

**DEVELOPMENT OF WEAPON DELIVERY MODELS
AND ANALYSIS PROGRAMS**

**Volume III. Testing and Demonstration of the Armament
Delivery Analysis Programming System (ADAPS)**

*A. FERIT KONAR
MICHAEL D. WARD*

Approved for public release; distribution unlimited.

FOREWORD

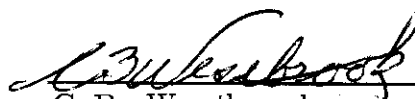
This document is the third of three volumes of the final report of a study conducted for the United States Air Force under Contract F33615-71-C-1059, "Development of Weapon Delivery Models and Analysis Programs". Approximately one man year of effort was covered by the contract. It was initiated under Project No. 8219, "Stability and Control Investigations", Task No. 821904, "Flight Control System Analysis," and administered by the Air Force Flight Dynamics Laboratory, Wright-Patterson Air Force Base, Ohio. Major Harvey M. Paskin (FGC), and Mr. Alonzo J. Connors (FGC) were project engineers.

The technical work reported was conducted by the Research Department of the Systems and Research Division of Honeywell Inc. Dr. A. Ferit Konar was the principal investigator; Mr. M. D. Ward was the programmer analyst. Dr. G. B. Skelton and Dr. E. E. Yore were project managers. Technical consultation was provided by Dr. Gunter Stein and Mr. C. R. Stone of Honeywell Inc.

The reporting period was October 1970 to July 1971. The report was first submitted in October 1971. The contractor's report number is Honeywell Report 12261-FR1.

The investigators in this study would like to thank Major Harvey H. Paskin for his enthusiastic support, for his technical leadership, and for his assistance in obtaining bomb data. The investigators would also like to thank Mr. Alonzo J. Connors for providing direction and assistance in testing the analysis programs.

This technical report was reviewed and is approved.



C. B. Westbrook
Chief, Control Criteria Branch
Flight Control Division
Air Force Flight Dynamics Laboratory

ABSTRACT

The testing and use of ADAPS is demonstrated by performing an analysis with a specified iron bomb (M117) and a representative tactical fighter-bomber aircraft (F4). The demonstration example revealed no appreciable performance difference between the time-invariant and time-varying optimal controllers for the weapon delivery process. The contribution matrix of an iron bomb indicated that the major contributors to the CEP are the velocity and the attitude-state errors at release.

Contrails

TABLE OF CONTENTS

	Page
SECTION I INTRODUCTION	1
SECTION II DATA PREPARATION	2
SECTION III TESTING THE AIRCRAFT SOFTWARE	26
Level Flight	26
40-Degree Dive and Pullup Trajectory	26
Frozen-Point Spectrum Analysis of the Linear Data	60
SECTION IV TESTING THE WEAPON AND GUST FILTER SOFTWARE	67
SECTION V TESTING THE CONTROLLER DESIGN SOFTWARE	72
SECTION VI CONTROLLER DESIGN	73
SECTION VII STATIONARY AND NONSTATIONARY GAINS AND SPECTRUMS	102
Gain Plots	102
Stationary, Free and Nonstationary Spectrums	152
SECTION VIII VARIANCE CONTRIBUTION AND CRITICAL PARAMETER IDENTIFICATION	174
SECTION IX CONCLUSIONS	182

LIST OF ILLUSTRATIONS

Figure		Page
1	Typical Parameter and Table Inputs to ADAP 1	13
2	Typical A-Array Dump Output from ADAP 1 During Simulation	25
3	Linear Data for Level Flight	27
4	Flight-Path-Angle Controller for Trim	28
5	Zero-Thrust, 40-degree Dive Trajectory	29
6	Stabilator, Angle-of-Attack and Flight-Path-Angle Profiles During Dive	29
7	Linear Data for 40-degree Dive	30
8	Dive and Pullup Trajectory	31
9	Flight-Path-Angle versus Time in Dive and Pullup	31
10	Stabilator Profile During Dive and Pull-up Maneuver Trim	32
11	Pitching Moment Coefficient of the Stabilator Along the Nominal Path	33
12	Augmented Aircraft and Reduced-Wind Dynamics	34
13	X_{eu} versus Time	35
14	$X_{e\theta}$ versus Time	35
15	X_{ew} versus Time	36
16	H_{eu} versus Time	36
17	$H_{e\theta}$ versus Time	37
18	H_{ew} versus Time	37
19	X_h versus Time	38
20	X_u versus Time	38
21	X_θ versus Time	39

LIST OF ILLUSTRATIONS --CONTINUED

22	X_q versus Time	39
23	X_w versus Time	40
24	M_h versus Time	40
25	M_u versus Time	41
26	M_q versus Time	41
27	M_w versus Time	42
28	Z_h versus Time	42
29	Z_u versus Time	43
30	Z_θ versus Time	43
31	Z_q versus Time	44
32	Z_w versus Time	44
33	Y_{ey} versus Time	45
34	$Y_{e\phi}$ versus Time	45
35	ψ_r versus Time	46
36	ψ_ϕ versus Time	46
37	N_r versus Time	47
38	N_v versus Time	47
39	N_p versus Time	48
40	Y_r versus Time	48
41	Y_v versus Time	49
42	Y_ϕ versus Time	49
43	Y_p versus Time	50
44	ϕ_r versus Time	50

LIST OF ILLUSTRATIONS -- CONTINUED

45	ϕ versus Time	51
46	L_r versus Time	51
47	L_v versus Time	52
48	L_p versus Time	52
49	Plotting Data Program Listing	53
50	Typical Aircraft Trajectory Input Data	54
51	δ_s versus Time	55
52	θ versus Time	56
53	γ versus Time	56
54	α versus Time	57
55	\dot{q} versus Time	57
56	q versus Time	58
57	$\dot{\alpha}$ versus Time	58
58	$\dot{\gamma}$ versus Time	59
59	V versus Time	59
60	Eigenvalue Analysis Program Listing	61
61	Short-Period Mode of Airframe During Dive	63
62	Phugoid Mode of Airframe During Dive	64
63	Dutch-Roll Mode of Airframe During Dive	65
64	Spiral Mode of Airframe versus Time During Dive	66
65	Roll-Convergence Mode of Airframe versus Time During Dive	66
66	Weapon Pitch-Axis Variables During Fall	69

LIST OF ILLUSTRATIONS -- CONCLUDED

67	Spectrum of Frozen Point - Longitudinal Matrix of M117	70
68	Spectrum of Frozen Point - Lateral Matrix of M117	71
69	Performance Evaluator Output - Free Airframe	77
70	Performance Evaluator Output - With Nonstationary Optimal Controller	85
71	Performance Evaluator Output -- With Fixed-Gain Optimal Controller	94
72	Gain Plotting Program Listing	103
73	Optimal Controller Gain Plots versus Time	104
74	Eigenvalue Spectrum Program Listing	153
75	Eigenvalue Spectrums	154
76	Variance Contribution Program Listing	177
77	Variance Contribution Program Outputs	178

Contrails

LIST OF TABLES

Table		Page
I	Typical Parameter Inputs for Aircraft	3
II	Typical Parameter Inputs for Weapon	6
III	Representation of Aircraft Coefficients in Stability Axes	8
IV	Representation of Bomb Aerodynamics	12
V	Comparison of Trajectory Data Obtained from ADAP 1 and Bomhtable	68
VI	Feedback Gains from Longitudinal States at 9 Seconds	74
VII	Feedback Gains from Lateral States at 9 Seconds	75
VIII	Feedback Gains from Wind States at 9 Seconds	75
IX	Performance Summary for Different Runs	76
X	Symbols for Controller Gains Corresponding to Aircraft States	102
XI	Sensitivity Matrix ϕ of a Weapon	175
XIII	Components of Nominal Impact Variances	176

SECTION I INTRODUCTION

This volume demonstrates the testing and use of the computer programs documented in Volume II by performing an analysis with a specified iron bomb (M117) and a representative tactical fighter-bomber aircraft (F4).

A typical delivery trajectory is chosen to be 40 degrees dive angle, 400 knots release velocity and 4000 feet release altitude. The measure of weapon delivery performance is chosen to be the CEP at impact.

First a typical data preparation and the input/output to the simulator and the linearizer (ADAP1) are treated. Then aircraft, weapon, and controller design software tests are described in that order.

Succeeding sections treat controller design, comparisons of stationary and nonstationary controllers, and variance contribution and critical-parameter identification in that order. A final section summarizes the conclusions drawn from the demonstration example.

SECTION II DATA PREPARATION

The major effort in data preparation for ADAPS is in punching cards for the parameter inputs and the aerodynamic tables.

Typical parameter inputs for an aircraft are shown in Table I, and weapon parameter inputs are shown in Table II. The representations of the airframe and the weapon aerodynamic tables in ADAPS are shown in Tables III and IV. Figure 1 shows the card images of the input data to ADAP 1 for the demonstration example. Figure 2 shows the A-Array dump output of the nonlinear trajectory data.

Table I. Typical Parameter Inputs for Aircraft

A(I)	Quantity	Mnemonic	Symbol	Description	Initial Value	Units
002	-13809.0	X	x_e	Range from target		ft
004	12000.0	H	h	Altitude		ft
016	422.5	VEL	V_a	Total velocity		ft/sec
026	0.03665	---	α	---		rad
029	0.03665	AL	α_a	Total angle of attack		rad
031	-0.8614	TH	θ	Pitch angle		rad
043	-0.001745	Q	q	Pitch rate		rad/sec
090	32.17	G	g	Gravity		ft/sec
115	38.67	B	b	Wing open		ft
116	16.04	C	c	Wing mean aerodynamic chord		ft
117	530.0	S	s	Wing area		ft ²
121	0.1	YDS	δ_s	Stabilator deflection		deg
122	0.00133	DELDS	$\Delta\delta_s$	Stabilator increment		deg/sec
131	100.0	N	N	No. of integration steps		---
132	1.0		ΔT	Time interval		sec
134	1.0	DTOUT		Output time interval		sec
140	0.7	YDSPU	$\delta_{s_{pu}}$	Stabilator deflection during pull-up		deg
141	7720	YTH(1)		Effective thrust output for engine 1		lbs
142	7720	YTH(2)		Effective thrust output for engine 2		lbs
156	10000.0	H1	h_1	Stabilator profile altitude breakpoint 1		ft
157	0.00075	DELDS1	$\Delta\delta_{s1}$	Stabilator increment 1		deg
170	12.0	NX, ANX	n_x	Number of nonlinear states		---
171	4.0	NU, ANU	n_u	Number of controls		---
172	6.0	NW, ANW	n_w	Number of disturbances		---
201	10.0	DX(1)	δ_u	Perturbation magnitude for u		ft/sec
202	5.0	DX(2)	δv		v	ft/sec
203	5.0	DX(3)	δw		w	ft/sec
204	0.01	DX(4)	δp		p	rad/sec
205	0.01	DX(5)	δq		q	rad/sec
206	0.01	DX(6)	δr		r	rad/sec
207	0.02	DX(7)	$\delta \theta$		θ	rad
208	0.02	DX(8)	$\delta \phi$		ϕ	rad
209	0.02	DX(9)	$\delta \psi$		ψ	rad
210	20.0	DX(10)	δx_e		x_e	ft
211	20.0	DX(11)	δy_e		y_e	ft
212	20.0	DX(12)	δh_e		h_e	ft
213	10.0		$\delta \dot{u}$		\dot{u}	ft/sec ²
214	5.0		$\delta \dot{v}$		\dot{v}	ft/sec ²
215	5.0		$\delta \dot{w}$		\dot{w}	ft/sec ²
216	0.01		$\delta \dot{p}$		\dot{p}	rad/sec ²
217	0.01		$\delta \dot{q}$		\dot{q}	rad/sec ²

Table I. Typical Parameter Inputs for Aircraft (continued)

A(1)	Quantity	Mnemonic	Symbol	Description	Initial Value	Units	
218	0.01		δr	Perturbation magnitude for \dot{r}		rad/sec ²	
221	0.05	DU(1)	$\delta(\delta_a)$		δ_a		deg
222	0.05	DU(2)	$\delta(\delta_g)$		δ_g		deg
223	0.05	DU(3)	$\delta(\delta_r)$		δ_r		deg
224	0.05	DU(4)	$\delta(\delta_{ap})$		δ_{sp}		deg
231	5.0	DW(1)	δu_a		u_a		ft/sec
232	5.0	DW(2)	δv_a		v_a		ft/sec
233	5.0	DW(3)	δw_a		w_a		ft/sec
234	0.01	DW(4)	δp_a		p_a		rad/sec
235	0.01	DW(5)	δq_a		q_a		rad/sec
236	0.01	DW(6)	δr_a	r_a		rad/sec	
256	0.2	KQDOT	$K_{\dot{q}}$	Trim stabilator gain on \dot{q}		deg/rad/sec ²	
257	0.25	KQ	K_q	Trim stabilator gain on q		deg/rad/sec	
258	0.1	KGAMDT	$K_{\dot{\gamma}}$	Trim stabilator gain on $\dot{\gamma}$		deg/rad/sec	
259	0.3	KGAM	K_{γ}	Trim stabilator gain on γ		deg/rad	
260	0.6981	GAMN	γ_0	Initial flight-path angle		rad	
261	1.0	TINT	---	---		---	
270	0.1047	QPU	q_{pu}	Pull-up pitch axis		rad/sec	
274	4000.0	HP	h_p	Pull-up altitude		ft	
283	30.0	TMAX	t_{max}	Maximum simulation time		sec	
290	0.5236	PSIB	$\bar{\psi}$	Mean wind azimuth angle		rad	
291	0.5236	THETAB	$\bar{\theta}$	Mean wind elevation angle		rad	
292	2000.0	HNAUT	h_0	Reference altitude for mean wind		ft	
293	30.0	VBNAUT	\bar{V}_0	Reference mean wind magnitude		ft/sec	
391	1.0	EA(1, 1)	e_{a11}	Accelerometer alignment matrix direction cosines			
395	1.0	EA(2, 2)	e_{a22}				
399	1.0	EA(3, 3)	e_{a33}				
400	1.0	EV(1, 1)	e_{v11}	Velocity sensor alignment matrix direction cosines			
404	1.0	EV(2, 2)	e_{v22}				
408	1.0	EV(3, 3)	e_{v33}				
409	1.0	ECOMEG(1, 1)	$e_{\Omega 11}$	Attitude gyros, alignment matrix direction cosines			
413	1.0	ECOMEG(2, 2)	$e_{\Omega 22}$				
417	1.0	ECOMEG(3, 3)	$e_{\Omega 33}$				
418	1.0	EOMEGD(1, 1)	$e_{\omega 11}$				
422	1.0	EOMEGD(2, 2)	$e_{\omega 22}$				
426	1.0	EOMEGD(3, 3)	$e_{\omega 33}$				
427	1.0	EOMEG(1, 1)	$e_{\omega 11}$				
431	1.0	EOMEG(2, 2)	$e_{\omega 22}$				
435	1.0	EOMEG(3, 3)	$e_{\omega 33}$				
501	313.5	XEX(1)	X_{ex}	X-coordinate of the thrust exit for engine 1		ft	
502	313.5	XEX(2)		X-coordinate of the thrust exit for engine 2		ft	
506	23.83	YEX(1)	Y_{ex}	Y-coordinate of the thrust exit for engine 1		ft	
507	23.83	YEX(2)		Y-coordinate of the thrust exit for engine 2		ft	
511	32.41	ZEX(1)	Z_{ex}	Z-coordinate of the thrust exit for engine 1		ft	
512	32.41	ZEX(2)		Z-coordinate of the thrust exit for engine 2		ft	
517	2.0	ANEX	N_{ex}	Number of thrust exits			

Table I. Typical Parameter Inputs for Aircraft (concluded)

A(1)	Quantity	Mnemonic	Symbol	Description	Initial Value	Units
559	20.0	XTH(1)	---	Thrust of engine 1		percent
560	20.0	XTH(2)	---	Thrust of engine 2		percent
579	316.0	XCA	---	X-coordinate of the moment reference center		ft
582	0.25	YAB(1)	---	Thrust vector azimuth bias for engine 1		deg
583	0.25	YAB(2)	---	Thrust vector azimuth bias for engine 2		deg
587	5.25	YEB(1)	---	Thrust vector elevation bias for engine 1		deg
588	5.25	YEB(2)	---	Thrust vector elevation bias for engine 2		deg
646	40.0	YDSB	δ_{sb}	Speed brakes deflection		deg
716	40420.0	WT	wt	Weight of the aircraft		lbs
901	7.0	AI(1)	$u(\text{loc})$	State component location of u		
902	8.0	AI(2)	$v(\text{loc})$	State component location of v		
903	9.0	AI(3)	$w(\text{loc})$	State component location of w		
904	42.0	AI(4)	$p(\text{loc})$	State component location for p		
905	43.0	AI(5)	$q(\text{loc})$	q		
906	44.0	AI(6)	$r(\text{loc})$	r		
907	31.0	AI(7)	$\theta(\text{loc})$	θ		
908	32.0	AI(8)	$\phi(\text{loc})$	ϕ		
909	33.0	AI(9)	$\psi(\text{loc})$	ψ		
910	2.0	AI(10)	$x_e(\text{loc})$	x_e		
911	3.0	AI(11)	$y_e(\text{loc})$	y_e		
912	4.0	AI(12)	$h_e(\text{loc})$	h_e		
913	17.0	AI(13)	$\dot{u}(\text{loc})$	\dot{u}		
914	18.0	AI(14)	$\dot{v}(\text{loc})$	\dot{v}		
915	19.0	AI(15)	$\dot{w}(\text{loc})$	\dot{w}		
916	45.0	AI(16)	$\dot{p}(\text{loc})$	\dot{p}		
917	46.0	AI(17)	$\dot{q}(\text{loc})$	\dot{q}		
918	47.0	AI(18)	$\dot{r}(\text{loc})$	\dot{r}		
919	39.0	AI(19)	$\dot{\theta}(\text{loc})$	$\dot{\theta}$		
920	40.0	AI(20)	$\dot{\phi}(\text{loc})$	$\dot{\phi}$		
921	41.0	AI(21)	$\dot{\psi}(\text{loc})$	$\dot{\psi}$		
922	13.0	AI(22)	$\dot{x}_e(\text{loc})$	\dot{x}_e		
923	14.0	AI(23)	$\dot{y}_e(\text{loc})$	\dot{y}_e		
924	15.0	AI(24)	$\dot{h}_e(\text{loc})$	\dot{h}_e		
925	123.0	AI(25)	$\delta_a(\text{loc})$	δ_a		
926	121.0	AI(26)	$\delta_s(\text{loc})$	δ_s		
927	125.0	AI(27)	$\delta_r(\text{loc})$	δ_r		
928	645.0	AI(18)	$\delta_{sp}(\text{loc})$	δ_{sp}		
929	101.0	AI(29)	$u_g(\text{loc})$	Disturbance input location for u_g		
930	102.0	AI(30)	$v_g(\text{loc})$	v_g		
931	103.0	AI(31)	$w_g(\text{loc})$	w_g		
932	104.0	AI(32)	$p_g(\text{loc})$	p_g		
933	105.0	AI(33)	$q_g(\text{loc})$	q_g		
934	106.0	AI(34)	$r_g(\text{loc})$	r_g		
995	2.0	SAC		Aircraft switch in Main		
996	2.0	SW		Weapon switch in Main		
998	1.00	ACWS		Aircraft weapon switch in wind filter		

Table II. Typical Parameter Inputs for Weapon

A(I)	Quantity	Mnemonic	Symbol	Description	Initial Value	Units	
002	-4081.0	X	x_e	Range from target at release		ft	
004	3995.0	H	h	Altitude		ft	
007	858.1	U	u	Velocity along x_b axis		ft/sec	
009	- 21.84	W	w	Velocity along z_b axis		ft/sec	
031	- 0.7158	TH	θ	Pitch attitude		rad	
043	- 0.01135	Q	q	Pitch rate		rad/sec	
083	5.6	IX	I_x	Moment of inertia about x axis		slug ft ²	
084	41.4	IY	I_y	Moment of inertia about y axis		slug ft ²	
085	41.4	IZ	I_z	Moment of inertia about z axis		slug ft ²	
090	32.17	G	g	Gravity		ft/sec ²	
091	25.6	MASS	m	Mass		slug	
115	1.33	B	b	Wing span of bomb		ft	
131	100.0	N	N	No. of integration steps			
132	1.0		ΔT	Time interval		sec	
134	1.0	DTOUT	---	Output interval		sec	
147	2.0	TAPEUNIT	---	---			
170	12.0	NX	n_x	No. of weapon states			
171	2.0	NU	n_u	No. of control inputs			
172	3.0	NW	n_w	No. of distribution inputs			
201	2.0	DX(1)	δu	Perturbation magnitude for u ↓		ft/sec	
202	2.0	DX(2)	δv		v		ft/sec
203	2.0	DX(3)	δw		w		ft/sec
204	0.004	DX(4)	δp		p		rad/sec
205	0.004	DX(5)	ψq		q		rad/sec
206	0.004	DX(6)	δr		r		rad/sec
207	0.004	DX(7)	$\delta \theta$		θ		rad/sec
208	0.004	DX(8)	$\delta \phi$		ϕ		rad
209	0.004	DX(9)	$\delta \psi$		ψ		rad
210	20.0	DX(10)	δx_e		x_e		ft
211	20.0	DX(11)	δy_e		y_e		ft
212	20.0	DX(12)	δh_e		h_e		ft
221	2.0	DU(1)	$\delta(\delta_a)$		δ_a		deg
222	2.0	DU(2)	$\delta(\delta_g)$	δ_g		deg	
231	2.0	DW(1)	δu_a	u_a		ft/sec	
232	2.0	DW(2)	δv_a	v_a		ft/sec	
233	2.0	DW(3)	δw_a	w_a		ft/sec	
261	1.0	TINT	---	---		---	

Table II. Typical Parameter Inputs for
Weapon (concluded)

A(I)	Quantity	Mnemonic	Symbol	Description	Initial Value	Units
290	0.5236	PSIB	ψ	Mean wind azimuth angle		rad
291	0.5236	THETAB	θ	Mean wind elevation angle		rad
292	2000.0	HNAUT	h_o	Reference altitude for mean wind		ft
293	30.0	VBNAUT	v_o	Reference mean wind magnitude		ft/sec
294	1.33	BMBD	b_d	Bomb diameter		ft
901	7.0	AI(1)	$u(\text{loc})$	State component location of u		
902	8.0	AI(2)	$v(\text{loc})$	v		
903	9.0	AI(3)	$w(\text{loc})$	w		
904	42.0	AI(4)	$p(\text{loc})$	p		
905	43.0	AI(5)	$q(\text{loc})$	q		
906	44.0	AI(6)	$r(\text{loc})$	r		
907	31.0	AI(7)	$\theta(\text{loc})$	θ		
908	32.0	AI(8)	$\phi(\text{loc})$	ϕ		
909	33.0	AI(9)	$\psi(\text{loc})$	ψ		
910	2.0	AI(10)	$x_e(\text{loc})$	x_e		
911	3.0	AI(11)	$y_e(\text{loc})$	y_e		
912	4.0	AI(12)	$h_e(\text{loc})$	h_e		
913	17.0	AI(13)	$\dot{u}(\text{loc})$	\dot{u}		
914	18.0	AI(14)	$\dot{v}(\text{loc})$	\dot{v}		
915	19.0	AI(15)	$\dot{w}(\text{loc})$	\dot{w}		
916	45.0	AI(16)	$\dot{p}(\text{loc})$	\dot{p}		
917	46.0	AI(17)	$\dot{q}(\text{loc})$	\dot{q}		
918	47.0	AI(18)	$\dot{r}(\text{loc})$	\dot{r}		
919	39.0	AI(19)	$\dot{\theta}(\text{loc})$	$\dot{\theta}$		
920	40.0	AI(20)	$\dot{\phi}(\text{loc})$	$\dot{\phi}$		
921	41.0	AI(21)	$\dot{\psi}(\text{loc})$	$\dot{\psi}$		
922	13.0	AI(22)	$\dot{x}_e(\text{loc})$	\dot{x}_e		
923	14.0	AI(23)	$\dot{y}_e(\text{loc})$	\dot{y}_e		
924	15.0	AI(24)	$\dot{h}_e(\text{loc})$	\dot{h}_e		
925	263.0	AI(25)	δx	Canted fin longitudinal input		deg
926	264.0	AI(26)	δy	Canted fin lateral input		deg
927	101.0	AI(27)	u_g	Gust disturbance input		ft/sec
928	102.0	AI(28)	v_g	Gust disturbance input		ft/sec
929	103.0	AI(29)	w_g	Gust disturbance input		ft/sec
995	2.0	SAC		Aircraft switch in main		
996	2.0	SW		Weapon switch in main		
997	1.0	ACWS		A/C weapon switch in wind filter		

Table III. Representation of Aircraft Coefficients in Stability Axes

Coefficient	Look-Up Representation	Mnemonic	Units
$C_L(M_a, h, \alpha_w^o)$	F1(1, 2, 3)	CL	
$C_{z_q}(h, M_a)$	F2(2, 1)	CZQ	per radian
$C_{z_\alpha}(h, M_a)$	F3(2, 1)	CZALDT	per radian
$C_{L_{\delta_s}}(h, \alpha_w^o, M_a)$	F4(2, 3, 1)	CLDS	per degree
$C_{L_{\delta_{sp}}}(h, M_a)$	F5(2, 1)	CLDSP	per degree
$C_{L_{\delta_a}}(h, M_a)$	F6(2, 1)	CLDA	per degree
$C_{L_{\delta_{sb}}}(\alpha_w^o, M_a)$	F7(3, 1)	CLDSB	per degree
$C_{L_{\delta_{lg}}}(\alpha_w^o)$	F8(3)	CLDLG	
$C_D(Pow, M_a, C_L)$	F9(4, 1, 5)	CD	
$C_D(\delta_{sb}^o, C_L, M_a)$	F10(6, 5, 1)	CDDSB	
$C_{D_{\delta_{lg}}}(CL)$	F11(5)	CDDLG	
$C_{mca}(M_a, h, \alpha_w^o)$	F12(1, 2, 3)	CMCA	
$C_{m_q}(h, M_a)$	F13(2, 1)	CMQ	per radian
$C_{m_\alpha}(h, M_a)$	F14(2, 1)	CMALDT	per radian

Table III. Representation of Aircraft Coefficients
in Stability Axes (continued)

Coefficient	Look-Up Representation	Mnemonic	Units
$C_{m_{\delta_s}}(h, \alpha_w^\circ, M_a)$	F15(2, 3, 1)	CMDS	per degree
$C_{m_{\delta_{sp}}}(\alpha_w^\circ, h, M_a)$	F16(3, 2, 1)	CMDSP	per degree
$C_{m_{\delta_a}}(\alpha_w^\circ, h, M_a)$	F17(3, 2, 1)	CMDA	per degree
$C_{m_{\delta_{sb}}}(M_a, \alpha_w^\circ)$	F18(3, 1)	CMDSB	per degree
$C_{m_{\delta_{lg}}}(\alpha_w^\circ)$	F19(3)	CMDLG	
$C_{y_\beta}(\alpha_w^\circ, h, M_a)$	F20(3, 2, 1)	CYBET	per degree
$C_{y_r}(\alpha_w^\circ, h, M_a)$	F21(3, 2, 1)	CYR	per radian
$C_{y_p}(h, \alpha_w^\circ, M_a)$	F22(2, 3, 1)	CYP	per radian
$C_{y_{\delta_{sp}}}(M_a)$	F23(1)	CYDSP	per degree
$C_{y_{\delta_a}}(M_a)$	F24(1)	CYDA	per degree
$C_{y_{\delta_r}}(h, M_a)$	F25(2, 1)	CYDR	per degree
$C_{n_\beta}(\alpha_w^\circ, h, M_a)$	F26(3, 2, 1)	CNBET	per degree
$C_{n_r}(M_a, h, \alpha_w^\circ)$	F27(3, 2, 1)	CNR	per radian

Table III. Representation of Aircraft Coefficients
in Stability Axes (continued)

Coefficient	Look-Up Representation	Mnemonic	Units
$C_{n_p}(h, \alpha_w^o, M_a)$	F28(2, 3, 1)	CNP	per radian
$C_{n_{\delta_{sp}}}(\alpha_w^o, M_a)$	F29(3, 1)	CNDSP	per degree
$C_{n_{\delta_a}}(\alpha_w^o, h, M_a)$	F30(3, 2, 1)	CNDA	per degree
$C_{n_{\delta_r}}(h, M_a)$	F31(2, 1)	CNDR	per degree
$C_{l_{\beta}}(\alpha_w^o, h, M_a)$	F32(3, 2, 1)	CLLBET	per degree
$C_{l_r}(\alpha_w^o, h, M_a)$	F33(3, 2, 1)	CLLR	per radian
$C_{l_p}(\alpha_w^o, h, M_a)$	F34(3, 2, 1)	CLLP	per radian
$C_{l_{\delta_{sp}}}(\alpha_w^o, h, M_a)$	F35(3, 2, 1)	CLLDSP	per degree
$C_{l_{\delta_a}}(\alpha_w^o, h, M_a)$	F36(3, 2, 1)	CLLDA	per degree
$C_{l_{\delta_r}}(\alpha_w^o, h, M_a)$	F37(3, 2, 1)	CLLDR	per degree
$X_{c.g.}(Y_{trm}, W_T)$	F45(10, 15)	XCG	inches
$Z_{c.g.}(Y_{trm}, W_T)$	F46(10, 15)	ZCG	inches
$I_x(Y_{trm}, W_T)$	F47(10, 15)	IX	slug/ft ²
$I_y(Y_{trm}, W_T)$	F48(10, 15)	IY	slug/ft ²

Table III. Representation of Aircraft Coefficients
in Stability Axes (concluded)

Coefficient	Look-Up Representation	Mnemonic	Units
$I_z(Y_{trm}, W_T)$	F49(10, 15)	IZ	slug/ft ²
$I_{xz}(Y_{trm}, W_T)$	F50(10, 15)	IXZ	slug/ft ²
$\rho(h)$	F53(2)	RHO	lbs/ft ³
$a(h)$	F54(2)	SOS	ft/sec
Argument	Look-Up Representation	Mnemonic	Units
M	V(1)	MACH	
h	V(2)	H	feet
α_w^o	V(3)	AL+1°	degrees
Power	V(4)	POW	per unit
C_L	V(5)	CL	
δ_{sb}	V(6)	YDSB	degree
δ_s	V(7)	YDS	degree
Y_{trm}	V(10)	YTRM	degree
W_T	V(15)	WT	lbs

Table IV. Representation of Bomb Aerodynamic Coefficients in Cross-Velocity Axes

Coefficient	Look-Up Representation	Mnemonic	Units.
$C_N(\hat{\alpha}^o, M_a)$	F75(3, 1)	CN	
$C_{N_\delta}(\hat{\alpha}^o, M_a)$	F76(3, 1)	CNDEL	per degree
$C_A(M_a)$	F77(1)	CA	
$C_m(\hat{\alpha}^o, M_a)$	F78(3, 1)	CM	per degree
$C_{m_q}(\hat{\alpha}^o, M_a)$	F79(3, 1)	CMQ	per degree
$C_{m_\delta}(\hat{\alpha}^o, M_a)$	F80(3, 1)	CMDEL	per degree
Argument	Look-Up Representation	Mnemonic	Units
M	V(1)	MACH	
h	V(2)	H	feet
$\hat{\alpha}^o$	V(3)	ALFH	degrees

1
C 03/23/72
C H0= 12000 FT,V0=250 KNTS
C INTEGRATION AND LINEARIZATION OF AIRPLANE
C NOMINAL PERTURBATION
C 40 DEGREE DIVE ANGLE
PCC
2 -.1381E+05 4 +.1200E+05 16 +.4225E+03 26 +.3665E-01 29 +.3665E-01
31 -.6614E+00 43 -.1745E-02 90 +.3217E+02 115 +.3867E+02 116 +.1604E+02
117 +.5300E+03 121 +.1000E+00 122 +.1330E-02 131 +.1000E+03 132 +.1000E+01
134 +.1000E+01 140 +.7000E+00 141 +.7720E+04 142 +.7720E+04 156 +.1000E+05
157 +.7500E-03 170 +.1200E+02 171 +.4000E+01 172 +.6000E+01 201 +.1000E+02
202 +.5000E+01 203 +.5000E+01 204 +.1000E-01 205 +.1000E-01 206 +.1000E-01
207 +.2000E-01 208 +.2000E-01 209 +.2000E-01 210 +.2000E+02 211 +.2000E+02
212 +.2000E+02 213 +.1000E+02 214 +.5000E+01 215 +.5000E+01 216 +.1000E-01
217 +.1000E-01 218 +.1000E-01 221 +.5000E-01 222 +.5000E-01 223 +.5000E-01
224 +.5000E-01 231 +.5000E+01 232 +.5000E+01 233 +.5000E+01 234 +.1000E-01
235 +.1000E-01 236 +.1000E-01 256 +.2000E+00 257 -.3000E+00 258 +.1000E+00
259 -.3000E+00 260 -.6981E+00 261 +.1000E+01 270 +.1047E+00 274 +.4000E+04
283 +.3000E+02 290 +.5236E+00 291 +.5236E+00 292 +.2000E+04 293 +.3000E+02
391 +.1000E+01 395 +.1000E+01 399 +.1000E+01 400 +.1000E+01 404 +.1000E+01
408 +.1000E+01 409 +.1000E+01 413 +.1000E+01 417 +.1000E+01 418 +.1000E+01
422 +.1000E+01 426 +.1000E+01 427 +.1000E+01 431 +.1000E+01 435 +.1000E+01
501 -.3135E+03 502 -.3135E+03 506 +.2383E+02 507 -.2383E+02 511 -.3241E+02
512 -.3241E+02 517 +.2000E+01 559 +.2000E+02 560 +.2000E+02 579 -.3162E+03
582 -.2500E+00 583 +.2500E+00 587 +.5250E+01 588 +.5250E+01 646 +.4000E+02
716 +.4042E+05 901 +.7000E+01 902 +.8000E+01 903 +.9000E+01 904 +.4200E+02
905 +.4300E+02 906 +.4400E+02 907 +.3100E+02 908 +.3200E+02 909 +.3300E+02
910 +.2000E+01 911 +.3000E+01 912 +.4000E+01 913 +.1700E+02 914 +.1800E+02
915 +.1900E+02 916 +.4500E+02 917 +.4600E+02 918 +.4700E+02 919 +.3900E+02
920 +.4000E+02 921 +.4100E+02 922 +.1300E+02 923 +.1400E+02 924 +.1500E+02
925 +.1230E+03 926 +.1210E+03 927 +.1250E+03 928 +.6450E+03 929 +.1010E+03
930 +.1020E+03 931 +.1030E+03 932 +.1040E+03 933 +.1050E+03 934 +.1060E+03
995 +.2000E+01 996 +.2000E+01 998 +.1000E+01

Figure 1. Typical Parameter and Table Inputs to ADAP 1

Contrails

```

RUN
 3  1 1  2 2  3 3  1
 1      0.5  0.9
 2      0.0 20000.0
 3      -4.0  8.0  16.0  20.0
      -0.22  .44  .78  .80
      -0.22  .47  .82  .85
      -0.25  .46  .74  .80
      -0.27  .51  .82  .89
-1
 2  5 2  4 1  2
 5      0.0 15000.0
 4      0.6  0.95
      -2.25 -2.15
      -2.40 -2.35
-1
 2  5 2  6 1  3
 5
 6      0.6  0.8  0.95
      -0.66 -0.62 -0.79
      -0.72 -0.71 -0.86
-1
 3  7 2  8 3  9 1  4
 7      0.0 20000.0
 8      6.0  12.0  16.0  20.0
 9      0.4  0.9
      .0069  .0057
      .0067  .0052
      .0064  .0046
      .0058  .0030
      .0071  .0064
      .0068  .0059
      .0065  .0050
      .0059  .0032
-1
 2 10 2 11 1  5
10      0.0 25000.0
11      0.4  1.1
      -.00040 -.00040
      -.00055 -.00055
-1
 2 10 2 12 1  6
10
12      0.4  0.7  1.05
      .00260 .00180 .00055
      .00270 .00220 .00140
-1

```

Figure 1. Typical Parameter and Table Inputs to ADAP 1 (continued)

Contrails

2	14	3	13	1	7						
14			0.0		4.0		8.0		12.0		
13			0.5		0.7		0.9				
			.00135		.00145		.00295				
			.00305		.00295		.00220				
			.00100		.00105		.00100				
			.00020		.00020		-.00030				
-1											
1	15	3				8					
15			-4.0		4.0		12.0		14.0	16.0	20.0
			-.0140		-.0145		-.0155		-.0175	-.0230	-.0460
-1											
3	16	4	17	1	18	5	9				
16			0.0		1.0						
17			0.4		0.8		1.0				
18			0.0		0.1		0.2				
			.0180		.0190		.0225				
			.0185		.0200		.0230				
			.0360		.0380		.0430				
			.0105		.0115		.0150				
			.0105		.0115		.0150				
			.0275		.0290		.0335				
-1											
3	19	6	21	5	20	1	10				
19			0.0		20.0		40.0				
21			0.3		0.7		0.9				
20			0.15		0.30		0.45		1.0		
			0.0		0.0		0.0		0.0		
			0.0		0.0		0.0		0.0		
			0.0		0.0		0.0		0.0		
			.0095		.0100		.0130		.0190		
			.0090		.0100		.0130		.0210		
			.0085		.0100		.0125		.0195		
			.0250		.0250		.0300		.0395		
			.0235		.0245		.0290		.0410		
			.0225		.0240		.0295		.0400		
-1											

Figure 1. Typical Parameter and Table Inputs to ADAP 1 (continued)

Contrails

```

1 22 5 11
22      -.2      .2      .4      .6      .7      .775
      .0194     .0165     .0146     .0118     .0090     .0030
-1

3 30 1 31 2 32 3 12
30      0.5      0.8      0.95
31      0.0 10000.0 30000.0
32      -4.0      6.0      10.0      18.0
      .025     -.014     -.026     -.025
      .026     -.015     -.028     -.028
      .028     -.016     -.029     -.031
      .023     -.011     -.021     -.028
      .030     -.015     -.025     -.032
      .034     -.018     -.029     -.038
      .029     -.026     -.032     -.052
      .034     -.035     -.040     -.063
      .039     -.041     -.048     -.07
-1

2 33 2 34 1 13
33      0.0 15000.0
34      0.6      0.8
      -2.30     -2.25
      -2.45     -2.40
-1

2 33 2 35 1 14
33
35      0.6      0.8      0.95
      -.97     -.95     -1.16
      -1.08     -1.03     -1.23
-1

3 36 2 37 3 38 1 15
36      0.0 20000.0
37      6.0      12.0      16.0      20.0
38      0.4      0.6      0.9
      -.0100     -.0093     -.0083
      -.0097     -.0089     -.0075
      -.0092     -.0082     -.0065
      -.0085     -.0072     -.0044
      -.0102     -.0099     -.0094
      -.0099     -.0094     -.0084
      -.0095     -.0087     -.0071
      -.0092     -.0076     -.0047
-1

3 39 3 40 2 42 1 16
39      0.0      8.0      16.0
40      0.0 15000.0
42      0.4      0.8      0.95
      .00012     .00018     .00035
      .00013     .00021     .00039
      .00006     .00015     .00030
      .00007     .00018     .00034
      .00003     .00018     .00036
      .00003     .00018     .00036
-1

```

Figure 1. Typical Parameter and Table Inputs to ADAP 1 (continued)

Contrails

```

3 39 3 40 2 41 1 17
39
40
41      0.5      0.7      0.9
      -.00097 -.00091 -.00103
      -.00101 -.00096 -.00111
      -.00080 -.00081 -.00096
      -.00085 -.00086 -.00105
      -.00066 -.00076 -.00104
      -.00070 -.00080 -.00110

-1
2 43 3 44 1      18
43      0.0      4.0      8.0      12.0
44      0.5      0.75     1.0
      0.00009 0.00009 -.00002
      -.00001 -.00016 0.00030
      0.00022 0.00022 0.00056
      0.00038 0.00040 0.00107

-1
1 45 3      19
45      -8.0     -4.0      4.0      16.0     20.0
      .0026     .0020     .0003  -0.0030  -0.0043

-1
3 39 3 40 2 46 1 20
39
40
46      .2      .8      1.0
      -.0114 -.0120 -.0124
      -.0114 -.0120 -.0125
      -.0105 -.0111 -.0108
      -.0105 -.0111 -.0112
      -.0096 -.0101 -.0098
      -.0096 -.0101 -.0100

-1
3 39 3 40 2 46 1 26
39
40
46      .00195 .00200 .00230
      .00195 .00205 .00240
      .00200 .00215 .00210
      .00200 .00215 .00225
      .00180 .00190 .00190
      .00180 .00190 .00200

-1

```

Figure 1. Typical Parameter and Table Inputs to ADAP 1 (continued)

Contrails

	3	39 3	40 2	47 1	32				
39									
40									
47		0.4	0.8	1.0					
		-.00055	-.00060	-.00063					
		-.00055	-.00060	-.00065					
		-.00135	-.00115	-.00105					
		-.00140	-.00135	-.00125					
		-.00 92	-.00075	-.00075					
		-.00 97	-.00103	-.00100					
-1									
	3	48 3	40 2	47 1	21				
48		0.0	4.0	8.0	12.0				
40									
47									
		.295	.320	.325					
		.295	.320	.330					
		.295	.310	.315					
		.295	.310	.320					
		.280	.300	.305					
		.280	.300	.320					
		.275	.295	.295					
		.275	.295	.310					
-1									
	3	48 3	40 2	47 1	27				
48									
40									
47									
		-.230	-.250	-.270					
		-.230	-.250	-.275					
		-.225	-.240	-.255					
		-.225	-.240	-.260					
		-.220	-.230	-.245					
		-.220	-.230	-.245					
		-.220	-.225	-.245					
		-.220	-.225	-.245					
-1									
	3	49 3	40 2	50 1	33				
49		-4.0	0.0	4.0	8.0	12.0	16.0		
40									
50		.4	.7	.95					
		-.012	-.017	-.016					
		.008	-.008	-.006					
		.029	.035	.041					
		.030	.037	.044					
		.012	.076	.083					
		.012	.081	.087					
		.012	.096	.113					
		.012	.097	.114					
		.032	.107	.140					
		.032	.109	.141					
		.089	.110	.156					
		.090	.111	.159					
-1									

Figure 1. Typical Parameter and Table Inputs to ADAP 1 (continued)

Contrails

```

      3  40 2  51 3  52 1  22
40
51      -12.0  -8.0      .0      8.0      12.0      16.0
52          .4      .8
          -.38  -.25
          -.39  -.35
          -.02  -.03
          .36   .27
          .35   .22
          .03   .00
          -.39  -.28
          -.40  -.37
          -.01  -.02
          .38   .30
          .34   .25
          .02   .00
-1
      3  40 2  51 3  53 1  28
40
51
53          .4      1.0
          .008   .032
          .060   .072
          .012   .023
          -.036  -.022
          .014  -.010
          .124   .070
          -.004  .048
          .072   .072
          .014   .020
          -.040  -.030
          .020  -.000
          .164   .084
-1
      3  54 3  55 2  56 1  34
54          0.0      4.0      8.0      12.0
55          0.0 10000.0 20000.0
56          .5      .9
          -.200  -.170
          -.210  -.185
          -.215  -.205
          -.210  -.165
          -.220  -.180
          -.225  -.205
          -.220  -.150
          -.230  -.165
          -.235  -.180
          -.200  -.115
          -.205  -.125
          -.215  -.135
-1

```

Figure 1. Typical Parameter and Table Inputs to ADAP 1 (continued)

Contrails

```

1 57 1 23
57 0.3 1.2 1.4 2.0
-.000060-.000060-.000130-.000060
-1
1 58 1 24
58 0.3 1.2 1.4 1.6 2.0
-.000165-.000165-.000030 .0000200.000020
-1
2 40 2 59 1 25
40
59 0.0 0.4 0.8
.00223 .00205 .00171
.00223 .00210 .00184
-1
2 60 3 61 1 29
60 0.0 8.0 16.0
61 0.5 0.9
.000055 .000068
.000022 .000017
-.000011-.0000 4
-1
3 60 3 40 2 62 1 30
60
40
62 0.4 0.9
-.000048-.000037
-.000048-.000037
-.000114-.000077
-.000116-.000083
-.000181-.000160
-.000184-.000165
-1
2 40 2 63 1 31
40
63 0.0 0.4 0.8
-.00140 -.00130 -.00101
-.00140 -.00134 -.00111
-1
3 70 3 71 2 72 1 35
70 0.0 4.0 8.0 12.0
71 0.0 10000.0 20000.0
72 0.3 .6 .8 .95
.000119 .000129 .000143 .000160
.000122 .000136 .000158 .000178
.000124 .000142 .000169 .000198
.000157 .000152 .000148 .000160
.000162 .000162 .000163 .000180
.000167 .000167 .000174 .000200
.000121 .000124 .000120 .000110
.000123 .000131 .000128 .000126
.000126 .000136 .000143 .000140
.000062 .000 62 .000062 .000059
.000065 .000 68 .000068 .000070
.000067 .000 71 .000073 .000076
-1

```

Figure 1. Typical Parameter and Table Inputs to ADAP 1 (continued)

Contrails

```

3  70 3  71 2  73 1  36
70
71
73      0.3      0.6      0.8      1.0
      .00053    .00039    .00023    .00000
      .00055    .00043    .00029    .00008
      .00057    .00047    .00035    .00015
      .00051    .00040    .00023    -.00001
      .00054    .00044    .00031    .00009
      .00057    .00048    .00034    .00019
      .00058    .00039    .00023    -.00001
      .00060    .00043    .00030    .00007
      .00062    .00047    .00035    .00014
      .00042    .00033    .00019    -.00001
      .00045    .00037    .00024    .00005
      .00047    .00041    .00029    .00013
-1
3  74 3  75 2  76 1  37
74      0.0      4.0     12.0     16.0
75      0.0 15000.0
76      0.0      0.4      0.8
      .000225 .000220 .000210
      .000225 .000225 .000225
      .000110 .000106 .000104
      .000110 .000108 .000110
      -.000110-.000109-.000110
      -.000110-.000109-.000115
      -.000225-.000220-.000210
      -.000225-.000225-.000225
-1
2  23 7  24 8          38
23     -21.0    -11.0    -1.0      7.0
24      0.0      2.0      3.0      4.0
      0.115    -.057    -.140    -.230
      0.077    -.110    -.197    -.284
      0.022    -.133    -.231    -.304
      -.014    -.176    -.245    -.304
-1
2  23 7  24 8          39
23
24
      .315     .157     .078     0.0
      .298     .150     .075     0.0
      .267     .134     .066     0.0
      .234     .119     .057     0.0
-1

```

Figure 1. Typical Parameter and Table Inputs to ADAP 1 (continued)

Contrails

2	23	7	24	8	40							
23												
24												
			.87	-0.24	-0.48	-0.68						
			.40	-0.55	-0.91	-1.28						
			0.13	-0.92	-1.46	-2.12						
			-0.13	-1.28	-2.00	-2.90						
-1												
1	23	7			41							
23												
			4.95	5.20	5.05	4.55						
-1												
1	25	9			42							
25			-10.38	-.0001	.0001	10.38						
			-11.55	-2.31	2.31	11.55						
-1												
2	28	12	27	11	43							
28			-8.0	8.0								
27			-3.0	-1.5	1.5	3.0						
			-75.0	-25.0	60.0	130.0						
			-130.0	-60.0	25.0	75.0						
-1												
1	64	1			44							
64			0.2	0.4	0.65	1.0	1.2	2.0				
			0.21	0.36	0.45	0.39	0.43	0.61				
-1												
2	65	10	66	15	45							
65			0.0	100.								
66			32000.0	37500.0	43000.0							
			317.4	317.9	325.4							
			317.4	317.9	325.4							
-1												
2	65	10	66	15	46							
65												
66			24.5	28.4	28.7							
			23.7	26.7	27.3							
-1												
2	65	10	66	15	47							
65												
66			21900.	24097.	27432.							
			23492.	26572.	29917.							
-1												
2	65	10	66	15	48							
65												
66			121000.	126665.	138521.							
			123716.	128976.	140844.							
-1												

Figure 1. Typical Parameter and Table Inputs to ADAP 1 (continued)

Contrails

```

2 6510 6615 49
65
66
    137000. 143576. 157697.
    139989. 146129. 160250.
-1
2 6510 6615 50
65
66
    3600.0 3801. 5880.
    3539. 3782. 5959.
-1
1 6713 51
67
    0.0 50.0 50.0001 100.0
    .000217 .000239 .000389 .000540
-1
1 6714 52 51
-1
1 68 2 53
68
    0.0 10000. 20000. 30000. 40000. 50000. 60000.
    .002377 .001755 .001266 .0008893.0005851.0003618.0002237
-1
1 69 2 54
69
    0.0 10000. 20000. 30000. 37000. 60000.
    1117. 1078. 1037. 995. 969. 969.
-1
-1
C 03/23/72
C INTEGRATION AND LINERIZATION OF WEAPON M117 DATA
C DOUBLE NOMINAL PERTURBATION
PCC
2 -.4081E+04 4 +.3995E+04 7 +.8581E+03 9 -.2184E+02 31 -.7158E+00
43 -.1135E-01 83 +.5600E+01 84 +.4140E+02 85 +.4140E+02 90 +.3217E+02
91 +.2560E+02 115 +.1330E+01 131 +.1000E+03 132 +.1000E+01 134 +.1000E+01
147 +.2000E+01 170 +.1200E+02 171 +.2000E+01 172 +.3000E+01 201 +.2000E+01
202 +.2000E+01 203 +.2000E+01 204 +.4000E-02 205 +.4000E-02 206 +.4000E-02
207 +.4000E-02 208 +.4000E-02 209 +.4000E-02 210 +.2000E+02 211 +.2000E+02
212 +.2000E+02 221 +.2000E+01 222 +.2000E+01 231 +.2000E+01 232 +.2000E+01
233 +.2000E+01 261 +.1000E+01 290 +.5236E+00 291 +.5236E+00 292 +.2000E+04
293 +.3000E+02 294 +.1330E+01 901 +.7000E+01 902 +.8000E+01 903 +.9000E+01
904 +.4200E+02 905 +.4300E+02 906 +.4400E+02 907 +.3100E+02 908 +.3200E+02
909 +.3300E+02 910 +.2000E+01 911 +.3000E+01 912 +.4000E+01 913 +.1700E+02
914 +.1800E+02 915 +.1900E+02 916 +.4500E+02 917 +.4600E+02 918 +.4700E+02
919 +.3900E+02 920 +.4000E+02 921 +.4100E+02 922 +.1300E+02 923 +.1400E+02
924 +.1500E+02 925 +.2630E+03 926 +.2640E+03 927 +.1010E+03 928 +.1020E+03
929 +.1030E+03 995 +.2000E+01 996 +.2000E+01 997 +.1000E+01
RUN
1 1 1 77
1 0.0 0.80 0.95 1.0 1.1 1.2 1.3 1.5
0.12 0.11 0.11 0.14 0.27 0.30 0.29 0.28
-1

```

Figure 1. Typical Parameter and Table Inputs to ADAP 1 (continued)

Contrails

	2	2 1	3 3	75				
	2	0.0	0.40	0.80	1.20	1.50		
	3	0.0	4.0	8.0	12.0	16.0	20.0	24.0
		0.0	0.24	0.62	1.02	1.59	2.04	2.70
		0.0	0.24	0.62	1.02	1.57	2.04	2.66
		0.0	0.24	0.63	1.08	1.60	2.08	2.62
		0.0	0.33	0.74	1.19	1.64	2.28	3.32
		0.0	0.35	0.71	1.17	1.83	2.63	3.71
-1	2	4 1	5 3	76				
	4	0.0	0.40	0.80	1.20	1.50		
	5	0.0	16.0	20.0	24.0			
		0.0	0.0	0.0	-0.09			
		0.0	0.0	0.0	-0.09			
		0.0	-0.03	-0.08	-0.23			
		0.0	-0.10	-0.13	-0.15			
		0.0	-0.06	-0.09	-0.11			
-1	2	6 1	7 3	78				
	6	0.0	0.40	0.80	1.2	1.5		
	7	0.0	4.0	8.0	12.0	16.0	20.0	24.0
		0.0	-0.30	-0.77	-1.65	-2.52	-3.56	-4.02
		0.0	-0.30	-0.77	-1.65	-2.52	-3.56	-4.02
		0.0	-0.24	-0.98	-1.72	-2.49	-3.25	-3.60
		0.0	-0.37	-1.04	-1.67	-2.17	-2.63	-3.14
		0.0	-0.27	-0.63	-1.10	-1.57	-2.07	-2.58
-1	2	8 1	9 3	80				
	8	0.0	0.5	0.9	1.3	1.5		
	9	0.0	10.	16.0	20.0	24.0		
		0.0	0.0	0.0	-0.08	-0.42		
		0.0	0.0	0.0	-0.08	-0.42		
		0.0	-0.03	-0.08	-0.27	-0.66		
		0.0	-0.04	-0.10	-0.16	-0.47		
		0.0	-0.04	-0.08	-0.12	-0.33		
-1	2	10 1	11 3	79				
	10	0.0	0.6	0.9	1.20	1.50		
	11	0.0	10.0	20.0	30.0			
		-75.0	-94.0	-125.0	-143.0			
		-75.0	-94.0	-125.0	-143.0			
		-80.0	-175.0	-200.0	-240.0			
		-158.0	-200.0	-215.0	-230.0			
		-155.0	-170.0	-180.0	-195.0			
-1	1	68 2	53					
	68	0.0	10000.	20000.	30000.	40000.	50000.	60000.
		.002377	.001755	.001266	.0008893	.0005851	.0003618	.0002237
-1	1	69 2	54					
	69	0.0	10000.	20000.	30000.	37000.	60000.	
		1117.	1078.	1037.	995.	969.	969.	
-1								
-1								
		STO						

Figure 1. Typical Parameter and Table Inputs to ADAP 1 (concluded)

LIST OF NON-ZERO FLUENTS IN A (1), THRU, A(1000)

1	1.0000E+00	2	-1.3476E+04	4	1.1714E+04	5	4.2214E-01	6	1.0709E+03	7	4.5165E+02	9	1.9763E+01
10	4.5165E+02	12	1.9763E+01	13	3.4457E+02	15	-2.9221E+02	16	4.5209E+02	17	2.9207E+01	19	2.1321E+00
20	9.5323E+00	22	-2.4214E+01	26	3.6650E-02	28	-7.0336E-01	29	4.3728E-02	31	-6.5963E-01	37	1.8874E-03
43	2.0050E-03	46	-4.4957E-03	48	-6.1422E-01	49	7.8913E-01	51	1.0000E+00	53	1.0000E+00	54	7.9022E-01
56	-6.1282E-01	58	1.0000E+00	60	6.1282E-01	62	7.9022E-01	70	1.7053E+02	71	-3.3982E+03	73	-2.9011E+04
78	3.3492E+03	81	2.0050E-03	83	2.5868E+04	84	1.3296E+05	85	1.5107E+05	88	4.9048E+03	89	1.0000E-02
90	3.2170E+01	91	1.2565E+03	92	6.9848E-01	93	-3.2089E-01	95	4.7348E-01	108	-2.9202E+02	111	1.5375E+04
112	-1.4128E+03	114	1.6709E-03	115	3.8670E-01	116	1.6040E+01	117	5.3000E+02	121	2.3300E-01	122	1.3300E-03
131	1.0000E+02	132	1.0000E+00	134	1.0000E+00	138	1.0000E+00	140	7.0000E-01	141	7.7200E+03	142	7.7200E+03
145	1.0000E+00	146	1.0000E+03	148	-4.6626E+03	150	-2.8835E+04	152	-1.0387E+04	156	1.0000E+04	157	7.5000E-04
163	-3.2387E-01	165	6.6408E-04	167	1.9399E-03	170	1.2000E+01	171	4.0000E+00	172	6.0000E+00	201	1.0000E+01
202	5.0000E+00	203	5.0000E+00	204	1.0000E-02	205	1.0000E-02	206	1.0000E-02	207	2.0000E-02	208	2.0000E-02
209	2.0000E-02	210	2.0000E+01	211	2.0000E-01	212	2.0000E-01	213	1.0000E+01	214	5.0000E+00	215	5.0000E+00
216	1.0000E-02	217	1.0000E-02	218	1.0000E-02	221	5.0000E-02	222	5.0000E-02	223	5.0000E-02	224	5.0000E-02
231	5.0000E+00	232	5.0000E+00	233	5.0000E+00	234	1.0000E-02	235	1.0000E-02	236	1.0000E-02	256	2.0000E-01
257	-3.0000E-01	258	1.0000E-01	259	-3.0000E-01	260	-6.9810E-01	261	1.0000E+00	265	2.5000E-03	266	5.0000E-03
270	1.0470E-01	274	4.0000E+03	283	3.0000E+01	288	4.6953E+01	290	5.2360E-01	291	5.2360E-01	292	2.0000E-03
293	3.0000E+01	295	1.3369E+01	296	2.0331E+01	297	-4.0155E+01	298	4.0885E+02	299	-2.0331E+01	300	5.5637E+01
301	4.1312E+02	302	5.1510E+00	303	5.1510E+00	304	5.1510E+00	305	3.4426E-02	306	3.4426E-02	307	3.4426E-02
308	8.3905E+00	309	8.3905E+00	310	1.1187E+01	311	4.2222E+02	313	1.5481E+01	315	-1.7450E-03	317	-6.6140E-01
320	1.7301E+01	322	7.2862E+00	324	4.7374E-02	326	1.8295E+04	328	-1.3768E+00	329	-9.6593E+01	331	-2.2482E-02
331	1.0000E+00	335	1.0000E+00	339	1.0000E+00	400	1.0000E+00	404	1.0000E+00	408	1.0000E+00	409	1.0000E+00
413	1.0000E+00	417	1.0000E+00	418	1.0000E+00	422	1.0000E+00	426	1.0000E+00	427	1.0000E+00	431	1.0000E+00
435	1.0000E+00	501	-3.1350E+02	502	-3.1350E+02	506	2.3830E+01	507	-2.3830E+01	511	-3.2410E+01	512	-3.2410E+01
517	2.0000E+00	558	2.5000E-05	559	2.5000E-01	560	2.0000E+01	574	7.7200E+03	575	7.7200E+03	579	-3.1620E+02
581	-2.8559E+01	582	-2.4500E-01	583	2.5000E-01	587	5.2500E+00	588	5.2500E+00	593	9.9580E-01	594	-9.1501E-02
595	-2.5563E-01	596	9.9580E-01	597	-9.1501E-02	598	-2.5563E-01	601	-3.9470E+03	611	3.2188E+02	612	2.8559E+01
636	4.0000E+01	661	2.6708E+02	700	-3.7794E+01	703	-4.0299E+01	705	-2.5758E-01	706	6.9775E+00	709	1.0814E-01
712	1.1488E-01	716	4.0420E+04	801	2.0374E-01	802	-2.3672E+00	803	-7.0688E-01	804	2.9062E-02	805	-4.7032E-04
806	2.5988E-03	807	2.8394E-03	808	-1.4469E-02	809	2.2527E-02	810	2.9062E-02	811	1.6465E-02	812	-4.7896E-03
813	-2.4172E+00	814	-1.0560E+00	815	-1.0066E-02	816	1.0638E-04	817	-9.3021E-04	818	2.3905E-06	819	4.0532E-04
820	-1.1288E-02	821	2.9589E-01	822	1.5542E-01	823	-6.0000E-05	824	-1.6500E-04	825	2.0739E-03	826	2.0147E-03
827	-2.2647E-01	828	-9.1984E-03	829	4.0544E-05	830	-7.6677E-05	831	-1.3180E-03	832	-9.1711E-04	833	1.8600E-02
834	-2.1962E-01	835	1.5858E-04	836	5.0534E-04	837	1.2202E-04	901	7.0000E+00	902	8.0000E+00	903	9.0000E+00
904	4.2000E+01	905	4.3000E+01	906	4.4000E+01	907	3.1000E+01	908	3.2000E+01	909	3.3000E+01	910	2.0000E+00
911	3.0000E+00	912	4.0000E+00	913	1.7000E+01	914	1.8000E+01	915	1.9000E+01	916	4.5000E+01	917	4.6000E+01
918	4.7000E+01	919	3.9000E+01	920	4.0000E+01	921	4.1000E+01	922	1.3000E+01	923	1.4000E+01	924	1.5000E+01
925	1.2300E+02	926	1.2100E+02	927	1.2500E+02	928	6.4500E+02	929	1.0100E+02	930	1.0200E+02	931	1.0300E+02
932	1.0400E+02	933	1.0500E+02	934	1.0600E+02	995	2.0000E+00	996	2.0000E+00	998	1.0000E+00		

Figure 2. Typical A-Array Dump Output From ADAP 1 During Simulation

SECTION III TESTING THE AIRCRAFT SOFTWARE

Aircraft software testing consisted of the following:

- Level-flight simulation and the linear data generation
- 40-degree dive and pull-up trajectory generation (with no thrust)
- 40-degree dive trajectory generation (with 75 percent of total thrust)
- Frozen-point spectrum analysis of the linear data

LEVEL FLIGHT

First, the main program was written to generate a level flight. This was accomplished by algebraic trimming and using the trimmed data in the aircraft flying mode. During level flight, linear data was obtained as shown in Figure 3.

40-DEGREE DIVE AND PULLUP TRAJECTORY

The main program was modified to generate a 40-degree dive trajectory for the linearization. This maneuver was accomplished by a proportional-plus-derivative controller from the flight-path angle to the stabilator as shown in Figure 4, with the gain values $K_{\dot{\gamma}} = -3.0$, and $K_{\gamma} = 2$ (subroutine PILOT).

The trajectory flown with zero thrust is shown in Figure 5. With a 40-degree dive, the exact crash point on the ground is 11,918 feet versus ADAP's result of 11,940 feet. The stabilator, angle-of-attack and flight-path angle profiles during a 40-degree dive maneuver are shown in Figure 6. As shown, the maximum deviation from the nominal flight path angle is about 0.1 degree. Figure 7 shows the time variation of various elements in the linear system matrix. As can be seen, the time variations during dive are in the form of

$$A(t) = A_0 + A_1 t$$

This fact should be exploited to reduce computations in nonstationary optimization processes.

	δu_i	δv_i	δw_i	δp_i	δq_i	δr_i	$\delta \theta_i$	$\delta \phi_i$	$\delta \psi_i$	δx_{ie}	δy_{ie}	δz_{ie}							
δu_i	-.0098	0	-.04986	0	-26.717	0	-32.145	0	0	0	0	0	.000080						
δv_i	€	-.16438	€	27.437	0	-674.36	€	32.145	0	0	0	0	€						
δw_i	-.05937	0	-.8409	0	671.15	0	-1.2538	0	0	0	0	0	.00086						
δp_i	€	-.02454	€	-1.9078	€	.4686							€						
δq_i	.000347	0	-.0055	0	-7073	0		0					-631 10 ⁻⁶						
δr_i	€	.0078	€	-.06839	€	-.3414	€						€						
$\delta \theta_i$																			
$\delta \phi_i$																			
$\delta \psi_i$																			
δx_{ie}	.9992	0	.03897				.543	0	.46 10 ⁻⁶										
δy_{ie}	€	1.0	€	0			€	-26.904	676.39				0						
δz_{ie}	.03897	€	-.9992				676.39	-.29 10 ⁻⁷	0										

		$\delta(u_i)$			$\delta(v_i)$			$\delta(w_i)$											
		0	-.0279	0	-.1346	0	-.02341	0	0	0	0	0	0	0	0	0			

		$\delta(u_e)$			$\delta(v_e)$			$\delta(w_e)$											
		0	0	0	0	0	0	0	0	0	0	0	0	0	0	0			

		$\delta(u_g)$			$\delta(v_g)$			$\delta(w_g)$										
		.0098	0	-.543	0	1.908	0	-.707	0	1.908	0	-.4717	0	0	0	0		
		€	-.16438	€	-.533	0	0	0	0	0	0	0	0	0	0	0		
		.06385	0	.8409	0	.4704	0											
		€	.0245	€	1.908	0	-.4717											
		-.00034	0	-.00552	0	-.707	0											
		€	-.00784	€	.0652	0	.341											

Figure 3. Linear Data for Level Flight

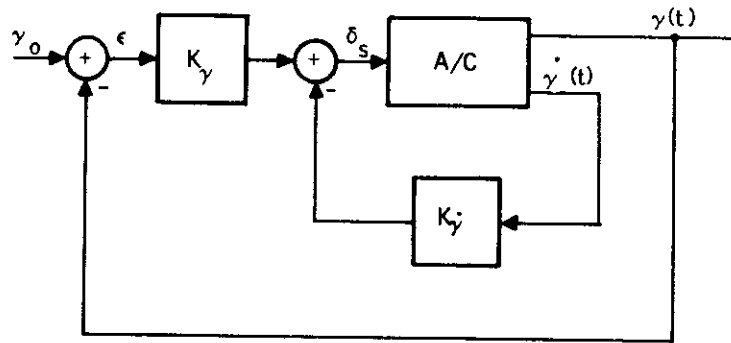


Figure 4. Flight-Path-Angle Controller for Trim

Next, the main program was modified to generate the pull-up nominal trajectory. A similar-type controller was used to obtain a constant pitch-up. The gain values were $K_{\dot{\gamma}} = -0.3$ and $K_{\gamma} = 0.2$. Figure 8 shows the flown nominal trajectory. Figure 9 shows the nominal flight-path angle flown. Figures 10 and 11 show respectively the nominal elevator profile and linear data for the pitching moment coefficient of the stabilator. Results can be refined further. For the purpose of linearization they were found to be satisfactory.

The 40-degree dive trajectory which has been obtained by using no thrust as discussed above, was modified by introducing 75 percent of the full thrust (i. e., 2×7720 pounds) into the program. The initial speed of the airplane was also modified from 400 knots down to 250 knots. Evidently this flight condition is very close to what a pilot does during dive bombing.

The flight-path angle was maintained within ± 1 degree using the stabilator profile with two line segments.

The nonlinear dive trajectory was flown, and the linear data were generated and plotted against time as shown in Figures 12 through 48.

The majority of the time-varying data can be represented by straight lines. Some of the linear data (with smaller relative magnitudes) show rapid changes as functions of time. These can be attributed to two sources: (a) approximate trim profile and initial conditions and (b) straight-line approximation in the nonlinear aerodynamic data.

Smoother data can be obtained by using a better stabilator profile and a higher-order approximation to aerodynamic table functions. These are refinements, however.

The program listing for the plotting data is given in Figure 49. This is followed by typical trajectory input data in Figure 50. The plots of important trajectory variables are shown in Figures 51 through 59.

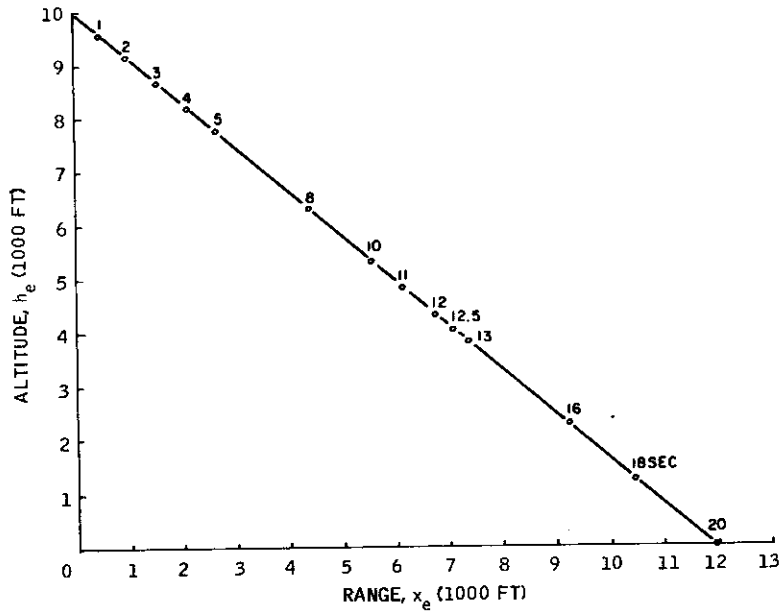


Figure 5. Zero-Thrust, 40-degree Dive Trajectory

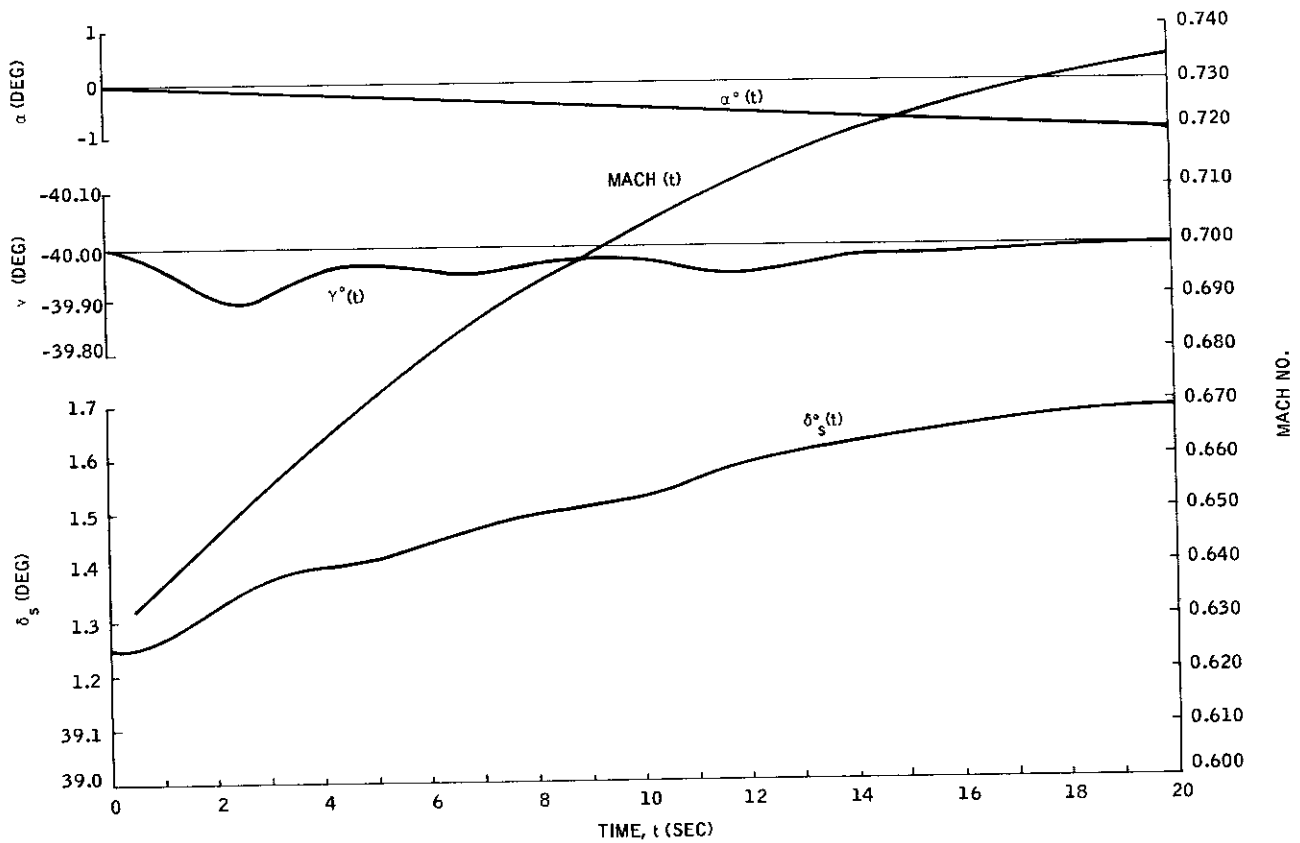


Figure 6. Stabilator, Angle-of-Attack and Flight-Path-Angle Profiles During Dive

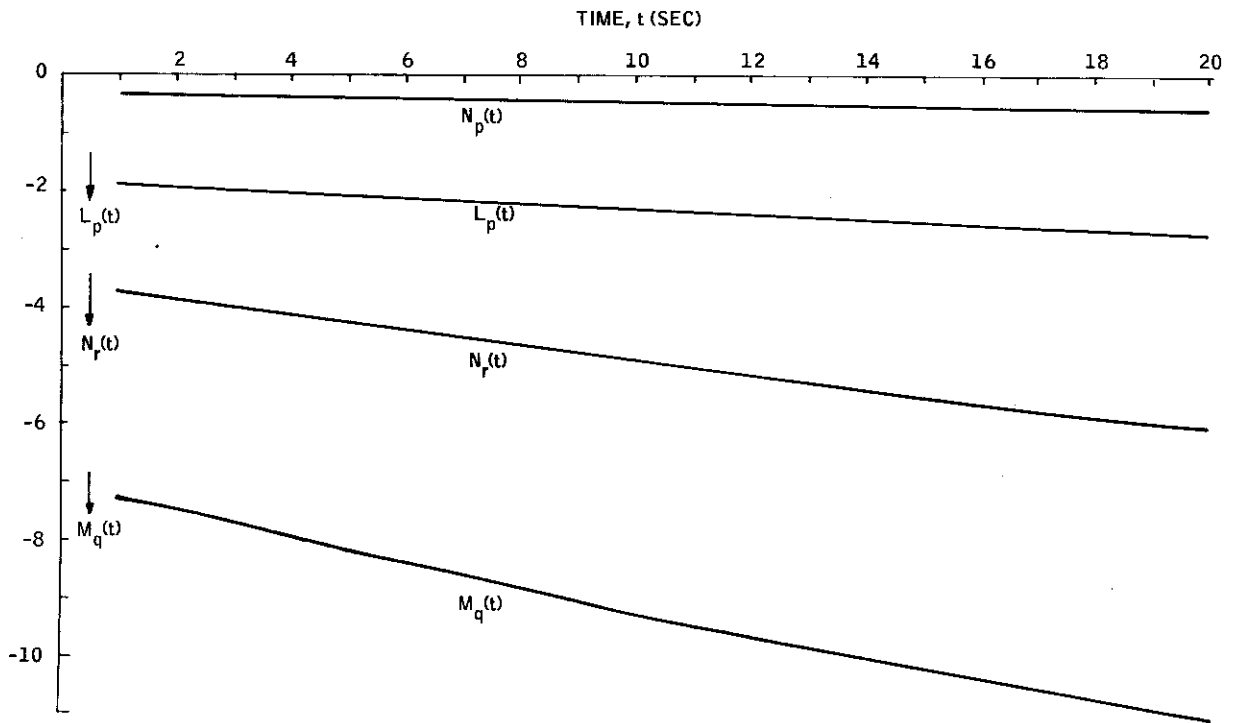
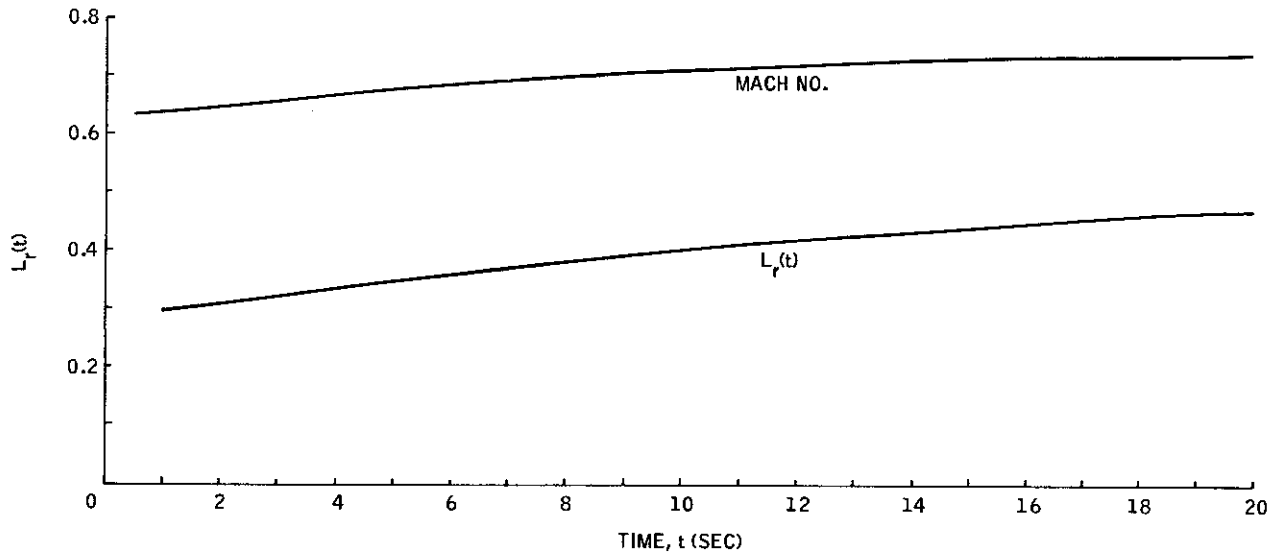


Figure 7. Linear Data for 40-degree Dive

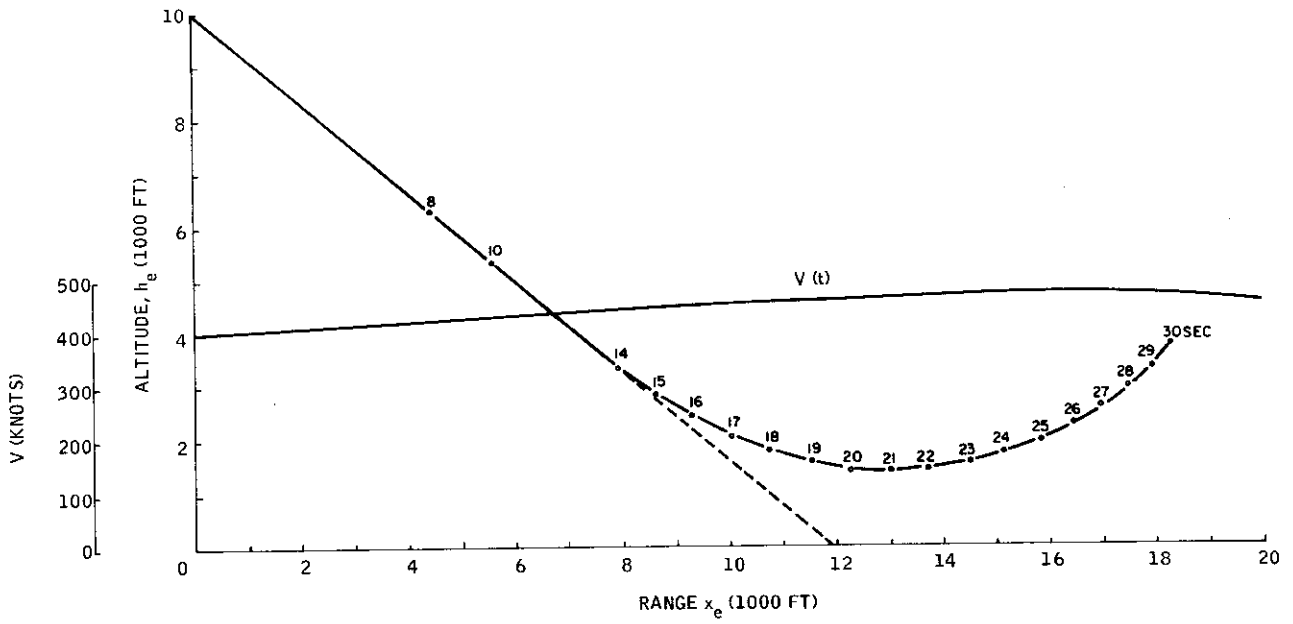


Figure 8. Dive and Pullup Trajectory

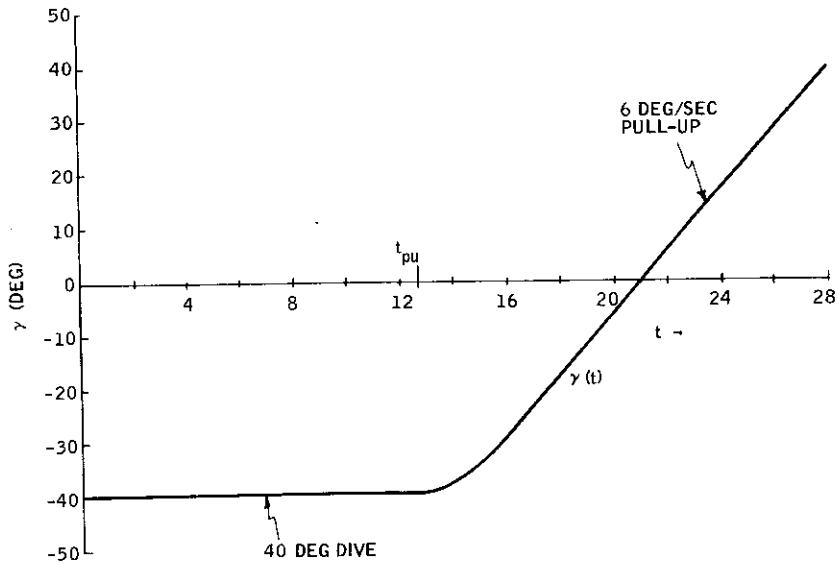


Figure 9. Flight-Path Angle versus Time in Dive and Pullup

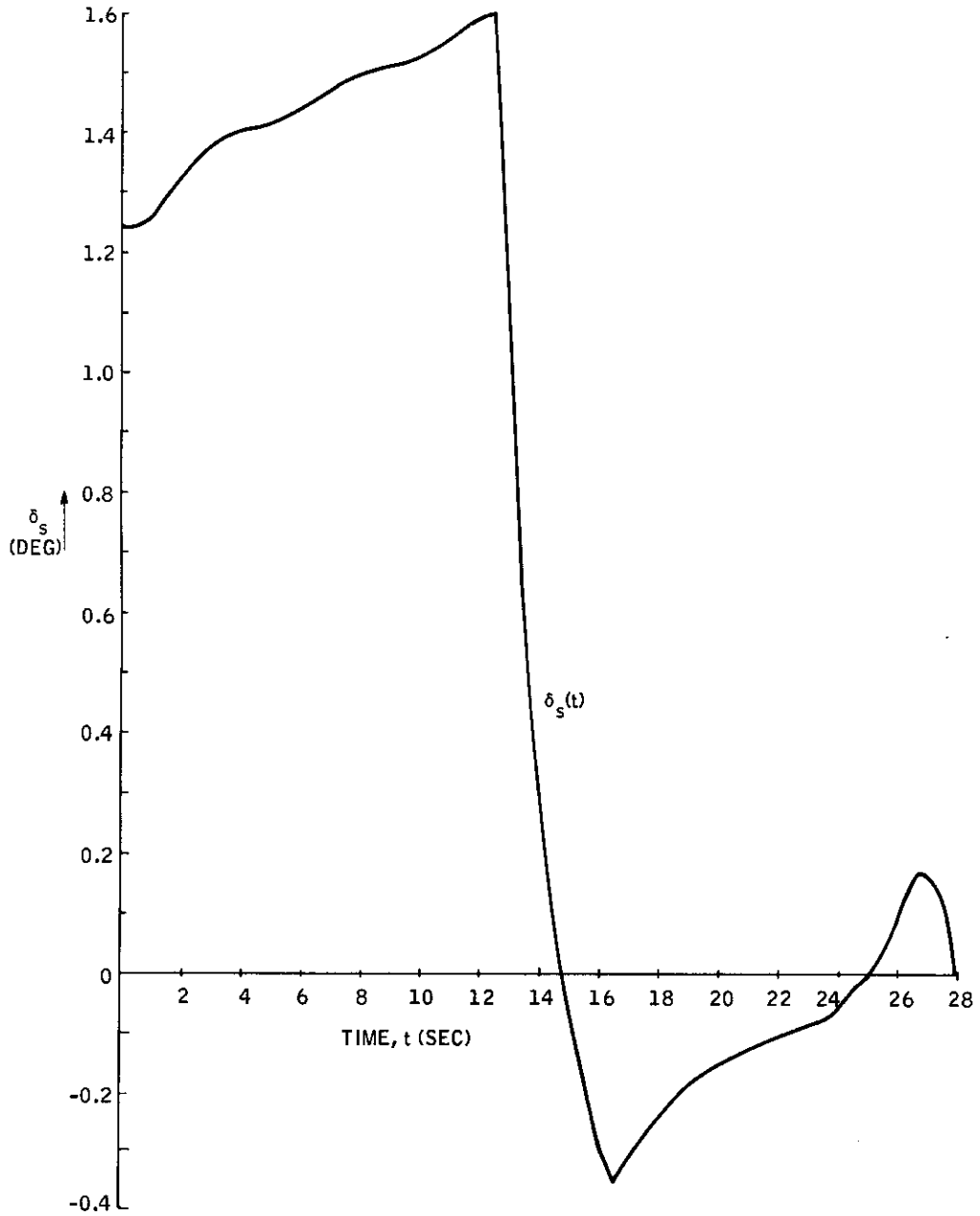


Figure 10. Stabilator Profile During Dive and Pull-up Maneuver Trim

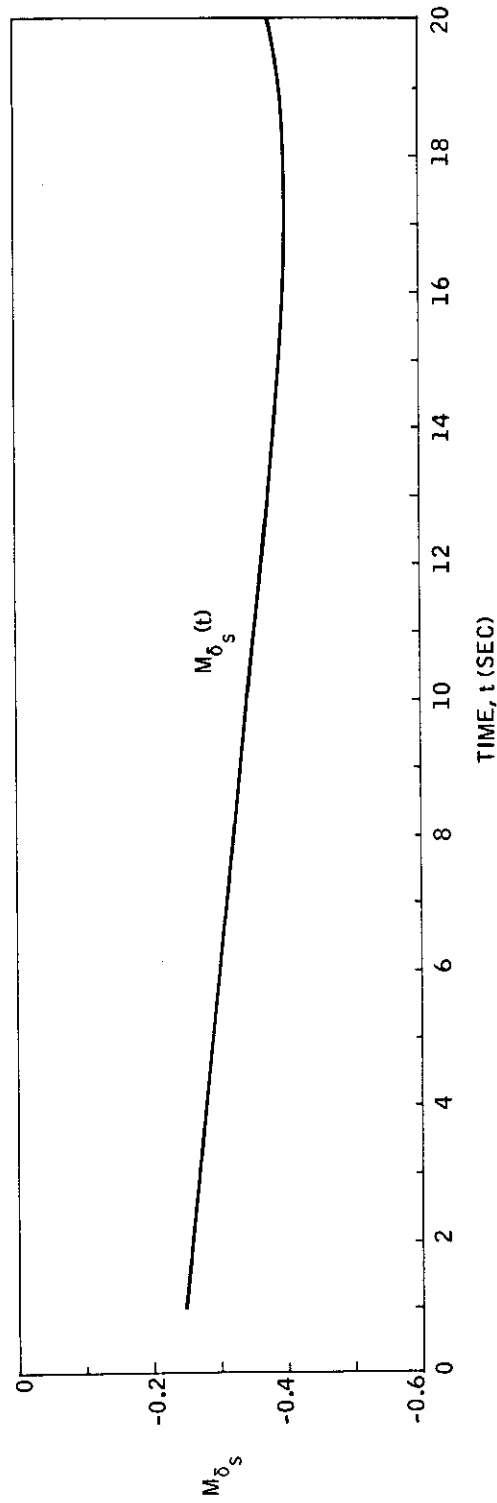


Figure 11. Pitching Moment Coefficient of the Stabilator Along the Nominal Path

\dot{x}_e	\dot{h}_c	\dot{u}	$\dot{\theta}$	\dot{q}	\dot{w}	\dot{y}_e	$\dot{\psi}$	\dot{r}	\dot{v}	$\dot{\phi}$	\dot{p}	\dot{w}_1	\dot{w}_3	\dot{w}_5	\dot{w}_2	\dot{w}_4
0	0	0	0	0	0	0	0	0	0	0	0	0	0	0	0	0
X_{eu}	$X_{ce\theta}$	X_{ew}	0	X_{eu}	X_{ew}	X_{eu}	X_{ew}	X_{uq}	X_{wq}	X_{uq}	X_{wq}	X_{uq}	X_{wq}	X_{uq}	X_{wq}	X_{uq}
H_{eu}	$H_{e\theta}$	H_{ew}	0	H_{eu}	H_{ew}	H_{eu}	H_{ew}	H_{uq}	H_{wq}	H_{uq}	H_{wq}	H_{uq}	H_{wq}	H_{uq}	H_{wq}	H_{uq}
M_{eu}	$M_{e\theta}$	M_{ew}	0	M_{eu}	M_{ew}	M_{eu}	M_{ew}	M_{uq}	M_{wq}	M_{uq}	M_{wq}	M_{uq}	M_{wq}	M_{uq}	M_{wq}	M_{uq}
Z_{eu}	$Z_{e\theta}$	Z_{ew}	0	Z_{eu}	Z_{ew}	Z_{eu}	Z_{ew}	Z_{uq}	Z_{wq}	Z_{uq}	Z_{wq}	Z_{uq}	Z_{wq}	Z_{uq}	Z_{wq}	Z_{uq}
0	0	0	0	0	0	0	0	0	0	0	0	0	0	0	0	0
$Y_{e\psi}$	$Y_{e\phi}$	$Y_{e\theta}$	$Y_{e\psi}$	$Y_{e\phi}$	$Y_{e\theta}$	$Y_{e\psi}$	$Y_{e\phi}$	$Y_{e\theta}$	$Y_{e\psi}$	$Y_{e\phi}$	$Y_{e\theta}$	$Y_{e\psi}$	$Y_{e\phi}$	$Y_{e\theta}$	$Y_{e\psi}$	$Y_{e\phi}$
0	0	0	0	0	0	0	0	0	0	0	0	0	0	0	0	0
$N_{e\psi}$	$N_{e\phi}$	$N_{e\theta}$	$N_{e\psi}$	$N_{e\phi}$	$N_{e\theta}$	$N_{e\psi}$	$N_{e\phi}$	$N_{e\theta}$	$N_{e\psi}$	$N_{e\phi}$	$N_{e\theta}$	$N_{e\psi}$	$N_{e\phi}$	$N_{e\theta}$	$N_{e\psi}$	$N_{e\phi}$
0	0	0	0	0	0	0	0	0	0	0	0	0	0	0	0	0
$L_{e\psi}$	$L_{e\phi}$	$L_{e\theta}$	$L_{e\psi}$	$L_{e\phi}$	$L_{e\theta}$	$L_{e\psi}$	$L_{e\phi}$	$L_{e\theta}$	$L_{e\psi}$	$L_{e\phi}$	$L_{e\theta}$	$L_{e\psi}$	$L_{e\phi}$	$L_{e\theta}$	$L_{e\psi}$	$L_{e\phi}$
0	0	0	0	0	0	0	0	0	0	0	0	0	0	0	0	0
a_u	a_ψ	a_r	a_v	a_ϕ	a_p	a_u	a_ψ	a_r	a_v	a_ϕ	a_p	a_u	a_ψ	a_r	a_v	a_ϕ
0	0	0	0	0	0	0	0	0	0	0	0	0	0	0	0	0
a_{2w}	a_{1w}	a_{2w}	a_{1w}	a_{2w}	a_{1w}	a_{2w}	a_{1w}	a_{2w}	a_{1w}	a_{2w}	a_{1w}	a_{2w}	a_{1w}	a_{2w}	a_{1w}	a_{2w}
0	0	0	0	0	0	0	0	0	0	0	0	0	0	0	0	0
a_{2v}	a_{1v}	a_{2v}	a_{1v}	a_{2v}	a_{1v}	a_{2v}	a_{1v}	a_{2v}	a_{1v}	a_{2v}	a_{1v}	a_{2v}	a_{1v}	a_{2v}	a_{1v}	a_{2v}
0	0	0	0	0	0	0	0	0	0	0	0	0	0	0	0	0
b_u	b_ψ	b_r	b_v	b_ϕ	b_p	b_u	b_ψ	b_r	b_v	b_ϕ	b_p	b_u	b_ψ	b_r	b_v	b_ϕ
0	0	0	0	0	0	0	0	0	0	0	0	0	0	0	0	0
b_{2w}	b_{1w}	b_{2w}	b_{1w}	b_{2w}	b_{1w}	b_{2w}	b_{1w}	b_{2w}	b_{1w}	b_{2w}	b_{1w}	b_{2w}	b_{1w}	b_{2w}	b_{1w}	b_{2w}
0	0	0	0	0	0	0	0	0	0	0	0	0	0	0	0	0
b_{2v}	b_{1v}	b_{2v}	b_{1v}	b_{2v}	b_{1v}	b_{2v}	b_{1v}	b_{2v}	b_{1v}	b_{2v}	b_{1v}	b_{2v}	b_{1v}	b_{2v}	b_{1v}	b_{2v}
0	0	0	0	0	0	0	0	0	0	0	0	0	0	0	0	0

$$\dot{x} = Fx + G_1 u + G_2 \bar{v} + G_3 \bar{w}, \quad G_2 = G_3$$

Figure 12. Augmented Aircraft and Reduced-Wind Dynamics

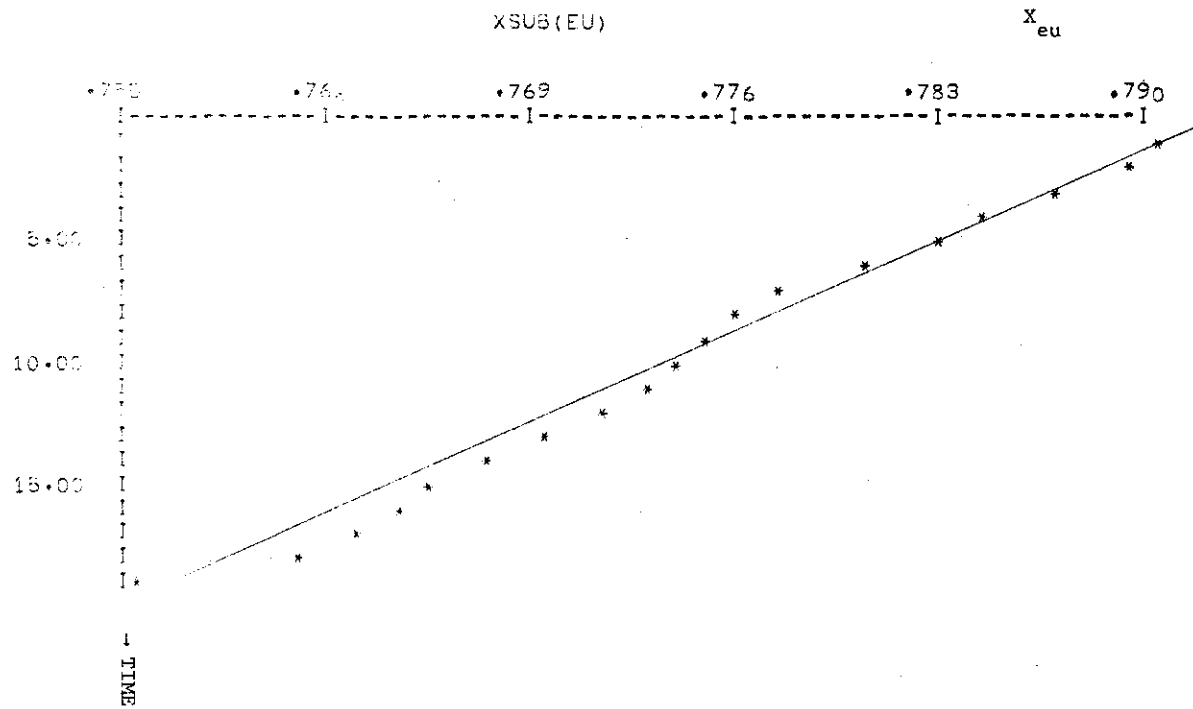


Figure 13. X_{eu} versus Time

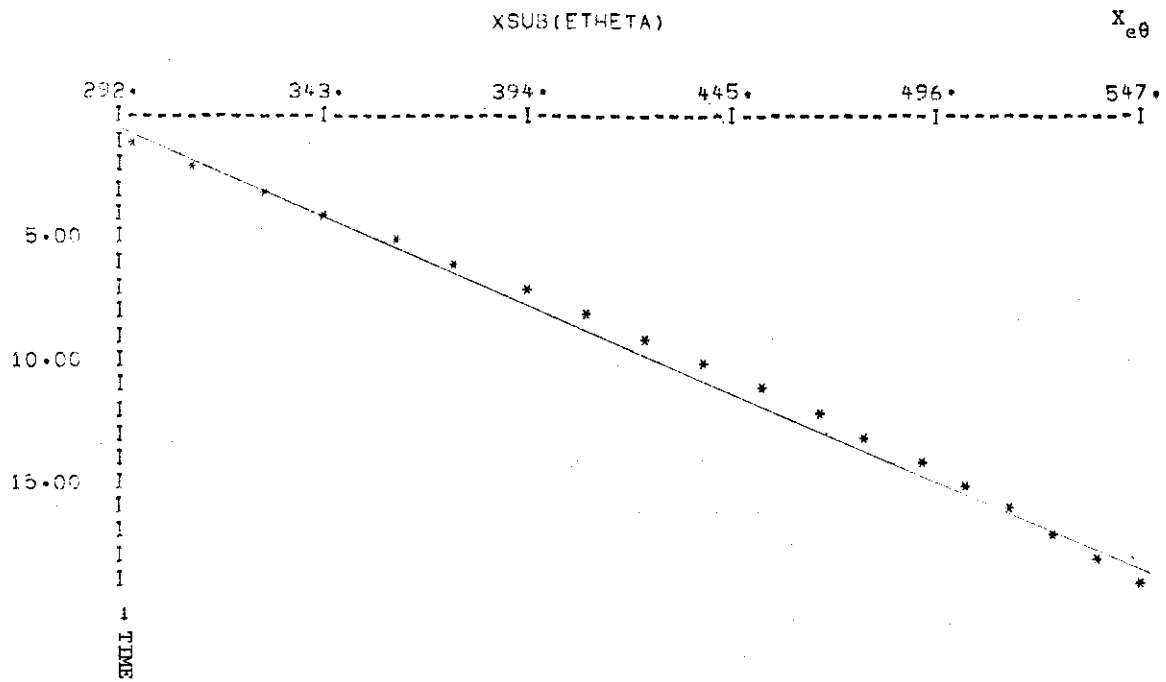


Figure 14. $X_{e\theta}$ versus Time

Contrails

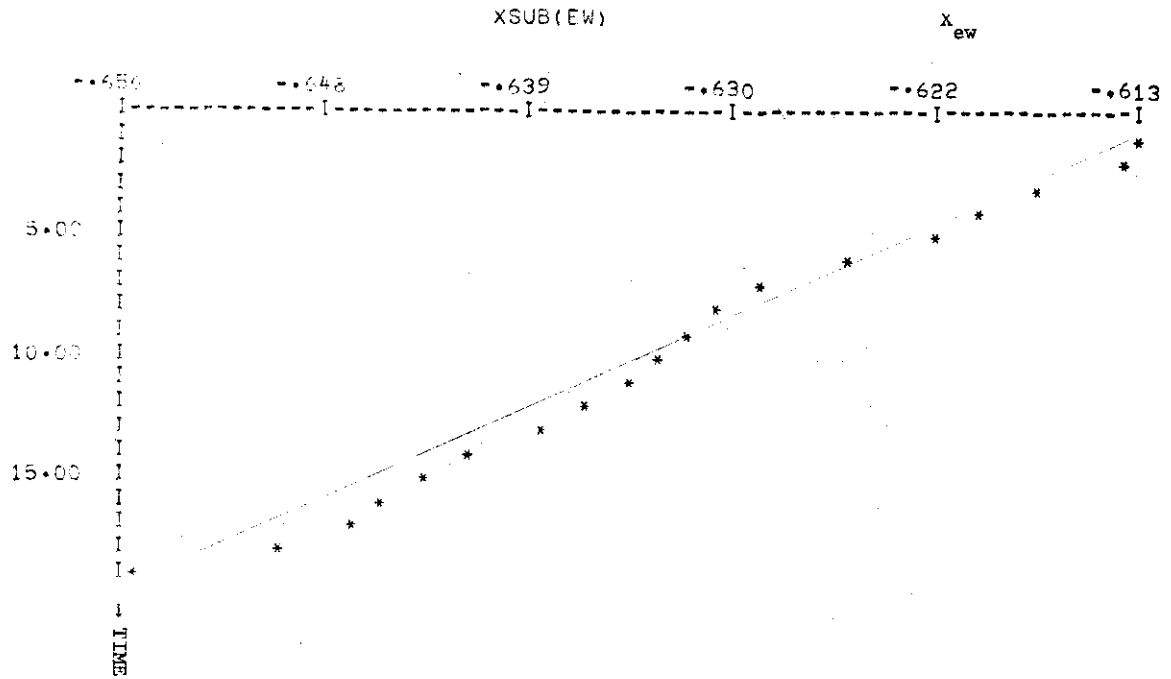


Figure 15. X_{ew} versus Time

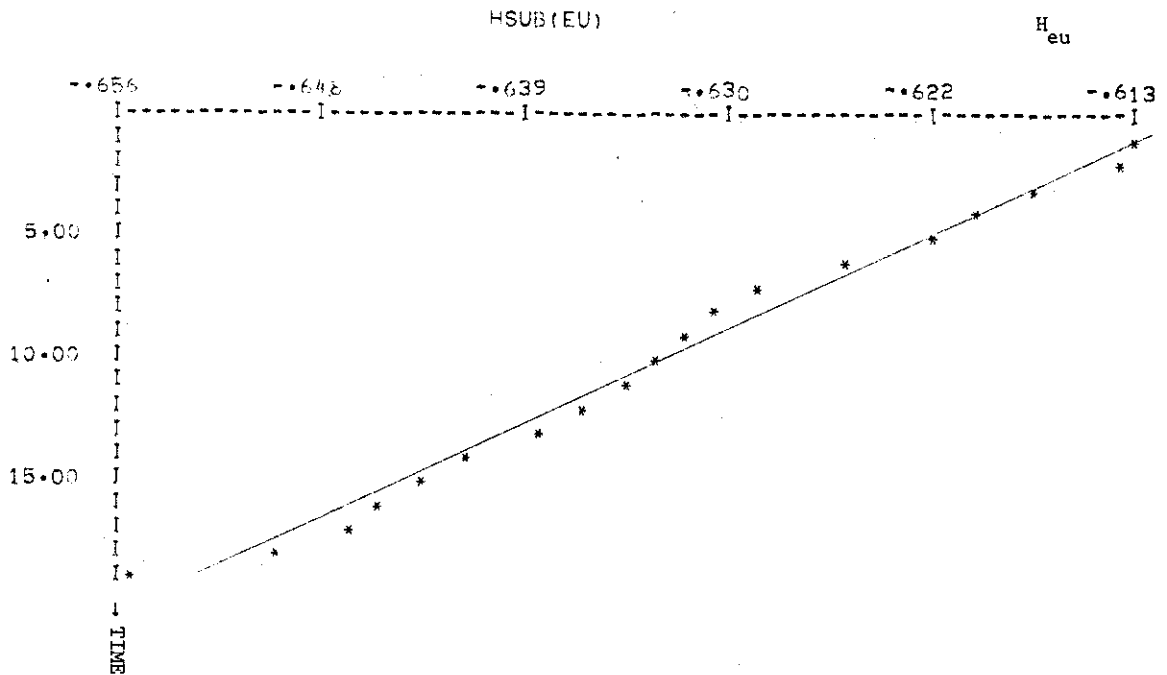


Figure 16. H_{eu} versus Time

Contrails

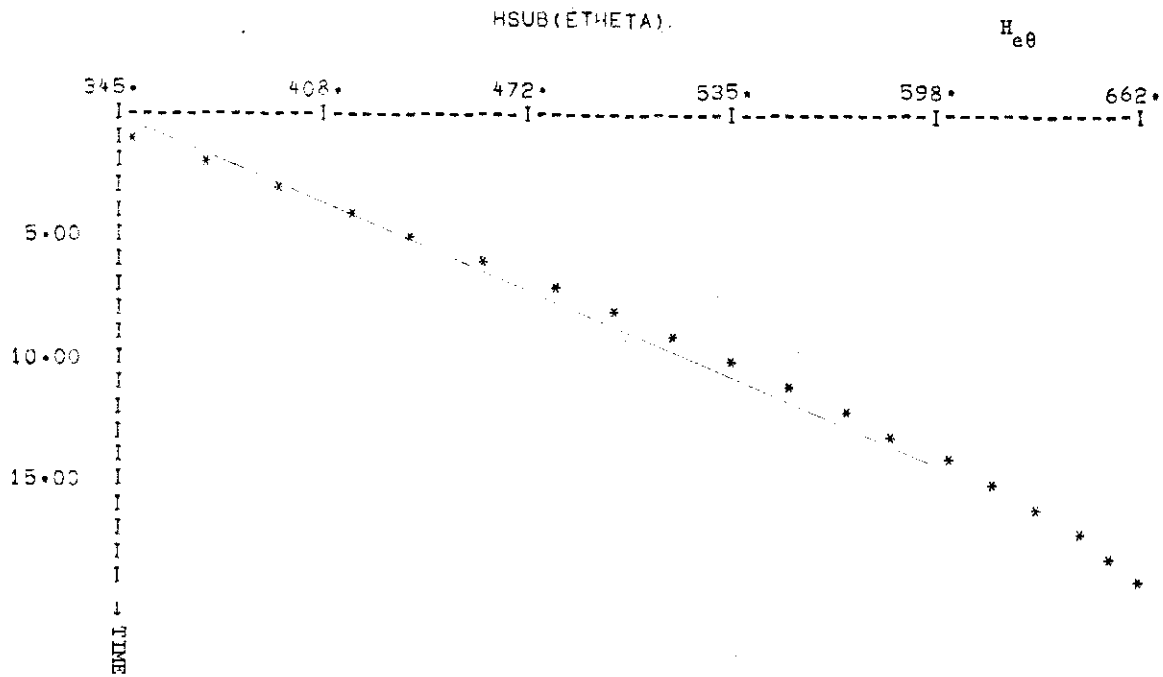


Figure 17. $H_{e\theta}$ versus Time

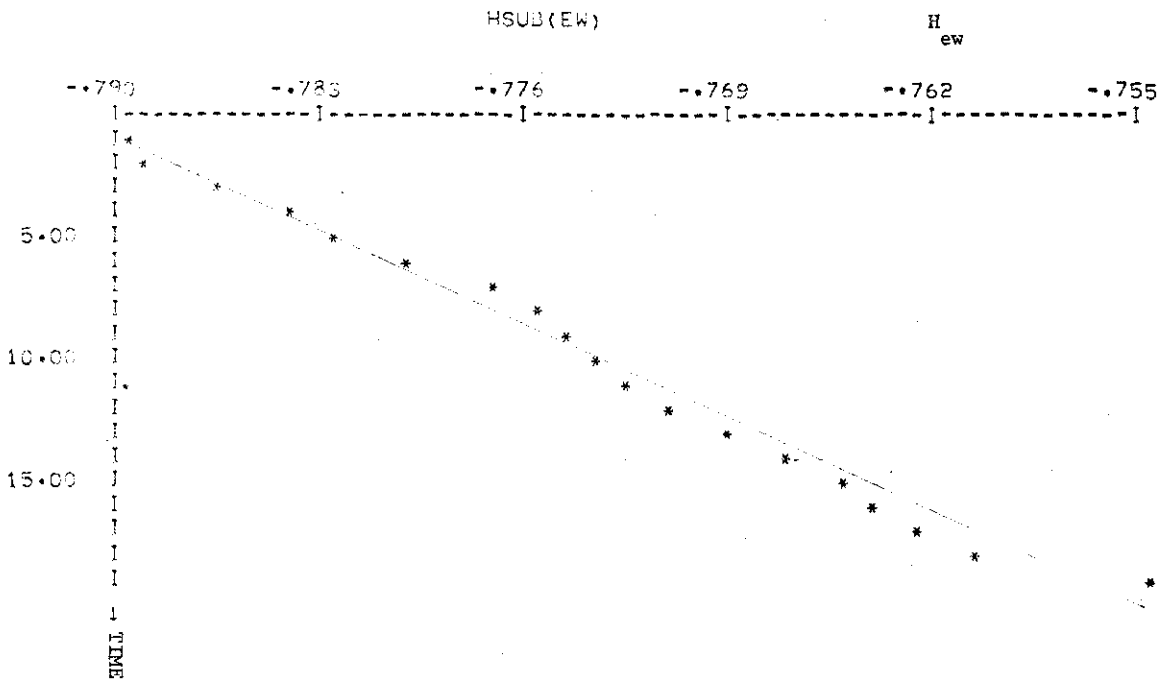


Figure 18. H_{ew} versus Time

Contrails

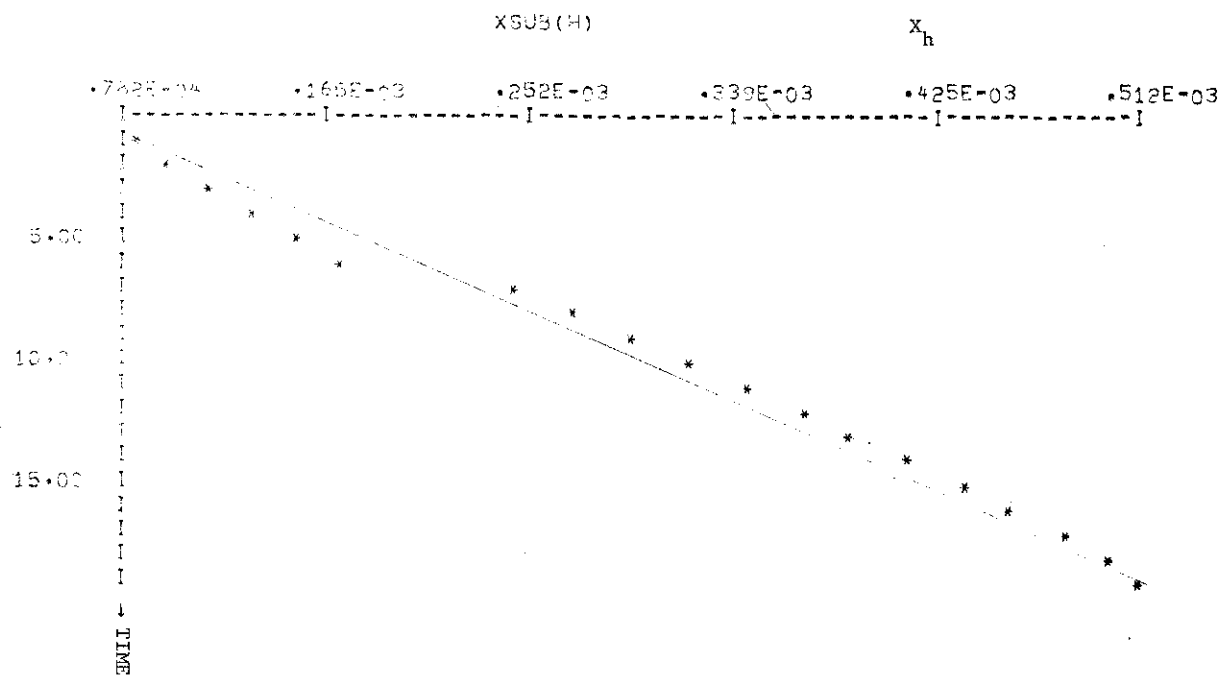


Figure 19. X_h versus Time

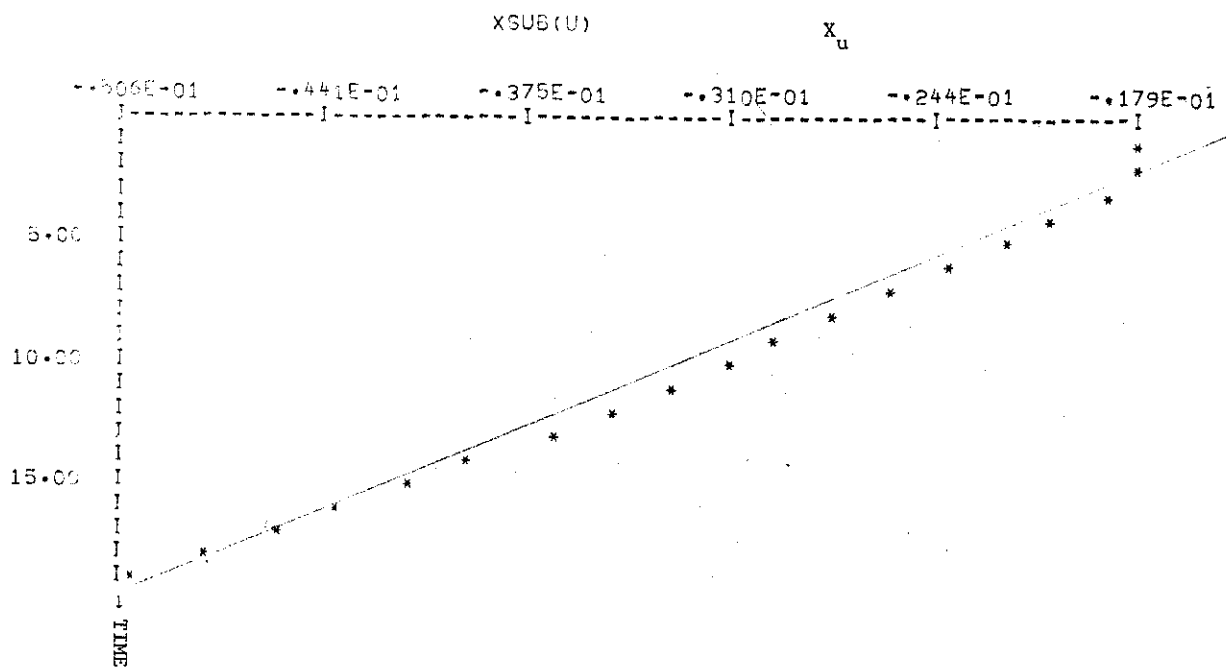


Figure 20. X_u versus Time

Contrails

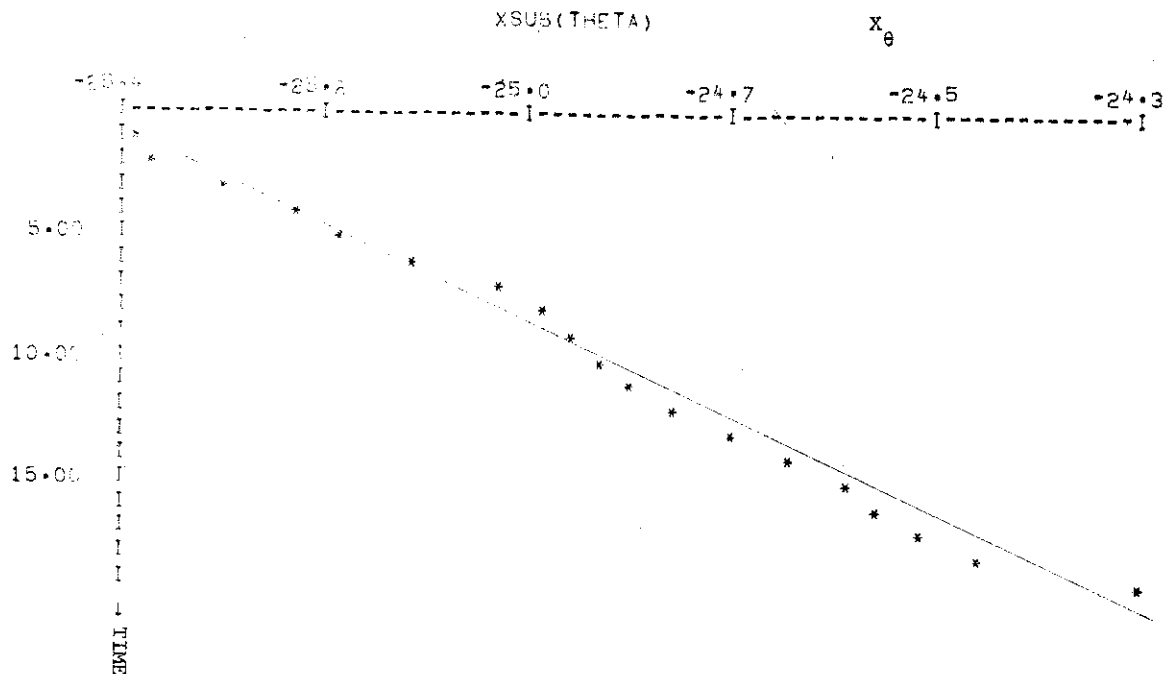


Figure 21. X_{θ} versus Time

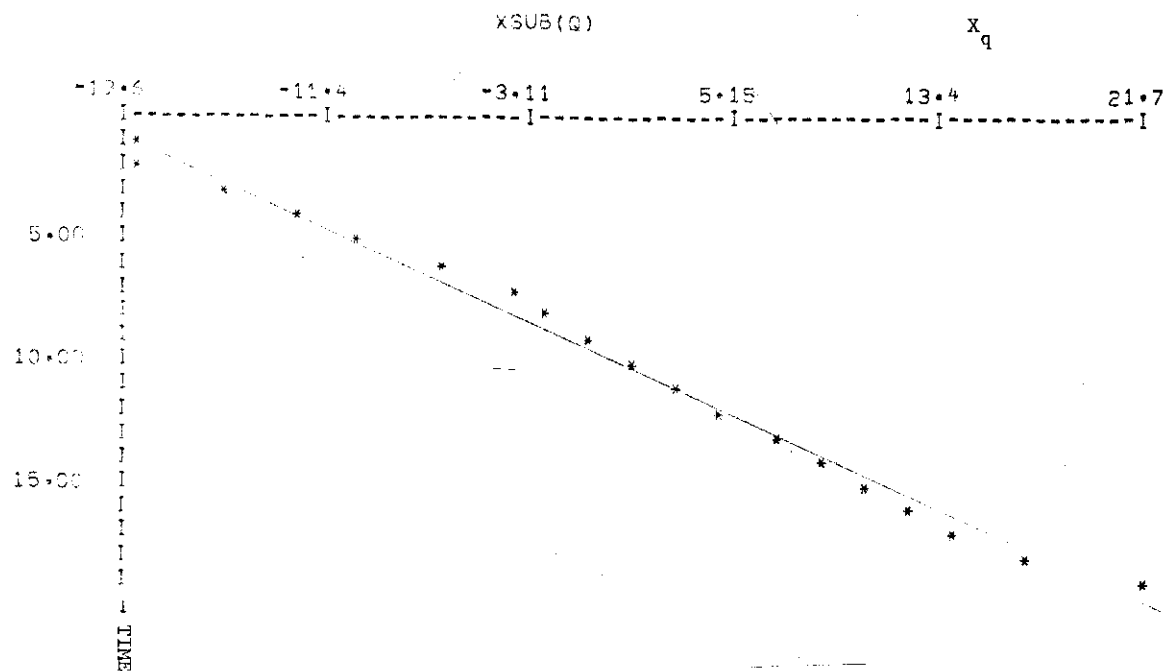


Figure 22. X_q versus Time

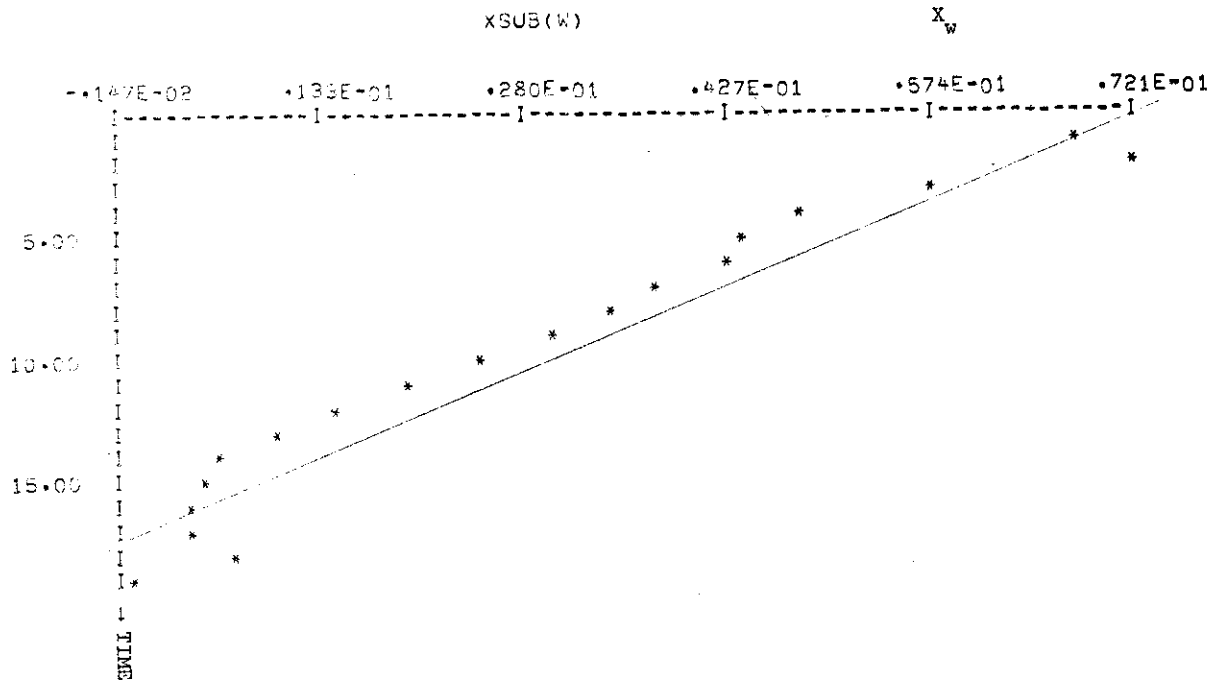


Figure 23. X_w versus Time

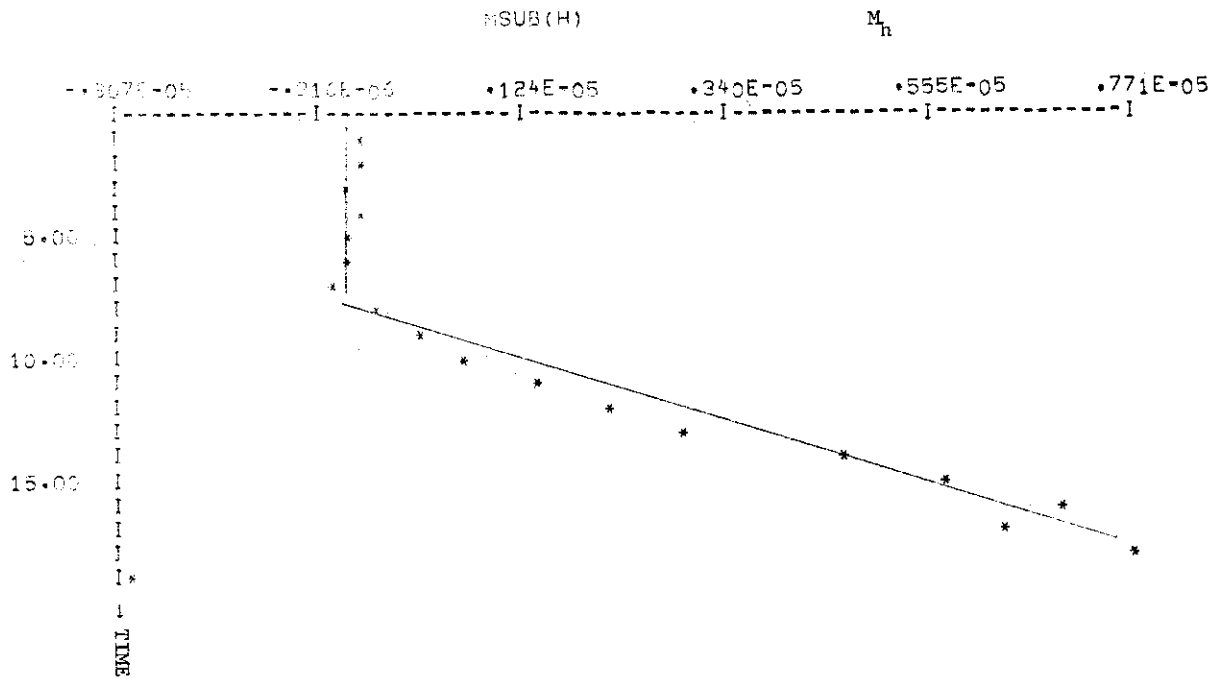


Figure 24. M_h versus Time

Contrails

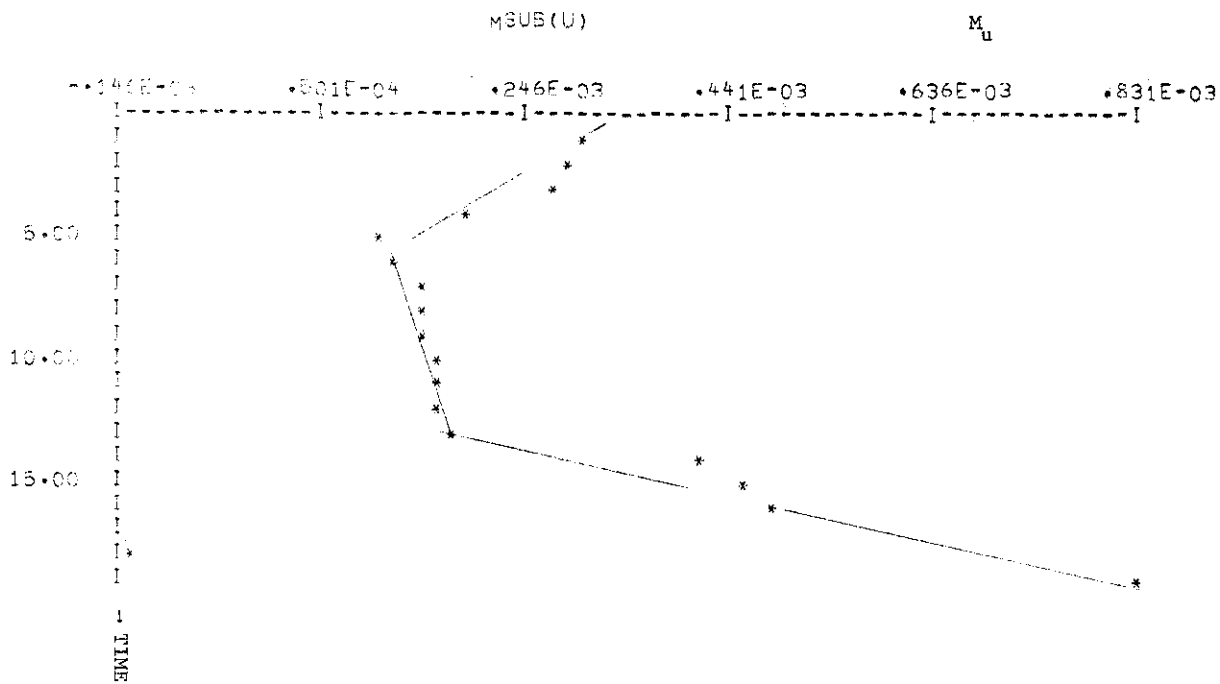


Figure 25. M_u versus Time

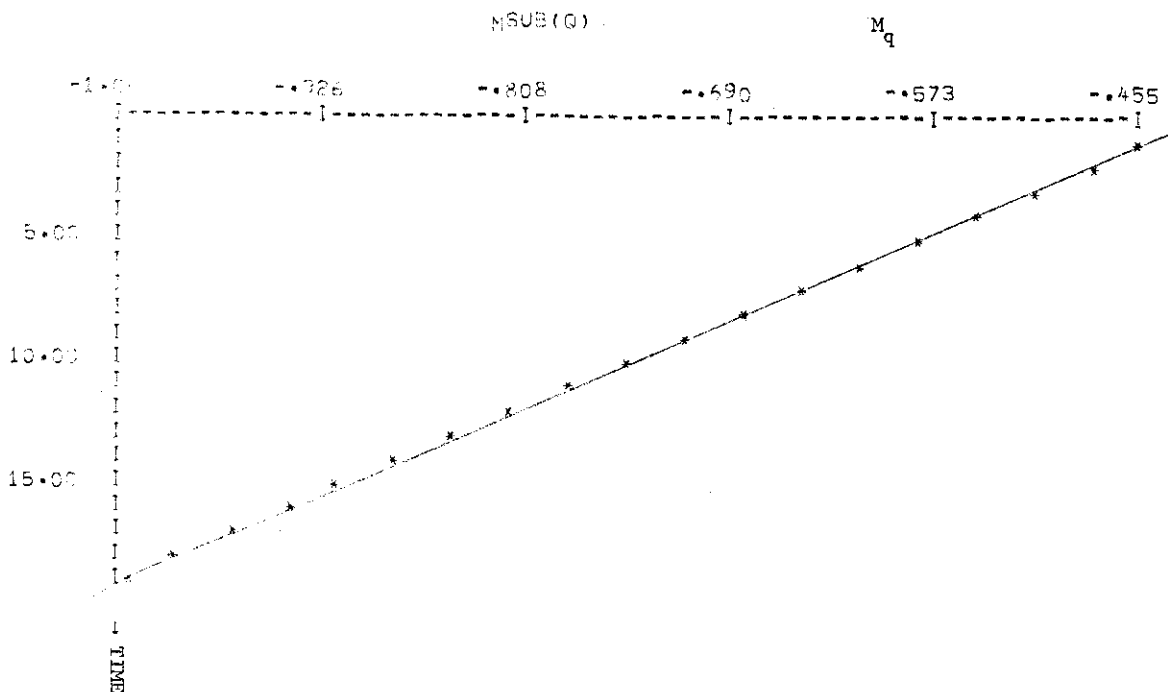


Figure 26. M_q versus Time

Contrails

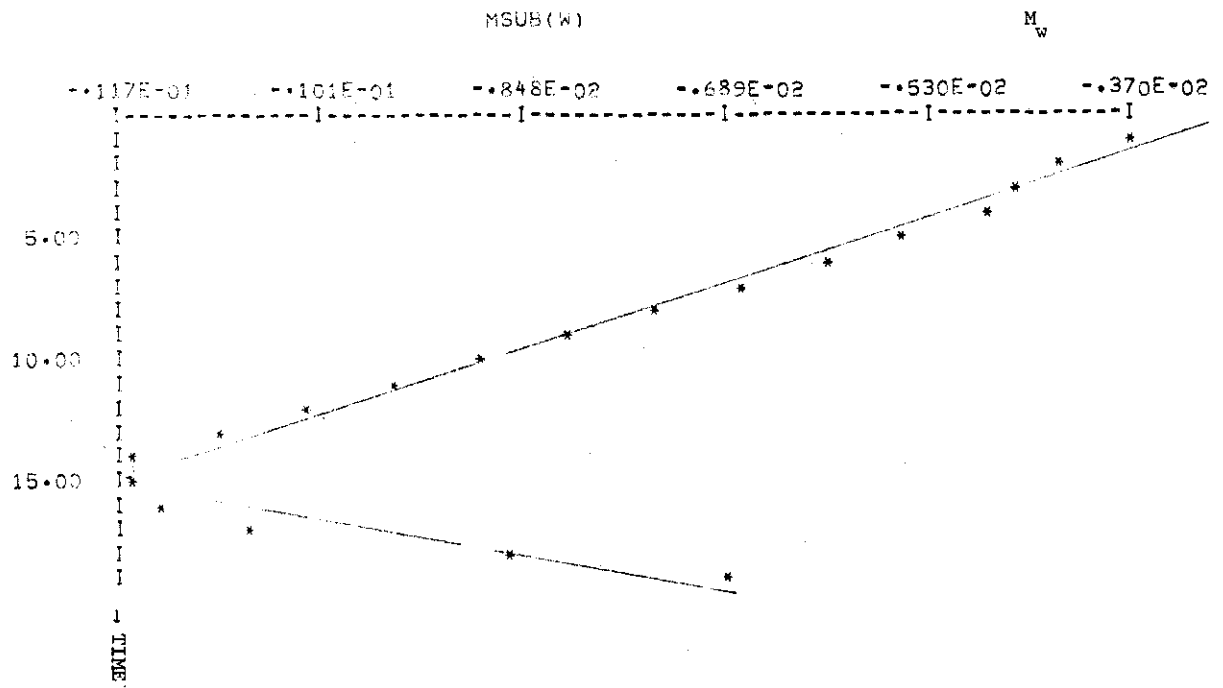


Figure 27. M_w versus Time

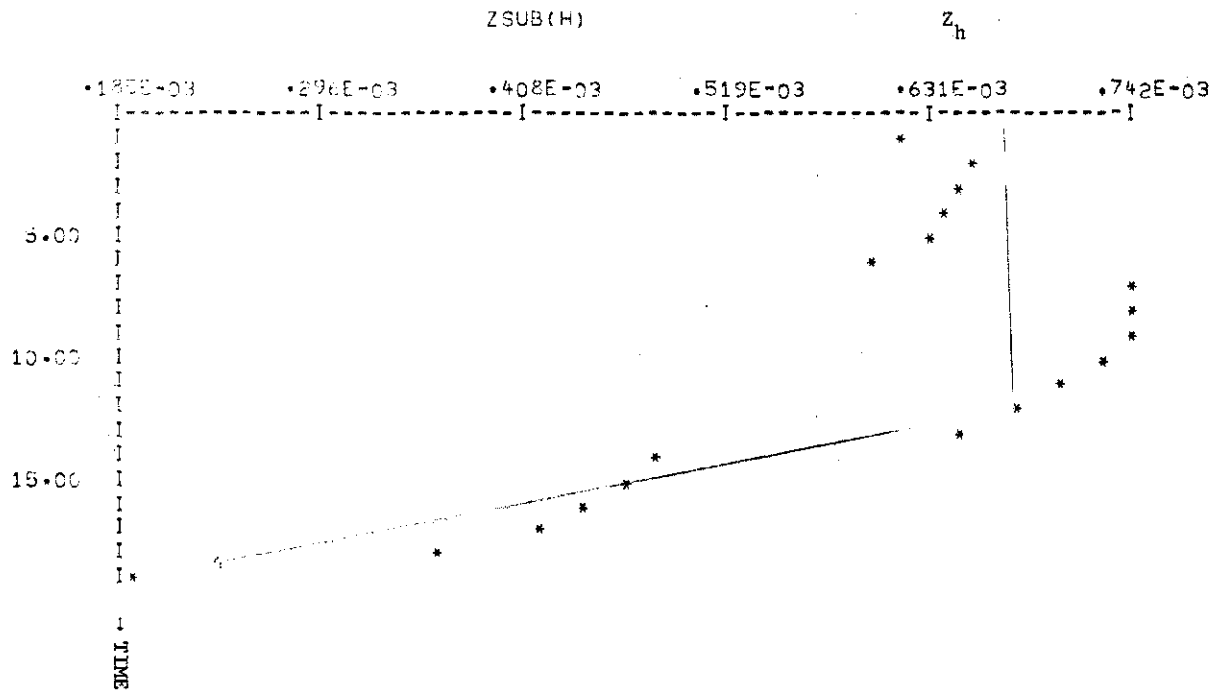


Figure 28. Z_h versus Time

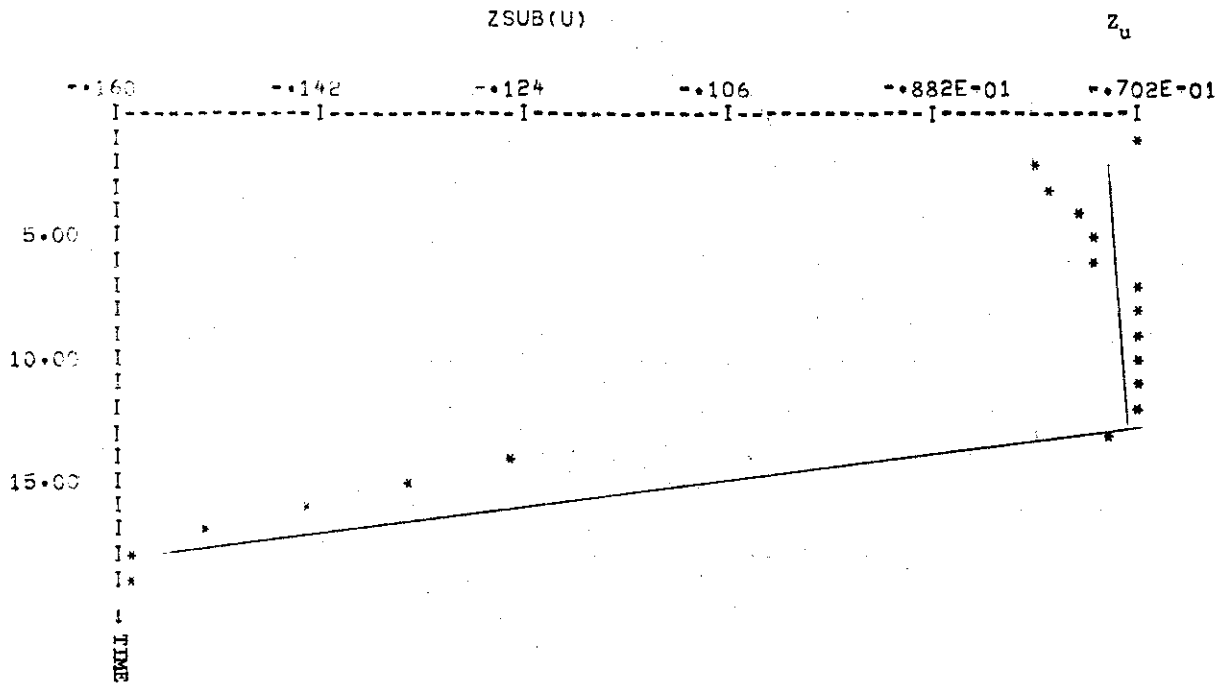


Figure 29. Z_u versus Time

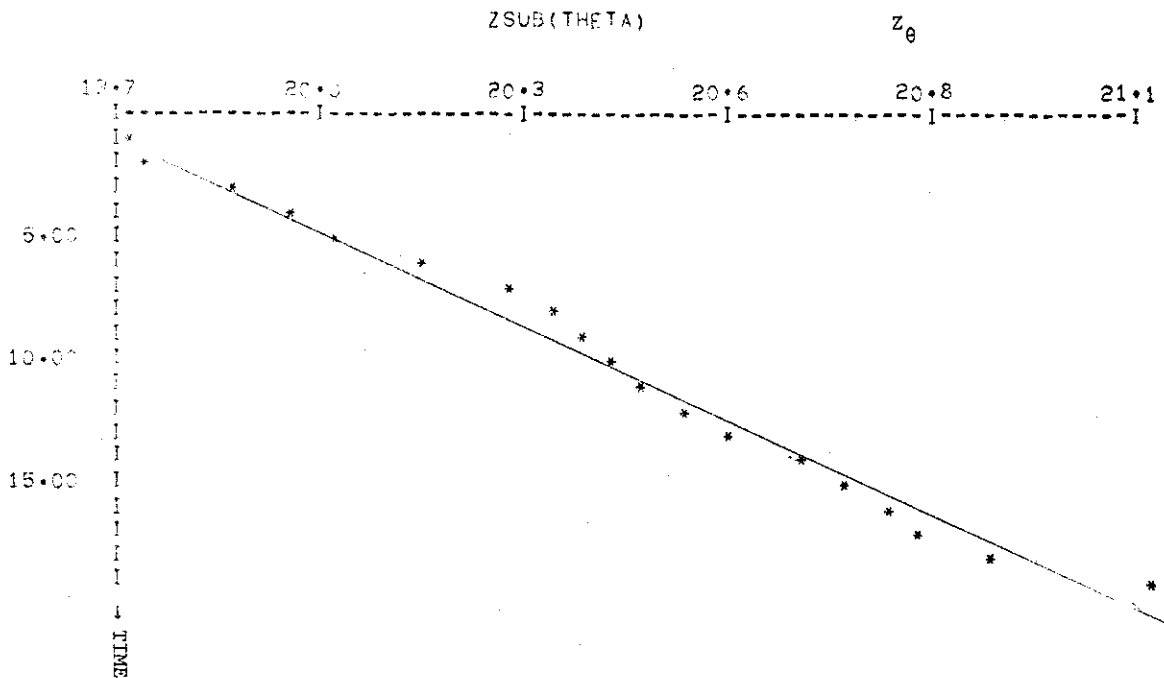


Figure 30. Z_θ versus Time

Contrails

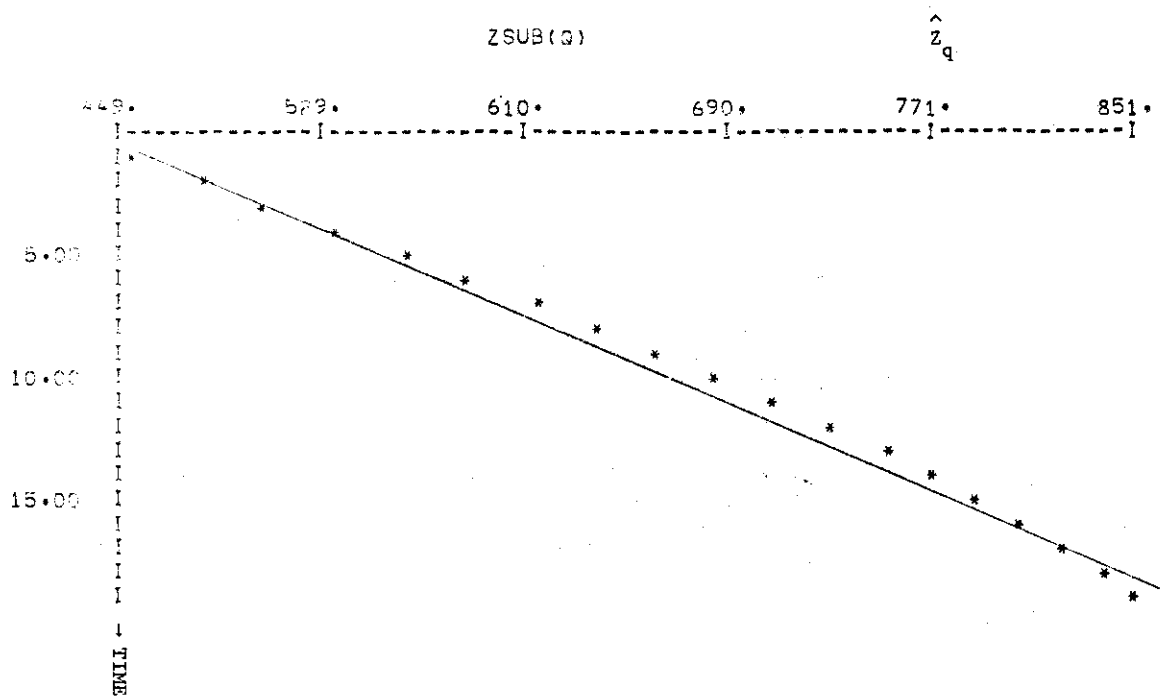


Figure 31. \hat{Z}_q versus Time

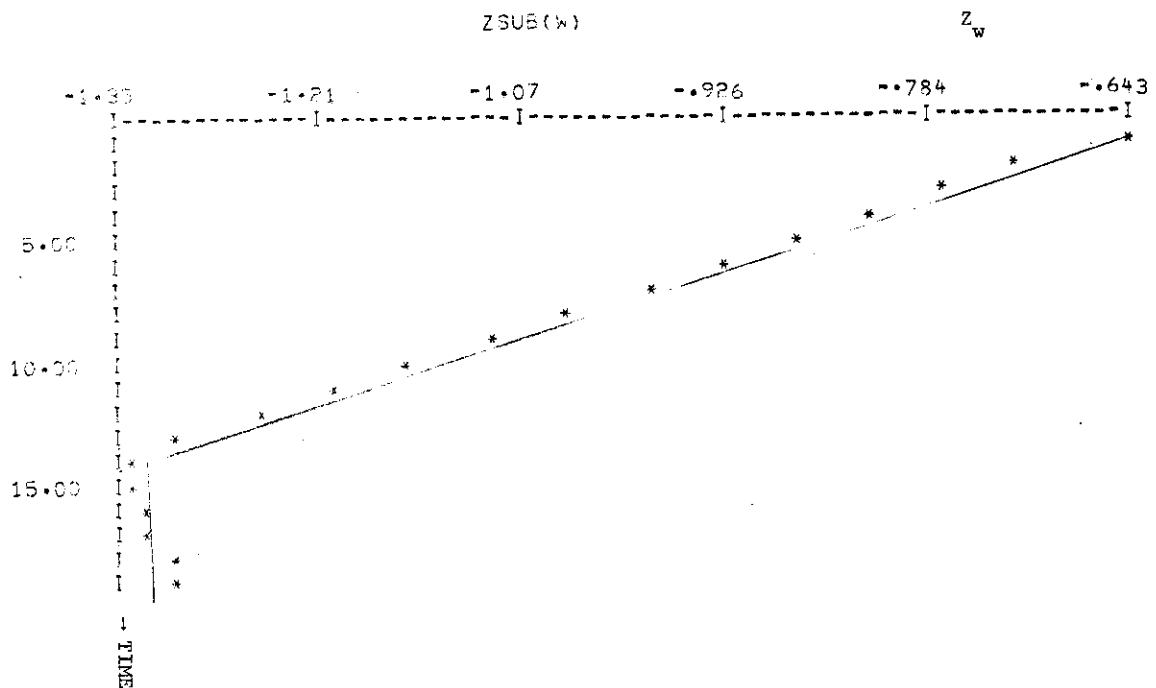


Figure 32. Z_w versus Time

Contrails

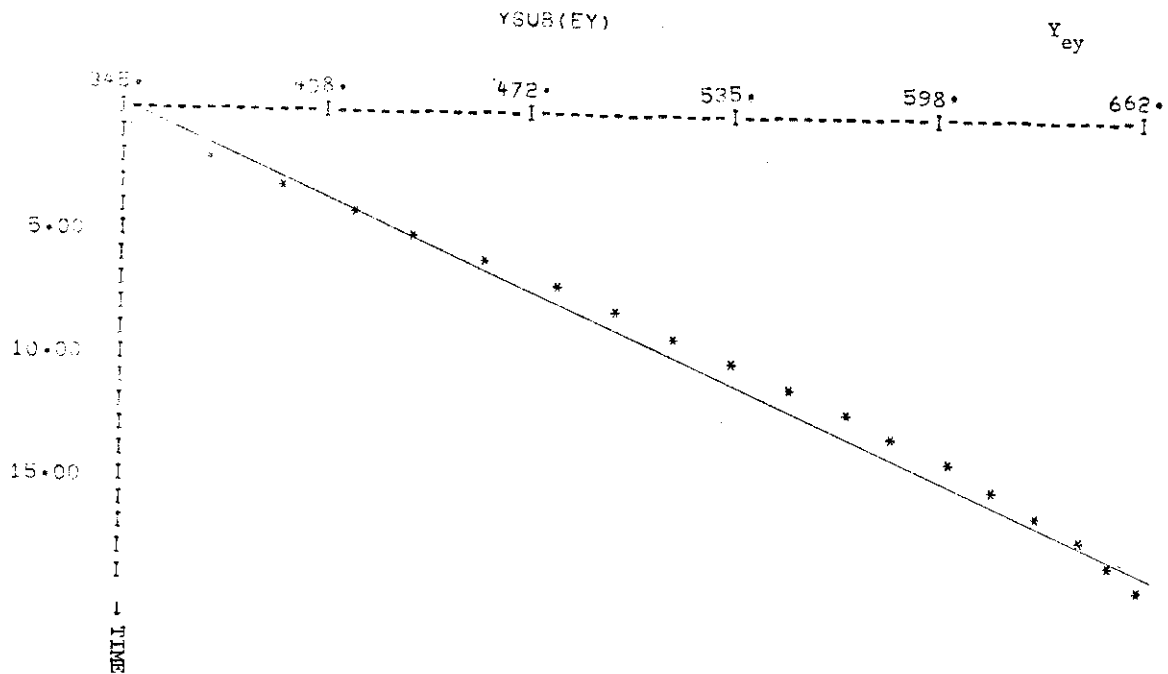


Figure 33. Y_{ey} versus Time

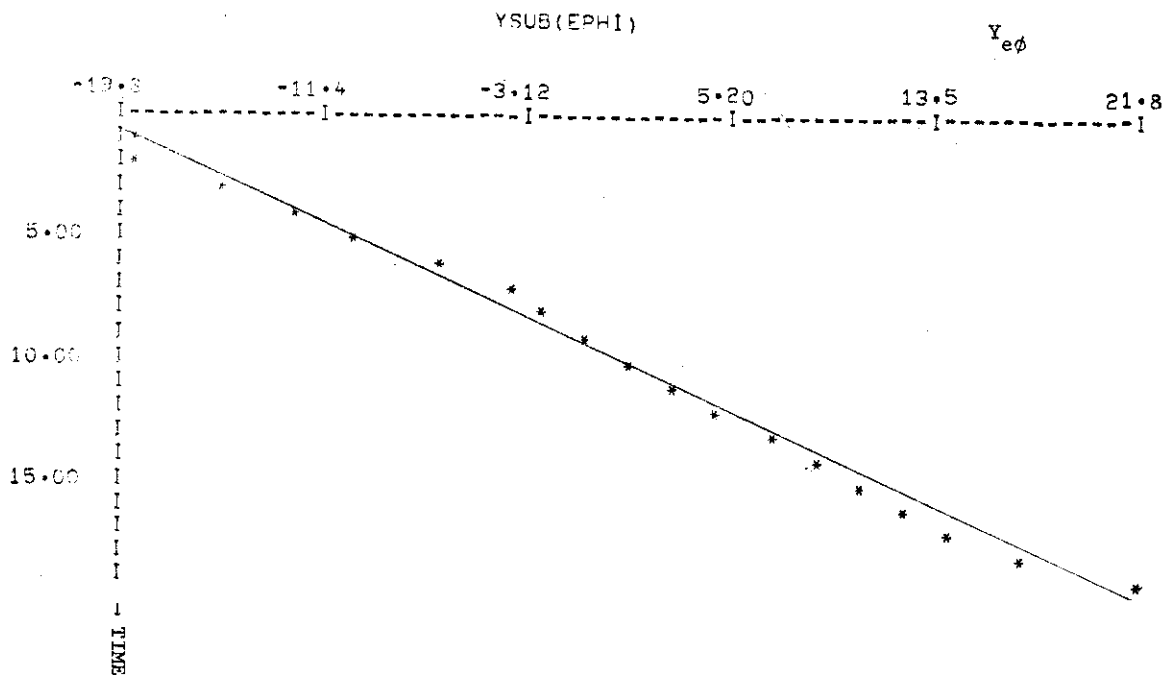


Figure 34. $Y_{e\phi}$ versus Time

Contrails

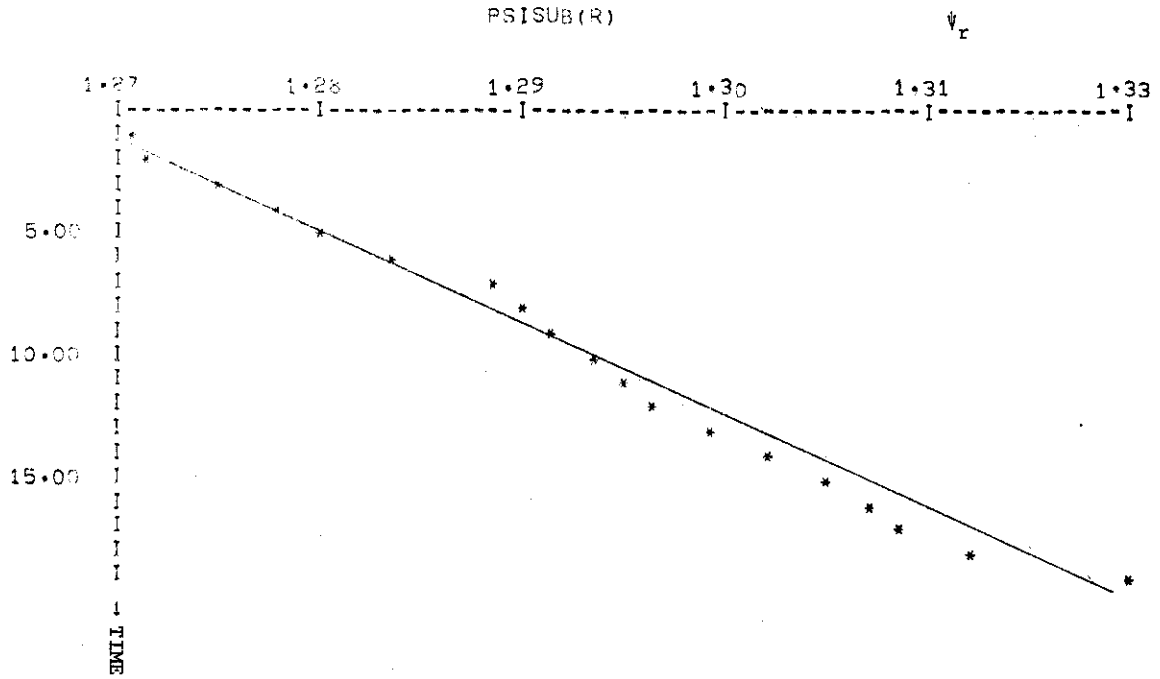


Figure 35. ψ_r versus Time

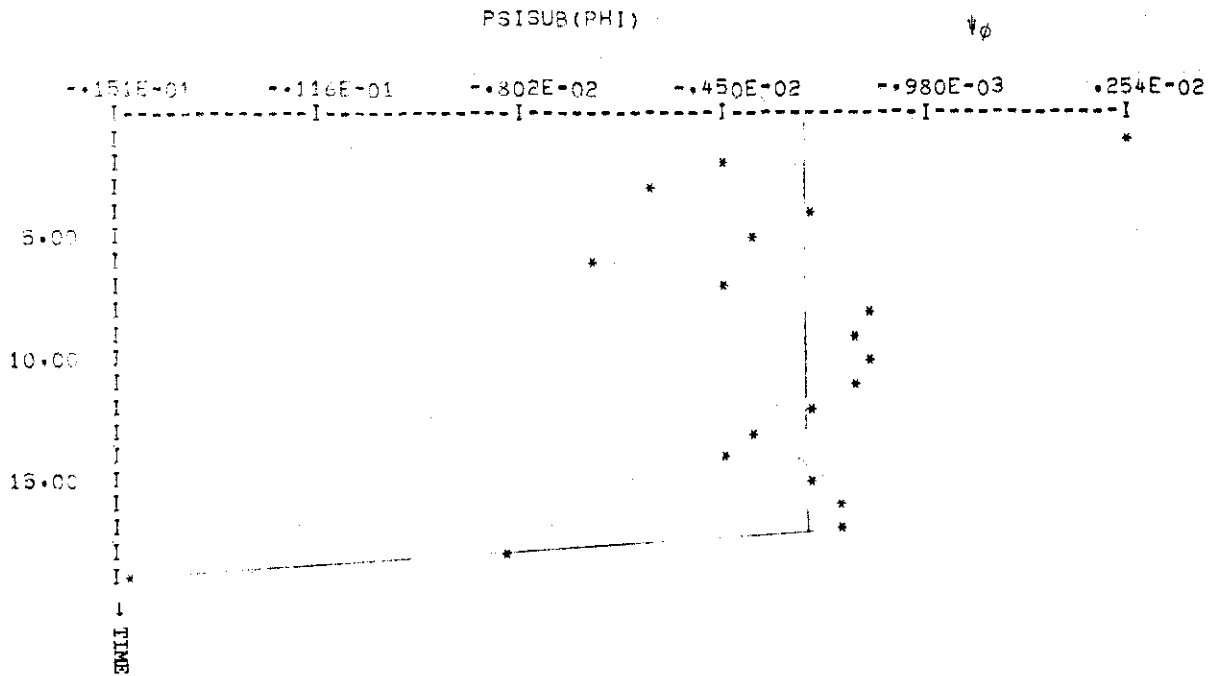


Figure 36. ψ_ϕ versus Time

Contrails

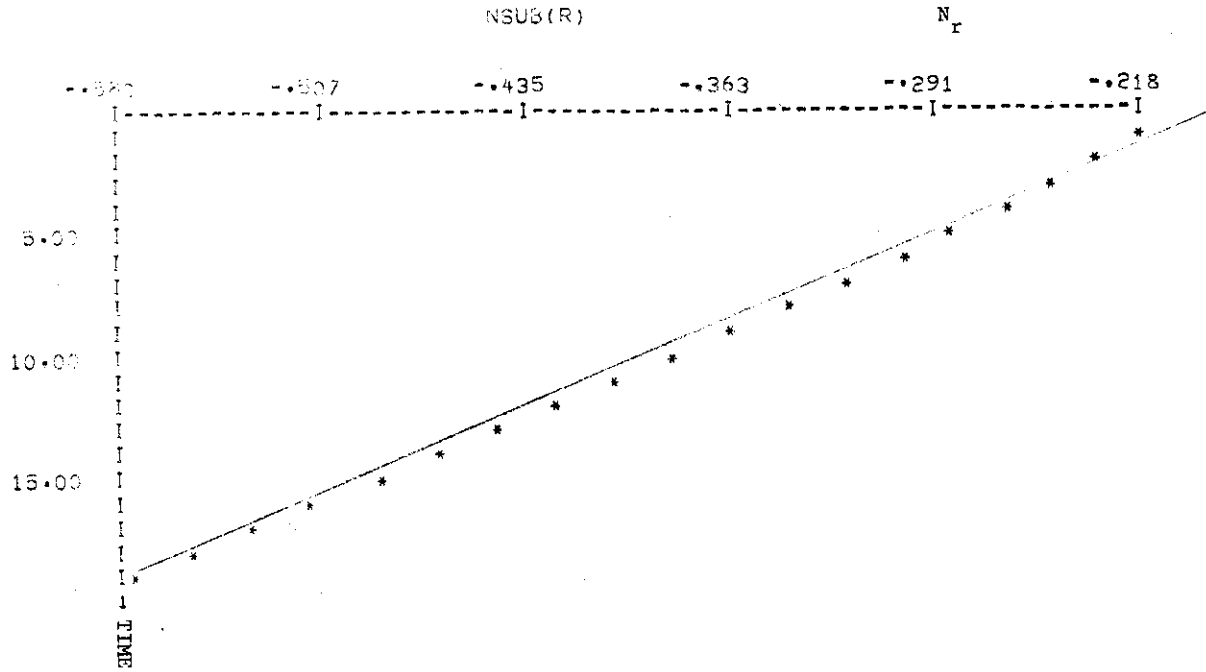


Figure 37. N_r versus Time

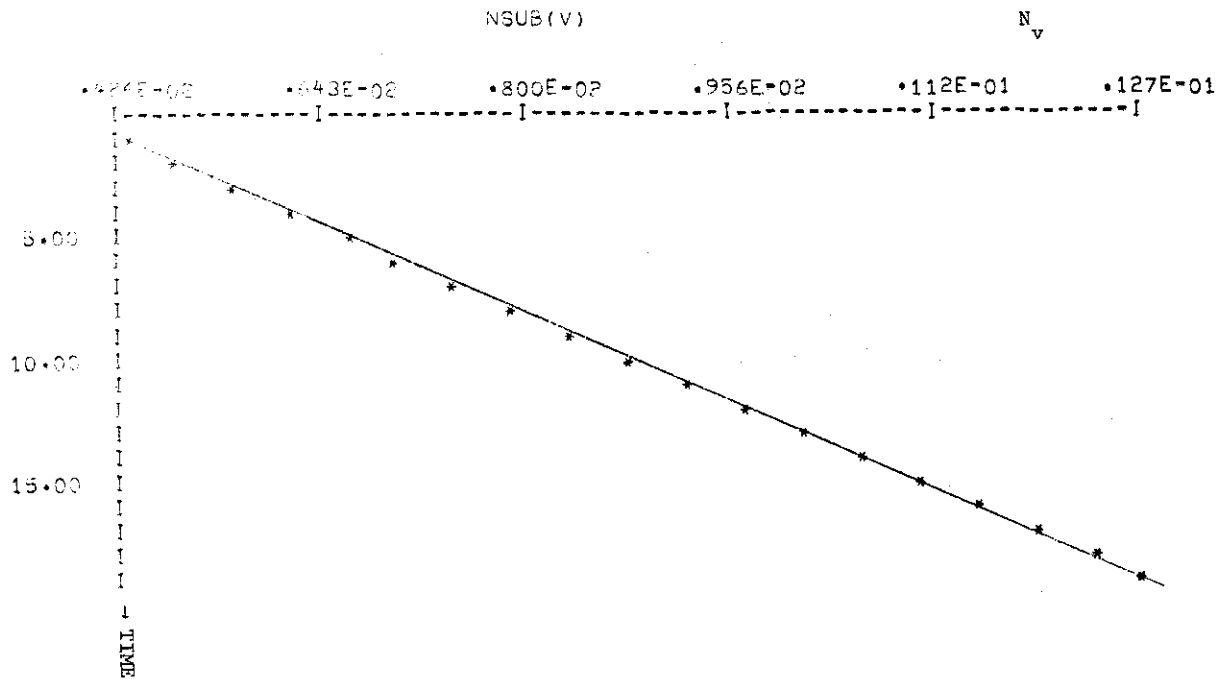


Figure 38. N_v versus Time

Contrails

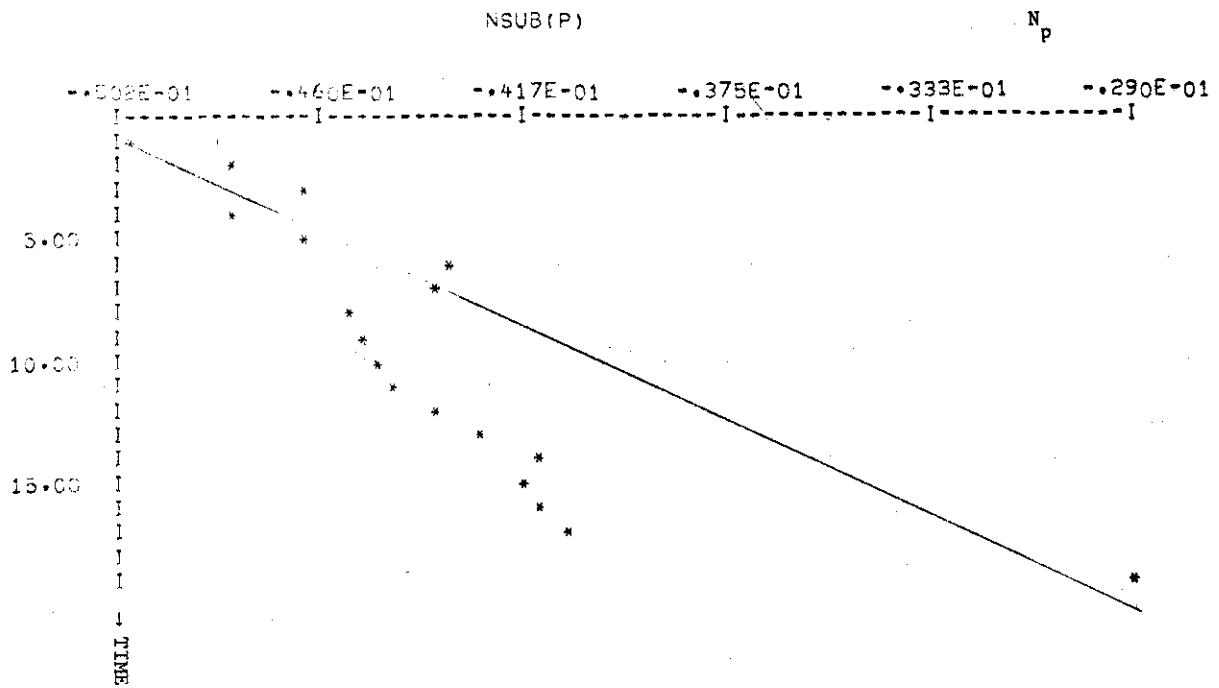


Figure 39. N_p versus Time

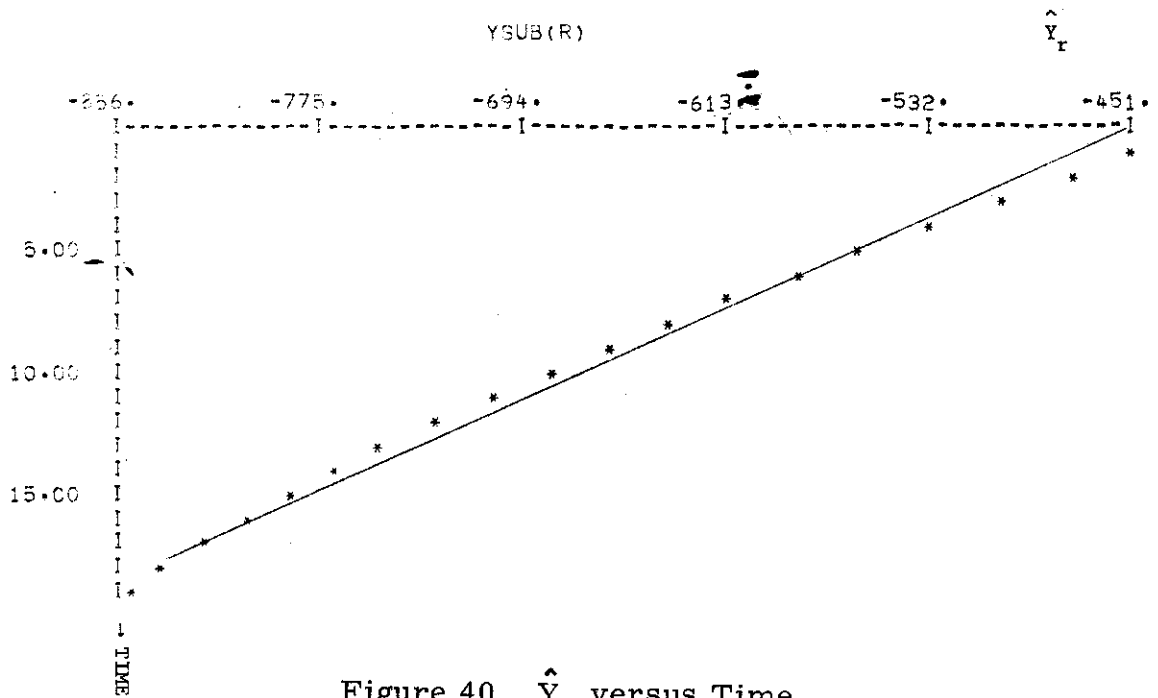


Figure 40. \hat{Y}_r versus Time

Contrails

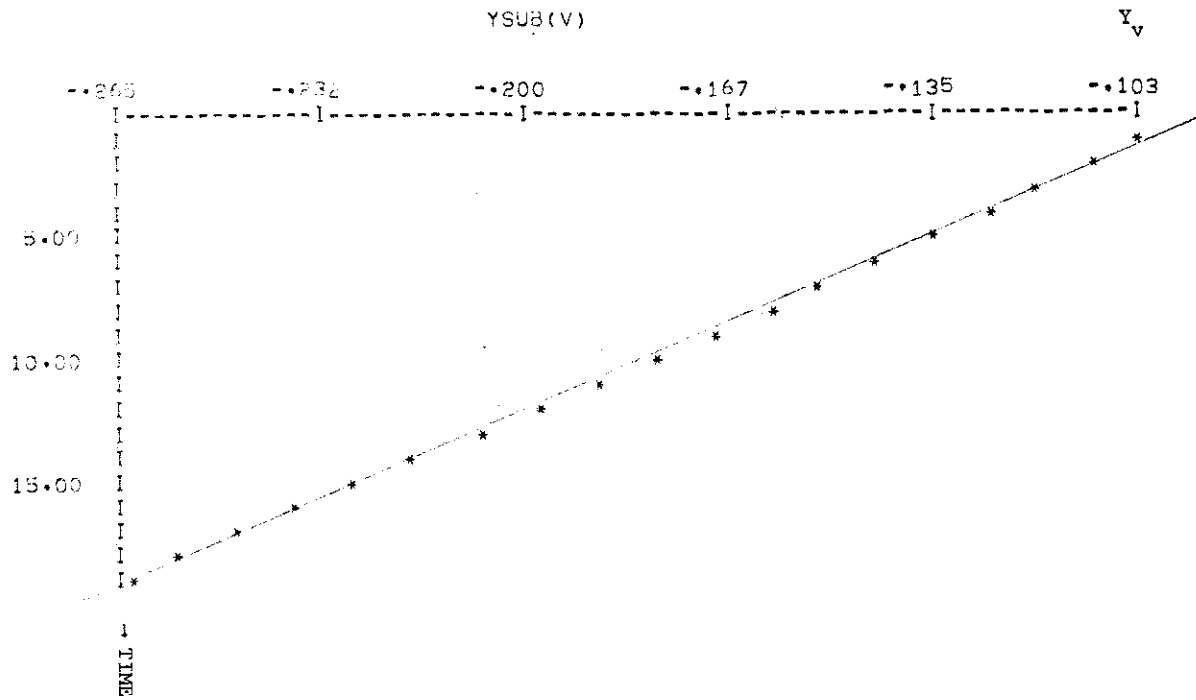


Figure 41. Y_V versus Time

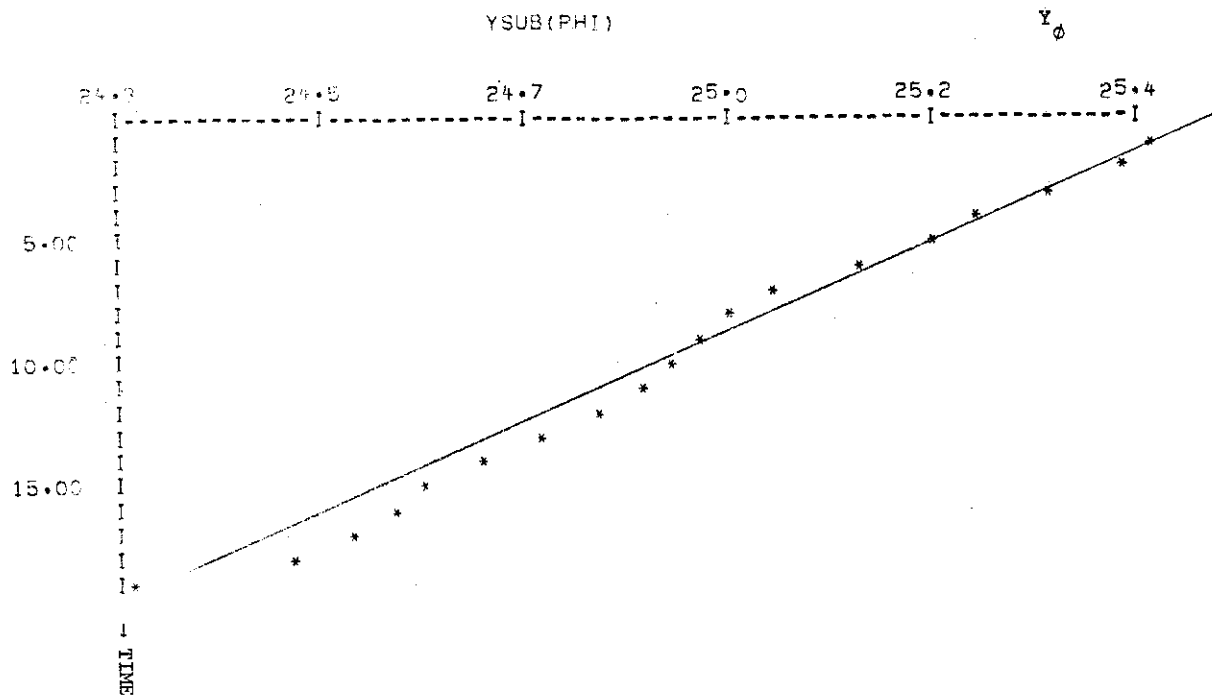


Figure 42. Y_ϕ versus Time

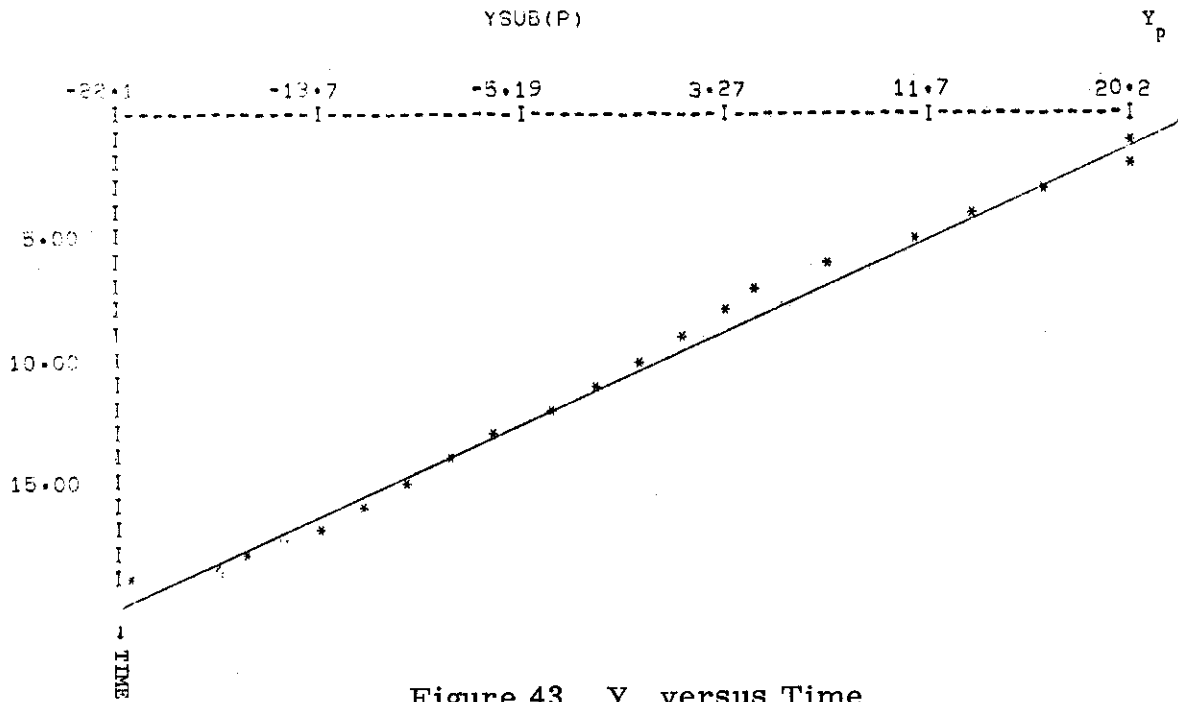


Figure 43. Y_p versus Time

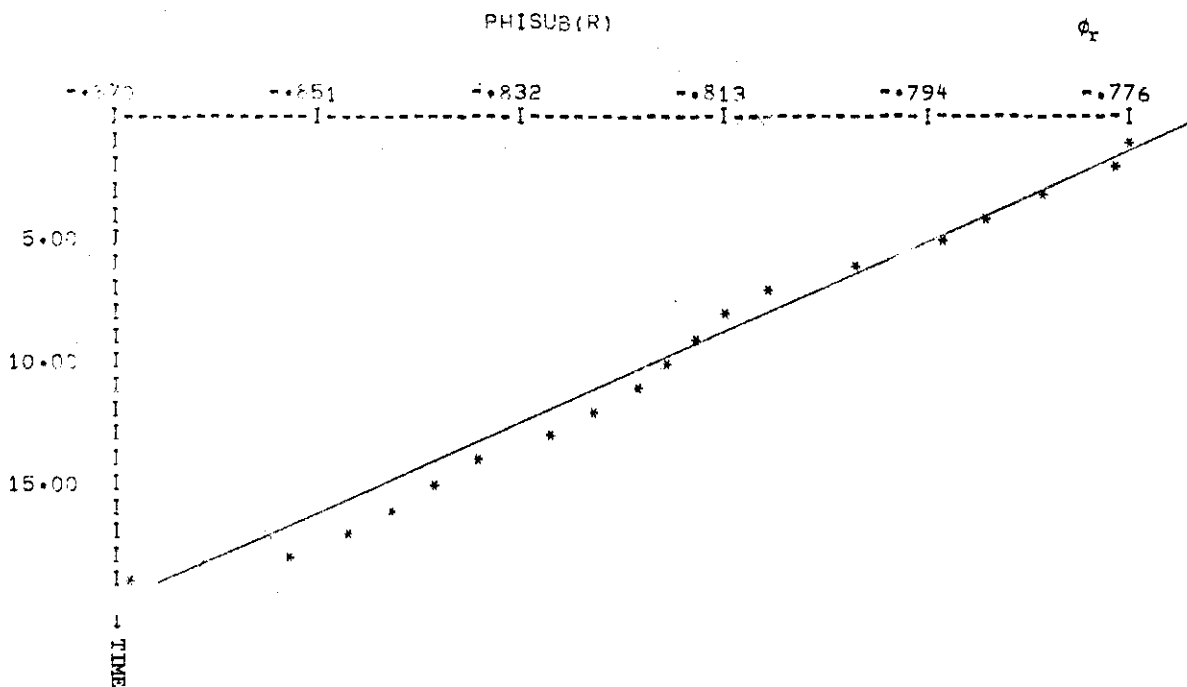


Figure 44. ϕ_r versus Time

Contrails

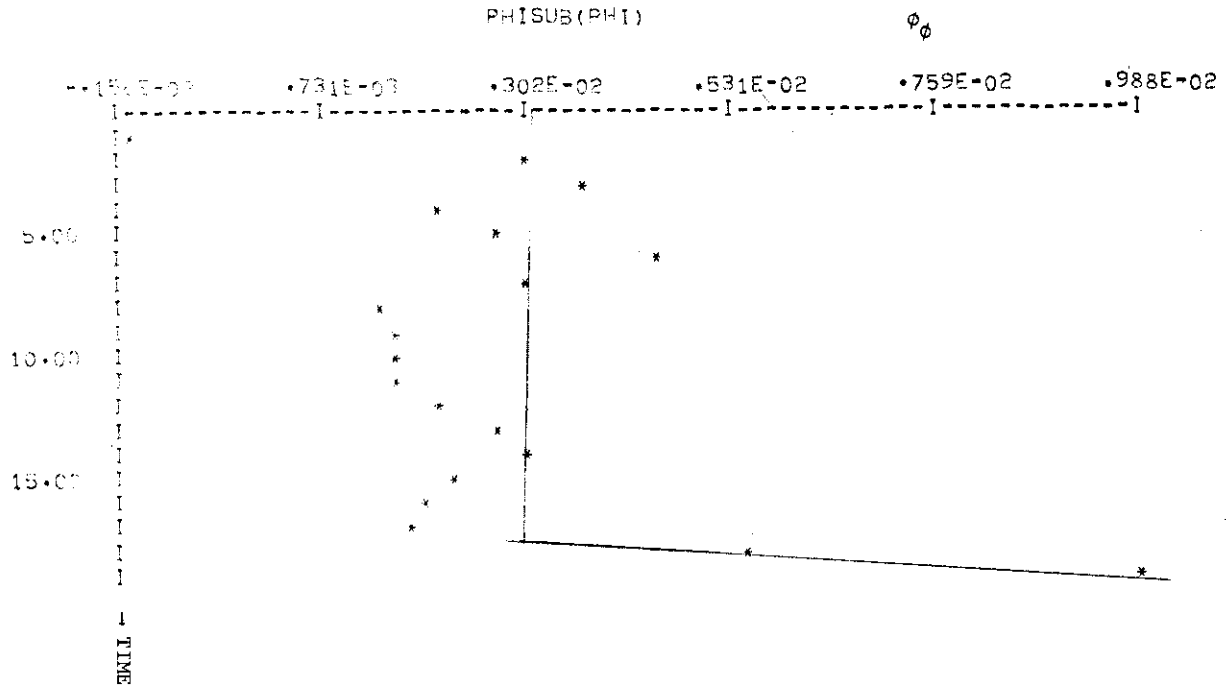


Figure 45. $\phi\phi$ versus Time

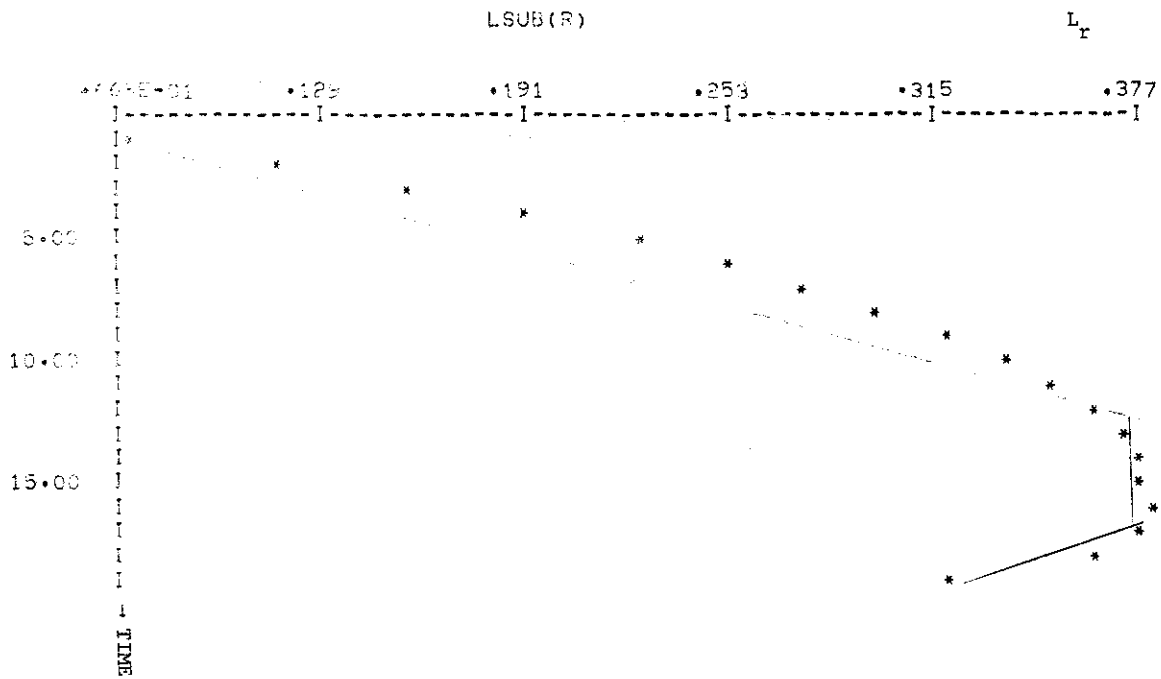


Figure 46. L_r versus Time

Contrails

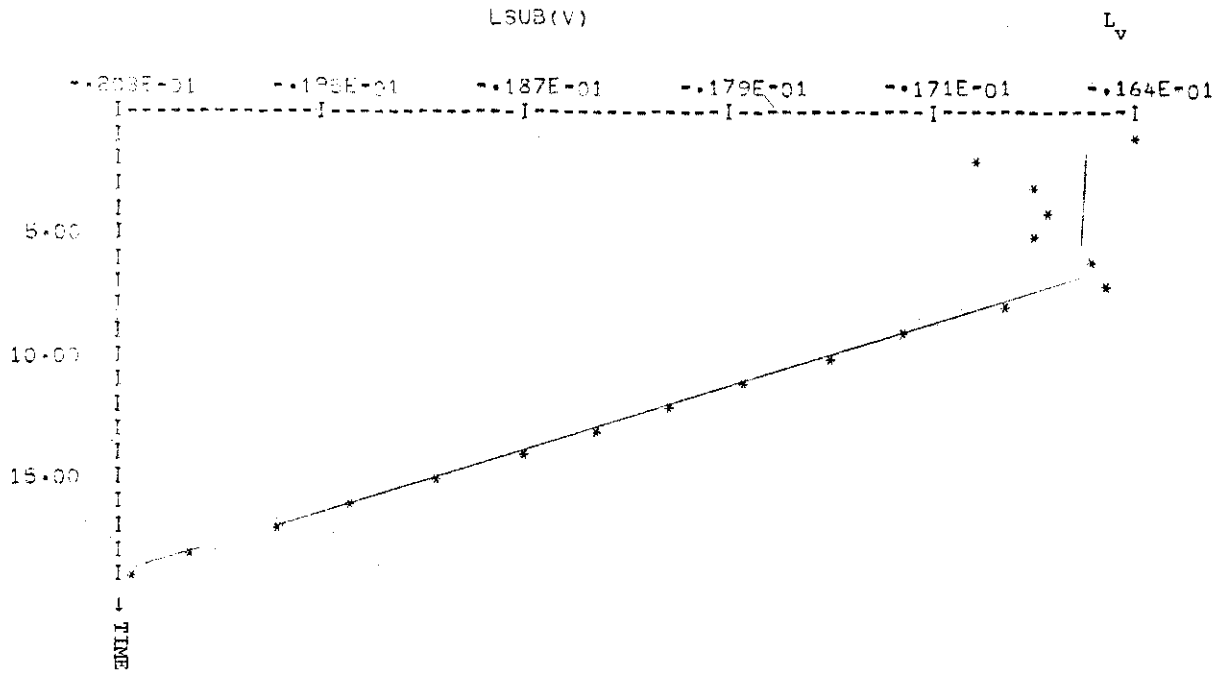


Figure 47. L_V versus Time

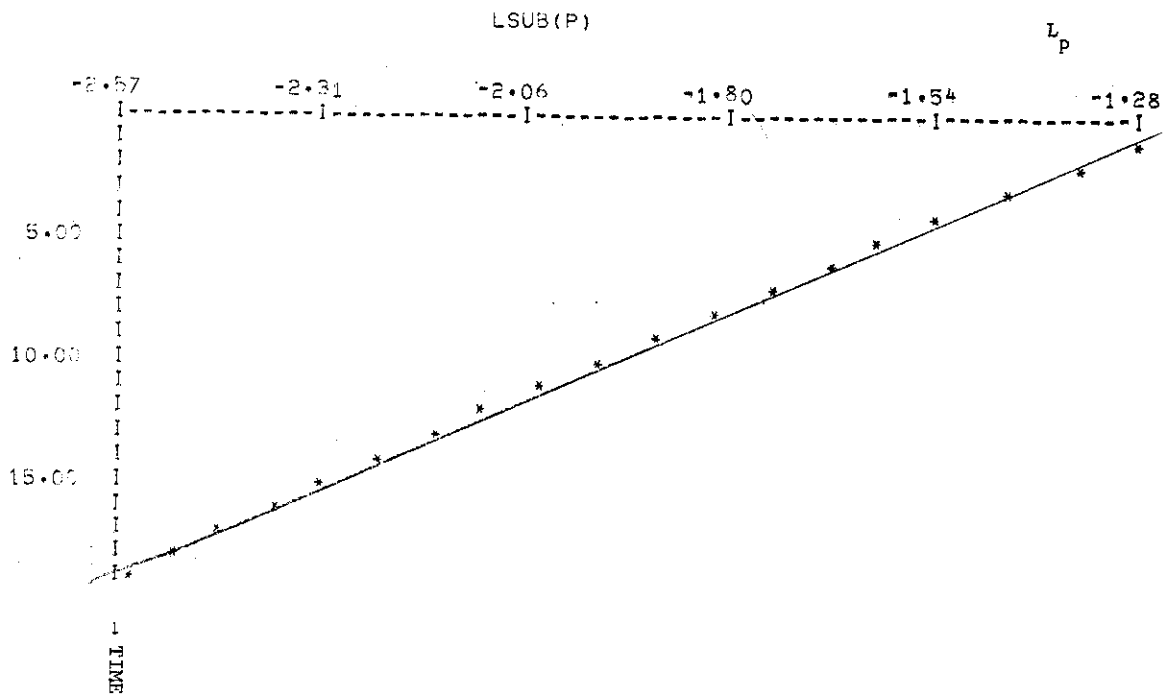


Figure 48. L_p versus Time

Contrails

```
▲FORTRAN LS,GS
 1: DIMENSION A(1000),IDX(20),IORD(20,8),YY(40,20),XX(40),AB(6)
 2: READ(5,1)NG
 3: DO 3 I=1,NG
 4:   3 READ(5,2)IDX(I),(IORD(I,J),J=1,8)
 5:   1 FORMAT(I2)
 6:   2 FORMAT(I4,8(A4))
 7: 999 PAUSE
 8: READ(5,998)NDP
 9: 998 FORMAT(I2)
10: REWIND 2
11: DO 4 I=1,NDP
12: READ(2)A
13: XX(I)=A(1)
14: DO 5 J=1,NG
15:   JJ=IDX(J)
16:   5 YY(I,J)=A(JJ)
17:   4 CONTINUE
18: DO 100 L=1,NG
19:   XMAX=-1.E+20
20:   XMIN=+1.E+20
21:   DO 10 I=1,NDP
22:     XMAX=AMAX(XMAX,YY(I,L))
23:     -10 XMIN=AMIN(XMIN,YY(I,L))
24:     R=XMAX-XMIN
25:     WRITE(9,200)(IORD(L,K),K=1,8)
26:     200 FORMAT(1H1,25X,8A4)
27:     AB(1)=XMIN
28:     DO 11 M=1,5
29:       11 AB(M+1)=AB(M)+R/5.
30:       WRITE(9,201)(AB(M),M=1,6)
31:       201 FORMAT(/6G14.3)
32:       WRITE(9,202)
33:       202 FORMAT(8X,'I',5('-----I'))
34:       JJ=5
35:       DO 300 J=1,NDP
36:         LL=(YY(J,L)-XMIN)*70./R
37:         IF(J.NE.JJ) GOT0 400
38:         T=XX(J)
39:         JJ=JJ+5
40:         WRITE(9,203)T,LL
41:         203 FORMAT(F6.2,' I',NX,'*')
42:         GOT0 300
43:       400 WRITE(9,204)LL
44:       204 FORMAT(6X,' I',NX,'*')
45:     300 CONTINUE
46:   100 CONTINUE
47:   GOT0 999
48: END
```

Figure 49. Plotting Data Program Listing

```
1
C 03/23/72
C H0= 12000 FT,V0=250 KNTS
C INTEGRATION AND LINEARIZATION OF AIRPLANE
C NOMINAL PERTURBATION
C 40 DEGREE DIVE ANGLE
PCC
 2 -.1381E+05   4 +.1200E+05  16 +.4225E+03  26 +.3665E-01  29 +.3665E-01
 31 -.6614E+00  43 -.1745E-02  90 +.3217E+02 115 +.3867E+02 116 +.1604E+02
117 +.5300E+03 121 +.1000E+00 122 +.1330E-02 131 +.1000E+03 132 +.1000E+01
134 +.1000E+01 140 +.7000E+00 141 +.7720E+04 142 +.7720E+04 156 +.1000E+05
157 +.7500E-03 170 +.1200E+02 171 +.4000E+01 172 +.6000E+01 201 +.1000E+02
202 +.5000E+01 203 +.5000E+01 204 +.1000E-01 205 +.1000E-01 206 +.1000E-01
207 +.2000E-01 208 +.2000E-01 209 +.2000E-01 210 +.2000E+02 211 +.2000E+02
212 +.2000E+02 213 +.1000E+02 214 +.5000E+01 215 +.5000E+01 216 +.1000E-01
217 +.1000E-01 218 +.1000E-01 221 +.5000E-01 222 +.5000E-01 223 +.5000E-01
224 +.5000E-01 231 +.5000E+01 232 +.5000E+01 233 +.5000E+01 234 +.1000E-01
235 +.1000E-01 236 +.1000E-01 256 +.2000E+00 257 -.3000E+00 258 +.1000E+00
259 -.3000E+00 260 -.6981E+00 261 +.1000E+01 270 +.1047E+00 274 +.4000E+04
283 +.3000E+02 290 +.5236E+00 291 +.5236E+00 292 +.2000E+04 293 +.3000E+02
391 +.1000E+01 395 +.1000E+01 399 +.1000E+01 400 +.1000E+01 404 +.1000E+01
408 +.1000E+01 409 +.1000E+01 413 +.1000E+01 417 +.1000E+01 418 +.1000E+01
422 +.1000E+01 426 +.1000E+01 427 +.1000E+01 431 +.1000E+01 435 +.1000E+01
501 -.3135E+03 502 -.3135E+03 506 +.2383E+02 507 -.2383E+02 511 -.3241E+02
512 -.3241E+02 517 +.2000E+01 559 +.2000E+02 560 +.2000E+02 579 -.3162E+03
582 -.2500E+00 583 +.2500E+00 587 +.5250E+01 588 +.5250E+01 646 +.4000E+02
716 +.4042E+05 901 +.7000E+01 902 +.8000E+01 903 +.9000E+01 904 +.4200E+02
905 +.4300E+02 906 +.4400E+02 907 +.3100E+02 908 +.3200E+02 909 +.3300E+02
910 +.2000E+01 911 +.3000E+01 912 +.4000E+01 913 +.1700E+02 914 +.1800E+02
915 +.1900E+02 916 +.4500E+02 917 +.4600E+02 918 +.4700E+02 919 +.3900E+02
920 +.4000E+02 921 +.4100E+02 922 +.1300E+02 923 +.1400E+02 924 +.1500E+02
925 +.1230E+03 926 +.1210E+03 927 +.1250E+03 928 +.6450E+03 929 +.1010E+03
930 +.1020E+03 931 +.1030E+03 932 +.1040E+03 933 +.1050E+03 934 +.1060E+03
995 +.2000E+01 996 +.2000E+01 998 +.1000E+01
```

Figure 50. Typical Aircraft Trajectory Input Data

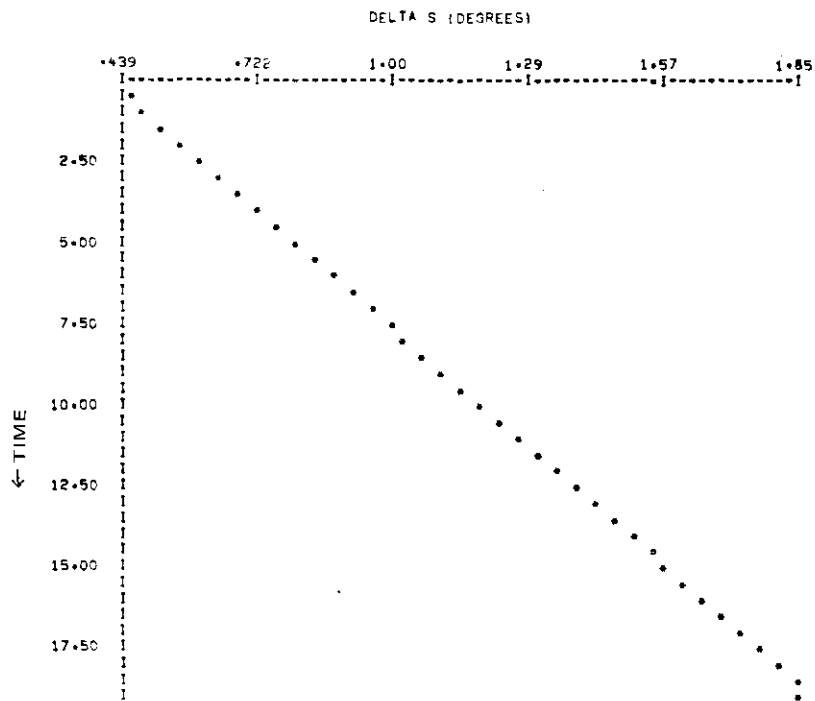


Figure 51. δ_s versus Time

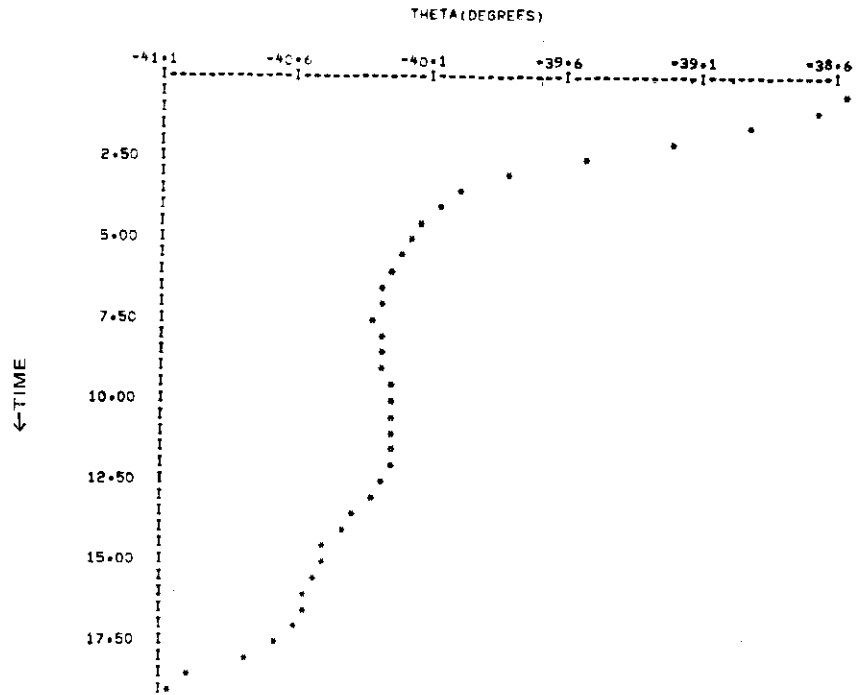


Figure 52. θ versus Time

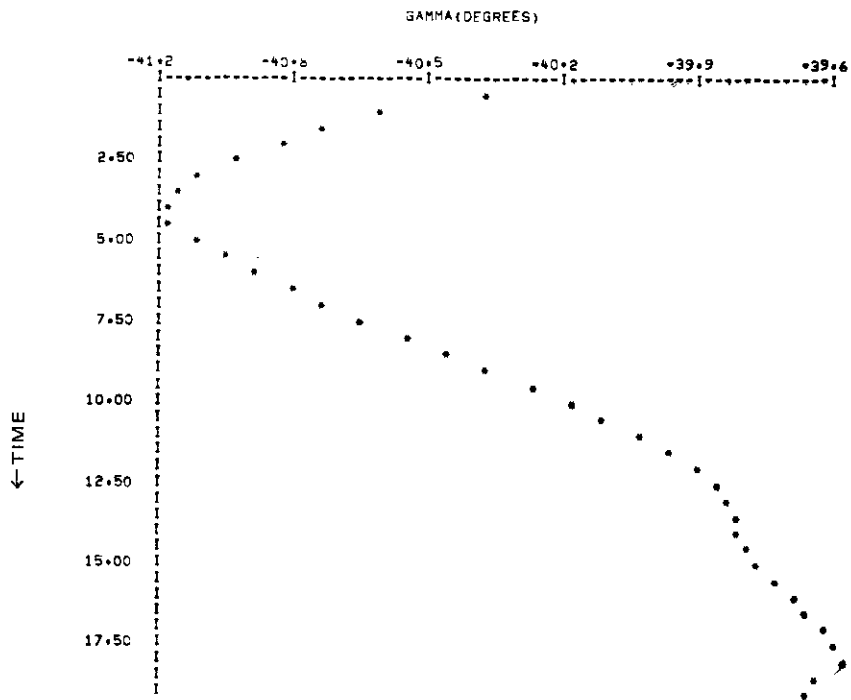


Figure 53. γ versus Time

Contrails

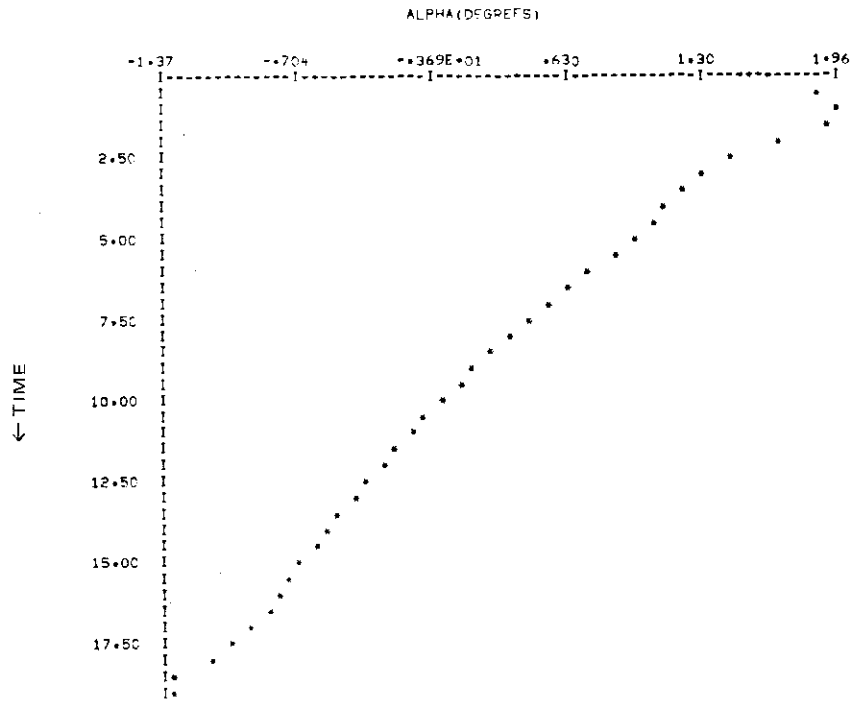


Figure 54. α versus Time

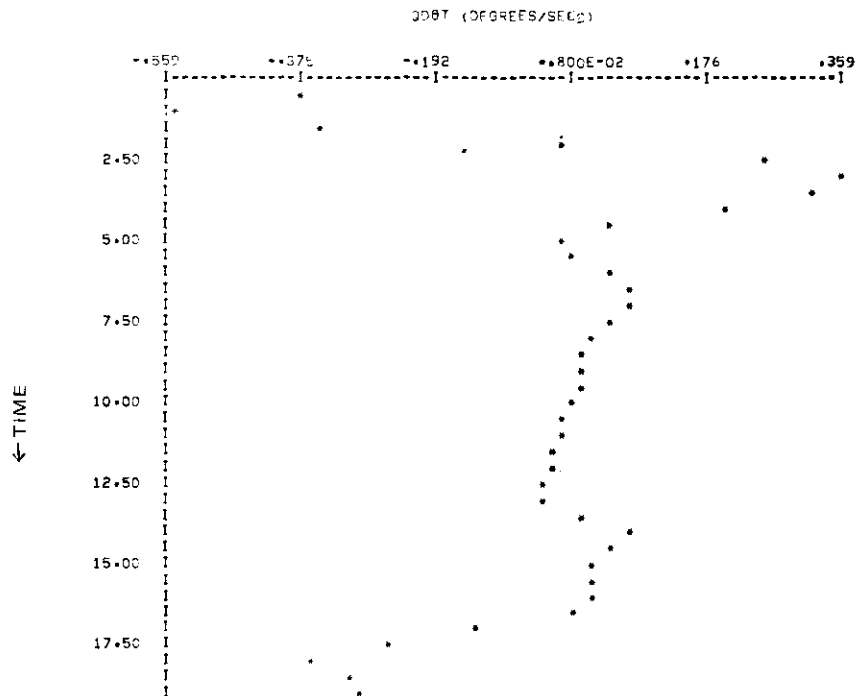


Figure 55. \dot{q} versus Time

Contrails

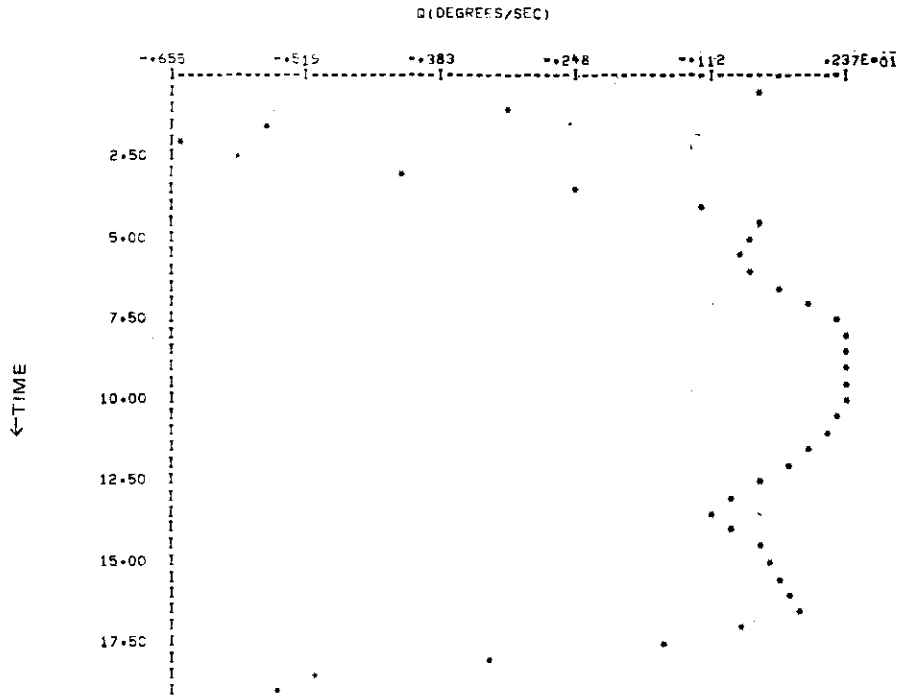


Figure 56. q versus Time

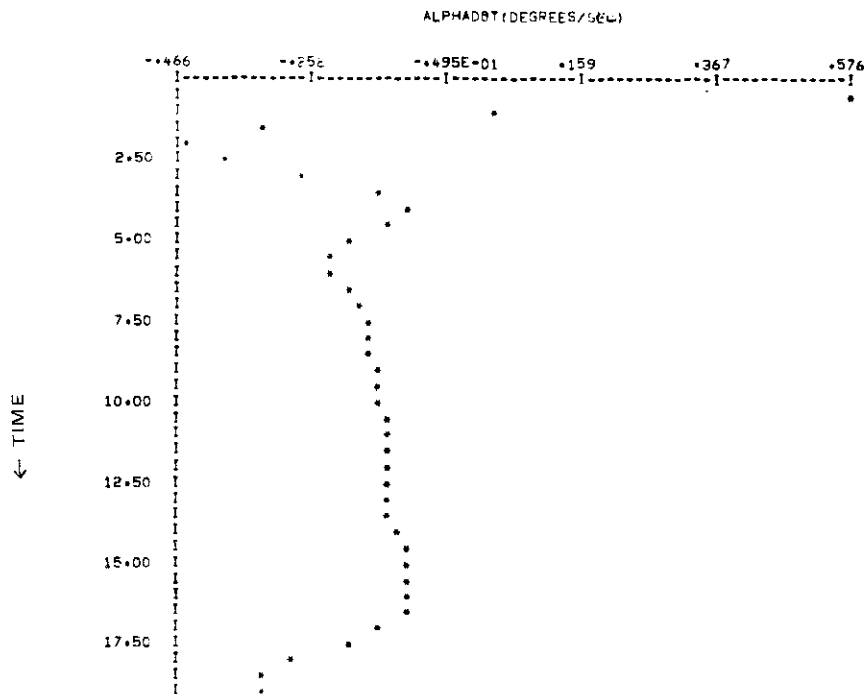


Figure 57. $\dot{\alpha}$ versus Time

Contrails

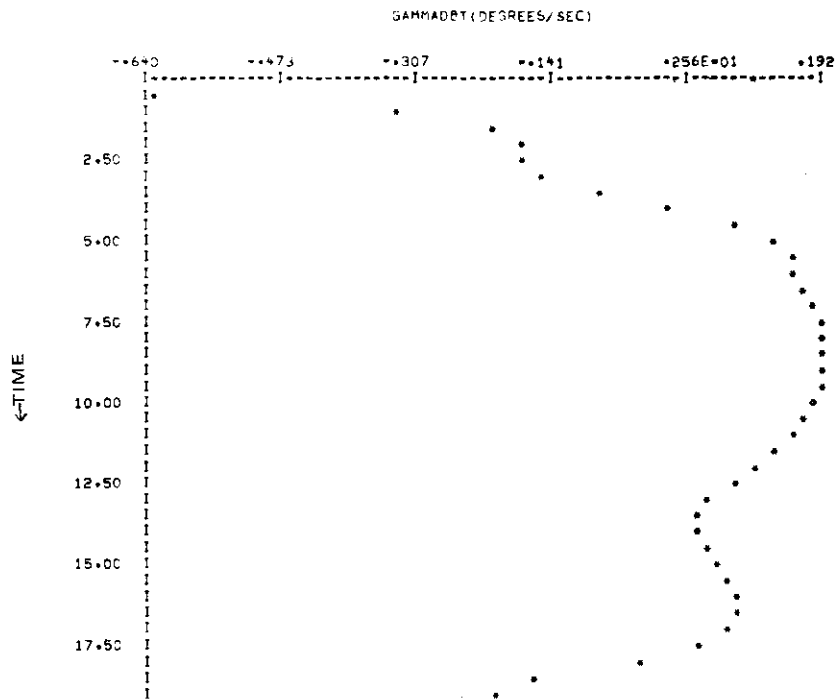


Figure 58. $\dot{\gamma}$ versus Time

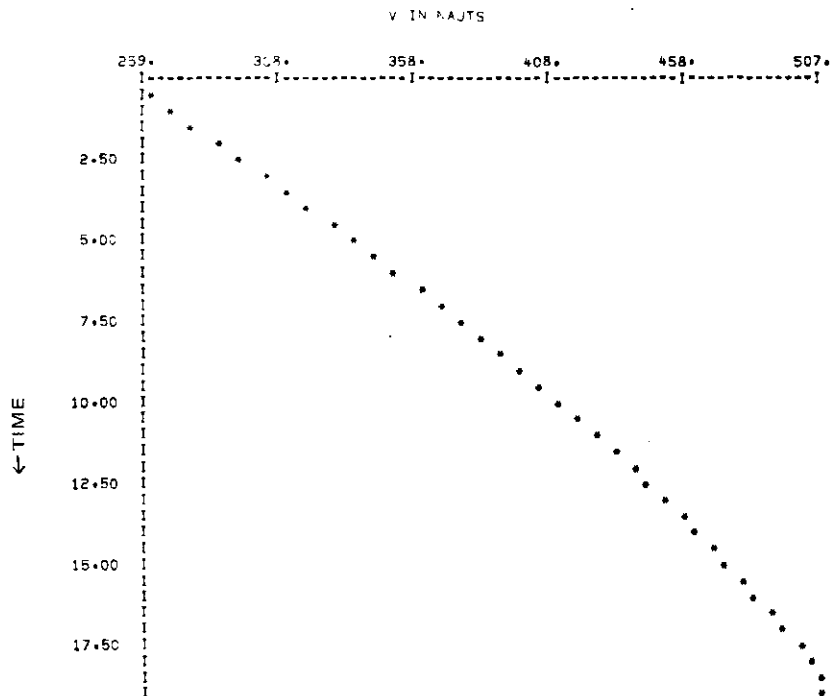


Figure 59. V versus Time

FROZEN-POINT SPECTRUM ANALYSIS OF THE LINEAR DATA

The linear aircraft data was then subjected to a frozen-point eigenvalue analysis. The eigenvalues were separated into the longitudinal and lateral channels. By properly partitioning the longitudinal matrix, the phugoid, and the short-period modes as well as the altitude and range modes were identified. Similarly the lateral matrix was partitioned, and the dutch-roll, the roll convergence and the spiral modes were identified. The matrices were partitioned as shown in Volume I, Figure 31.

The program listing for the eigenvalue analysis is given in Figure 60. The short-period mode and the phugoid mode of the airframe during dive are plotted in Figures 61 and 62, respectively at 1-second data time points. The dutch-roll mode, the spiral mode, and the roll convergence mode are similarly plotted in Figures 63, 64 and 65.

Contrails

FORTRAN LS.60

```
1: DIMENSION D(12,12), ISH(12), FU(4,4), FU1(3,3), FU2(2,2), FL(6,6)
2: DIMENSION FL1(2,2), FL2(4,4), F(12,12), FH(12,12)
3: DIMENSION A(50)
4: LW=9
5: KK=16
6: READ(5,1001) ISH
7: 1001 FORMAT(12I2)
8: DO 10 L=1, KK
9: READ(2) F
10: DO 4001 I=1, 12
11: DO 4001 J=1, 12
12: IF (ABS(F(I,J)).GT..00000001) GO TO 4001
13: F(I,J)=0.
14: 4001 CONTINUE
15: DO 300 I=1,12
16: DO 300 J=1,12
17: 300 FH(I,J)= F(I,J)
18: CALL SHUF(FH,12,12,1,ISH,12,12,D)
19: FH(1,8)=0.
20: FH(1,11)=0.
21: FH(4,5)=1.1
22: FH(7,10)=1.1
23: FH(11,12)=1.1
24: FH(2,11)=0.
25: 4000 FORMAT(1H1/7X,1CH F MATRIX /)
26: WRITE(LW,4000)
27: CALL MP(12,12,12,12,FH,9)
28: ICBT=0
29: DO 4022 I=1,12
30: DO 4022 J=1,12
31: IF ((FH(I,J).EQ.0.).OR.(FH(I,J).EQ.1.)) GO TO 4022
32: ICBT=ICBT+1
33: A(ICBT)=FH(I,J)
34: 4022 CONTINUE
35: WRITE(3) A
36: DO 4002 I=1,4
37: II=I+2
38: DO 4002 J=1,4
39: JJ=J+2
40: 4002 FU(I,J)=FH(II,JJ)
41: DO 4003 I=1,3
42: II=I+1
43: DO 4003 J=1,3
44: JJ=J+1
45: 4003 FU1(I,J)=FU(II,JJ)
46: DO 4004 J=1,2
47: JJ=J+1
48: DO 4004 I=1,2
49: II=I+1
50: 4004 FU2(I,J)=FU1(II,JJ)
51: DO 4005 I=1,6
52: II=I+6
53: DO 4005 J=1,6
54: JJ=J+6
55: 4005 FL(I,J)=FH(II,JJ)
56: DO 4006 I=1,4
57: DO 4006 J=1,4
58: 4006 FL2(I,J)=FL(I,J)
59: DO 4007 I=1,2
```

Figure 60. Eigenvalue Analysis Program Listing

Contrails

```
60:      II=I+2
61:      D9 4007 J=1,2
62:      JJ=J+2
63: 4007 FL1(I,J)=FL2(II,JJ)
64:      WRITE(9,4008)
65:      CALL MP(4,4,4,4,FU,9)
66:      CALL ROOT(FU,4)
67:      WRITE(9,4009)
68:      CALL MP(3,3,3,3,FU1,9)
69:      CALL ROOT(FU1,3)
70:      WRITE(9,4010)
71:      CALL MP(2,2,2,2,FU2,9)
72:      CALL ROOT(FU2,2)
73:      WRITE(9,4011)
74:      CALL MP(6,6,6,6,FL,9)
75:      CALL ROOT(FL,6)
76:      WRITE(9,4012)
77:      CALL MP(4,4,4,4,FL2,9)
78:      CALL ROOT(FL2,4)
79:      WRITE(9,4013)
80:      CALL MP(2,2,2,2,FL1,9)
81:      CALL ROOT(FL1,2)
82: 4008 FORMAT(1H1/7X,10HF11 MATRIX/)
83: 4009 FORMAT(//7X,15HF11(3X3) MATRIX/)
84: 4010 FORMAT(//7X,15HF11(2X2) MATRIX/)
85: 4011 FORMAT(1H1/7X,10HF22 MATRIX/)
86: 4012 FORMAT(//7X,15HF22(4X4) MATRIX/)
87: 4013 FORMAT(//7X,15HF22(2X2) MATRIX/)
88:      10 CONTINUE
89:      END
```

```
1:      SUBROUTINE ROOT(A,NX)
2:      DIMENSION A(NX,NX),RR(40)
3:      LWR=9
4:      CALL HESSEN(NX,A,NX)
5:      CALL QRCALL(NX,A,RR,MM,NX)
6:      WRITE(LWR,900)
7: 900 FORMAT(///5X,23H          REAL          IMAG/)
8:      MN=MM/2
9:      D9 901 K=1,MN
10:     I=2*K-1
11:     II=2*K
12: 901 WRITE(LWR,802)RP(I),RR(II)
13: 802 FORMAT(2E20.8)
14:     RETURN
15:     END
```

Figure 60. Eigenvalue Analysis Program Listing (concluded)

Contrails

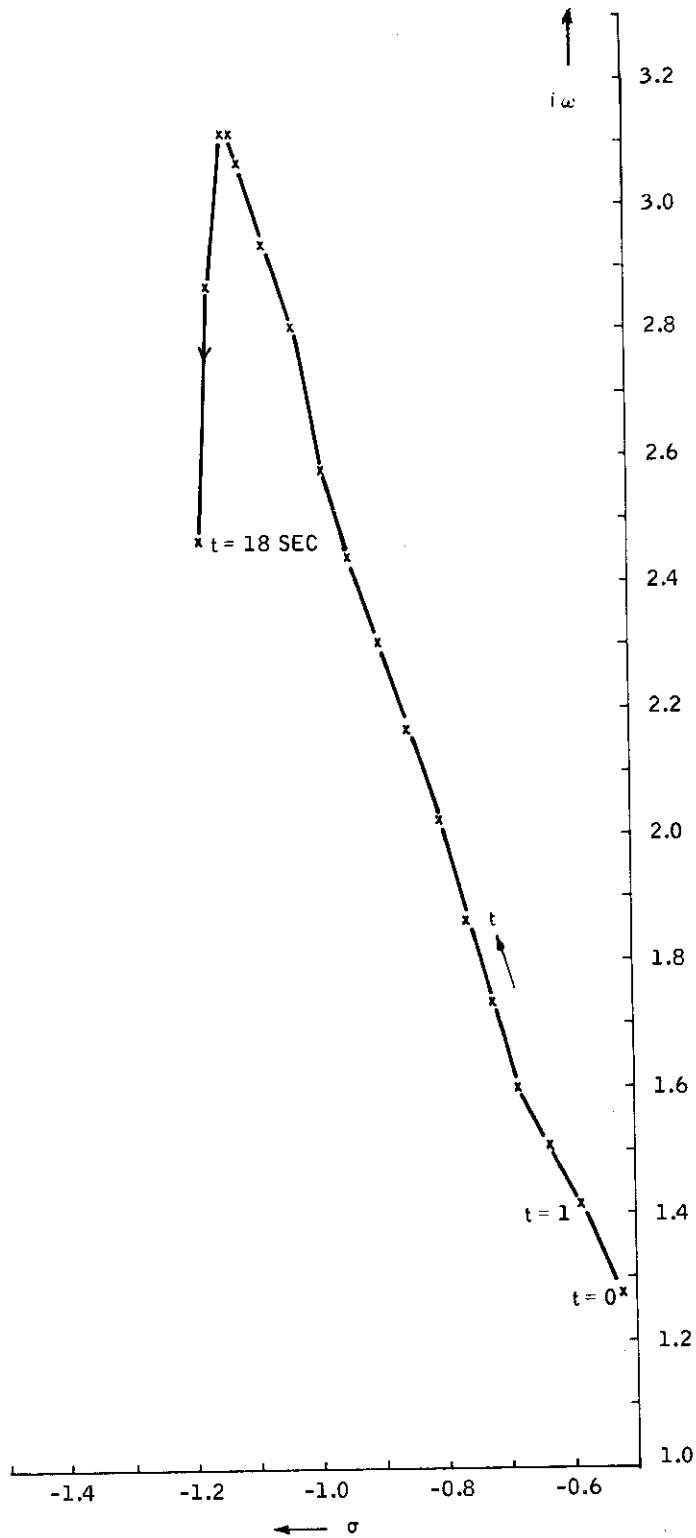


Figure 61. Short-Period Mode of Airframe During Dive

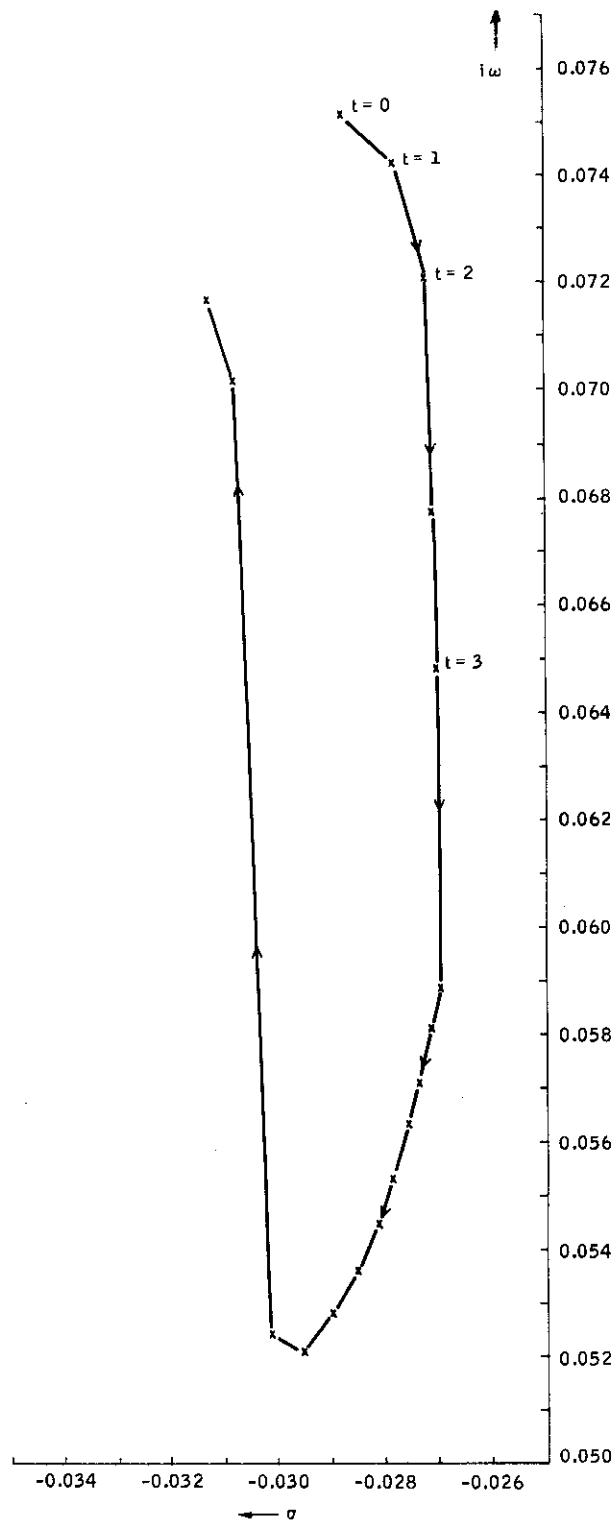


Figure 62. Phugoid Mode of Airframe During Dive

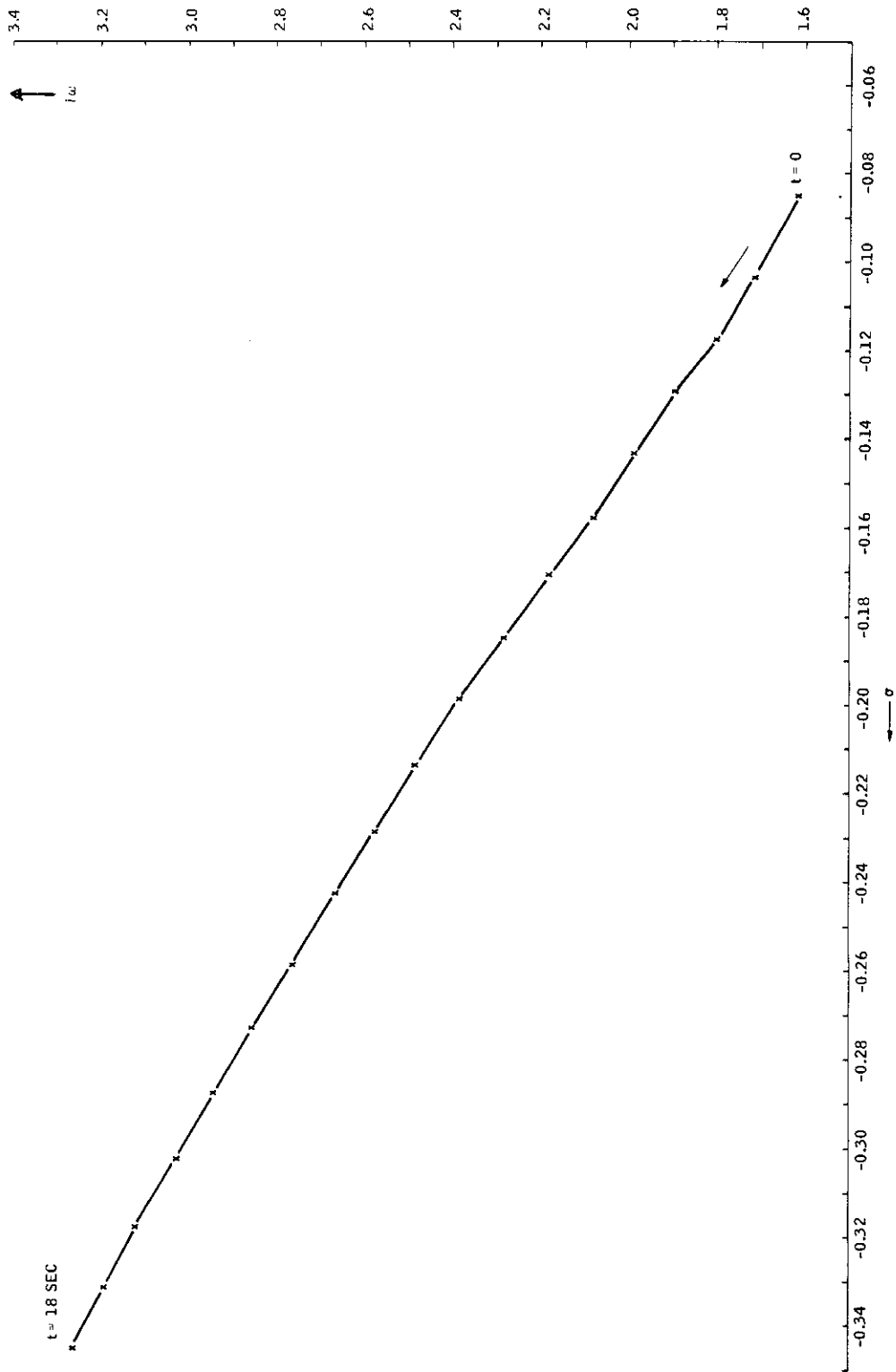


Figure 63. Dutch-Roll Mode of Airframe During Dive

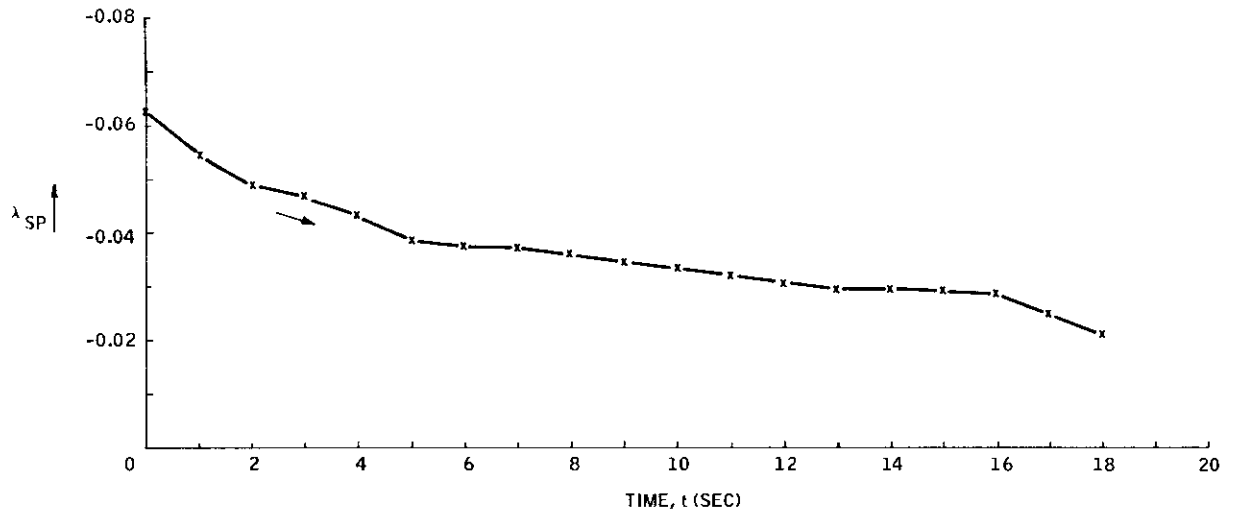


Figure 64. Spiral Mode of Airframe versus Time During Dive

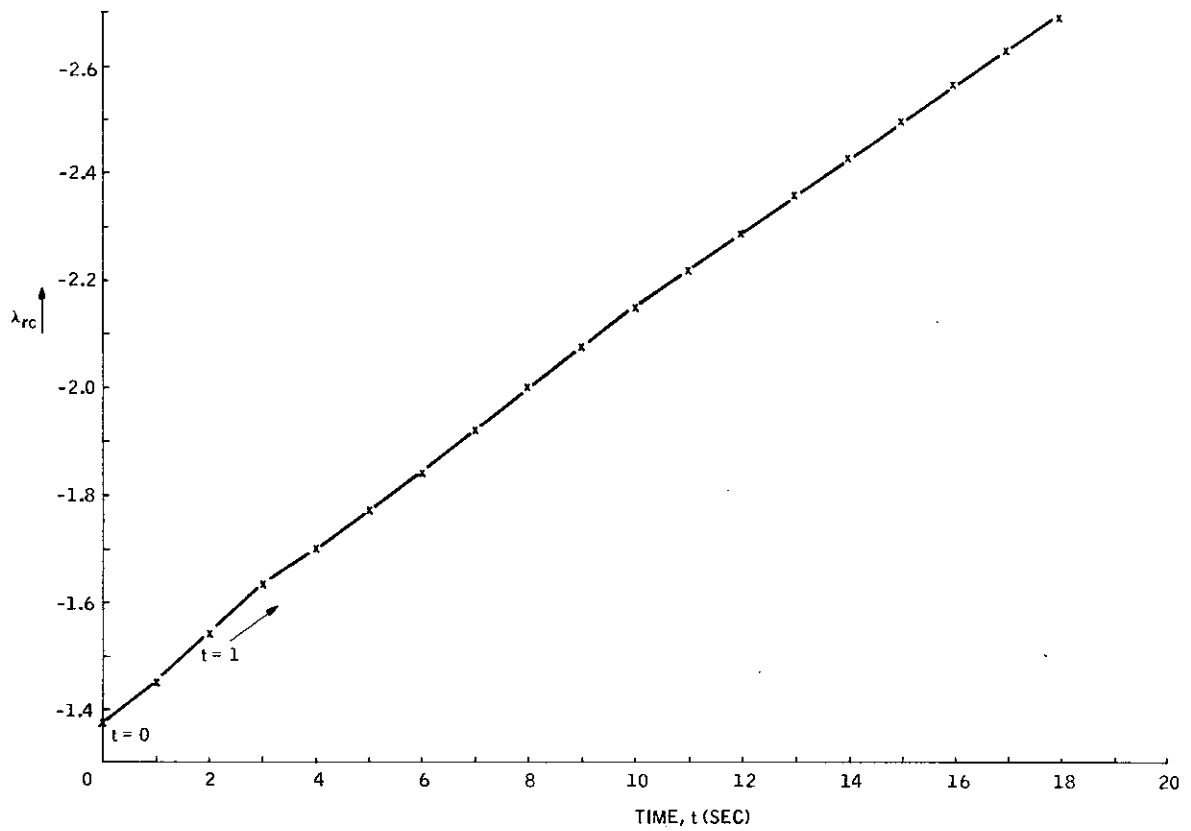


Figure 65. Roll-Convergence Mode of Airframe versus Time During Dive

SECTION IV TESTING THE WEAPON AND GUST FILTER SOFTWARE

First, a main program was written to generate the weapon's nonlinear trajectory. The M117 bomb was dropped from a specified altitude with a specified velocity and dive angles. The results obtained from the program were checked against bombtable TH 61 A1-3-2/NAVAIR 00-130-ASR-2. Table V shows these checks. The results were found to be satisfactory. Next, the main program was modified to include linearization at specified time intervals during the weapon trajectory generation with different perturbation magnitudes. Almost the same linearization matrices (F, G) are obtained by doubling and halving the nominal perturbations. Figure 66 shows the pitch-axis variables during fall.

The lateral response was also checked by two experiments, one starting with the side velocity of $v = 20$ feet, with $\psi = 0$, and the other by $v = 0$ and $\psi = 10$ -degree azimuth angle in bomb orientation.

The linear data obtained from the nominal initial condition were subjected to the frozen-point spectrum (eigenvalue) analysis. The short-period and the dutch-roll modes of the M117 were found to be stable at all frozen-time points. The phugoid mode and the spiral mode became slightly unstable at some points of the free fall. Figures 67 and 68 show the longitudinal and the lateral eigenvalues of the weapon.

The gust filter, which is a part of WINDK, was checked out by integrating numerically its covariance differential equation with a unity covariance input until steady state is reached. The result was found to be

$$\lim_{t \rightarrow \infty} E \begin{bmatrix} u^2 \\ v^2 \\ w^2 \\ g \end{bmatrix} = \frac{1}{\pi} \begin{bmatrix} \sigma_u^2 \\ \sigma_v^2 \\ \sigma_w^2 \\ \sigma \end{bmatrix}$$

A brief analysis was presented in Section IV of Volume I to justify the result. This shows that, in order to obtain a variance σ^2 at the output of the Dryden filter, the input noise η must have a variance

$$\sigma_{\eta}^2 = \pi$$

instead of the usually assumed value of unity.

Contrails

The pole locations of the roll, pitch and yaw gust filters for the aircraft are inversely proportional to wingspan b . The corresponding term for the weapon would be its diameter. When weapon diameter is used in place of wingspan, the magnitudes of the poles of the roll pitch, and yaw filters become excessively large. Numerical integration (i. e., non-real-time simulation) of these extremely fast dynamics requires a very small integration step size.

For small weapons, the space gradient effects of wind gust, (i. e., roll, pitch and yaw filters) are small. For this reason, these filters are omitted in the simulation of weapons in ADAPS.

The overall state of the weapon and wind dynamics are defined as

$$(x', w') \triangleq (\delta x_e, \delta h_e, \delta u, \delta \theta, \delta q, \delta w | \delta y, \delta \psi, \delta r, \delta v | w_1, w_3, w_5 | w_2, w_4)$$

in which the roll dynamics of the weapon and the roll-pitch-yaw dynamics of wind gust are omitted.

Table V. Comparison of Trajectory Data Obtained from ADAP 1 and Bomhtable

FC	Rlse Alt Above Burst (ft)	Eject Vel (ft/sec)	Dive Angle (deg)	Rlse Vel (kts)	Time of Fall (sec)	Horiz Range (ft)	Impact Angle (deg)	Impact Vel (ft/sec)	Source of Data
1	4000	0	40	400	7.40	3740	52.6	814	Bomhtable
					7.37	3749	51.7	817.6	ADAP 1
2	4000	0	30	400	8.60	4900	46.7	810	Bomhtable
					8.57	4907	46.8	813.5	ADAP 1

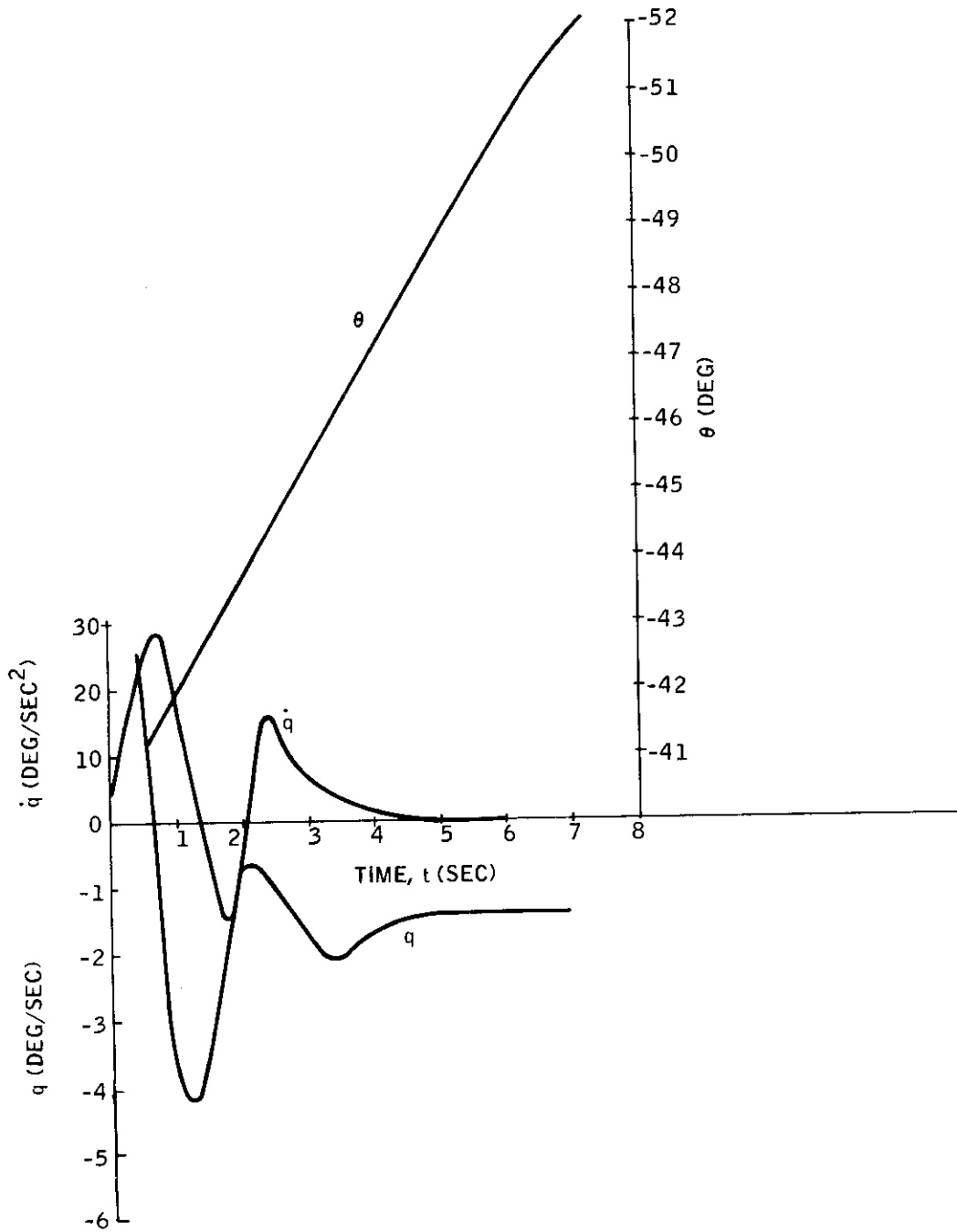


Figure 66. Weapon Pitch-Axis Variables During Fall

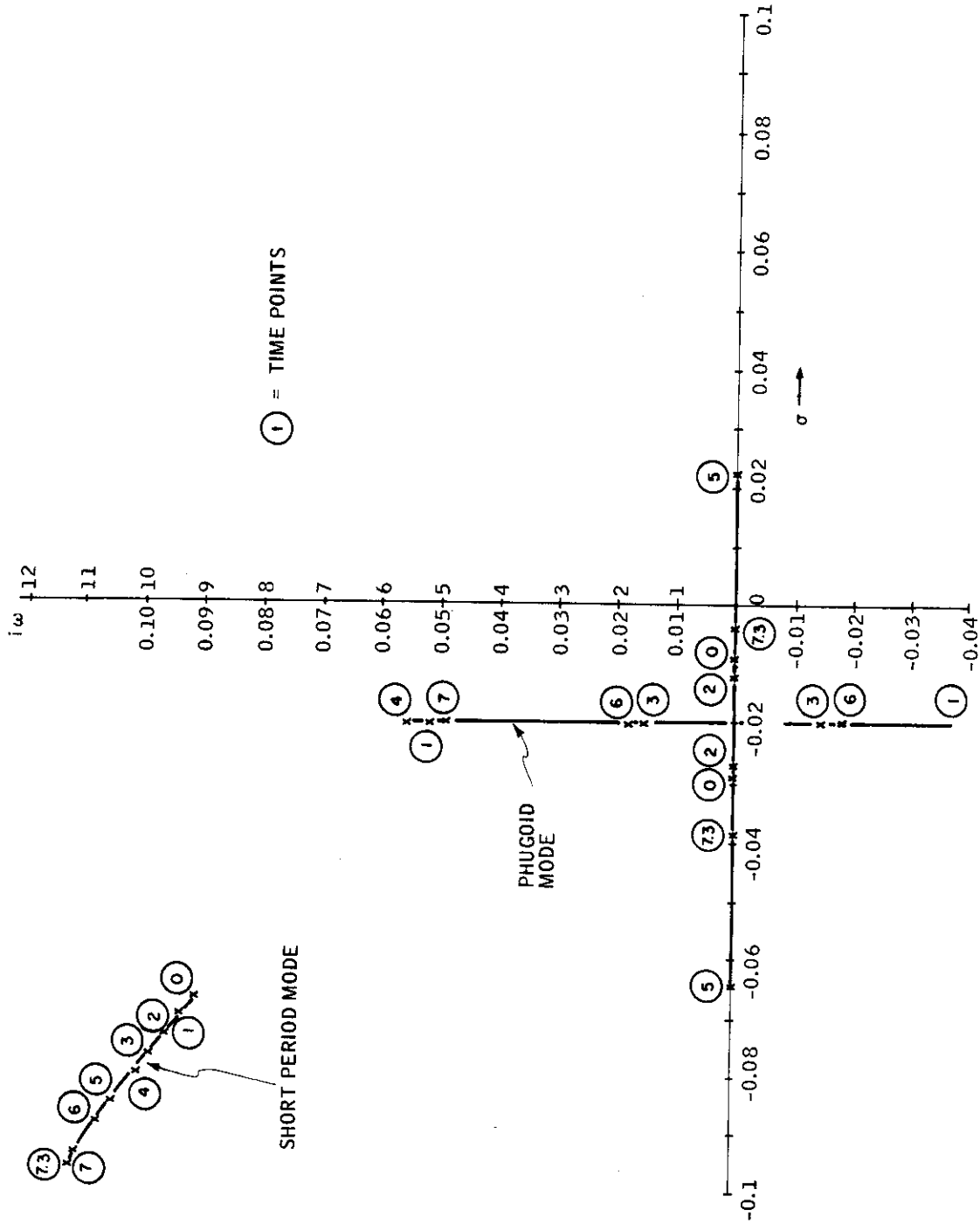


Figure 67. Spectrum of Frozen Point - Longitudinal Matrix of M117

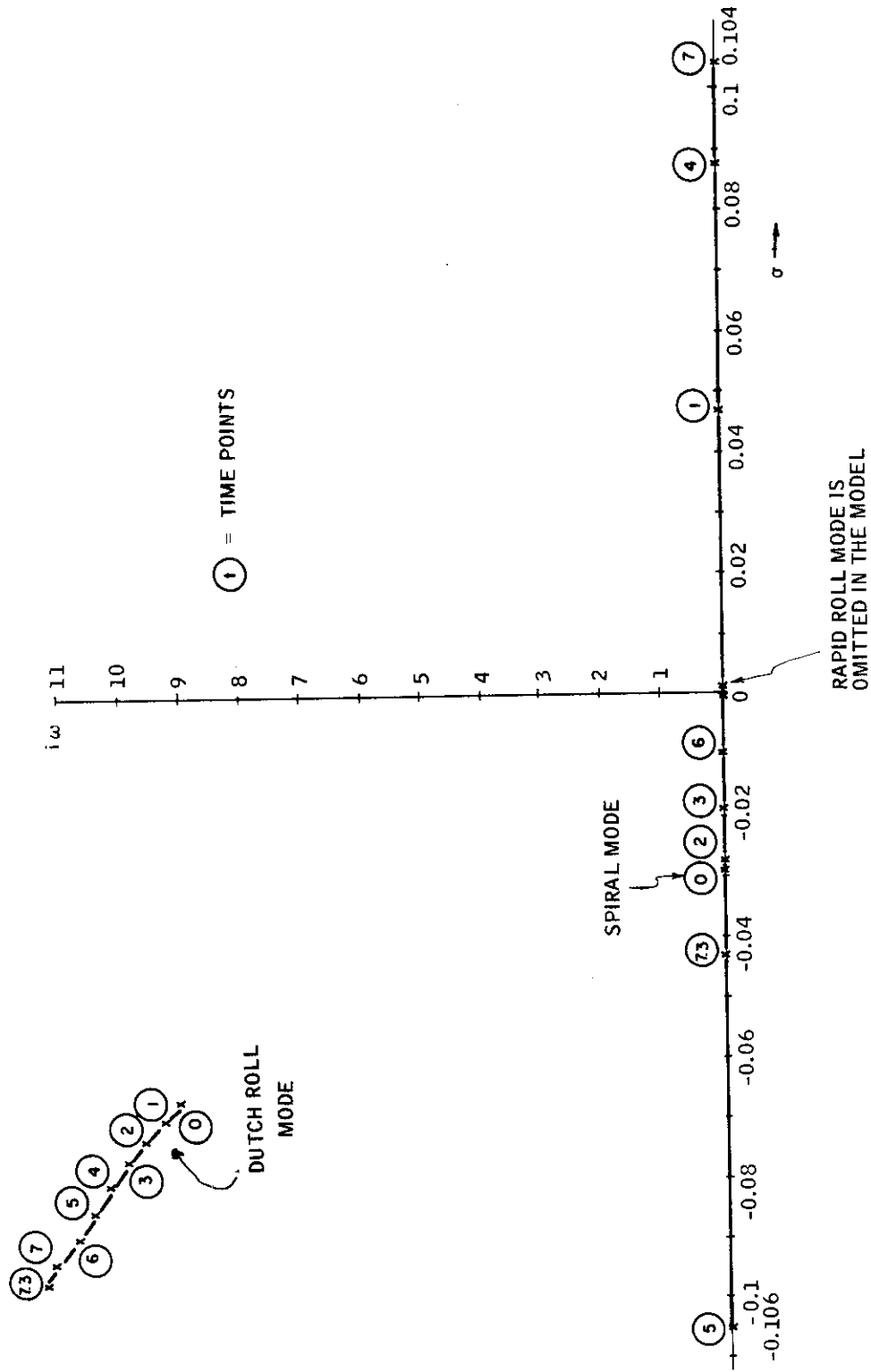


Figure 68. Spectrum of Frozen Point - Lateral Matrix of M117

SECTION V TESTING THE CONTROLLER DESIGN SOFTWARE

The nonstationary optimization program (DISCOP) was debugged using a dynamical system (catalytic cracker) with a known solution. This known solution was for the continuous controller. The sample time of DISCOP which essentially computes discrete controller had to be reduced to 0.001 to approximate the continuous controller. The same steady-state gains were produced by DISCOP.

The second test was conducted for a system described by a set of proper identity matrices. Feedback and estimator gains were computed by DISCOP. The results were identical with the known answers.

The stationary optimization program DIAK was tested similarly. Simple system matrices were used, and the costate, optimal controller gains, minimum estimation error covariance, optimal estimator gains and the total covariance matrices were computed and checked against known answers.

SECTION VI CONTROLLER DESIGN

The linear data obtained from ADAP 1, as previously described, were used for controller design.

The first run was made to determine how much improvement in performance would be obtained by using a controller. For this, first the performance corresponding to the airframe with no controller was evaluated, and the CEP at impact was computed. This was compared against performance with the optimal controller. As expected, a large improvement in the performance (reducing the CEP) was obtained.

To establish the adequacy or inadequacy of the stationary analysis, first a nonstationary optimization program was run, and the CEP at impact was computed with the time-varying controller gains. Next, a time point, nine seconds, was chosen within the airplane flight time interval $0 \leq t \leq 19$ seconds. The linear data of the 9-second time point were used for computing the time-invariant (i. e., steady-state) optimal gains. Subsequently, the CEP at impact was computed with these fixed gains.

In these two iterations it was assumed that the aircraft states were measured completely but imperfectly and the wind states together with the aircraft states had to be estimated. The control points were assumed to be the ailerons, the stabilator, the spoilers and the rudder. The gains corresponding to stationary and nonstationary designs for the 9-second data points are shown in Tables VI, VII and VIII.

No appreciable difference in performance was noticed between the two results. The performance results are summarized in Table IX. On the basis of this experiment, the performance obtained from the fixed-gain optimal system is thought to be satisfactory. We emphasize that the performance computations are based on the actual physical time-varying, finite-time system with a variable or fixed set of gains in it. The steady-state variances of the position and the attitude states of the closed-loop system corresponding to some of the frozen-point linear data are finite but considerably different than that of finite time covariances. This is due to low damping of the position and attitude integrators by the optimal controller.

The output of the performance evaluator (ADAP 3) corresponding to the free airframe is shown in Figure 69. Figure 70 shows the performance outputs with the nonstationary optimal controller. The performance outputs for the fixed-gain optimal controller are shown in Figure 71.

The controller weights corresponding to the stabilator, aileron, rudder and the spoiler were all the same, and the value used in the example was 10^4 . Since the bomb dynamics did not have the roll states p and ϕ , no weightings were computed for these variables when using the impact covariance matrix. The weighting values used for these variables were selected to be:

$$q_\phi = 10^3, q_p = 10^2$$

Table VI. Feedback Gains from Longitudinal States at 9 Seconds

Control	x_e (ft)	h_e (ft)	u (ft/sec)	θ (rad)	q (rad/sec)	w (ft/sec)	Optimization
δ_s (deg)	0.00121	0.00106	0.00545	10.437	1.864	-0.0130	Nonstationary
	0.00124	0.00108	0.00551	10.559	1.863	-0.0133	Stationary
δ_a (deg)	0.000104	0.00009	0.00039	0.86642	0.15553	-0.00106	Nonstationary
	0.000097	0.00008	0.00031	0.76507	0.13655	-0.00094	Stationary
δ_r (deg)	0.000015	0.000013	0.00011	0.15521	0.02688	-0.00020	Nonstationary
	0.000021	0.000018	0.00015	0.21582	0.03684	-0.00028	Stationary
δ_{sp} (deg)	-0.00003	-0.00002	-0.00016	-0.2787	-0.04918	-0.000352	Nonstationary
	-0.00003	-0.00003	-0.00020	-0.32738	-0.05687	-0.000421	Stationary

Table VII. Feedback Gains from Lateral States at 9 Seconds

Control	y_e (ft)	ψ (rad)	r (rad/sec)	v (rad/sec)	ϕ (rad)	p (rad/sec)	Optimization
δ_s (deg)	0.000079	0.6950	0.1603	0.00105	0.1488	0.06737	Nonstationary
	0.000070	0.7030	0.2224	0.00099	0.2093	0.09943	Stationary
δ_a (deg)	-0.00137	-11.412	-2.4919	-0.01759	-2.3055	-1.037	Nonstationary
	-0.00134	-11.548	-3.0831	-0.1721	-2.8890	-1.3530	Stationary
δ_r (deg)	0.001056	8.3445	1.7659	0.01298	1.600	0.7163	Nonstationary
	0.00099	8.077	2.0522	0.01224	1.8752	0.8731	Stationary
δ_{sp} (deg)	-0.00058	-4.8339	-1.0511	-0.0074	-0.9702	-0.4362	Nonstationary
	-0.000571	-4.868	-1.2917	-0.0072	-1.2073	-0.5650	Stationary

Table VIII. Feedback Gains from Wind States at 9 Seconds

Control	w_1 (ft/sec)	w_3 (ft/sec)	w_5	w_2 (ft/sec)	w_4	Optimization
δ_s (deg)	-0.00204	-0.00048	-0.00217	0.000037	0.000145	Nonstationary
	-0.00215	-0.00075	-0.00157	0.000151	0.000650	Stationary
δ_a (deg)	-0.00013	-0.00003	-0.00013	-0.00051	-0.00185	Nonstationary
	-0.00008	-0.00001	-0.00012	-0.00217	-0.00582	Stationary
δ_r (deg)	-0.00005	-0.00001	-0.00006	0.00027	0.001181	Nonstationary
	-0.00008	-0.00003	-0.000001	0.00135	0.00324	Stationary
δ_{sp} (deg)	0.00006	0.000016	0.000075	-0.00021	-0.00077	Nonstationary
	0.00009	0.000038	0.000044	0.00090	-0.00239	Stationary

Table IX. Performance Summary for Different Runs

Description of Run	Variances at the Nominal Impact Time		Variances at the Horizontal Impact Plane		Horizontal CEP	Variances at the Vertical Impact Plane		Vertical CEP
	σ_x^2	σ_y^2	$\tilde{\sigma}_x^2$	$\tilde{\sigma}_y^2$		$\tilde{\sigma}_h^2$	$\tilde{\sigma}_v^2$	
Free airframe	58430	59212	17099	59212	337.7	143940	59212	364.29
Nonstationary optimal controller	17386	1052	19412	1052.8	27.77	201.5	1052.8	28.96
Fixed-gain optimal controller	17581	870	22343	870.0	32.27	849.98	870.0	34.31

INITIAL COVARIANCE OF RBMB

RBW 1	.33478E 05	.80399E 04	.28117E 03	.26896E 01	.48895E-01	-.34751E 00	.12140E 02	-.28100E-13	.72533E-14	.44572E-12
	-.52562E 01	-.43002E 01	.43174E 00	.00000E 00	.00000E 00					
RBW 2	.80399E 04	.70649E 04	-.89702E 02	.71480E 00	-.45088E-01	.11704E 01	.39441E-09	.23204E-13	-.59896E-14	-.36807E-12
	-.19701E 02	-.22112E 01	-.12014E 00	.00000E 00	.00000E 00					
RBW 3	.28117E 03	-.89702E 02	.33195E 02	.18339E-01	.22762E-02	.23915E 00	-.10616E-10	-.62459E-15	.16122E-15	.99072E-14
	.20555E 01	-.35162E 00	.37054E-01	.00000E 00	.00000E 00					
RBW 4	.26896E 01	.71480E 00	.18539E-01	.23372E-03	.37864E-05	.11196E-01	.81913E-14	.48192E-18	-.12440E-18	-.76442E-17
	-.52864E-02	.83308E-02	.69035E-03	.00000E 00	.00000E 00					
RBW 5	.48895E-01	-.45088E-01	.22762E-02	.37864E-05	.11804E-04	.15403E-02	.32787E-14	.19290E-18	-.49791E-19	-.30597E-17
	-.23661E-02	.26874E-02	.46213E-03	.00000E 00	.00000E 00					
RBW 6	.34751E 00	.11704E 01	.23915E 00	.11196E-01	.15403E-02	.16497E 02	.37896E-11	.22296E-15	-.57551E-16	-.35365E-14
	-.13524E 00	.90336E 01	.72884E 00	.00000E 00	.00000E 00					
RBW 7	.12140E 02	.39441E-09	-.10616E-10	.81913E-14	.32787E-14	.37896E-11	.27398E 05	.30982E 01	.27916E-02	-.21837E 02
	.00000E 00	.00000E 00	.00000E 00	.15381E 01	-.22529E 00					
RBW 8	-.28100E-13	.23204E-13	-.62459E-15	.48192E-18	.19290E-18	.22296E-15	.30982E 01	.43224E-03	-.15450E-05	-.23888E-01
	.00000E 00	.00000E 00	.00000E 00	-.13414E-01	-.11648E-02					
RBW 9	.72533E-14	-.59896E-14	.16122E-15	.36721E-02	-.61270E-03	-.57551E-16	.27916E-02	-.15450E-05	.10762E-03	-.44409E-03
	.00000E 00	.00000E 00	.00000E 00	.00000E 00	.00000E 00					
RBW 10	.44572E-12	-.36807E-12	.99072E-14	.76442E-17	-.30597E-17	-.35365E-14	-.21837E 02	-.23888E-01	-.44409E-03	.21057E 02
	.00000E 00	.00000E 00	.00000E 00	.93049E 01	.77086E 00					
RBW 11	-.52562E 01	-.43002E 01	.43174E 00	.20555E 01	-.52944E-02	-.13524E 00	.00000E 00	.00000E 00	.00000E 00	.00000E 00
	.98318E 01	.00000E 00	.00000E 00	.00000E 00	.00000E 00					
RBW 12	-.43002E 01	-.22112E 01	-.35162E 00	.83308E-02	.26874E-02	.90336E 01	.00000E 00	.00000E 00	.00000E 00	.00000E 00
	.00000E 00	.95895E 01	.82433E 00	.00000E 00	.00000E 00					
RBW 13	.43174E 00	-.12014E 00	.37054E-01	.69035E-03	.46213E-03	.72884E 00	.00000E 00	.00000E 00	.00000E 00	.00000E 00
	.00000E 00	.32433E 00	.30732E-01	.00000E 00	.00000E 00					
RBW 14	.00000E 00	.00000E 00	.00000E 00	.00000E 00	.00000E 00	.00000E 00	.15381E 01	-.13414E-01	-.36721E-02	.93049E 01
	.00000E 00	.00000E 00	.00000E 00	.00000E 00	.00000E 00					
RBW 15	.00000E 00	.00000E 00	.00000E 00	.00000E 00	.00000E 00	.00000E 00	.00000E 00	-.22529E 00	-.11648E-02	-.61270E-03
	.00000E 00	.00000E 00	.00000E 00	.00000E 00	.00000E 00					

Figure 69. Performance Evaluator Output - Free Airframe

XSUBF BATHIX I= 4.28

R8W 1	60394E 00	-22304E 00	17036E 00	-26569E-04	18072E-03	-34479E-01	-69096E-09	-10555E-11	-95899E-12	46555E+09
R8W 2	20729E 00	-21954E-02	23953E-01	46564E-03	19755E-08					
R8W 3	62304E 00	58341E 00	-19133E 00	-33500E-04	15761E-03	-30660E-01	00000E 00	00000E 00	00000E 00	00000E 00
R8W 4	21732E 00	-85040E-02	16660E-01	00000E 00	00000E 00					
R8W 5	17936E 00	-19133E 00	62515E-01	-10596E-04	-65221E-05	-11883E-01	00000E 00	00000E 00	00000E 00	00000E 00
R8W 6	26569E-04	-33500E-04	10596E-04	42610E-04	91194E-05	41113E-01	00000E 00	00000E 00	00000E 00	00000E 00
R8W 7	23479E-04	10553E-01	14673E-01	00000E 00	00000E 00					
R8W 8	18072E-03	15761E-03	-65221E-05	91194E-05	58511E-02	14627E-01	00000E 00	00000E 00	00000E 00	00000E 00
R8W 9	43567E-04	10335E 00	44073E 00	00000E 00	00000E 00					
R8W 10	3479E-01	-30660E-01	-11883E-01	41113E-01	14627E-01	39676E 02	00000E 00	00000E 00	00000E 00	00000E 00
R8W 11	17314E-01	19745E 02	14602E 02	00000E 00	00000E 00					
R8W 12	69096E-09	00000E 00	00000E 00	00000E 00	00000E 00	00000E 00	36046E-01	-36501E-03	36531E-03	24418E 00
R8W 13	00000E 00	00000E 00	00000E 00	19077E 00	61763E-02					
R8W 14	10555E-11	00000E 00	00000E 00	00000E 00	00000E 00	00000E 00	-36601E-03	25254E-03	75961E-04	-16194E 00
R8W 15	00000E 00	00000E 00	00000E 00	-10390E 00	-59320E-01					
R8W 16	95899E-12	00000E 00	00000E 00	00000E 00	00000E 00	00000E 00	36531E-03	75961E-04	74214E-02	-57265E+01
R8W 17	00000E 00	00000E 00	00000E 00	-18401E 00	-14661E 00					
R8W 18	46555E-09	00000E 00	00000E 00	00000E 00	00000E 00	00000E 00	24418E 00	-16194E 00	-57265E+01	10386E 03
R8W 19	20729E 00	-21632E 00	43977E 00	23447E-04	43567E-04	17814E-01	00000E 00	00000E 00	00000E 00	00000E 00
R8W 20	64663E 02	00000E 00	00000E 00	00000E 00	00000E 00					
R8W 21	91954E-02	-85040E-02	-29561E-02	10552E-01	10938E 00	10315E 02	00000E 00	00000E 00	00000E 00	00000E 00
R8W 22	00000E 00	17072E 02	49839E 02	00000E 00	00000E 00					
R8W 23	23533E-01	16660E-01	-40228E-02	14673E-01	44073E 00	14602E 02	00000E 00	00000E 00	00000E 00	00000E 00
R8W 24	00000E 00	49839E 02	17389E 03	00000E 00	00000E 00					
R8W 25	46546E-09	00000E 00	00000E 00	00000E 00	00000E 00	00000E 00	19077E 00	-10390E 00	-18401E 00	66839E 02
R8W 26	00000E 00	00000E 00	00000E 00	71744E 02	42611E 02					
R8W 27	19755E-08	00000E 00	00000E 00	00000E 00	00000E 00	00000E 00	61763E-02	-59320E-01	-14661E 00	38155E 02
R8W 28	00000E 00	00000E 00	00000E 00	42611E 02	27159E 02					

Figure 69. Performance Evaluator Output - Free Airframe (continued)

PHI(T,TR) MATRIX

R0W 1	.20172E-02	.49408E 01	.33662E 04	.45008E 01	--.40420E 01	.00000E 00	.18626E-05	.37485E-08	.28731E-08
.10000E 01	.24374E 00	.26440E 00	--.74333E-09	--.27066E-08					
R0W 2	.00000E 00	.93811E 00	.35517E 01	.40640E 04	.54825E 01	.00000E 00	.00000E 00	.00000E 00	.00000E 00
--.78244E-01	--.24596E 00	--.34527E 00	.00000E 00	.00000E 00	--.46249E 01	.00000E 00	.00000E 00	.00000E 00	.00000E 00
R0W 3	.00000E 00	.91130E+03	.90393E 00	--.12584E 03	.12189E 00	.00000E 00	.00000E 00	.00000E 00	.00000E 00
.29157E-01	.62774E-01	.84009E-01	.00000E 00	.00000E 00					
R0W 4	.00000E 00	.59415E+07	.23798E-03	.84406E 00	.11545E-02	.00000E 00	.00000E 00	.00000E 00	.00000E 00
.48130E-05	.55006E-05	--.12574E-04	.00000E 00	.00000E 00					
R0W 5	.00000E 00	.16224E-07	.15072E-04	--.23961E-01	.70367E-04	.00000E 00	.00000E 00	.00000E 00	.00000E 00
.47200E-06	.44400E-05	.46416E-06	.00000E 00	.00000E 00	.24306E-04	.00000E 00	.00000E 00	.00000E 00	.00000E 00
R0W 6	.00000E 00	--.12225E-05	--.47617E-03	.37410E 00	.17895E-01	.00000E 00	.00000E 00	.00000E 00	.00000E 00
--.16530E-05	.20554E-05	--.23702E-02	.00000E 00	.00000E 00					
R0W 7	.00000E 00	.00000E 00	.00000E 00	.00000E 00	.00000E 00	.10000E 01	.40807E 04	.83505E 01	.62797E 01
.00000E 00	.00000E 00	.00000E 00	.00000E 00	.00000E 00	.00000E 00	.00000E 00	.00000E 00	.00000E 00	.00000E 00
R0W 8	.00000E 00	.00000E 00	.00000E 00	.00000E 00	.00000E 00	.00000E 00	.00000E 00	.00000E 00	.00000E 00
.00000E 00	.00000E 00	.00000E 00	.00000E 00	.00000E 00	.00000E 00	.00000E 00	.00000E 00	.00000E 00	.00000E 00
R0W 9	.00000E 00	.00000E 00	.00000E 00	.00000E 00	.00000E 00	.00000E 00	.00000E 00	.00000E 00	.00000E 00
.00000E 00	.00000E 00	.00000E 00	.00000E 00	.00000E 00	.00000E 00	.00000E 00	.00000E 00	.00000E 00	.00000E 00
R0W 10	.00000E 00	.00000E 00	.00000E 00	.00000E 00	.00000E 00	.00000E 00	.00000E 00	.00000E 00	.00000E 00
.00000E 00	.00000E 00	.00000E 00	.00000E 00	.00000E 00	.00000E 00	.00000E 00	.00000E 00	.00000E 00	.00000E 00
R0W 11	.00000E 00	.00000E 00	.00000E 00	.00000E 00	.00000E 00	.00000E 00	.00000E 00	.00000E 00	.00000E 00
.41583E+01	.00000E 00	.00000E 00	.00000E 00	.00000E 00	.00000E 00	.00000E 00	.00000E 00	.00000E 00	.00000E 00
R0W 12	.00000E 00	.00000E 00	.00000E 00	.00000E 00	.00000E 00	.00000E 00	.00000E 00	.00000E 00	.00000E 00
.00000E 00	.00000E 00	.00000E 00	.00000E 00	.00000E 00	.00000E 00	.00000E 00	.00000E 00	.00000E 00	.00000E 00
R0W 13	.00000E 00	.00000E 00	.00000E 00	.00000E 00	.00000E 00	.00000E 00	.00000E 00	.00000E 00	.00000E 00
.00000E 00	.00000E 00	.00000E 00	.00000E 00	.00000E 00	.00000E 00	.00000E 00	.00000E 00	.00000E 00	.00000E 00
R0W 14	.00000E 00	.00000E 00	.00000E 00	.00000E 00	.00000E 00	.00000E 00	.00000E 00	.00000E 00	.00000E 00
.00000E 00	.00000E 00	.00000E 00	.00000E 00	.00000E 00	.00000E 00	.00000E 00	.00000E 00	.00000E 00	.00000E 00
R0W 15	.00000E 00	.00000E 00	.00000E 00	.00000E 00	.00000E 00	.00000E 00	.00000E 00	.00000E 00	.00000E 00
.00000E 00	.00000E 00	.00000E 00	.00000E 00	.00000E 00	.00000E 00	.00000E 00	.00000E 00	.00000E 00	.00000E 00
.00000E 00	.00000E 00	.00000E 00	.00000E 00	.00000E 00	.00000E 00	.00000E 00	.00000E 00	.00000E 00	.00000E 00

Figure 69. Performance Evaluator Output - Free Airframe (continued)

X(T) MATRIX

R6W 1	.58430E 05	.22643E 05	.19286E 02	.31226E 01	.77186E+01	.10357E 01	.42140E 02	.75918E+09	.80676E-12	.59646E+09
R6W 2	.26856E 00	-.11685E-01	-.24896E-01	.59308E-09	.21799E-08	.60687E 00	.55182E+09	.25651E-13	-.18315E-17	.59068E+16
R6W 3	.22643E 05	.17099E 09	.31187E 03	.13041E 01	.39556E+01	.29250E+01	.12102E+10	.56255E+15	.40167E-19	.12954E+17
R6W 4	.22392E 01	-.11544E-01	-.59551E-02	.00000E 00	.00000E 00	.41174E-01	.83351E-15	.38745E+19	-.27665E-23	.89220E+22
R6W 5	.19296E 02	.31187E 03	.26491E 02	-.34648E-02	.69077E-03	.14625E-01	.39676E 02	.81958E-18	-.27202E+22	.87729E+21
R6W 6	.55526E 00	.30732E-02	-.43378E-02	.00000E 00	.00000E 00	.14625E-01	.39676E 02	.81958E-18	-.27202E+22	.87729E+21
R6W 7	.31226E 01	.15701E 01	-.34648E-02	.21577E-03	.47371E-05	.41174E-01	.83351E-15	.38745E+19	-.27665E-23	.89220E+22
R6W 8	.13475E-03	.16351E-01	.14668E-01	.00000E 00	.00000E 00	.14625E-01	.39676E 02	.81958E-18	-.27202E+22	.87729E+21
R6W 9	.77186E-01	-.39556E-01	.69077E-03	.47371E-05	.58512E-02	.41174E-01	.83351E-15	.38745E+19	-.27665E-23	.89220E+22
R6W 10	.00000E 00	.10315E 02	.44073E 00	.00000E 00	.00000E 00	.14625E-01	.39676E 02	.81958E-18	-.27202E+22	.87729E+21
R6W 11	.10357E 01	.50687E 00	.29250E+01	.41174E-01	.14625E+01	.41174E-01	.83351E-15	.38745E+19	-.27665E-23	.89220E+22
R6W 12	.12140E 02	.55182E-09	-.12102E-10	.83351E-15	.31782E-15	.41174E-01	.83351E-15	.38745E+19	-.27665E-23	.89220E+22
R6W 13	.00000E 00	.00000E 00	.00000E 00	.61455E-01	-.13013E 00	.14625E-01	.39676E 02	.81958E-18	-.27202E+22	.87729E+21
R6W 14	.75918E+09	.25651E-13	.56255E+15	.38745E+19	.14774E-19	.41174E-01	.83351E-15	.38745E+19	-.27665E-23	.89220E+22
R6W 15	.80676E-12	.59646E-09	.59060E 00	.59060E 00	.59349E-01	.41174E-01	.83351E-15	.38745E+19	-.27665E-23	.89220E+22
R6W 16	.59646E-09	.59060E-16	.12954E-17	.89220E+22	-.34020E-22	.41174E-01	.83351E-15	.38745E+19	-.27665E-23	.89220E+22
R6W 17	.00000E 00	.00000E 00	.00000E 00	.66842E 02	.38150E 02	.14625E-01	.39676E 02	.81958E-18	-.27202E+22	.87729E+21
R6W 18	.26856E 00	.22392E 01	.55526E 00	.13475E-03	.50171E-04	.17691E-01	.00000E 00	.00000E 00	.00000E 00	.00000E 00
R6W 19	.64680E 02	.00000E 00	.00000E 00	.00000E 00	.00000E 00	.10315E 02	.00000E 00	.00000E 00	.00000E 00	.00000E 00
R6W 20	.16955E-01	.11348E-01	.43053E-02	.49839E 02	.10938E 00	.10315E 02	.00000E 00	.00000E 00	.00000E 00	.00000E 00
R6W 21	.24906E-01	.59551E-02	-.43378E-02	.14668E-01	.44073E 00	.14660E 02	.00000E 00	.00000E 00	.00000E 00	.00000E 00
R6W 22	.00000E 00	.49839E 02	.17389E 03	.00000E 00	.00000E 00	.14660E 02	.00000E 00	.00000E 00	.00000E 00	.00000E 00
R6W 23	.59308E-09	.00000E 00	.00000E 00	.00000E 00	.00000E 00	.00000E 00	.00000E 00	.00000E 00	.00000E 00	.00000E 00
R6W 24	.00000E 00	.00000E 00	.00000E 00	.71747E 02	.42616E 02	.00000E 00	.61455E+01	-.10393E 00	.18400E 00	.14660E 02
R6W 25	.21799E-08	.00000E 00	.00000E 00	.00000E 00	.00000E 00	.00000E 00	.00000E 00	.00000E 00	.00000E 00	.00000E 00
R6W 26	.00000E 00	.00000E 00	.00000E 00	.42616E 02	.27167E 02	.00000E 00	.00000E 00	.00000E 00	.00000E 00	.00000E 00

Figure 69. Performance Evaluator Output - Free Airframe (continued)

XSDM 715 0411A

RBW 1	.42706E 01	.44558E 01	.12140E 02	.75921E 09	.38592E 12	.79234E 09
RBW 2	.45775E 03	.81810E 02	.21799E 04	.00000E 00	.00000E 00	.00000E 00
RBW 3	.00000E 00	.00000E 00	.00000E 00	.00000E 00	.00000E 00	.00000E 00
RBW 4	.28156E 01	.88335E 04	.59411E 16	.32507E 14	.53389E 12	
RBW 5	.21420E 02	.44148E 00	.00000E 00	.00000E 00	.00000E 00	
RBW 6	.28156E 01	.70217E 05	.12563E 10	.38746E 19	.41260E 16	.67763E 14
RBW 7	.20228E 01	.28301E 02	.00000E 00	.00000E 00	.00000E 00	
RBW 8	.46248E 04	.44049E 00	.14625E 01	.30164E 19	.30372E 18	.49882E 16
RBW 9	.00000E 00	.46670E 02	.18407E 10	.23447E 17	.60616E 16	.99554E 14
RBW 10	.41274E 01	.14625E 01	.59212E 05	.47316E 01	.19951E 03	.11420E 00
RBW 11	.12140E 02	.18885E 09	.12563E 10	.93131E 13	.75954E 04	.74214E 02
RBW 12	.11126E 12	.61455E 01	.13013E 00	.00000E 00	.00000E 00	
RBW 13	.00000E 00	.38746E 19	.30164E 19	.23447E 17	.66117E 03	.75954E 04
RBW 14	.00000E 00	.11134E 15	.10393E 00	.59349E 01	.60616E 16	.19951E 03
RBW 15	.38746E 19	.41274E 01	.12563E 10	.93131E 13	.75954E 04	.74214E 02
RBW 16	.00000E 00	.11134E 15	.10393E 00	.59349E 01	.60616E 16	.19951E 03
RBW 17	.00000E 00	.11134E 15	.10393E 00	.59349E 01	.60616E 16	.19951E 03
RBW 18	.00000E 00	.11134E 15	.10393E 00	.59349E 01	.60616E 16	.19951E 03
RBW 19	.00000E 00	.11134E 15	.10393E 00	.59349E 01	.60616E 16	.19951E 03
RBW 20	.00000E 00	.11134E 15	.10393E 00	.59349E 01	.60616E 16	.19951E 03
RBW 21	.00000E 00	.11134E 15	.10393E 00	.59349E 01	.60616E 16	.19951E 03
RBW 22	.00000E 00	.11134E 15	.10393E 00	.59349E 01	.60616E 16	.19951E 03
RBW 23	.00000E 00	.11134E 15	.10393E 00	.59349E 01	.60616E 16	.19951E 03
RBW 24	.00000E 00	.11134E 15	.10393E 00	.59349E 01	.60616E 16	.19951E 03
RBW 25	.00000E 00	.11134E 15	.10393E 00	.59349E 01	.60616E 16	.19951E 03
RBW 26	.00000E 00	.11134E 15	.10393E 00	.59349E 01	.60616E 16	.19951E 03
RBW 27	.00000E 00	.11134E 15	.10393E 00	.59349E 01	.60616E 16	.19951E 03
RBW 28	.00000E 00	.11134E 15	.10393E 00	.59349E 01	.60616E 16	.19951E 03
RBW 29	.00000E 00	.11134E 15	.10393E 00	.59349E 01	.60616E 16	.19951E 03
RBW 30	.00000E 00	.11134E 15	.10393E 00	.59349E 01	.60616E 16	.19951E 03
RBW 31	.00000E 00	.11134E 15	.10393E 00	.59349E 01	.60616E 16	.19951E 03
RBW 32	.00000E 00	.11134E 15	.10393E 00	.59349E 01	.60616E 16	.19951E 03
RBW 33	.00000E 00	.11134E 15	.10393E 00	.59349E 01	.60616E 16	.19951E 03
RBW 34	.00000E 00	.11134E 15	.10393E 00	.59349E 01	.60616E 16	.19951E 03
RBW 35	.00000E 00	.11134E 15	.10393E 00	.59349E 01	.60616E 16	.19951E 03
RBW 36	.00000E 00	.11134E 15	.10393E 00	.59349E 01	.60616E 16	.19951E 03
RBW 37	.00000E 00	.11134E 15	.10393E 00	.59349E 01	.60616E 16	.19951E 03
RBW 38	.00000E 00	.11134E 15	.10393E 00	.59349E 01	.60616E 16	.19951E 03
RBW 39	.00000E 00	.11134E 15	.10393E 00	.59349E 01	.60616E 16	.19951E 03
RBW 40	.00000E 00	.11134E 15	.10393E 00	.59349E 01	.60616E 16	.19951E 03
RBW 41	.00000E 00	.11134E 15	.10393E 00	.59349E 01	.60616E 16	.19951E 03
RBW 42	.00000E 00	.11134E 15	.10393E 00	.59349E 01	.60616E 16	.19951E 03
RBW 43	.00000E 00	.11134E 15	.10393E 00	.59349E 01	.60616E 16	.19951E 03
RBW 44	.00000E 00	.11134E 15	.10393E 00	.59349E 01	.60616E 16	.19951E 03
RBW 45	.00000E 00	.11134E 15	.10393E 00	.59349E 01	.60616E 16	.19951E 03
RBW 46	.00000E 00	.11134E 15	.10393E 00	.59349E 01	.60616E 16	.19951E 03
RBW 47	.00000E 00	.11134E 15	.10393E 00	.59349E 01	.60616E 16	.19951E 03
RBW 48	.00000E 00	.11134E 15	.10393E 00	.59349E 01	.60616E 16	.19951E 03
RBW 49	.00000E 00	.11134E 15	.10393E 00	.59349E 01	.60616E 16	.19951E 03
RBW 50	.00000E 00	.11134E 15	.10393E 00	.59349E 01	.60616E 16	.19951E 03

CEP HORIZONTAL = .34773675E 03 CEP VERTICAL = .16410525E 03

Figure 69. Performance Evaluator Output - Free Airframe (continued)

WEIGHTING MATRIX GH

ROW 1	.15708E 01	.13834E 01	.28494E 01	.10908E 05	.14651E 02	-.12745E 02	.00000E 00	.29258E 05	.58881E 08	.45131E 08
	.49917E 01	.49377E 01	-.59603E 01	-.11674E 08	-.42515E 08					
ROW 2	.13834E 01	.12184E 01	.25095E 01	.96064E 04	.12303E 02	-.11224E 02	-.30208E 10	.24535E 05	.49334E 08	.37850E 08
	.43962E 01	.49404E 01	-.51864E 01	-.10263E 08	-.37458E 08					
ROW 3	.28494E 01	.25095E 01	.51489E 01	.19787E 05	.26578E 02	.23119E 02	.10750E 09	.57462E 05	.11579E 07	.88619E 08
	.90550E 01	.83222E 01	-.10703E 00	-.21252E 08	-.77067E 08					
ROW 4	.10908E 05	.26064E 04	.19787E 05	.75742E 08	.10174E 06	-.88499E 05	-.12300E 06	.19815E 01	.39860E 04	.30567E 04
	.34662E 03	.31857E 03	-.40971E 03	-.80998E 05	-.29529E 04					
ROW 5	.14651E 02	.12303E 02	.26578E 02	.10174E 06	.13666E 03	-.11887E 03	-.16593E 09	.26613E 04	.53534E 07	.41053E 07
	.46559E 00	.42791E 00	-.55033E 00	-.10880E 07	-.39663E 07					
ROW 6	.11274E 02	-.11224E 02	.23119E 02	-.88499E 05	-.11887E 03	.10340E 03	.13998E 09	-.23168E 04	-.46604E 07	-.35738E 07
	.40500E 00	-.37222E 00	.47872E 00	.94642E 08	.34502E 07					
ROW 7	.00000E 00	.30208E 10	.10750E 09	-.12300E 06	-.16593E 09	.13998E 09	.31416E 01	.12820E 05	.26234E 02	.19728E 02
	.23681E 11	.74441E 11	.10450E 10	-.20891E 00	.16120E 00					
ROW 8	.29258E 05	.24535E 05	.57462E 05	.19815E 01	.26013E 04	-.23168E 04	.12820E 05	.52313E 08	.10705E 06	.80505E 05
	.10264E 06	.11583E 06	.67259E 07	-.85249E 03	.65781E 03					
ROW 9	.58881E 08	.49134E 08	.11579E 07	.39860E 04	.53534E 07	-.46604E 07	.26234E 02	.10705E 06	.21907E 03	.16474E 03
	.20683E 09	.23413E 09	-.13391E 09	-.17445E 01	.13461E 01					
ROW 10	.45131E 08	.37850E 08	.88619E 08	.30567E 04	.41053E 07	-.35738E 07	.19728E 02	.80505E 05	.16474E 03	.12389E 03
	.15229E 09	.17454E 09	-.10390E 09	-.13119E 01	.10123E 01					
ROW 11	.39917E 01	.43962E 01	.90550E 01	.34662E 03	.46559E 00	-.40500E 00	.23681E 11	.10264E 06	.20689E 09	.15829E 09
	.15863E 02	.14579E 02	-.18750E 02	-.37222E 10	-.13998E 09					
ROW 12	.45377E 01	.40404E 01	.83222E 01	.31857E 03	.42791E 00	-.37222E 00	.74441E 11	.11583E 06	.23413E 09	.17856E 09
	.14579E 02	.13399E 02	-.17232E 02	-.34597E 10	-.12379E 09					
ROW 13	.29208E 01	-.51364E 01	-.10703E 00	-.40971E 03	-.55033E 00	.47872E 00	.10450E 10	-.67259E 07	-.13391E 09	-.10390E 09
	-.18750E 02	-.17232E 02	.22183E 02	.43164E 10	.16223E 09					
ROW 14	.11674E 08	-.10263E 08	-.80998E 05	-.10880E 07	-.13892E 01	.84642E 08	-.20891E 00	-.85249E 03	-.17445E 01	-.13119E 01
	-.37222E 10	-.34507E 10	.43164E 10	.13892E 01	-.10720E 01					
ROW 15	.42515E 08	.37458E 08	-.77067E 08	-.29529E 04	-.39663E 07	.34502E 07	.16120E 00	.65781E 03	.13461E 01	.10123E 01
	-.13494E 09	-.12379E 09	.16093E 09	-.10720E 01	.82717E 02					

Figure 69. Performance Evaluator Output - Free Airframe (continued)

WEIGHTING TABLE CV

RBW 1	.1750E-01	.3676E-01	.1407E-05	.1890E-02	.1644E-02	.3437E-10	.3915E-05	.7884E-08	.6039E-08
.6440E-01	.3619E-01	.7613E-01	.1528E-08	.4543E-08					
RBW 2	.1735E-01	.1573E-01	.3238E-01	.1239E-05	.1654E-02	.1448E-02	.6935E-13	.3325E-05	.6691E-08
.5672E-01	.6215E-01	.4704E-01	.1326E-08	.4483E-08					
RBW 3	.3676E-01	.3238E-01	.4669E-01	.2533E-05	.3429E-02	.2983E-02	.1698E-09	.7541E-05	.1523E-07
.1144E-00	.1078E-00	.1310E-00	.2744E-04	.4994E-04					
RBW 4	.1407E-05	.1239E-05	.3553E-05	.9729E-08	.1312E-06	.1141E-06	.1157E-06	.2668E-04	.7215E-07
.4472E-03	.4115E-03	.5286E-03	.1046E-04	.3808E-04					
RBW 5	.1890E-02	.1407E-02	.3429E-02	.1312E-06	.1763E-03	.1533E-03	.1547E-09	.3584E-04	.7215E-07
.6007E-00	.5512E-00	.7109E-00	.1406E-07	.5113E-07					
RBW 6	.1644E-02	.1448E-02	.4293E-02	.1141E-06	.1533E-03	.1334E-03	.1389E-09	.3119E-04	.6280E-07
.5225E-00	.4812E-00	.6174E-00	.1293E-07	.4450E-07					
RBW 7	.3437E-10	.5930E-10	.1698E-09	.1157E-06	.1547E-03	.1389E-09	.3141E-01	.1282E-05	.2623E-02
.3460E-11	.3443E-11	.6152E-11	.2089E-00	.1612E-00					
RBW 8	.3915E-05	.3238E-05	.7541E-05	.2648E-04	.3584E-04	.3119E-04	.1282E-05	.5231E-08	.1070E-06
.1340E-06	.1447E-06	.1044E-06	.8524E-03	.6578E-03					
RBW 9	.7884E-08	.6619E-08	.1528E-07	.5372E-04	.7215E-07	.6280E-07	.1070E-06	.2190E-03	.1647E-03
.2703E-03	.2943E-03	.2089E-03	.1744E-01	.1346E-01					
RBW 10	.6039E-08	.5169E-08	.1163E-07	.4116E-04	.5528E-07	.4811E-07	.1972E-02	.8050E-05	.1647E-03
.2072E-03	.2243E-03	.1612E-03	.1311E-01	.1012E-01					
RBW 11	.6440E-01	.5673E-01	.1163E-00	.4472E-03	.6007E-00	.5225E-00	.3460E-11	.1340E-06	.2703E-09
.2046E-03	.1811E-03	.2413E-03	.4810E-10	.1744E-09					
RBW 12	.5913E-01	.5213E-01	.1073E-00	.4110E-03	.5512E-00	.4802E-00	.8448E-11	.1447E-06	.2924E-09
.1811E-02	.1739E-02	.1293E-02	.4456E-10	.1597E-09					
RBW 13	.7613E-01	.6744E-01	.1351E-00	.5286E-03	.7109E-00	.6176E-00	.9158E-11	.1044E-06	.2088E-09
.2419E-03	.2293E-03	.2849E-03	.5591E-10	.2052E-09					
RBW 14	.1508E-08	.1326E-08	.2744E-03	.1104E-07	.1406E-07	.1223E-07	.2089E-00	.8524E-03	.1744E-01
.4812E-11	.4456E-11	.5589E-11	.1329E-01	.1072E-01					
RBW 15	.5483E-02	.4812E-02	.9942E-03	.3308E-04	.5115E-07	.4450E-07	.1612E-00	.6578E-03	.1346E-01
.1741E-09	.1527E-09	.2065E-09	.1072E-01	.8271E-02					

GV(1,1) = .1670763E 01 GV(7,7) = .31415926E 01 GV(2,2) = .15707963E 01 GV(7,7) = .31415926E 01

JSUBH= .36124401E 06 JSUBV= .44210889E 06

APPROXIMATE CEPH= .33909813E 03 APPROXIMATE CEPV= .36218550E 03

STEP 00000000

Figure 69. Performance Evaluator Output - Free Airframe (concluded)

INITIAL COVARIANCE OF BOMB

ROW 1	1.1231E+04	-1.2100E+04	6.2666E+02	-1.2345E-01	2.8161E-01	-1.9587E+01	5.1099E+01	1.2963E-02	3.0050E-03	1.7084E+00
ROW 2	-2.7736E-01	-1.7128E+00	-1.7599E-01	1.5678E+00	-3.1939E-03					
ROW 3	-1.2100E+04	1.3132E+04	-6.7626E+02	1.2800E-01	-3.0198E-01	1.7482E+01	-4.4949E+01	-5.5781E-04	-5.0576E-03	-1.3407E+01
ROW 4	-1.7670E+00	-1.1718E+00	-1.3584E-01	-1.3042E+01	-3.8957E+00					
ROW 5	6.2666E+02	-6.7626E+02	3.5253E+01	-7.1777E-03	1.5715E-02	-1.0999E+00	3.3424E+00	-1.9828E-03	3.9143E-04	1.9876E+00
ROW 6	3.6175E-01	-1.2104E-01	-1.0527E-02	1.9570E+00	6.5051E-01					
ROW 7	-1.2345E-01	1.2800E-01	-7.1777E-03	6.5759E-06	-2.8379E-06	4.1604E-03	-2.4884E-03	2.8134E-06	1.7130E-07	-1.6643E-03
ROW 8	-6.9085E-04	3.4602E-03	5.0477E-04	-1.6427E-03	-8.5289E-04					
ROW 9	2.8161E-01	-3.0198E-01	1.5715E-02	-2.8379E-06	1.1033E-05	3.0757E-04	8.9617E-04	2.7456E-06	4.6916E-07	-1.5797E-03
ROW 10	-8.9391E-04	1.2425E-03	2.4739E-04	-1.5909E-03	-9.3084E-04					
ROW 11	-1.9587E+01	1.7482E+01	-1.0999E+00	4.1604E-03	3.0757E-04	4.1791E+00	-2.0236E-02	-2.3719E-04	4.6128E-05	1.2378E-01
ROW 12	1.0549E-02	3.7253E+00	5.5411E-01	1.3357E-01	3.3837E-02					
ROW 13	5.1099E+01	-4.4949E+01	3.3424E+00	-2.4884E-03	8.9617E-04	-2.0236E-02	7.2908E+02	-1.7118E-01	-2.5842E-03	3.1442E+01
ROW 14	1.3947E+00	1.0625E-02	5.8381E-04	3.3863E+01	6.7822E+00					
ROW 15	1.2963E-02	-5.5781E-04	-1.9828E-03	2.8134E-06	2.7456E-06	-2.3719E-04	-1.7118E-01	1.8891E-04	-1.0990E-05	-7.6143E-02
ROW 16	-7.8881E-03	3.7539E-06	2.5662E-07	-7.3660E-02	-1.9230E-02					
ROW 17	3.0050E-03	-5.0576E-03	3.9143E-04	1.7130E-07	4.6916E-07	4.6128E-05	-2.5842E-03	-1.0990E-05	3.2515E-05	8.8942E-03
ROW 18	-7.5286E-04	2.1750E-07	2.4026E-08	7.4394E-03	8.2861E-04					
ROW 19	1.7084E+00	-1.3407E+01	1.9876E+00	-1.6643E-03	-1.5797E-03	1.2378E-01	3.1442E+01	-7.6143E-02	8.8942E-03	5.2942E+01
ROW 20	5.4030E+00	-2.2603E-05	-2.2352E-06	5.0479E+01	1.3201E+01					
ROW 21	-2.7736E-01	-1.7670E+00	3.6175E-01	-6.9085E-04	-8.9391E-04	1.0549E-02	1.3947E+00	-7.8881E-03	-7.5286E-04	5.4030E+00
ROW 22	3.0539E+00	0.	0.	5.4414E+00	3.1353E+00					
ROW 23	-1.7128E+00	-1.1718E+00	-1.2104E-01	3.4602E-03	1.2425E-03	3.7253E+00	1.0625E-02	3.7539E-06	2.1750E-07	-2.2603E-05
ROW 24	0.	3.9854E+00	6.1008E-01	0.	0.					
ROW 25	-1.7599E-01	-1.3584E-01	-1.0527E-02	5.0477E-04	2.4739E-04	5.5411E-01	5.8381E-04	2.5662E-07	2.4026E-08	-2.2352E-06
ROW 26	0.	6.1008E-01	9.5997E-02	0.	0.					
ROW 27	1.5678E+00	-1.3042E+01	1.9570E+00	-1.6427E-03	-1.5909E-03	1.3357E-01	3.3863E+01	-7.3660E-02	7.4394E-03	5.0479E+01
ROW 28	5.4414E+00	0.	0.	5.0062E+01	1.3141E+01					
ROW 29	-3.1939E-03	-3.8957E+00	6.5051E-01	-8.5289E-04	-9.3084E-04	3.3837E-02	6.7822E+00	-1.9230E-02	8.2861E-04	1.3201E+01
ROW 30	3.1353E+00	0.	0.	1.3141E+01	4.6854E+00					

Figure 70. Performance Evaluator Output - With Nonstationary Optimal Controller

PHI(T,TR) MATRIX

ROW 1	1.0000E+00	2.0176E-03	4.9408E+00	3.3664E+03	4.5009E+00	-4.0420E+00	0.	0.	0.	0.	0.	0.
ROW 2	1.0066E-01	2.4572E-01	2.6649E-01	0.	0.	0.	0.	0.	0.	0.	0.	0.
ROW 3	0.	9.9810E-01	-3.5517E+00	4.0642E+03	5.4825E+00	-4.6249E+00	0.	0.	0.	0.	0.	0.
ROW 4	0.	-7.6240E-02	-2.4594E-01	-3.4534E-01	0.	0.	0.	0.	0.	0.	0.	0.
ROW 5	0.	9.1472E-04	9.0391E-01	-1.2583E+02	-1.8118E-01	1.2187E-01	0.	0.	0.	0.	0.	0.
ROW 6	0.	2.9155E-02	6.2769E-02	8.4039E-02	0.	0.	0.	0.	0.	0.	0.	0.
ROW 7	0.	5.9640E-08	2.3799E-04	8.4406E-01	1.1545E-03	-9.8671E-04	0.	0.	0.	0.	0.	0.
ROW 8	0.	4.8137E-06	5.4981E-06	-1.2531E-05	0.	0.	0.	0.	0.	0.	0.	0.
ROW 9	0.	4.7815E-07	1.5067E-08	1.5074E-05	-2.3965E-02	6.9076E-05	2.4303E-05	0.	0.	0.	0.	0.
ROW 10	0.	0.	4.5088E-06	8.9634E-08	0.	0.	0.	0.	0.	0.	0.	0.
ROW 11	0.	-1.6720E-06	2.0238E-04	-2.3384E-03	0.	0.	0.	0.	0.	0.	0.	0.
ROW 12	0.	0.	0.	0.	0.	0.	0.	0.	0.	0.	0.	0.
ROW 13	0.	0.	0.	0.	0.	0.	0.	0.	0.	0.	0.	0.
ROW 14	0.	0.	0.	0.	0.	0.	0.	0.	0.	0.	0.	0.
ROW 15	0.	0.	0.	0.	0.	0.	0.	0.	0.	0.	0.	0.
ROW 16	0.	0.	0.	0.	0.	0.	0.	0.	0.	0.	0.	0.
ROW 17	0.	0.	0.	0.	0.	0.	0.	0.	0.	0.	0.	0.
ROW 18	0.	0.	0.	0.	0.	0.	0.	0.	0.	0.	0.	0.
ROW 19	0.	0.	0.	0.	0.	0.	0.	0.	0.	0.	0.	0.
ROW 20	0.	0.	0.	0.	0.	0.	0.	0.	0.	0.	0.	0.
ROW 21	0.	0.	0.	0.	0.	0.	0.	0.	0.	0.	0.	0.
ROW 22	0.	0.	0.	0.	0.	0.	0.	0.	0.	0.	0.	0.
ROW 23	0.	0.	0.	0.	0.	0.	0.	0.	0.	0.	0.	0.
ROW 24	0.	0.	0.	0.	0.	0.	0.	0.	0.	0.	0.	0.
ROW 25	0.	0.	0.	0.	0.	0.	0.	0.	0.	0.	0.	0.
ROW 26	0.	0.	0.	0.	0.	0.	0.	0.	0.	0.	0.	0.
ROW 27	0.	0.	0.	0.	0.	0.	0.	0.	0.	0.	0.	0.
ROW 28	0.	0.	0.	0.	0.	0.	0.	0.	0.	0.	0.	0.
ROW 29	0.	0.	0.	0.	0.	0.	0.	0.	0.	0.	0.	0.
ROW 30	0.	0.	0.	0.	0.	0.	0.	0.	0.	0.	0.	0.
ROW 31	0.	0.	0.	0.	0.	0.	0.	0.	0.	0.	0.	0.
ROW 32	0.	0.	0.	0.	0.	0.	0.	0.	0.	0.	0.	0.
ROW 33	0.	0.	0.	0.	0.	0.	0.	0.	0.	0.	0.	0.
ROW 34	0.	0.	0.	0.	0.	0.	0.	0.	0.	0.	0.	0.
ROW 35	0.	0.	0.	0.	0.	0.	0.	0.	0.	0.	0.	0.
ROW 36	0.	0.	0.	0.	0.	0.	0.	0.	0.	0.	0.	0.
ROW 37	0.	0.	0.	0.	0.	0.	0.	0.	0.	0.	0.	0.
ROW 38	0.	0.	0.	0.	0.	0.	0.	0.	0.	0.	0.	0.
ROW 39	0.	0.	0.	0.	0.	0.	0.	0.	0.	0.	0.	0.
ROW 40	0.	0.	0.	0.	0.	0.	0.	0.	0.	0.	0.	0.
ROW 41	0.	0.	0.	0.	0.	0.	0.	0.	0.	0.	0.	0.
ROW 42	0.	0.	0.	0.	0.	0.	0.	0.	0.	0.	0.	0.
ROW 43	0.	0.	0.	0.	0.	0.	0.	0.	0.	0.	0.	0.
ROW 44	0.	0.	0.	0.	0.	0.	0.	0.	0.	0.	0.	0.
ROW 45	0.	0.	0.	0.	0.	0.	0.	0.	0.	0.	0.	0.
ROW 46	0.	0.	0.	0.	0.	0.	0.	0.	0.	0.	0.	0.
ROW 47	0.	0.	0.	0.	0.	0.	0.	0.	0.	0.	0.	0.
ROW 48	0.	0.	0.	0.	0.	0.	0.	0.	0.	0.	0.	0.
ROW 49	0.	0.	0.	0.	0.	0.	0.	0.	0.	0.	0.	0.
ROW 50	0.	0.	0.	0.	0.	0.	0.	0.	0.	0.	0.	0.
ROW 51	0.	0.	0.	0.	0.	0.	0.	0.	0.	0.	0.	0.
ROW 52	0.	0.	0.	0.	0.	0.	0.	0.	0.	0.	0.	0.
ROW 53	0.	0.	0.	0.	0.	0.	0.	0.	0.	0.	0.	0.
ROW 54	0.	0.	0.	0.	0.	0.	0.	0.	0.	0.	0.	0.
ROW 55	0.	0.	0.	0.	0.	0.	0.	0.	0.	0.	0.	0.
ROW 56	0.	0.	0.	0.	0.	0.	0.	0.	0.	0.	0.	0.
ROW 57	0.	0.	0.	0.	0.	0.	0.	0.	0.	0.	0.	0.
ROW 58	0.	0.	0.	0.	0.	0.	0.	0.	0.	0.	0.	0.
ROW 59	0.	0.	0.	0.	0.	0.	0.	0.	0.	0.	0.	0.
ROW 60	0.	0.	0.	0.	0.	0.	0.	0.	0.	0.	0.	0.
ROW 61	0.	0.	0.	0.	0.	0.	0.	0.	0.	0.	0.	0.
ROW 62	0.	0.	0.	0.	0.	0.	0.	0.	0.	0.	0.	0.
ROW 63	0.	0.	0.	0.	0.	0.	0.	0.	0.	0.	0.	0.
ROW 64	0.	0.	0.	0.	0.	0.	0.	0.	0.	0.	0.	0.
ROW 65	0.	0.	0.	0.	0.	0.	0.	0.	0.	0.	0.	0.
ROW 66	0.	0.	0.	0.	0.	0.	0.	0.	0.	0.	0.	0.
ROW 67	0.	0.	0.	0.	0.	0.	0.	0.	0.	0.	0.	0.
ROW 68	0.	0.	0.	0.	0.	0.	0.	0.	0.	0.	0.	0.
ROW 69	0.	0.	0.	0.	0.	0.	0.	0.	0.	0.	0.	0.
ROW 70	0.	0.	0.	0.	0.	0.	0.	0.	0.	0.	0.	0.
ROW 71	0.	0.	0.	0.	0.	0.	0.	0.	0.	0.	0.	0.
ROW 72	0.	0.	0.	0.	0.	0.	0.	0.	0.	0.	0.	0.
ROW 73	0.	0.	0.	0.	0.	0.	0.	0.	0.	0.	0.	0.
ROW 74	0.	0.	0.	0.	0.	0.	0.	0.	0.	0.	0.	0.
ROW 75	0.	0.	0.	0.	0.	0.	0.	0.	0.	0.	0.	0.
ROW 76	0.	0.	0.	0.	0.	0.	0.	0.	0.	0.	0.	0.
ROW 77	0.	0.	0.	0.	0.	0.	0.	0.	0.	0.	0.	0.
ROW 78	0.	0.	0.	0.	0.	0.	0.	0.	0.	0.	0.	0.
ROW 79	0.	0.	0.	0.	0.	0.	0.	0.	0.	0.	0.	0.
ROW 80	0.	0.	0.	0.	0.	0.	0.	0.	0.	0.	0.	0.
ROW 81	0.	0.	0.	0.	0.	0.	0.	0.	0.	0.	0.	0.
ROW 82	0.	0.	0.	0.	0.	0.	0.	0.	0.	0.	0.	0.
ROW 83	0.	0.	0.	0.	0.	0.	0.	0.	0.	0.	0.	0.
ROW 84	0.	0.	0.	0.	0.	0.	0.	0.	0.	0.	0.	0.
ROW 85	0.	0.	0.	0.	0.	0.	0.	0.	0.	0.	0.	0.
ROW 86	0.	0.	0.	0.	0.	0.	0.	0.	0.	0.	0.	0.
ROW 87	0.	0.	0.	0.	0.	0.	0.	0.	0.	0.	0.	0.
ROW 88	0.	0.	0.	0.	0.	0.	0.	0.	0.	0.	0.	0.
ROW 89	0.	0.	0.	0.	0.	0.	0.	0.	0.	0.	0.	0.
ROW 90	0.	0.	0.	0.	0.	0.	0.	0.	0.	0.	0.	0.
ROW 91	0.	0.	0.	0.	0.	0.	0.	0.	0.	0.	0.	0.
ROW 92	0.	0.	0.	0.	0.	0.	0.	0.	0.	0.	0.	0.
ROW 93	0.	0.	0.	0.	0.	0.	0.	0.	0.	0.	0.	0.
ROW 94	0.	0.	0.	0.	0.	0.	0.	0.	0.	0.	0.	0.
ROW 95	0.	0.	0.	0.	0.	0.	0.	0.	0.	0.	0.	0.
ROW 96	0.	0.	0.	0.	0.	0.	0.	0.	0.	0.	0.	0.
ROW 97	0.	0.	0.	0.	0.	0.	0.	0.	0.	0.	0.	0.
ROW 98	0.	0.	0.	0.	0.	0.	0.	0.	0.	0.	0.	0.
ROW 99	0.	0.	0.	0.	0.	0.	0.	0.	0.	0.	0.	0.
ROW 100	0.	0.	0.	0.	0.	0.	0.	0.	0.	0.	0.	0.

Figure 70. Performance Evaluator Output - With Nonstationary Optimal Controller (continued)

X(I) MATRIX

ROW 1	1.7386E+04	-1.8291E+04	7.0681E+02	8.2631E-02	1.4714E-02	-4.2882E-01	1.4863E+02	2.2046E-02	-9.8227E-05	-1.0398E-01
ROW 2	1.8410E-01	-9.7972E-03	1.7753E-02	-1.0270E-01	-1.5407E-01	3.8972E-01	-1.6255E-02	-2.3483E-02	-8.6551E-04	-7.9701E-02
ROW 3	-1.8291E+04	1.9412E+04	-7.4902E+02	-7.8475E-02	-1.5472E-02	-2.8343E-02	7.0208E+00	9.0553E-04	6.8501E-05	6.8984E-03
ROW 4	-4.7178E-01	-8.7145E-03	1.2761E-02	-7.7058E-02	6.1022E-01	4.6114E-01	-2.9763E-03	-4.0496E-03	6.6824E-03	-4.6948E-02
ROW 5	7.0681E+02	-7.4902E+02	2.9194E+01	2.8493E+03	6.0628E-04	4.1158E-02	8.6690E-04	5.4723E-07	-6.9391E-08	-1.9198E-05
ROW 6	4.6114E-01	-2.9763E-03	-4.0496E-03	6.6824E-03	-4.6948E-02	4.4612E-05	1.0945E-01	6.1617E-07	-1.5396E-06	8.2831E-02
ROW 7	8.2831E-02	-7.8475E-02	2.8493E-03	4.4091E-05	9.1304E-06	1.4752E-02	-1.8855E-05	1.8771E-05	1.4615E-02	1.4292E-04
ROW 8	2.9608E-06	1.0554E-02	1.4752E-02	-1.8855E-05	1.8771E-05	4.4612E-05	1.0945E-01	6.1617E-07	-1.5396E-06	4.4612E-05
ROW 9	1.4714E-02	-1.5472E-02	6.0628E-04	9.1304E-06	5.8585E-03	3.9722E+01	-3.8893E-03	-3.4868E-07	-6.2795E-08	-1.0133E-05
ROW 10	-4.2882E-01	3.8972E-01	-1.6255E-02	4.1158E-02	1.4615E-02	3.9722E+01	-3.8893E-03	-3.4868E-07	-6.2795E-08	-1.0133E-05
ROW 11	1.7827E-02	1.0318E+01	1.4680E+01	-9.8958E-06	3.4053E-05	1.4680E+01	1.0318E+01	9.3751E-06	1.2811E-09	-1.1858E-14
ROW 12	1.4863E+02	-1.6255E+02	7.0208E+00	8.6690E-04	1.4292E-04	-3.8893E-03	1.0528E+03	2.0300E-01	6.6348E-04	-1.3902E-01
ROW 13	1.2160E-01	9.3751E-06	6.4515E-05	-1.8967E-01	-1.1692E+00	2.0300E-01	2.0300E-01	3.3294E-04	7.5944E-05	-1.6229E-01
ROW 14	2.2046E-02	-2.3483E-02	9.0553E-04	5.4723E-07	7.6757E-09	-3.4868E-07	2.0300E-01	3.3294E-04	7.5944E-05	-1.6229E-01
ROW 15	1.0752E-05	1.2811E-09	8.9170E-09	-1.0412E-01	-5.9563E-02	-3.4868E-07	2.0300E-01	3.3294E-04	7.5944E-05	-1.6229E-01
ROW 16	-9.8227E-05	-8.6551E-04	6.8501E-05	-6.9391E-08	3.2770E-09	-6.2795E-08	6.6348E-04	7.5944E-05	7.4368E-03	-5.7234E-02
ROW 17	-1.0398E-01	-7.9701E-02	6.8984E-03	-1.9198E-05	6.2954E-07	-1.0133E-05	-1.3902E-01	-1.6229E-01	-5.7234E-02	1.0408E+02
ROW 18	4.3562E-03	-1.3467E-12	-1.0617E-11	6.6969E+01	3.8258E+01	1.7827E-02	1.2160E-01	1.0752E-05	1.5559E-05	4.3562E-03
ROW 19	1.8410E-01	-4.7178E-01	4.6114E-01	2.9608E-06	4.4612E-05	4.2794E-03	4.0901E-03	1.7827E-02	1.2160E-01	1.0752E-05
ROW 20	6.4778E+01	0.	0.	4.2794E-03	-4.0901E-03	1.0318E+01	1.0318E+01	9.3751E-06	1.2811E-09	-1.1858E-14
ROW 21	-9.7972E-03	-8.7145E-03	-2.9763E-03	1.0554E-02	1.0945E-01	1.4680E+01	1.4680E+01	6.4515E-05	8.9170E-09	-8.8982E-14
ROW 22	0.	1.7082E+01	4.9928E+01	0.	0.	4.4101E-01	4.4101E-01	4.4101E-01	4.4101E-01	-1.0617E-11
ROW 23	1.7753E-02	1.2761E-02	-4.0496E-03	1.4752E-02	4.4101E-01	4.9928E+01	1.7422E+02	0.	0.	0.
ROW 24	0.	4.9928E+01	1.7422E+02	0.	0.	4.4101E-01	4.4101E-01	4.4101E-01	4.4101E-01	-1.0617E-11
ROW 25	-1.0270E-01	-7.7058E-02	6.6824E-03	-1.8855E-05	6.1617E-07	-9.8958E-06	-1.8967E-01	-1.0412E-01	-1.8419E-01	6.6969E+01
ROW 26	4.2794E+03	0.	0.	7.1872E+01	4.2709E+01	4.2794E+03	0.	0.	0.	0.
ROW 27	-1.407E-01	6.1022E-01	-4.6948E-02	1.8771E-05	-1.5396E-06	1.8771E-05	-1.5396E-06	3.4053E-05	-1.1692E+00	-5.9563E-02
ROW 28	-4.0901E-03	0.	0.	4.2709E+01	2.7255E+01	4.2709E+01	2.7255E+01	4.2709E+01	4.2709E+01	2.7255E+01

∞∞

Figure 70. Performance Evaluator Output - With Nonstationary Optimal Controller (continued)

VARIANCE CONTRIBUTION MATRIX

ROW 1	1.3967E+04	-3.0378E+01	3.8530E+03	-5.1319E+02	1.5671E+00	1.0835E+02	0.	0.	0.	0.
	-5.6222E-02	-1.1241E+00	-1.5779E-01	0.	0.	0.	0.	0.	0.	0.
ROW 2	0.	1.5917E+04	2.9273E+03	6.4919E+02	-2.0310E+00	-8.2459E+01	0.	0.	0.	0.
	4.8109E-01	1.2518E+00	2.7325E-01	0.	0.	0.	0.	0.	0.	0.
ROW 3	0.	0.	0.	0.	0.	2.2605E+02	5.1167E+02	6.8812E-02	3.1749E+02	0.
	0.	0.	0.	-3.1702E+00	5.4268E-01	0.	0.	0.	0.	0.

NORMALIZED VARIANCE CONTRIBUTION MATRIX

ROW 1	8.0340E+01	-1.7473E-01	2.2163E+01	-2.9519E+00	9.0141E-03	6.2326E-01	0.	0.	0.	0.
	-3.2339E-04	-6.4661E-03	-9.0763E-04	0.	0.	0.	0.	0.	0.	0.
ROW 2	0.	8.2000E+01	1.5081E+01	3.3444E+00	-1.0463E-02	-4.2481E-01	0.	0.	0.	0.
	2.4784E-03	6.4490E-03	1.4077E-03	0.	0.	0.	0.	0.	0.	0.
ROW 3	0.	0.	0.	0.	0.	2.1472E+01	4.8603E+01	6.5364E-03	3.0168E+01	0.
	0.	0.	0.	-3.0114E-01	5.1548E-02	0.	0.	0.	0.	0.

Figure 70. Performance Evaluator Output - With Nonstationary Optimal Controller (continued)

XSUBH WIG MATRIX

ROW 1	0.	1.8274E+01	1.3745E-02	-1.0115E-03	-1.7771E-01	5.5295E+00	1.3728E-03	-8.6018E-04	-1.7414E-01
ROW 2	-2.3123E-01	-1.7469E-02	-5.1857E+00	-2.7779E+00	3.8314E-01	0.	0.	0.	0.
ROW 3	0.	0.	0.	0.	0.	0.	0.	0.	0.
ROW 4	1.8274E+01	0.	4.2839E+00	9.4651E-04	-2.5647E-04	3.0794E+00	3.3615E-04	4.7515E-05	4.9659E-03
ROW 5	4.4970E-01	-3.1876E-03	-1.2119E+00	-5.9925E-01	-3.2152E-02	4.1152E-02	8.6690E-04	5.4723E-07	-6.9391E-08
ROW 6	1.3745E-02	0.	9.4651E-04	4.4091E-05	8.9930E-06	1.7617E-02	-1.4185E-04	-3.3463E-08	1.7607E-09
ROW 7	2.9608E-06	1.0554E-02	1.4412E-02	-1.8916E-04	1.8771E-05	3.9722E+01	-1.6333E-02	2.0322E-01	6.4347E-04
ROW 8	-1.0115E-03	0.	-2.5647E-04	4.4109E+01	4.0700E-05	-1.6333E-02	1.0528E+03	2.0322E-01	6.4347E-04
ROW 9	4.3785E-05	1.0945E-01	4.4109E+01	4.0700E-05	-4.7059E-07	-2.1464E-06	2.0300E-01	3.3294E-04	7.5944E-05
ROW 10	-1.7771E-01	0.	-4.0202E-02	4.1152E-02	1.4617E-02	3.9722E+01	-1.6333E-02	2.0322E-01	6.4347E-04
ROW 11	1.7791E-02	1.0318E-01	1.4688E+01	4.0550E-03	0.0768E-05	-1.6333E-02	1.0528E+03	2.0322E-01	6.4347E-04
ROW 12	5.295E+00	0.	3.0794E+00	8.6690E-04	-1.4185E-04	-1.6333E-02	1.0528E+03	2.0322E-01	6.4347E-04
ROW 13	1.2160E-01	9.3751E-06	-7.0548E-01	-5.4244E-01	-1.1692E+00	-2.1464E-06	2.0300E-01	3.3294E-04	7.5944E-05
ROW 14	1.3728E-03	0.	3.3010E-04	5.4723E-07	-3.3463E-08	-2.1464E-06	2.0300E-01	3.3294E-04	7.5944E-05
ROW 15	1.0752E-05	1.2831E-04	-1.0192E-04	-1.0417E-01	-5.9563E-02	-1.2905E-07	1.6229E-01	-5.7234E-02	1.0440E-01
ROW 16	-8.6018E-04	0.	4.7515E-05	-6.9391E-08	1.7607E-09	-1.2905E-07	1.6229E-01	-5.7234E-02	1.0440E-01
ROW 17	1.5559E-05	-3.8314E-01	-3.7507E-06	-1.0417E-01	-1.4675E-01	-1.2905E-07	1.6229E-01	-5.7234E-02	1.0440E-01
ROW 18	-1.7414E-01	0.	4.9659E-03	-1.0417E-01	3.8258E+01	-1.2905E-07	1.6229E-01	-5.7234E-02	1.0440E-01
ROW 19	4.3562E-03	-1.3467E-12	-3.4594E-04	6.6900E+01	3.8258E+01	-1.2905E-07	1.6229E-01	-5.7234E-02	1.0440E-01
ROW 20	-2.3123E-01	0.	4.9707E-01	2.9608E-06	4.3785E-05	1.7791E-02	1.2100E-01	1.0752E-05	4.5559E-05
ROW 21	6.4778E+01	0.	-2.0477E-03	3.2555E-03	-4.0901E-03	1.7791E-02	1.2100E-01	1.0752E-05	4.5559E-05
ROW 22	-1.7469E-02	0.	-3.1876E-03	1.0554E-02	1.0945E-01	1.0318E+01	9.3751E-06	1.2811E-09	-1.1858E-14
ROW 23	0.	1.7082E+01	4.9928E+01	-1.8912E-05	0.	1.4688E+01	-7.0548E-01	-1.0192E-04	-3.7567E-06
ROW 24	-5.1857E+00	0.	-1.2119E+00	1.4412E-02	4.4109E-01	1.4688E+01	-7.0548E-01	-1.0192E-04	-3.7567E-06
ROW 25	-2.0477E-03	4.9928E+01	1.7459E+02	1.8254E-01	2.6486E-03	4.0550E-03	-5.4244E-01	-1.0417E-01	-1.8419E-01
ROW 26	-2.7779E+00	0.	-5.9925E-01	-1.8916E-04	4.0706E-05	4.0550E-03	-5.4244E-01	-1.0417E-01	-1.8419E-01
ROW 27	3.2555E-03	-1.8912E-05	1.8254E-01	7.1963E+01	4.2710E+01	8.0768E-05	-1.1692E+00	-5.9563E-02	-1.4675E-01
ROW 28	3.8314E-01	0.	-3.2152E-02	1.8771E-05	-4.7059E-07	8.0768E-05	-1.1692E+00	-5.9563E-02	-1.4675E-01
ROW 29	-4.0901E-03	0.	2.6486E-03	4.2710E+01	2.7255E+01	0.	0.	0.	0.

CEP HORIZONTAL= 2.77745770E+01

Figure 70. Performance Evaluator Output - With Nonstationary Optimal Controller (continued)

XSUBV #IG MATRIX

ROW 1	0.	0.	0.	0.	0.	0.	0.	0.	0.	0.	0.	0.	0.	0.	0.	0.	0.	0.	0.	0.					
ROW 2	0.	0.	0.	0.	0.	0.	0.	0.	0.	0.	0.	0.	0.	0.	0.	0.	0.	0.	0.	0.					
ROW 3	2.9152E+02	1.3689E+01	1.5613E-02	-1.6596E-03	-2.2418E-01	6.2810E+00	1.5594E-03	-9.7708E-04	-1.9781E-01	-2.6266E-01	-1.9843E-02	-7.1558E+00	-3.7881E+00	4.3521E-01	-3.6355E-02	2.9271E+00	2.9834E-04	7.1206E-05	9.7622E-03	4.5607E-01	-2.7065E-03	-1.1285E+00	-5.5245E-01	-4.2704E-02	
ROW 4	1.3689E+01	3.4486E+00	5.6793E-04	-2.5260E-04	4.1150E-02	8.6690E-04	5.4723E-07	-6.9391E-08	-1.9198E-05	1.5613E-02	5.6793E-04	4.4091E-05	8.9656E-06	1.8771E-05	1.4618E-02	-1.5285E-04	-3.6195E-08	3.4724E-09	8.3645E-07	2.9608E-06	1.9555E-02	1.4344E-02	-2.2305E-04	1.8771E-05	
ROW 5	1.9555E-02	1.4344E-02	-2.2305E-04	1.8771E-05	1.4618E-02	-1.5285E-04	-3.6195E-08	3.4724E-09	8.3645E-07	4.4245E-05	1.0945E-01	4.4111E-01	4.9836E-05	-1.2330E-06	-1.6596E-03	-2.5260E-04	8.9656E-06	5.8585E-03	4.245E-05	1.0945E-01	4.4111E-01	4.9836E-05	-1.2330E-06	-1.6596E-03	
ROW 6	-2.2418E-01	-3.6355E-02	4.1150E-02	1.4618E-02	3.9722E+01	-1.6814E-02	-2.2658E-06	-5.4254E-08	-1.0910E-06	1.7811E-02	1.0318E+01	9.3751E-06	1.2811E-09	-1.1857E-14	6.2810E+00	1.0528E+03	2.0300E-01	6.6348E-04	-1.3902E-01	1.7811E-02	1.2160E-01	1.0752E-05	1.5559E-05	4.3562E-03	
ROW 7	6.2810E+00	2.9271E+00	8.6690E-04	-1.5285E-04	-1.6814E-02	1.0528E+03	2.0300E-01	6.6348E-04	-1.3902E-01	1.2160E-01	1.0752E-05	1.5559E-05	4.3562E-03	4.5607E-01	-2.7065E-03	-1.9843E-02	1.0945E-02	1.0318E+01	9.3751E-06	1.2811E-09	-1.1857E-14	-1.3466E-12	1.4690E+01	4.9928E+01	
ROW 8	1.9843E-02	7.1558E+00	3.7881E+00	4.3521E-01	4.7831E-03	4.7831E-03	4.7831E-03	4.7831E-03	4.7831E-03	4.7831E-03	4.7831E-03	4.7831E-03	4.7831E-03	4.7831E-03	4.7831E-03	4.7831E-03	4.7831E-03	4.7831E-03	4.7831E-03	4.7831E-03	4.7831E-03	4.7831E-03	4.7831E-03	4.7831E-03	4.7831E-03
ROW 9	1.5594E-03	2.9834E-04	5.4723E-07	-3.6195E-08	-2.2658E-06	2.0300E-01	3.3298E-04	7.5944E-05	-1.6229E-01	1.7811E-02	1.0318E+01	9.3751E-06	1.2811E-09	-1.1857E-14	6.6348E-04	7.5944E-05	7.4368E-03	-5.7234E-02	1.0408E+02	1.7811E-02	1.2160E-01	1.0752E-05	1.5559E-05	4.3562E-03	
ROW 10	1.5594E-03	2.9834E-04	5.4723E-07	-3.6195E-08	-2.2658E-06	2.0300E-01	3.3298E-04	7.5944E-05	-1.6229E-01	1.7811E-02	1.0318E+01	9.3751E-06	1.2811E-09	-1.1857E-14	6.6348E-04	7.5944E-05	7.4368E-03	-5.7234E-02	1.0408E+02	1.7811E-02	1.2160E-01	1.0752E-05	1.5559E-05	4.3562E-03	
ROW 11	1.5594E-03	2.9834E-04	5.4723E-07	-3.6195E-08	-2.2658E-06	2.0300E-01	3.3298E-04	7.5944E-05	-1.6229E-01	1.7811E-02	1.0318E+01	9.3751E-06	1.2811E-09	-1.1857E-14	6.6348E-04	7.5944E-05	7.4368E-03	-5.7234E-02	1.0408E+02	1.7811E-02	1.2160E-01	1.0752E-05	1.5559E-05	4.3562E-03	
ROW 12	6.4778E+01	0.	-9.0769E-04	3.8255E-03	-4.0901E-03	0.	0.	0.	0.	0.	0.	0.	0.	0.	0.	0.	0.	0.	0.	0.	0.	0.	0.	0.	
ROW 13	-1.9843E-02	-2.7065E-03	1.0554E-02	1.0945E-02	1.0318E+01	9.3751E-06	1.2811E-09	-1.1857E-14	-1.3466E-12	1.4690E+01	4.9928E+01	2.4152E-05	0.	0.	0.	0.	0.	0.	0.	0.	0.	0.	0.	0.	
ROW 14	-1.1558E+00	-1.1285E-01	1.4344E-02	4.4111E-01	4.4111E-01	4.4111E-01	4.4111E-01	4.4111E-01	4.4111E-01	4.4111E-01	4.4111E-01	4.4111E-01	4.4111E-01	4.4111E-01	4.4111E-01	4.4111E-01	4.4111E-01	4.4111E-01	4.4111E-01	4.4111E-01	4.4111E-01	4.4111E-01	4.4111E-01	4.4111E-01	
ROW 15	-3.7881E+00	-5.5245E-01	-2.2305E-04	4.9836E-05	4.9836E-05	4.9836E-05	4.9836E-05	4.9836E-05	4.9836E-05	4.9836E-05	4.9836E-05	4.9836E-05	4.9836E-05	4.9836E-05	4.9836E-05	4.9836E-05	4.9836E-05	4.9836E-05	4.9836E-05	4.9836E-05	4.9836E-05	4.9836E-05	4.9836E-05	4.9836E-05	
ROW 16	4.3521E-03	2.4152E-05	2.1177E-01	7.1978E+01	4.2709E+01	4.2709E+01	4.2709E+01	4.2709E+01	4.2709E+01	4.2709E+01	4.2709E+01	4.2709E+01	4.2709E+01	4.2709E+01	4.2709E+01	4.2709E+01	4.2709E+01	4.2709E+01	4.2709E+01	4.2709E+01	4.2709E+01	4.2709E+01	4.2709E+01	4.2709E+01	
ROW 17	4.3521E-03	2.4152E-05	2.1177E-01	7.1978E+01	4.2709E+01	4.2709E+01	4.2709E+01	4.2709E+01	4.2709E+01	4.2709E+01	4.2709E+01	4.2709E+01	4.2709E+01	4.2709E+01	4.2709E+01	4.2709E+01	4.2709E+01	4.2709E+01	4.2709E+01	4.2709E+01	4.2709E+01	4.2709E+01	4.2709E+01	4.2709E+01	
ROW 18	-4.0901E-03	0.	4.2709E-04	4.2709E+01	2.7255E+01	2.7255E+01	2.7255E+01	2.7255E+01	2.7255E+01	2.7255E+01	2.7255E+01	2.7255E+01	2.7255E+01	2.7255E+01	2.7255E+01	2.7255E+01	2.7255E+01	2.7255E+01	2.7255E+01	2.7255E+01	2.7255E+01	2.7255E+01	2.7255E+01	2.7255E+01	

CEP VERTICAL= 2.89696347E+01

Figure 70. Performance Evaluator Output - With Nonstationary Optimal Controller (continued)

WEIGHTING MATRIX QH

ROW 1	3.1416E+00	2.7668E+00	5.6989E+00	2.1816E+04	2.9303E+01	-2.5489E+01	0.	0.	0.	0.
ROW 2	9.9846E-02	9.1745E-02	-1.1791E-01	0.	0.	0.	0.	0.	0.	0.
ROW 3	2.7668E+00	2.44367E+00	5.0190E+00	1.9214E+04	2.5807E+01	-2.2449E+01	-1.5104E-11	-6.1637E-08	-1.2613E-10	-9.4850E-11
ROW 4	8.7934E-02	8.0800E-02	-1.0384E-01	1.0044E-12	-7.7468E-13	0.	0.	0.	0.	0.
ROW 5	5.6989E+00	5.0190E+00	1.0338E+01	3.9575E+04	5.3156E+01	-4.6238E+01	5.3748E-11	2.1933E-07	4.4882E-10	3.3752E-10
ROW 6	1.8112E-01	1.6644E-01	-2.1389E-01	-3.5741E-12	2.7567E-12	0.	0.	0.	0.	0.
ROW 7	2.1816E+04	1.9214E+04	3.9575E+04	1.5150E+08	2.0349E+05	-1.7701E+05	-6.1502E-08	-2.5098E-04	-5.1358E-07	-3.8622E-07
ROW 8	6.9336E+02	6.3711E+02	-8.1879E+02	4.0898E-09	-3.1544E-09	0.	0.	0.	0.	0.
ROW 9	2.9303E+01	2.5807E+01	5.3156E+01	2.0349E+05	2.7332E+02	-2.3775E+02	-8.2967E-11	-3.3857E-07	-6.9281E-10	-5.2101E-10
ROW 10	9.3131E-01	8.5575E-01	-1.0998E+00	5.5171E-12	-4.2553E-12	0.	0.	0.	0.	0.
ROW 11	-2.5489E+01	-2.2449E+01	-4.6238E+01	-1.7701E+05	-2.3775E+02	2.0681E+02	6.9987E-11	2.8560E-07	5.8443E-10	4.3950E-10
ROW 12	-8.1010E-01	-7.4443E-01	9.5665E-01	-4.6540E-12	3.5896E-12	0.	0.	0.	0.	0.
ROW 13	0.	-1.5104E-11	5.3748E-11	-6.1502E-08	-8.2967E-11	6.9987E-11	1.5708E+00	6.4101E+03	1.3117E+01	9.8642E+00
ROW 14	1.1840E-12	3.7218E-12	5.2259E-12	-1.0446E-01	8.0565E-02	0.	0.	0.	0.	0.
ROW 15	0.	-6.1637E-08	2.1933E-07	-2.5098E-04	-3.3857E-07	2.8560E-07	6.4101E+03	2.6158E+07	5.3528E+04	4.0254E+04
ROW 16	4.8316E-09	1.5188E-08	2.1326E-08	-4.2626E+02	3.2877E+02	0.	0.	0.	0.	0.
ROW 17	0.	-1.2613E-10	4.4882E-10	-5.1358E-07	-6.9281E-10	5.8443E-10	1.3117E+01	5.3528E+04	1.0953E+02	8.2371E+01
ROW 18	9.8870E-12	3.1079E-11	4.3639E-11	-8.7225E-01	6.7276E-01	0.	0.	0.	0.	0.
ROW 19	0.	-9.4850E-11	3.3752E-10	-3.8622E-07	-5.2101E-10	4.3950E-10	9.8642E+00	4.0254E+04	8.2371E+01	6.1945E+01
ROW 20	7.4352E-12	2.3372E-11	3.2817E-11	-6.5595E-01	5.0593E-01	0.	0.	0.	0.	0.
ROW 21	9.9846E-02	8.7934E-02	1.8112E-01	6.9336E+02	9.3131E-01	-8.1010E-01	1.1840E-12	4.8316E-09	9.8870E-12	7.4352E-12
ROW 22	3.1733E-03	2.9158E-03	-3.7474E-03	-7.8734E-14	6.0726E-14	0.	0.	0.	0.	0.
ROW 23	9.1745E-02	8.0800E-02	1.6644E-01	6.3711E+02	8.5575E-01	-7.4443E-01	3.7218E-12	1.5188E-08	3.1079E-11	2.3372E-11
ROW 24	2.9158E-03	2.6793E-03	-3.4433E-03	-2.4749E-13	1.9089E-13	0.	0.	0.	0.	0.
ROW 25	-1.1791E-01	-1.0384E-01	-2.1389E-01	-8.1879E+02	-1.0998E+00	9.5665E-01	5.2259E-12	2.1326E-08	4.3639E-11	3.2817E-11
ROW 26	-3.7474E-03	-3.4433E-03	4.4253E-03	-3.4751E-13	2.6803E-13	0.	0.	0.	0.	0.
ROW 27	0.	1.0044E-12	-3.5741E-12	4.0898E-09	5.5171E-12	-4.6540E-12	-1.0446E-01	-4.2626E+02	-8.7225E-01	-6.5595E-01
ROW 28	-7.8734E-14	-2.4749E-13	-3.4751E-13	6.9461E-03	-5.3574E-03	0.	0.	0.	0.	0.
ROW 29	0.	-7.7468E-13	2.7567E-12	-3.1544E-09	-4.2553E-12	3.5896E-12	8.0565E-02	3.2877E+02	6.7276E-01	5.0593E-01
ROW 30	6.0726E-14	1.9089E-13	2.6803E-13	-5.3574E-03	4.1321E-03	0.	0.	0.	0.	0.

Figure 70. Performance Evaluator Output - With Nonstationary Optimal Controller (continued)

WEIGHTING MATRIX QV

ROW 1	4.0535E+00	3.5700E+00	7.3532E+00	2.8149E+04	3.7809E+01	-3.2889E+01	1.7190E-11	7.0147E-08	1.4354E-10	1.0795E-10
ROW 2	1.2883E-01	1.1838E-01	-1.5214E-01	-1.1431E-12	8.8164E-13					
ROW 3	3.5700E+00	3.1441E+00	6.4760E+00	2.4791E+04	3.3299E+01	-2.8965E+01	3.4682E-14	1.4153E-10	2.8961E-13	2.1779E-13
ROW 4	1.1346E-01	1.0426E-01	-1.1339E-01	-2.3063E-15	1.7789E-15					
ROW 5	7.3532E+00	6.4760E+00	1.3339E+01	5.1063E+04	6.8587E+01	-5.9660E+01	8.4930E-11	3.4658E-07	7.0921E-10	5.3334E-10
ROW 6	2.3370E-01	2.1474E-01	-2.7598E-01	-5.6477E-12	4.3560E-12					
ROW 7	2.8149E+04	2.4791E+04	5.1063E+04	1.9548E+08	2.6250E+05	-2.2839E+05	5.7867E-08	2.3614E-04	4.8322E-07	3.6339E-07
ROW 8	8.9463E+02	8.2205E+02	-1.0565E+03	-3.8481E-09	2.9680E-09					
ROW 9	3.7809E+01	3.3299E+01	6.8587E+01	2.6256E+05	3.5266E+02	-3.0677E+02	7.7368E-11	3.1572E-07	6.4606E-10	4.8585E-10
ROW 10	1.2016E+00	1.1042E+00	-1.4190E+00	-5.1448E-12	3.9681E-12					
ROW 11	-3.2889E+01	-2.8965E+01	-5.9660E+01	-2.2839E+05	-3.0677E+02	2.6684E+02	-6.9480E-11	-2.8353E-07	-5.8020E-10	-4.3632E-10
ROW 12	-1.0453E+00	-9.6046E-01	1.2344E+00	4.6203E-12	-3.5636E-12					
ROW 13	1.7190E-11	3.4682E-14	8.4930E-11	5.7867E-08	7.7368E-11	-6.9480E-11	1.5708E+00	6.4101E+03	1.3117E+01	9.8642E+00
ROW 14	1.7303E-12	4.2238E-12	4.5808E-12	-1.0446E-01	8.0565E-02					
ROW 15	7.0147E-08	1.4153E-10	3.4658E-07	2.3614E-04	3.1572E-07	-2.8353E-07	6.4101E+03	2.6158E+07	5.3528E+04	4.0254E+04
ROW 16	7.0610E-09	1.7236E-08	1.8693E-08	-4.2626E+02	3.2877E+02					
ROW 17	1.4354E-10	2.8961E-13	7.0921E-10	4.8322E+07	6.4606E-10	-5.8020E-10	1.3117E+01	5.3528E+04	1.0953E+02	8.2371E+01
ROW 18	1.4449E-11	3.5271E-11	3.8252E-11	-8.7225E-01	6.7276E-01					
ROW 19	1.0795E-10	2.1779E-13	5.3334E-10	3.6339E+07	4.8595E-10	-4.3632E-10	9.8642E+00	4.0254E+04	8.2371E+01	6.1945E+01
ROW 20	1.0866E-11	2.6524E-11	2.8766E-11	-6.5595E-01	5.0593E-01					
ROW 21	1.2883E-01	1.1346E-01	2.3370E-01	8.9463E+02	1.2016E+00	-1.0453E+00	1.7303E-12	7.0610E-09	1.4449E-11	1.0866E-11
ROW 22	4.0944E-03	3.7623E-03	-4.8352E-03	-1.1506E-13	8.8746E-14					
ROW 23	1.1838E-01	1.0426E-01	2.1474E-01	8.2205E+02	1.1042E+00	-9.6046E-01	4.2238E-12	1.7236E-08	3.5271E-11	2.6524E-11
ROW 24	3.7623E-03	3.4570E-03	-4.4429E-03	-2.8087E-13	2.1663E-13					
ROW 25	-1.5214E-01	-1.3399E-01	-2.7598E-01	-1.0565E+03	-1.4190E+00	1.2344E+00	5.5808E-12	1.8693E-08	3.8252E-11	2.8766E-11
ROW 26	-4.8352E-03	-4.4429E-03	5.7099E-03	-3.0461E-13	2.3494E-13					
ROW 27	-1.1431E-12	-2.3063E-15	-5.6477E-12	-3.8481E-09	-5.1448E-12	4.6203E-12	-1.0446E-01	-4.2626E+02	-8.7225E-01	-6.5595E-01
ROW 28	-1.1506E-13	-2.8087E-13	-3.0461E-13	6.9461E-03	-5.3574E-03					
ROW 29	8.8164E-13	1.7788E-15	4.3560E-12	2.9680E-09	3.9681E-12	-3.5636E-12	8.0565E-02	3.2877E+02	6.7276E-01	5.0593E-01
ROW 30	8.8746E-14	2.1663E-13	2.3494E-13	-5.3574E-03	4.1321E-03					

QH(1,1) = 3.14159265E+00 QH(7,7) = 1.57079633E+00 QV(2,2) = 3.14159265E+00 QV(7,7) = 1.57079633E+00

JSUBH= 2.36351968E+03 JSUBV= 2.56956184E+03

APPROXIMATE CEPH= 2.74286653E+01 APPROXIMATE CEPV= 2.85992472E+01

Figure 70. Performance Evaluator Output - With Nonstationary Optimal Controller (concluded)

INITIAL COVARIANCE OF BOMB

R0W 1	-.1154E 05	-.12638E 05	.63510E 03	-.24038E 00	.59369E 01	-.64165E 02	.15566E 01	-.67844E 02	.86535E 03	.33890E 01
	-.52492E-01	-.15347E 01	-.16677E 00	.32353E 01	.50046E 00					
R0W 2	.12638E 05	.14447E 05	-.72268E 03	.26913E 00	-.68796E 01	.68870E 02	-.25353E 01	.18539E 01	-.14010E 02	-.10935E 02
	-.14521E 01	-.10338E 01	-.12511E 00	-.10520E 02	-.31578E 01					
R0W 3	.63510E 03	-.72268E 03	.61559E 02	-.13913E 01	.35444E 02	-.31677E 01	.29973E 00	-.31073E 02	.20176E 03	.19087E 01
	.35266E 00	-.12495E 00	-.10707E 01	.18814E 01	.62846E 00					
R0W 4	.24038E 00	.26913E 00	-.13513E 01	.11635E 04	-.11077E 05	.61717E 02	-.24546E 05	.50859E 06	.59567E 06	.29678E 03
	-.40438E 03	.37556E 02	.54321E 03	-.37802E 03	.38652E 03					
R0W 5	.59369E 01	-.68796E 01	.15444E 02	-.11077E 05	.90486E 05	.10848E 02	.38080E 05	-.12340E 06	.22926E 06	.74967E 04
	-.57603E 03	.13008E 02	.25611E 03	-.24147E 03	-.42903E 03					
R0W 6	-.64165E 02	.68870E 02	-.31677E 01	.61717E 02	.10848E 02	.11310E 02	.84482E 01	-.79631E 03	.20121E 03	.52900E 00
	.94042E 01	.33007E 01	.56573E 00	.44957E 00	.15680E 00					
R0W 7	.15566E 01	-.25353E 01	.29973E 00	-.24546E 05	.38080E 05	.84482E 01	.13777E 03	-.24812E 01	.13157E 02	.10041E 02
	.50942E 00	.15754E 01	.13640E 02	.92413E 01	.19545E 01					
R0W 8	.67844E 02	.18349E 01	-.31073E 02	.50859E 06	.12340E 06	-.79631E 03	-.24512E 01	.17177E 03	-.15223E 04	.83426E 01
	.84643E 02	.22346E 04	.29879E 05	-.82740E 01	-.21252E 01					
R0W 9	.25353E 03	-.14107E 02	.20176E 03	.59667E 06	.22826E 06	.20121E 03	.13157E 02	-.15223E 04	.55923E 04	.76154E 02
	-.88781E 03	-.24432E 03	-.29166E 06	.68818E 02	.61243E 03					
R0 10	.33890E 01	-.10338E 02	.19087E 01	-.29478E 03	.74967E 04	.82900E 00	.10041E 02	-.83426E 01	.76154E 02	.56334E 02
	.54702E 01	-.59369E 02	-.12641E 02	.48723E 02	.12975E 02					
R0W 11	-.52492E 01	-.14521E 01	.35266E 00	-.40438E 03	-.57603E 03	.94042E 01	.50942E 00	-.84643E 02	-.88781E 03	.54702E 01
	.30539E 01	.00000E 00	.30000E 00	.54414E 01	.31353E 01					
R0W 12	-.14947E 01	.10338E 01	-.12495E 00	.37556E 02	.13008E 02	.38007E 01	.15754E 01	.22366E 04	-.24482E 05	.69999E 02
	.00000E 00	.30454E 01	.61008E 00	.00000E 00	.00000E 00					
R0W 13	.16677E 00	-.12495E 00	-.10707E 01	.54321E 03	.25611E 03	.56573E 00	.13660E 02	.29879E 05	-.29166E 06	.12661E 02
	.00000E 00	.61008E 00	.05997E 01	.00000E 00	.00000E 00					
R0W 14	.32353E 01	-.10338E 02	.18814E 01	-.37802E 03	-.24147E 03	.44957E 00	.92413E 01	-.82740E 01	.68818E 02	.48739E 02
	.54414E 01	.00000E 00	.00000E 00	.50062E 02	.13141E 02					
R0W 15	.50942E 00	-.31578E 01	.62846E 00	-.38652E 03	-.42903E 03	.15680E 00	.19545E 01	-.21252E 01	.61243E 03	.12975E 02
	.31353E 01	.00000E 00	.00000E 00	.13141E 02	.46854E 01					

Figure 71. Performance Evaluator Output - With Fixed-Gain Optimal Controller

XSUBF MATRIX T. 6.28

R0W 1	.6094E 00	-.6230E 00	.1793E 00	-.2659E-04	.18072E-03	-.34479E-01	-.69096E-09	-.10555E-11	-.95899E-17	.46555E-09
	.20729E 00	-.91954E-02	.23553E-01	.46546E-09	.19755E-08					
R0W 2	.62304E 00	.68351E 00	-.15133E 00	-.33500E-04	.15761E-03	.30660E-01	.00000E 00	.00000E 00	.00000E 00	.00000E 00
	-.21632E 00	-.85040E-02	.16660E-01	.00000E 00	.00000E 00					
R0W 3	.17936E 00	-.19133E 00	.62315E-01	-.10596E-04	-.65221E-05	-.11883E-01	.00000E 00	.00000E 00	.00000E 00	.00000E 00
	.43977E 00	-.29561E-02	-.40228E-02	.00000E 00	.00000E 00					
R0W 4	-.2659E-04	-.33500E-04	-.10696E-04	.42610E-04	.91194E-05	.41113E-01	.00000E 00	.00000E 00	.00000E 00	.00000E 00
	.23479E-04	.10552E-01	.14673E-01	.00000E 00	.00000E 00					
R0W 5	.18072E-03	.15741E-03	-.65221E-05	.91194E-05	.58511E-02	.14627E-01	.00000E 00	.00000E 00	.00000E 00	.00000E 00
	.43967E-04	.10938E 00	.44073E 00	.00000E 00	.00000E 00					
R0W 6	-.34479E-01	-.30660E-01	-.11883E-01	.41113E-01	.14627E-01	.39676E 02	.00000E 00	.00000E 00	.00000E 00	.00000E 00
	.17814E-01	.10315E 02	.14602E 02	.00000E 00	.00000E 00					
R0W 7	-.69096E-09	.00000E 00	.00000E 00	.00000E 00	.00000E 00	.00000E 00	.36046E-01	-.36601E-03	.36531E-03	.24418E 00
	.00000E 00	.00000E 00	.00000E 00	.00000E 00	.00000E 00					
R0W 8	-.10555E-11	.00000E 00	.00000E 00	.00000E 00	.00000E 00	.00000E 00	.36601E-03	.25254E-03	.75961E-04	-.16194E 00
	.00000E 00	.00000E 00	.00000E 00	.00000E 00	.00000E 00					
R0W 9	-.95899E-12	.00000E 00	.00000E 00	.00000E 00	.00000E 00	.00000E 00	.36531E-03	.75961E-04	.74214E-02	-.57265E-01
	.00000E 00	.00000E 00	.00000E 00	.00000E 00	.00000E 00					
R0W 10	.46555E-09	.00000E 00	.00000E 00	.00000E 00	.00000E 00	.00000E 00	.24418E 00	-.16194E 00	-.57265E-01	.10386E 03
	.00000E 00	.00000E 00	.00000E 00	.00000E 00	.00000E 00					
R0W 11	.20729E 00	-.21632E 00	.43977E 00	.23479E-04	.43967E-04	.17814E-01	.00000E 00	.00000E 00	.00000E 00	.00000E 00
	.64663E 02	.00000E 00	.00000E 00	.00000E 00	.00000E 00					
R0W 12	-.91954E-02	-.85040E-02	-.23553E-02	.10552E-01	.10938E 00	.10315E 02	.00000E 00	.00000E 00	.00000E 00	.00000E 00
	.00000E 00	.17072E 02	.49839E 02	.00000E 00	.00000E 00					
R0W 13	.23553E-01	.16660E-01	-.40228E-02	.14673E-01	.44073E 00	.14602E 02	.00000E 00	.00000E 00	.00000E 00	.00000E 00
	.00000E 00	.49839E 02	.17389E 03	.00000E 00	.00000E 00					
R0W 14	.46546E-09	.00000E 00	.00000E 00	.00000E 00	.00000E 00	.00000E 00	.19077E 00	-.10390E 00	-.18401E 00	.66839E 02
	.00000E 00	.00000E 00	.00000E 00	.71744E 02	.42611E 02					
R0W 15	.19755E-08	.00000E 00	.00000E 00	.00000E 00	.00000E 00	.00000E 00	.61769E-02	-.59320E-01	-.14661E 00	.38155E 02
	.00000E 00	.00000E 00	.00000E 00	.42611E 02	.27159E 02					

Figure 71. Performance Evaluator Output - With Fixed-Gain Optimal Controller (continued)

x(1) .ATMIX

R0 ¹	1	.1791E 05	-.1244E 03	.2249E 03	.6874E-01	.1835E-01	-.5263E 00	-.7199E 01	-.2247E-02	.1989E-04	-.9830E-01
R0 ²	2	.2171E 00	-.2643E-02	.1919E-01	-.9736E-01	-.2501E 00					
R0 ³	3	-.1544E 03	.2234E 03	-.9070E 03	-.3749E-03	-.2116E-01	.5271E 00	.6916E 01	.2682E-02	-.7017E-03	-.7793E-01
R0 ⁴	4	.4291E 00	-.2611E-02	.1446E-01	-.7556E-01	.4534E 00					
R0 ⁵	5	.5269E 03	-.9470E 03	.5170E 02	.4470E-02	.1029E-02	-.4224E-01	-.4369E 00	-.1786E-03	.6363E-04	.6800E-02
R0 ⁶	6	.4522E 00	-.2842E-02	-.0735E-02	.6592E-02	-.4271E-01					
R0 ⁷	7	.6872E-01	-.3749E-03	.4794E-02	.5100E-04	.9033E-05	.4111E-01	-.6406E-04	.9461E-08	-.4661E-07	-.1720E-04
R0 ⁸	8	.9463E-05	.1065E-01	.1467E-01	-.1693E-04	.2425E-05					
R0 ⁹	9	.1810E-01	-.2116E-01	.1012E-02	.9033E-05	.5851E-02	.1462E-01	-.8824E-05	-.4382E-08	.2563E-08	.5732E-06
R0 ¹⁰	10	.4434E-04	.1592E 00	.5417E 00	.5618E-06	-.1014E-05					
R0 ¹¹	11	.5263E 00	.3271E 00	-.4241E-01	.4111E-01	.1462E-01	.3967E 02	.2679E-03	.1127E-06	-.4955E-07	-.9078E-05
R0 ¹²	12	.1773E-01	-.1244E 00	.1467E 02	-.8879E-05	.2437E-04					
R0 ¹³	13	-.7199E 01	.5916E 01	.4249E 00	-.6406E-04	-.8824E-05	.2679E-03	.8700E 03	.1880E 00	.6383E-03	.5784E 00
R0 ¹⁴	14	.4691E-02	.1715E-04	.1244E-03	.5166E 00	.6540E 00					
R0 ¹⁵	15	-.2249E-03	.5603E-02	.1767E-03	.9461E-08	.4382E-08	.1127E-06	.1880E 00	.3008E-03	.7600E-04	-.1618E 00
R0 ¹⁶	16	.8515E-05	.3129E-04	.2387E-07	-.1038E 00	-.5912E-01					
R0 ¹⁷	17	.1523E-04	-.7117E-03	.6347E-04	-.4661E-07	.2563E-08	.4955E-07	.6383E-03	.7600E-04	.7421E-02	-.5725E-01
R0 ¹⁸	18	.3830E-01	.1773E-01	.6808E-02	-.1720E-04	.5732E-06	.9078E-05	.5784E 00	.1618E 00	-.5725E-01	.1038E 03
R0 ¹⁹	19	.4752E-02	-.1124E-01	-.1544E-03	.6694E 02	.3163E 02					
R0 ²⁰	20	.2171E 00	-.2244E 00	.4522E 00	.4298E-02	.4083E-02	.1779E-01	.4691E-02	.8915E-05	.1560E-04	.4375E-02
R0 ²¹	21	.4469E 02	.2900E 02	.4070E 00	.4298E-02	.4083E-02					
R0 ²²	22	-.5645E-02	.2611E-02	-.2942E-02	.1055E-01	.1933E 00	.1031E 02	.1715E-04	.3123E-08	.1022E-11	.5112E-10
R0 ²³	23	.0000E 00	.1737E 02	.4983E 02	.0000E 00	.0000E 00					
R0 ²⁴	24	.1910E-01	.1466E-01	.4073E-02	.1467E-01	.4407E 00	.1460E 02	.1264E-03	.2308E-07	.6339E-11	-.1544E-09
R0 ²⁵	25	.0000E 00	.4298E 02	.1729E 03	.0000E 00	.0000E 00					
R0 ²⁶	26	-.9736E-01	.7564E-01	.4596E-02	-.1693E-04	.5618E-06	.8879E-05	.5156E 00	.1038E 00	-.1839E 00	.6684E 02
R0 ²⁷	27	.4298E-02	.4070E 00	.2900E 00	.7175E 02	.4261E 02					
R0 ²⁸	28	-.2501E 00	.4691E 00	-.4271E-01	.2425E-05	-.1014E-05	.2437E-04	.6540E 00	-.5912E-01	-.1466E 00	.3816E 02
R0 ²⁹	29	-.4083E-02	.4070E 00	.2900E 00	.4261E 02	.2718E 02					

Figure 71. Performance Evaluator Output - With Fixed-Gain
Optimal Controller (continued)

XSUBH WIG NATRIA

R0 ¹	.6576E 03	.0000E 00	.3312E 02	.6841E-01	-.1928E-03	-.4509E-01	-.1111E 01	.1135E-03	.5978E-09	.1669E 00
R0 ²	.1505E 00	-.1713E-01	.1003E 01	.3216E 00	.1577E 00	.0000E 00	.0000E 00	.0000E 00	.0000E 00	.0000E 00
R0 ³	.0000E 00	.0000E 00	.0000E 00	.0000E 00	.0000E 00	.0000E 00	.0000E 00	.0000E 00	.0000E 00	.0000E 00
R0 ⁴	.3312E 02	.0000E 00	.2020E 02	.4612E-02	-.6179E-04	-.5748E-01	-.2692E 00	-.1136E-03	.4662E-04	.4911E-02
R0 ⁵	.4489E 00	-.3189E-02	-.1593E 01	.7898E 00	-.3147E-01	.4111E-01	-.6406E-04	.9461E-08	.4661E-07	-.1720E-04
R0 ⁶	.6841E-01	.0000E 00	.4612E-02	.5100E-04	.9032E-05	.1462E-01	.3291E-05	.3156E-09	.1334E-08	.4367E-06
R0 ⁷	.9465E-05	.1052E-01	.1467E-01	-.1775E-04	.2425E-05	.3967E 02	.7973E-03	.3181E-06	.1032E-06	-.1504E-04
R0 ⁸	.1928E-03	.0000E 00	-.6179E-04	.9032E-05	.5851E-02	.7973E-03	.8700E 03	.1880E 00	.6383E-03	.5784E 00
R0 ⁹	.4359E-04	.1033E 00	.4408E 00	.3943E-04	-.2028E-06	.3181E-06	.1880E 00	.3008E-03	.7600E-04	-.1618E 00
R0 ¹⁰	.4509E-01	.0000E 00	-.5748E-01	.4111E-01	.1462E-01	.3967E 02	.7973E-03	.3181E-06	.1032E-06	-.1504E-04
R0 ¹¹	.1776E-01	.1031E 02	.1461E 02	.4841E-02	.5984E-04	.7973E-03	.8700E 03	.1880E 00	.6383E-03	.5784E 00
R0 ¹²	.1111E 01	.0000E 00	-.2692E 00	-.6406E-04	.3291E-05	.3181E-06	.1880E 00	.3008E-03	.7600E-04	-.1618E 00
R0 ¹³	.4691E-02	.1715E-04	.3014E-01	.5305E 00	.6540E 00	.3181E-06	.1880E 00	.3008E-03	.7600E-04	-.1618E 00
R0 ¹⁴	.1135E-03	.0000E 00	-.1136E-03	.9461E-08	.3156E-09	.3181E-06	.1880E 00	.3008E-03	.7600E-04	-.1618E 00
R0 ¹⁵	.8915E-05	.3123E-08	.1164E-04	-.1038E 00	-.4591E-01	.1032E-06	.6383E-03	.7600E-04	.7421E-02	-.5725E-01
R0 ¹⁶	.5978E-03	.0000E 00	.4642E-04	-.4661E-07	.1334E-08	-.1032E-06	.6383E-03	.7600E-04	.7421E-02	-.5725E-01
R0 ¹⁷	.1560E-04	.1022E-11	-.3045E-05	-.1839E 00	-.1466E 00	.1504E-04	.5784E 00	.1618E 00	.5725E-01	.1038E 03
R0 ¹⁸	.1669E 00	.0000E 00	.4911E-02	-.1720E-04	.4367E-06	.1504E-04	.5784E 00	.1618E 00	.5725E-01	.1038E 03
R0 ¹⁹	.4375E-02	.5110E-10	-.8382E-03	.6684E 02	.3816E 02	.1776E-01	.4691E-02	.8915E-05	.1560E-04	.4375E-02
R0 ²⁰	.1505E 00	.0000E 00	.8489E 00	.9465E-05	.4359E-04	.1776E-01	.4691E-02	.8915E-05	.1560E-04	.4375E-02
R0 ²¹	.6469E 02	.0000E 00	-.1845E-02	.3375E-02	-.4083E-02	.1031E 02	.1715E-04	.3123E-08	.1022E-11	.5110E-10
R0 ²²	.1713E-01	.2000E 00	-.3189E-02	.1052E-01	.1033E 00	.1031E 02	.1715E-04	.3123E-08	.1022E-11	.5110E-10
R0 ²³	.0000E 00	.1712E 02	.4983E 02	-.1847E-04	.8000E 00	.1461E 02	.3014E-02	.1166E-04	.3045E-05	-.3382E-03
R0 ²⁴	.1030E 01	.0000E 00	.1553E 01	.1467E-01	.4408E 00	.1461E 02	.3014E-02	.1166E-04	.3045E-05	-.3382E-03
R0 ²⁵	.1215E-02	.4911E 04	.1743E 03	.2104E 00	.2011E-02	.4841E-02	.5306E 00	.1038E 00	.1839E 00	.6684E 02
R0 ²⁶	.3214E 02	.0000E 00	-.7858E 00	.1775E-04	.9943E-04	.4841E-02	.5306E 00	.1038E 00	.1839E 00	.6684E 02
R0 ²⁷	.3375E-02	-.1347E-04	.2104E 00	.7183E 02	.4262E 02	.5984E-04	.6540E-04	.5912E-01	.1466E 00	.3816E 02
R0 ²⁸	.1577E 00	.0000E 00	-.3147E-01	.2425E-05	-.2028E-06	.5984E-04	.6540E-04	.5912E-01	.1466E 00	.3816E 02
R0 ²⁹	.4083E-02	.0000E 00	.2011E-02	.4262E 02	.2718E 02					

CEP HORIZ TOTAL= .31270228E 02 CEP VERTICAL= .19492559E 02

Figure 71. Performance Evaluator Output - With Fixed-Gain Optimal Controller (continued)

KFISOLVERS - CATALAN .BT

R8 ¹	.31414E-01	.07364E-01	.6592E-01	.23315E-05	.2932E-02	.25489E-02	.00000E-00	.58517E-05	.11776E-07	.90263E-08
	.29938E-01	.31754E-01	.11160E-00	.23353E-08	.8530E-08					
R8 ²	.07668E-01	.24367E-01	.2019E-01	.19213E-05	.25307E-02	.22449E-02	.15104E-10	.50919E-05	.10245E-07	.78544E-08
	.37524E-01	.33307E-01	.16394E-00	.20557E-08	.74839E-08					
R8 ³	.36928E-01	.50120E-01	.1033E-02	.39573E-05	.53155E-02	.446238E-02	.53748E-10	.10834E-04	.21811E-07	.16711E-07
	.18114E-00	.14444E-00	.31406E-00	.42398E-08	.15422E-07					
R8 ⁴	.21815E-02	.16619E-02	.25772E-05	.15144E-09	.20348E-06	.17700E-06	.61500E-07	.40383E-01	.81260E-04	.62292E-04
	.69325E-03	.63714E-03	.51543E-03	.16212E-04	.59048E-04					
R8 ⁵	.29802E-02	.25307E-02	.3135E-02	.20348E-06	.27331E-03	.23775E-03	.82366E-10	.54242E-04	.10915E-06	.83669E-07
	.93114E-01	.25339E-01	.11107E-01	.21776E-07	.79314E-07					
R8 ⁶	.25489E-02	.22449E-02	.46138E-02	.17700E-06	.23775E-03	.20681E-03	.69988E-10	.47192E-04	.94961E-07	.72795E-07
	.61000E-00	.74044E-00	.5744E-00	.18442E-07	.6892E-07					
R8 ⁷	.00000E-00	.13104E-10	.3748E-10	.61500E-07	.82966E-10	.69988E-10	.15708E-01	.64099E-04	.13117E-02	.98642E-01
	.11841E-11	.37231E-11	.1273E-11	.10445E-00	.80601E-01					
R8 ⁸	.88512E-05	.90712E-05	.10334E-04	.40383E-01	.54242E-04	.47192E-04	.64099E-04	.26156E-08	.53526E-05	.40252E-05
	.19079E-06	.13009E-06	.19848E-06	.42624E-03	.32891E-03					
R8 ⁹	.11776E-07	.10245E-07	.31311E-07	.81260E-04	.10915E-06	.94961E-07	.13117E-02	.53526E-05	.10953E-03	.82371E-02
	.28411E-09	.37307E-09	.30971E-09	.87225E-00	.67306E-00					
R8 ¹⁰	.20263E-03	.73346E-03	.16711E-07	.62292E-04	.83669E-07	.72795E-07	.98642E-01	.40252E-05	.82371E-02	.61945E-02
	.29427E-03	.35730E-03	.30644E-03	.65599E-00	.50613E-00					
R8 ¹¹	.59838E-01	.37324E-01	.18110E-00	.69325E-03	.93118E-00	.81000E-00	.11841E-11	.19079E-06	.38411E-09	.29427E-09
	.21725E-02	.09154E-02	.17500E-02	.74289E-10	.27315E-09					
R8 ¹²	.11754E-01	.30335E-01	.16144E-00	.63714E-03	.85882E-00	.74445E-00	.37221E-11	.18609E-06	.37502E-09	.28700E-09
	.29153E-02	.26759E-02	.3445E-02	.68451E-10	.24813E-09					
R8 ¹³	.11801E-00	.10339E-00	.21406E-00	.81343E-03	.11007E-01	.95744E-00	.52250E-11	.19348E-06	.39871E-09	.30624E-09
	.37503E-02	.34464E-02	.4594E-02	.87370E-10	.31964E-09					
R8 ¹⁴	.23353E-08	.20348E-08	.42398E-08	.16212E-04	.21776E-07	.18942E-07	.10445E-00	.42624E-03	.87225E-00	.65599E-00
	.74239E-10	.63051E-10	.7373E-10	.69460E-02	.53593E-02					
R8 ¹⁵	.25038E-06	.74044E-06	.19422E-07	.59448E-04	.79314E-07	.68992E-07	.80601E-01	.32891E-03	.67306E-00	.50613E-00
	.27013E-09	.24415E-09	.31666E-09	.53599E-02	.41358E-02					

Figure 71. Performance Evaluator Output - With Fixed-Gain
Optimal Controller (continued)

WEIGHTING DATA

R0# 1	.40535E-01	.35740E-01	.73032E-01	.28144E-05	.37309E-02	-.32889E-02	.17190E-10	.76205E-05	.15338E-07	.11754E-07
R0# 2	.12241E-00	.11439E-00	-.15726E-00	-.30143E-08	-.10975E-07					
R0# 3	.35700E-01	.31441E-01	.44766E-01	.24790E-05	.33298E-02	-.28965E-02	.34675E-13	.68497E-05	.13382E-07	.10257E-07
R0# 4	.11345E-00	.10437E-00	-.11341E-00	-.26537E-08	-.96624E-08					
R0# 5	.73520E-01	.64740E-01	.13339E-02	.51760E-05	.68583E-02	-.59660E-02	.84930E-10	.14043E-04	.28272E-07	.21660E-07
R0# 6	.23367E-00	.21476E-00	-.27220E-00	-.54715E-08	-.19898E-07					
R0# 7	.28144E-05	.24740E-05	.51760E-05	.19446E-09	.26254E-06	-.22838E-06	.57864E-07	.52666E-01	.10599E-03	.81236E-04
R0# 8	.89448E-03	.82248E-03	-.10573E-04	-.20227E-04	-.76181E-04					
R0# 9	.37400E-02	.33249E-02	.88585E-02	.26254E-06	.35265E-03	-.30676E-03	.77366E-10	.70740E-04	.14237E-06	.10912E-06
R0# 10	.12315E-01	.11142E-01	-.14202E-01	-.28410E-07	-.10233E-06					
R0# 11	.32889E-02	.28448E-02	.59660E-02	.22238E-06	-.30675E-03	.26684E-03	.69479E-10	.61543E-04	-.12386E-06	.94930E-07
R0# 12	.10451E-01	.10455E-01	.12354E-01	.24452E-07	.89012E-07					
R0# 13	.17190E-10	.34475E-13	.84930E-10	.57864E-07	.77366E-10	-.69479E-10	.15708E-01	.64099E-04	.13117E-02	.98642E-01
R0# 14	.17403E-11	.42241E-11	.45793E-11	-.10445E-00	.80601E-01					
R0# 15	.76205E-05	.66437E-05	.14043E-04	.52666E-01	.70740E-04	-.61543E-04	.64099E-04	.26156E-08	.53526E-05	.40252E-05
R0# 16	.24740E-06	.23775E-06	-.26492E-06	-.42624E-03	.32891E-03					
R0# 17	.15338E-07	.13332E-07	.28272E-07	.10599E-03	.14237E-06	-.12386E-06	.13117E-02	.53526E-05	.10953E-03	.82371E-02
R0# 18	.42730E-09	.47305E-09	-.53250E-09	-.87225E-00	.67306E-00					
R0# 19	.11754E-07	.10257E-07	.21660E-07	.81236E-04	.10912E-06	-.94930E-07	.98642E-01	.40252E-05	.82371E-02	.61945E-02
R0# 20	.38097E-09	.36682E-09	-.40871E-09	-.65595E-00	.50615E-00					
R0# 21	.12381E-00	.11345E-00	.23367E-00	.89448E-03	.12015E-01	-.10451E-01	.17303E-11	.24700E-06	.49730E-09	.38097E-09
R0# 22	.40335E-02	.37622E-02	-.48386E-02	-.95867E-10	-.34856E-09					
R0# 23	.11439E-00	.10437E-00	.21476E-00	.82239E-03	.11042E-01	-.96055E-00	.42241E-11	.23775E-06	.47905E-09	.36668E-09
R0# 24	.37422E-02	.34577E-02	-.44470E-02	-.88283E-10	-.32021E-09					
R0# 25	.15226E-00	-.13410E-00	-.27620E-00	-.10573E-04	-.14202E-01	.12354E-01	.45793E-11	.26492E-06	-.53250E-09	-.40871E-09
R0# 26	.48386E-02	-.44470E-02	.57193E-02	.11238E-09	.41234E-09					
R0# 27	.30143E-08	-.26537E-08	-.54715E-08	-.20927E-04	-.28110E-07	.24452E-07	-.10445E-00	.42624E-03	.87225E-00	.65595E-00
R0# 28	.95367E-10	-.88283E-10	.11238E-09	.69460E-02	-.53598E-02					
R0# 29	.10970E-07	-.96624E-08	-.19498E-07	-.76181E-04	-.10233E-06	.89012E-07	.80601E-01	.32891E-03	.67306E-00	.50615E-00
R0# 30	.34856E-09	-.32021E-09	.41234E-09	-.45359E-02	.41358E-02					

QH(1,1) = .31415226E 01 QH(7,7) = .15707963E 01 QV(2,2) = .31415226E 01 QV(7,7) = .15707963E 01

JSUBH# .34362248E 04 JSUBV# .40369832E 04

APPROXIMATE CEPH# .33072410E 02 APPROXIMATE CEPV# .35847059E 02

STOP 00000200

Figure 71. Performance Evaluator Output - With Fixed-Gain Optimal Controller (concluded)

SECTION VII
STATIONARY AND NONSTATIONARY GAINS AND SPECTRUMS

GAIN PLOTS

Plots of optimal controller gains corresponding to the aircraft states were made, one for the time-varying optimal gains and the other for the fixed-optimal gains for each frozen-time point linear data. The symbols for the controller gains are given in Table X. Figure 72 shows the program listing used for plotting the gains. The plots corresponding to nonstationary and stationary designs for each gain element are shown as Figure 73. The gain values are expressed as per-radian deflection. It is seen that the values for stationary and nonstationary designs are reasonably close to each other.

Table X. Symbols for Controller Gains Corresponding to Aircraft States

	δ_{xe}	δ_{he}	δ_u	δ_θ	δ_q	δ_w	δ_{ye}	δ_ψ	δ_r	δ_v	δ_ϕ	δ_p
δ_s	$K_{\delta_s, xe}$	$K_{\delta_s, he}$	$K_{\delta_s, u}$	$K_{\delta_s, \theta}$	$K_{\delta_s, q}$	$K_{\delta_s, w}$	$K_{\delta_s, ye}$	$K_{\delta_s, \psi}$	$K_{\delta_s, r}$	$K_{\delta_s, v}$	$K_{\delta_s, \phi}$	$K_{\delta_s, p}$
δ_a	$K_{\delta_a, xe}$	$K_{\delta_a, he}$	$K_{\delta_a, u}$	$K_{\delta_a, \theta}$	$K_{\delta_a, q}$	$K_{\delta_a, w}$	$K_{\delta_a, ye}$	$K_{\delta_a, \psi}$	$K_{\delta_a, r}$	$K_{\delta_a, v}$	$K_{\delta_a, \phi}$	$K_{\delta_a, p}$
δ_r	$K_{\delta_r, xe}$	$K_{\delta_r, he}$	$K_{\delta_r, u}$	$K_{\delta_r, \theta}$	$K_{\delta_r, q}$	$K_{\delta_r, w}$	$K_{\delta_r, ye}$	$K_{\delta_r, \psi}$	$K_{\delta_r, r}$	$K_{\delta_r, v}$	$K_{\delta_r, \phi}$	$K_{\delta_r, p}$
δ_{sp}	$K_{\delta_{sp}, xe}$	$K_{\delta_{sp}, he}$	$K_{\delta_{sp}, u}$	$K_{\delta_{sp}, \theta}$	$K_{\delta_{sp}, q}$	$K_{\delta_{sp}, w}$	$K_{\delta_{sp}, ye}$	$K_{\delta_{sp}, \psi}$	$K_{\delta_{sp}, r}$	$K_{\delta_{sp}, v}$	$K_{\delta_{sp}, \phi}$	$K_{\delta_{sp}, p}$

Contrails

```
▲FORTRAN LS,G9
1:   DIMENSION XX(20),IORD(48,8),YY(20,48),AK(4,18,20),AB(6)
2:   DIMENSION AKK(4,17)
3:   READ(5,1)NG
4:   1 FORMAT(I2)
5:   DO 3 I=1,NG
6:   3 READ(5,2)((IORD(I,J),J=1,8)
7:   2 FORMAT(8(A4))
8:   READ(5,998)NDP
9:   998 FORMAT(I2)
10:  DO 2022 L=1,20
11:  READ(6)AKK
12:  DO 3033 I=1,4
13:  DO 3033 J=1,17
14:  3033 AK(I,J,L)=AKK(I,J)
15:  2022 CONTINUE
16:  DO 2023 I=1,19
17:  2023 XX(I)=I-1
18:  XX(20)=18.97
19:  DO 4 L=1,NDP
20:  ICOT=0
21:  DO 5 I=1,4
22:  DO 5 J=1,12
23:  ICOT=ICOT+1
24:  5 YY(L,ICOT)=AK(I,J,L)/57.3
25:  4 CONTINUE
26:  DO 100 L=1,NG
27:  XMAX=-1.E+20
28:  XMIN=+1.E+20
29:  DO 10 I=1,NDP
30:  XMAX=AMAX(XMAX,YY(I,L))
31:  10 XMIN=AMIN(XMIN,YY(I,L))
32:  R=XMAX-XMIN
33:  WRITE(9,200)((IORD(L,K),K=1,8)
34:  200 FORMAT(1H1,25X,8A4)
35:  AB(1)=XMIN
36:  DO 11 M=1,5
37:  11 AB(M+1)=AB(M)+R/5.
38:  WRITE(9,201)(AB(M),M=1,6)
39:  201 FORMAT(//6G14.3)
40:  WRITE(9,202)
41:  202 FORMAT(8X,'I',5('-----I'))
42:  JJ=6
43:  DO 300 J=1,NDP
44:  LL=(YY(J,L)-XMIN)*70./R
45:  IF(J.NE.0) GOT0 400
46:  T=XX(J)
47:  JJ=JJ+5
48:  WRITE(9,203)T,LL
49:  203 FORMAT(F6.2,' I',NX,'*')
50:  GOT0 300
51:  400 WRITE(9,204)LL
52:  204 FORMAT(6X,' I',NX,'*')
53:  300 CONTINUE
54:  100 CONTINUE
55:  END
```

Figure 72. Gain Plotting Program Listing

Contrails

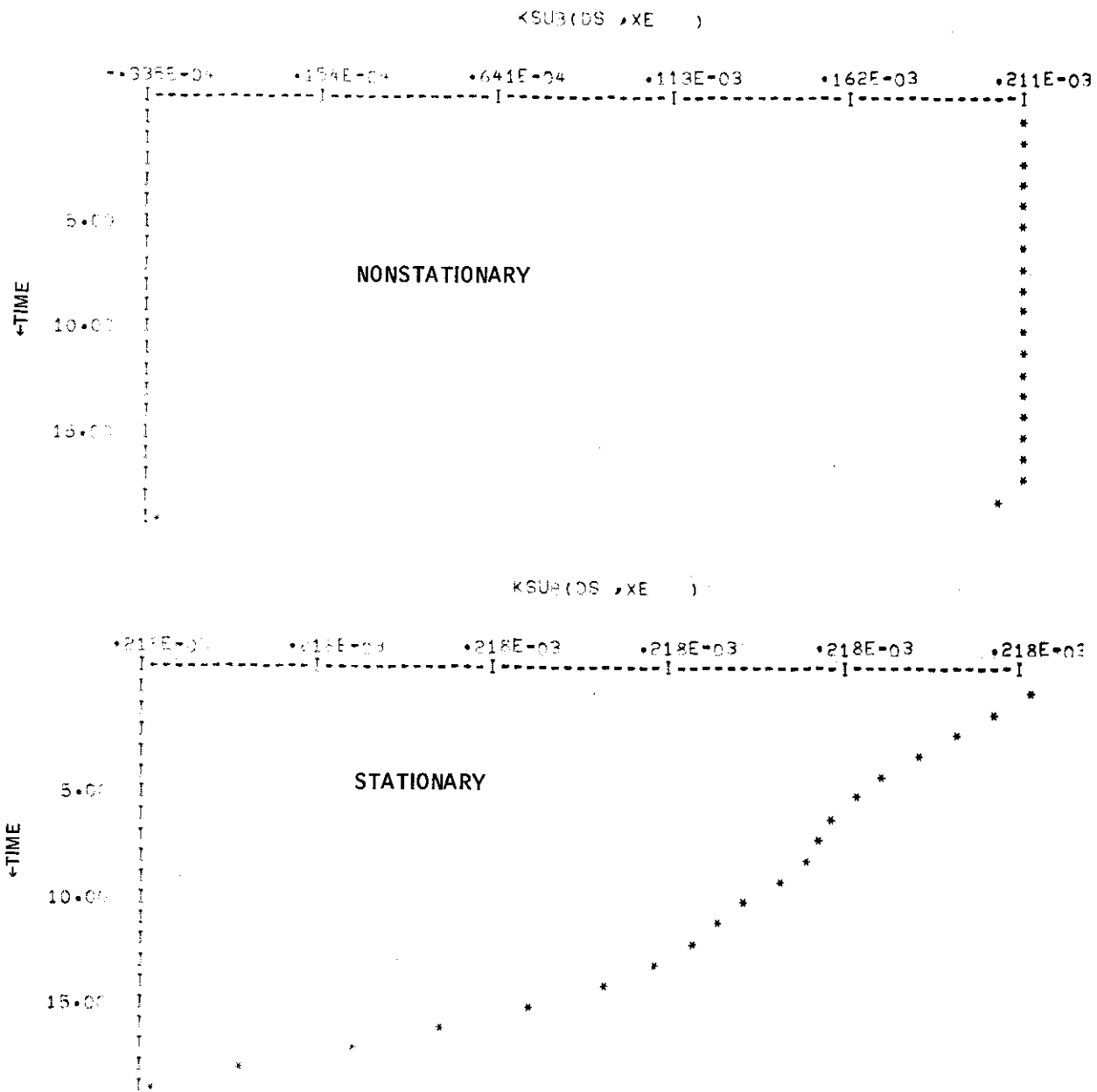


Figure 73. Optimal Controller Gain Plots versus Time

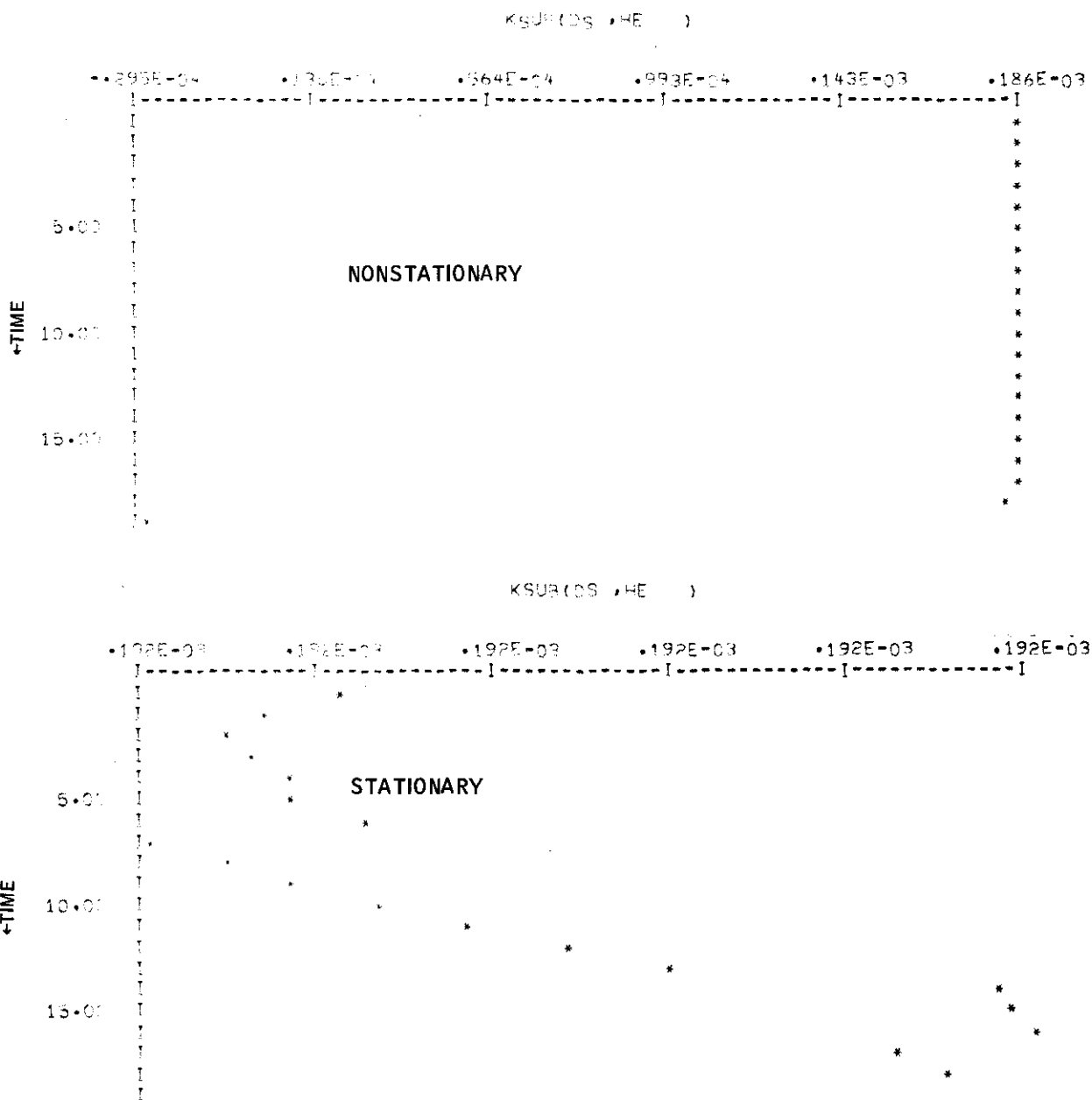


Figure 73. Optimal Controller Gain Plots (continued)

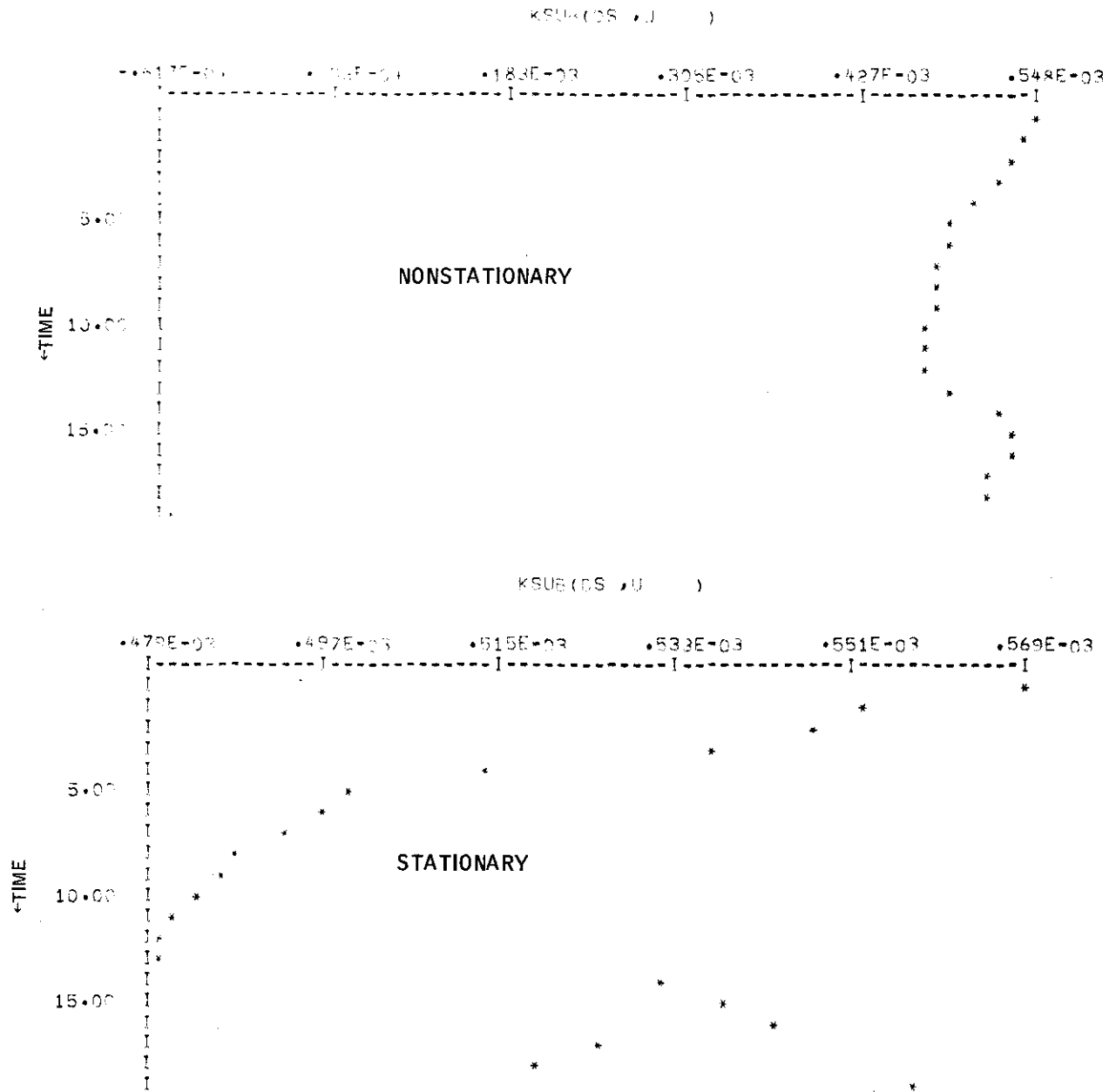


Figure 73. Optimal Controller Gain Plots (continued)

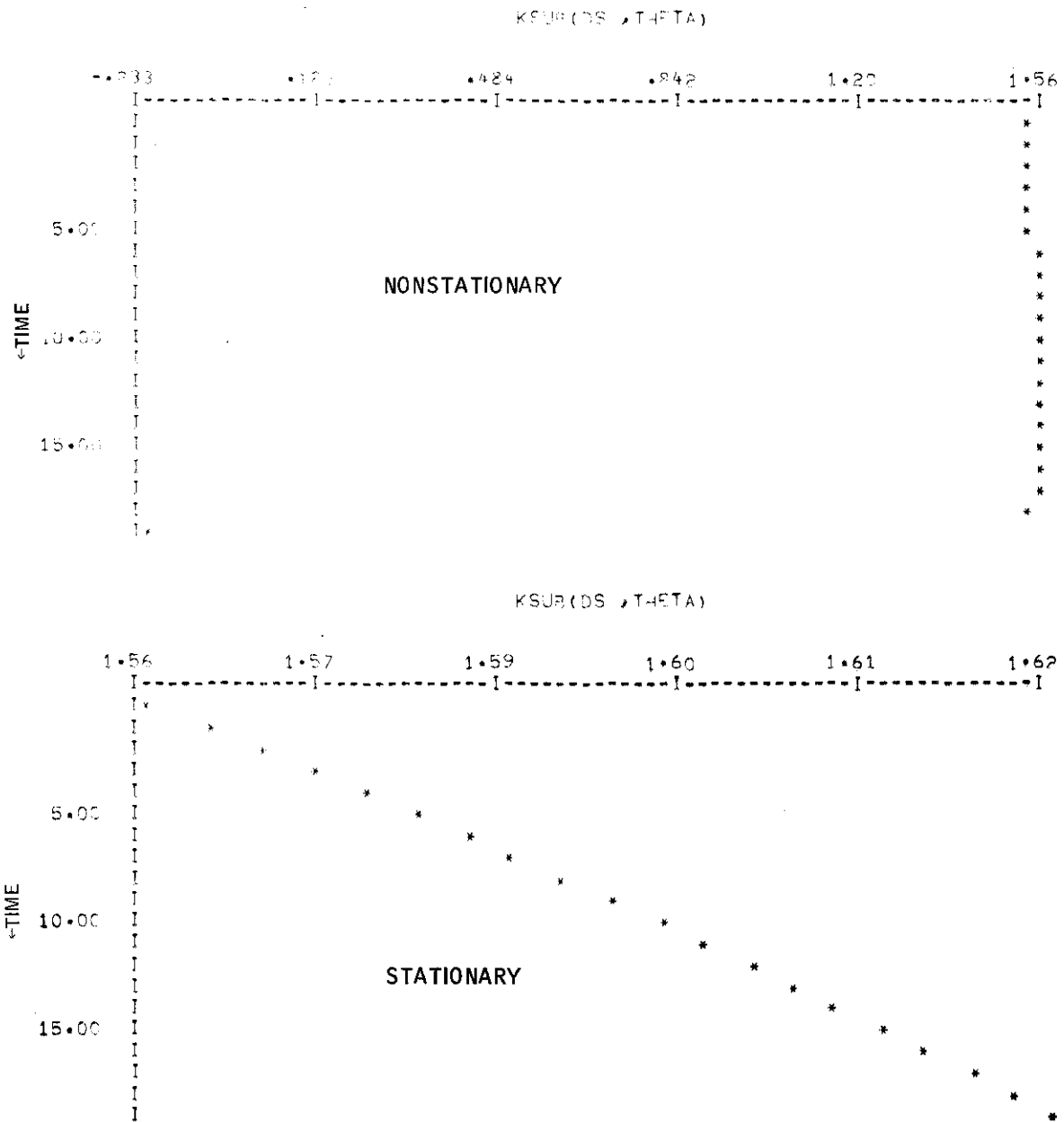


Figure 73. Optimal Controller Gain Plots (continued)

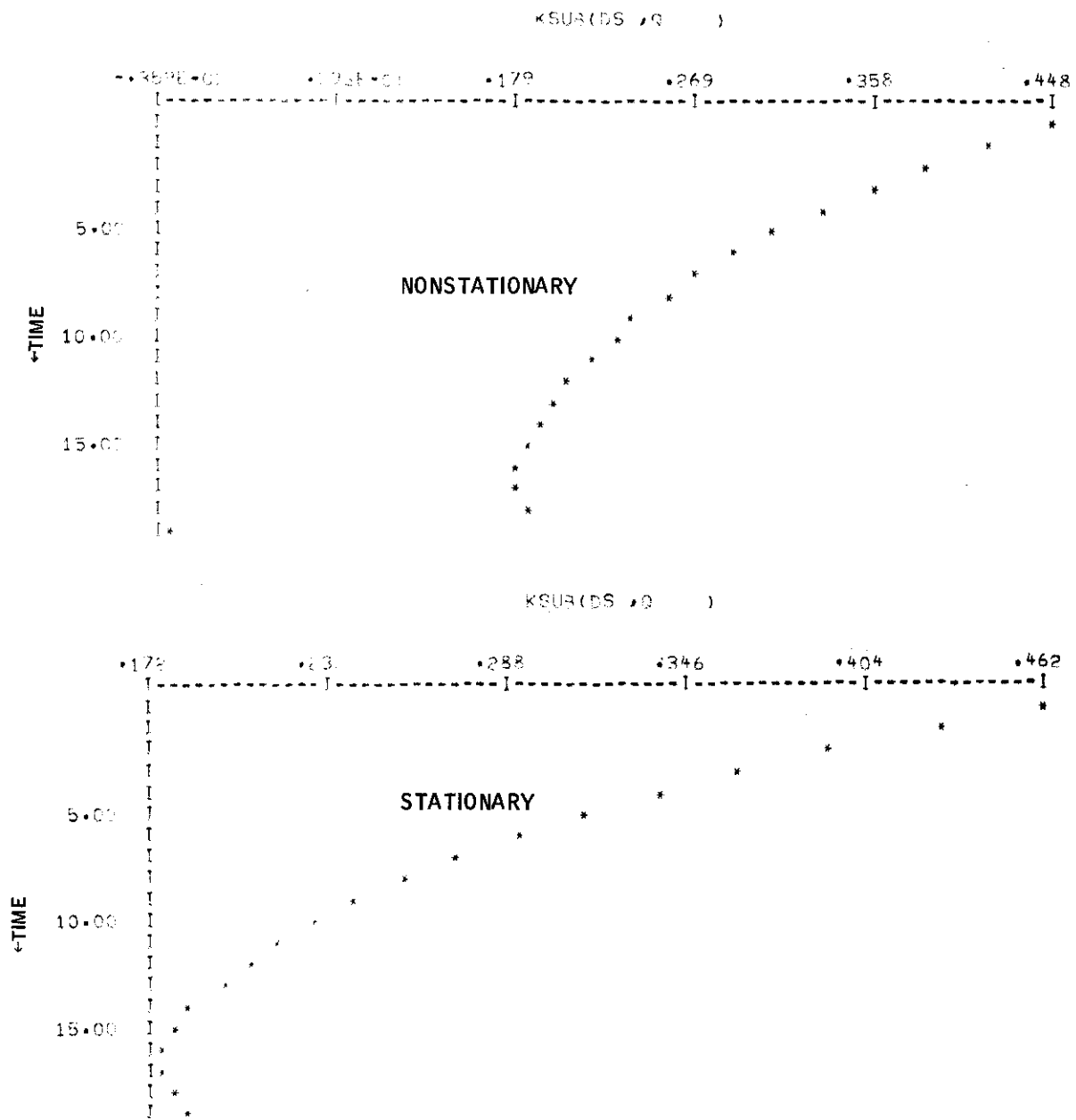


Figure 73. Optimal Controller Gain Plots (continued)

Contrails

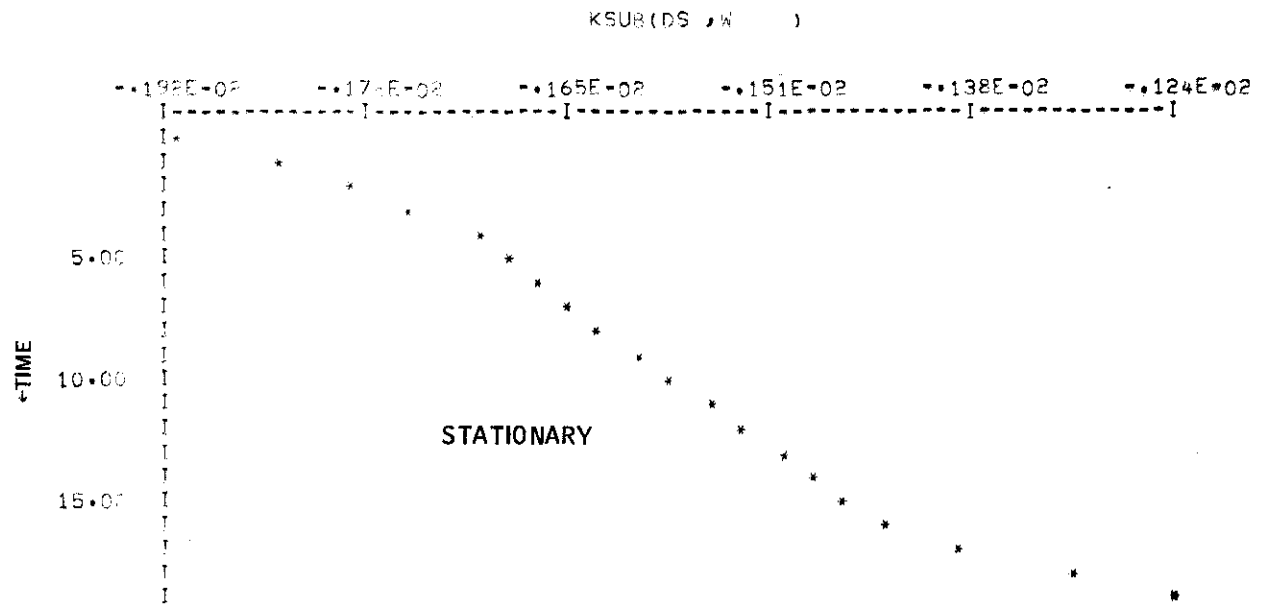
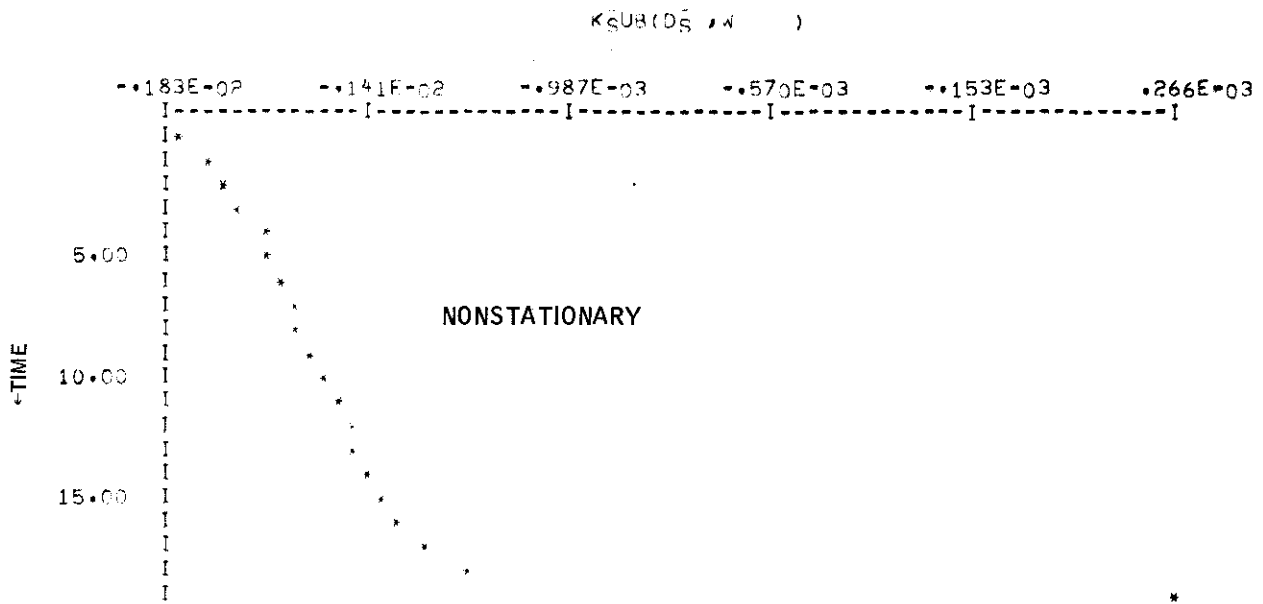


Figure 73. Optimal Controller Gain Plots (continued)

Contrails

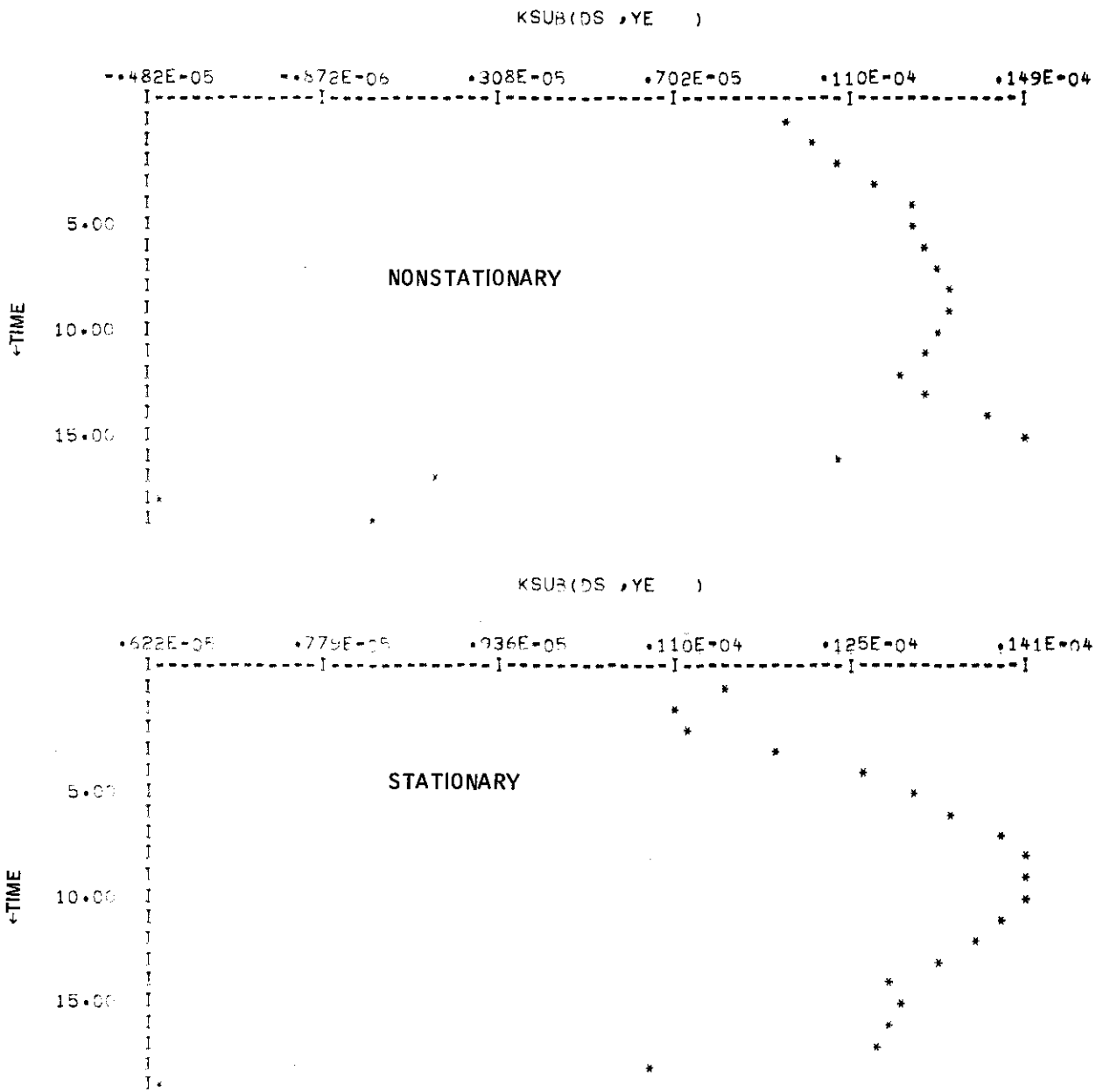


Figure 73. Optimal Controller Gain Plots (continued)

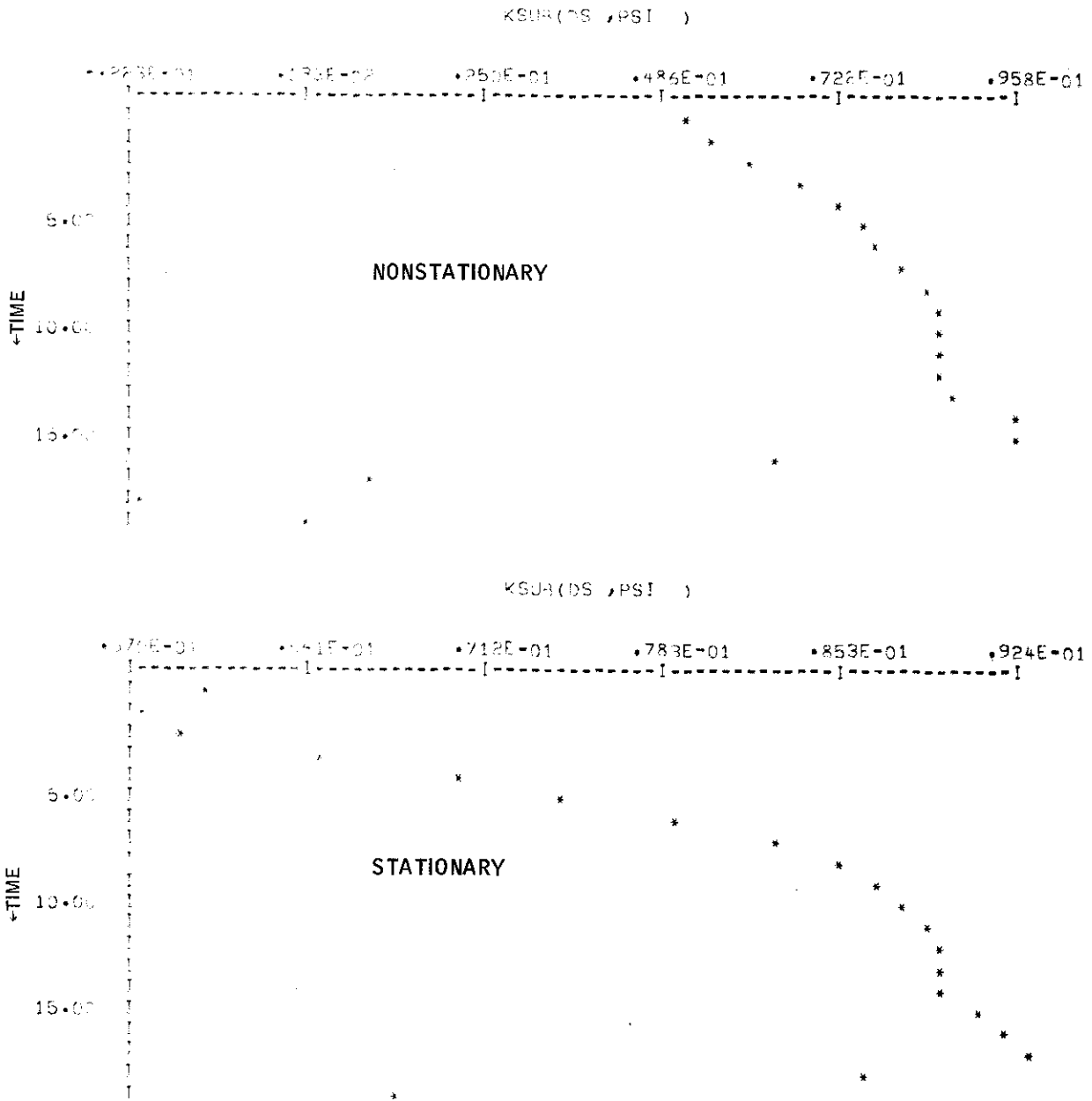


Figure 73. Optimal Controller Gain Plots (continued)

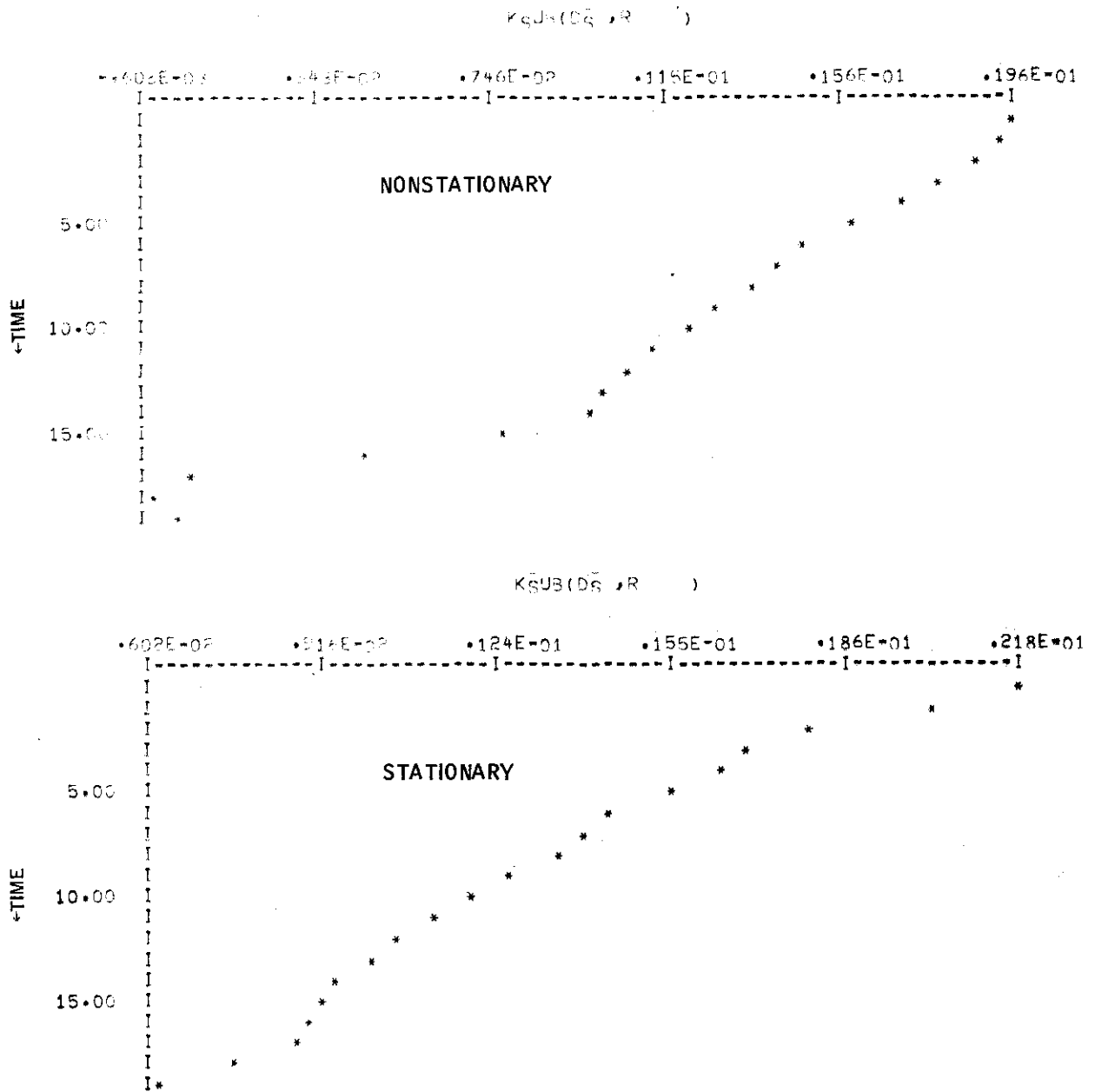


Figure 73. Optimal Controller Gain Plots (continued)

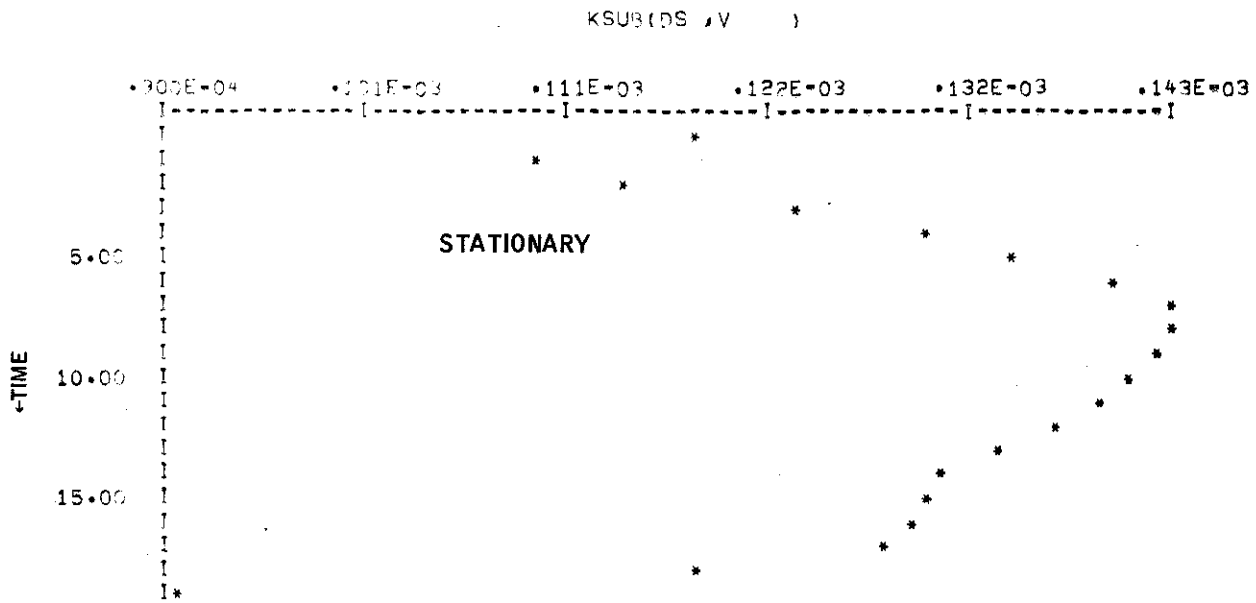
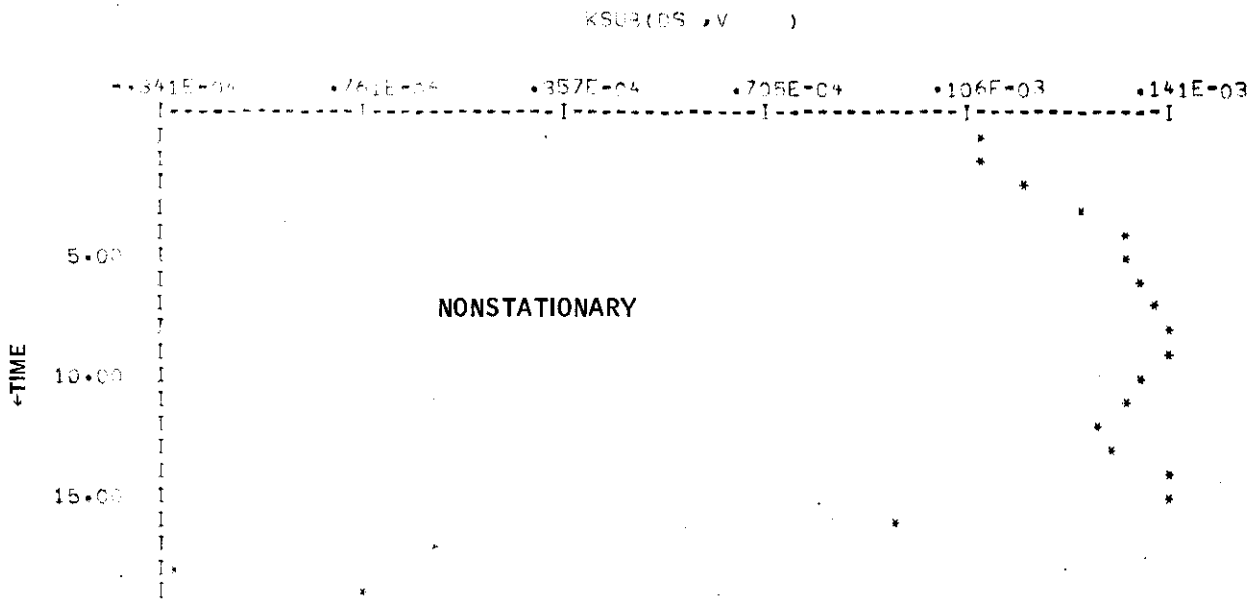


Figure 73. Optimal Controller Gain Plots (continued)

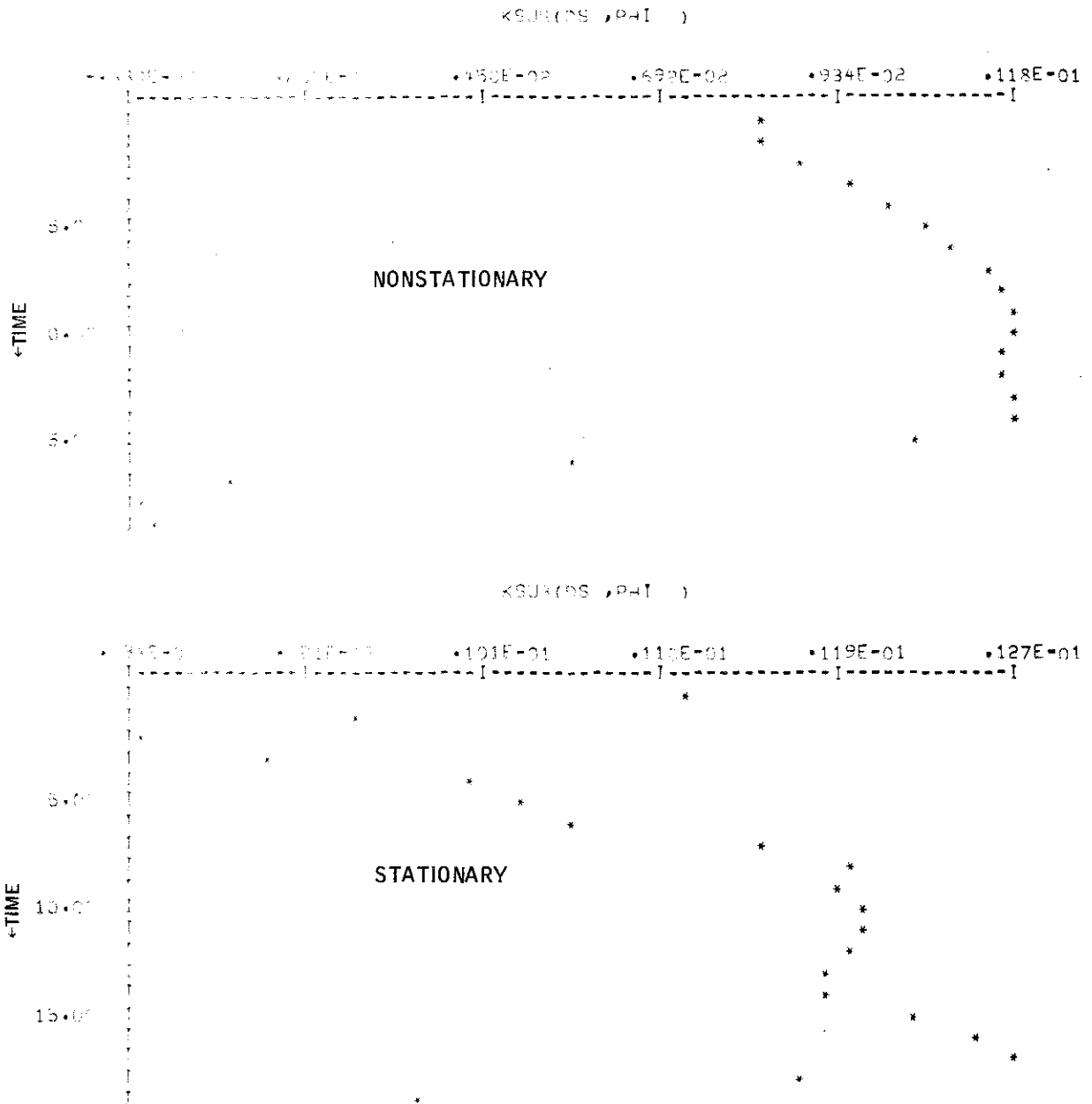


Figure 73. Optimal Controller Gain Plots (continued)

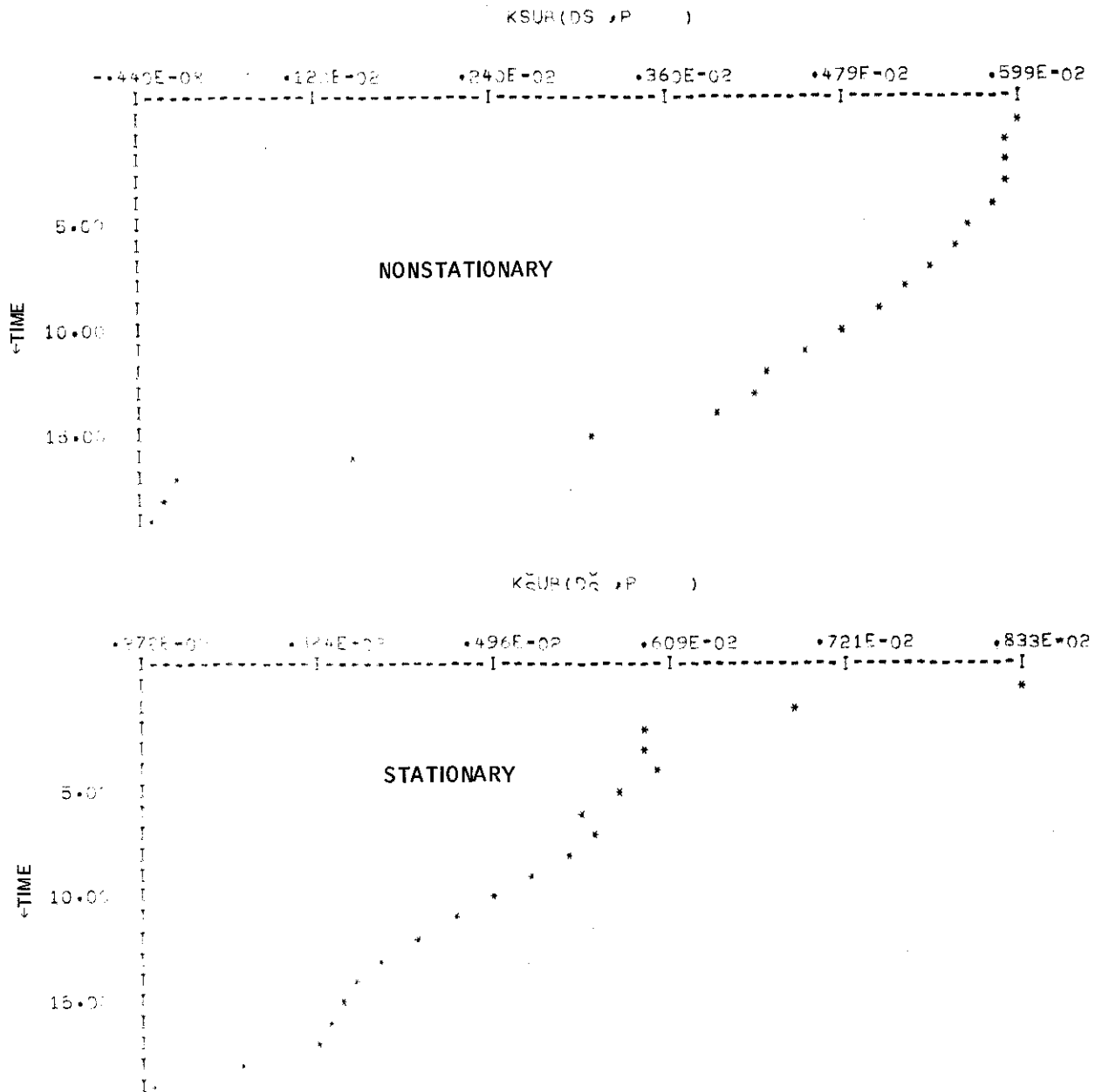


Figure 73. Optimal Controller Gain Plots (continued)

Contrails

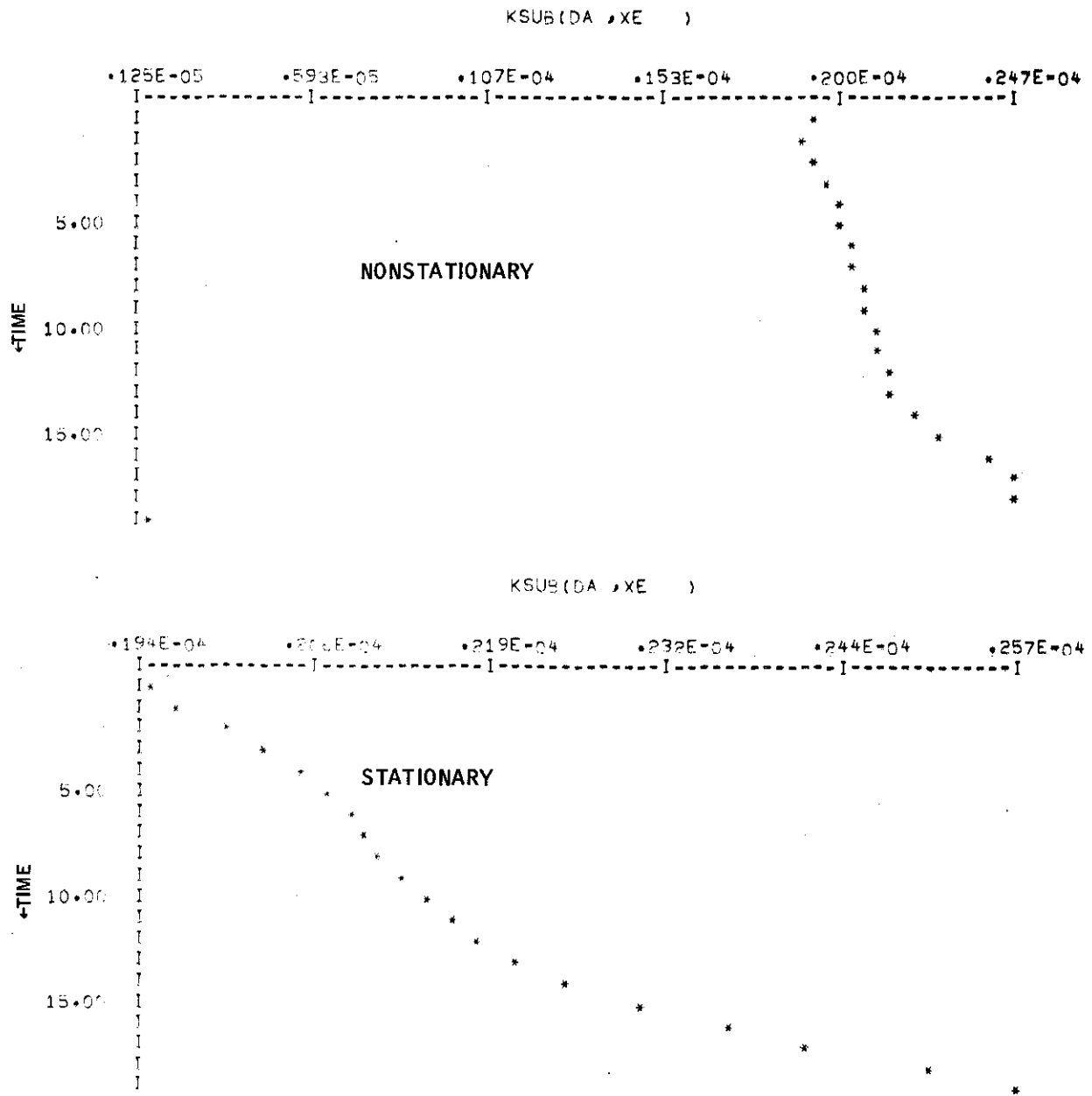


Figure 73. Optimal Controller Gain Plots (continued)

Contrails

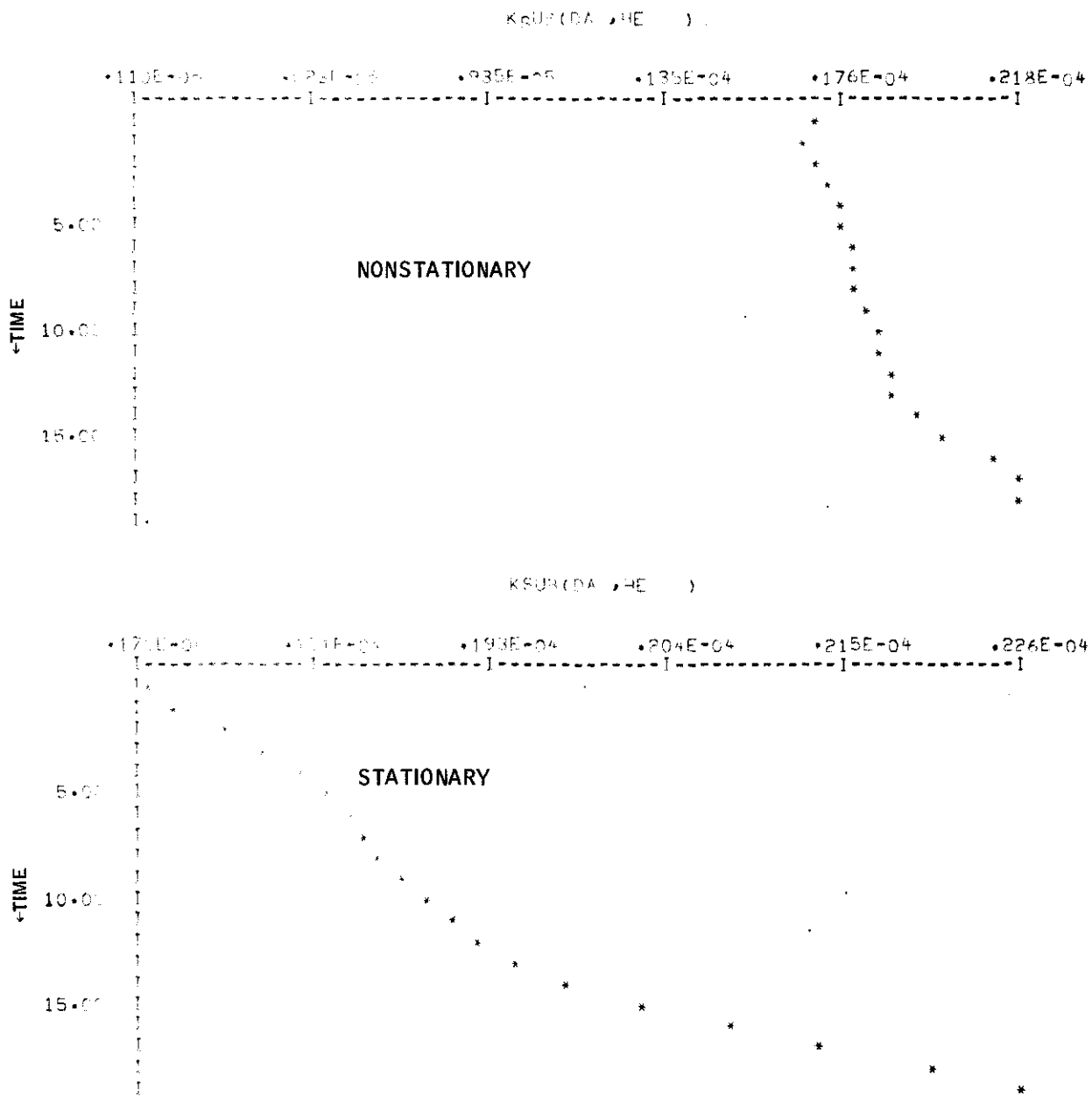


Figure 73. Optimal Controller Gain Plots (continued)

Contrails

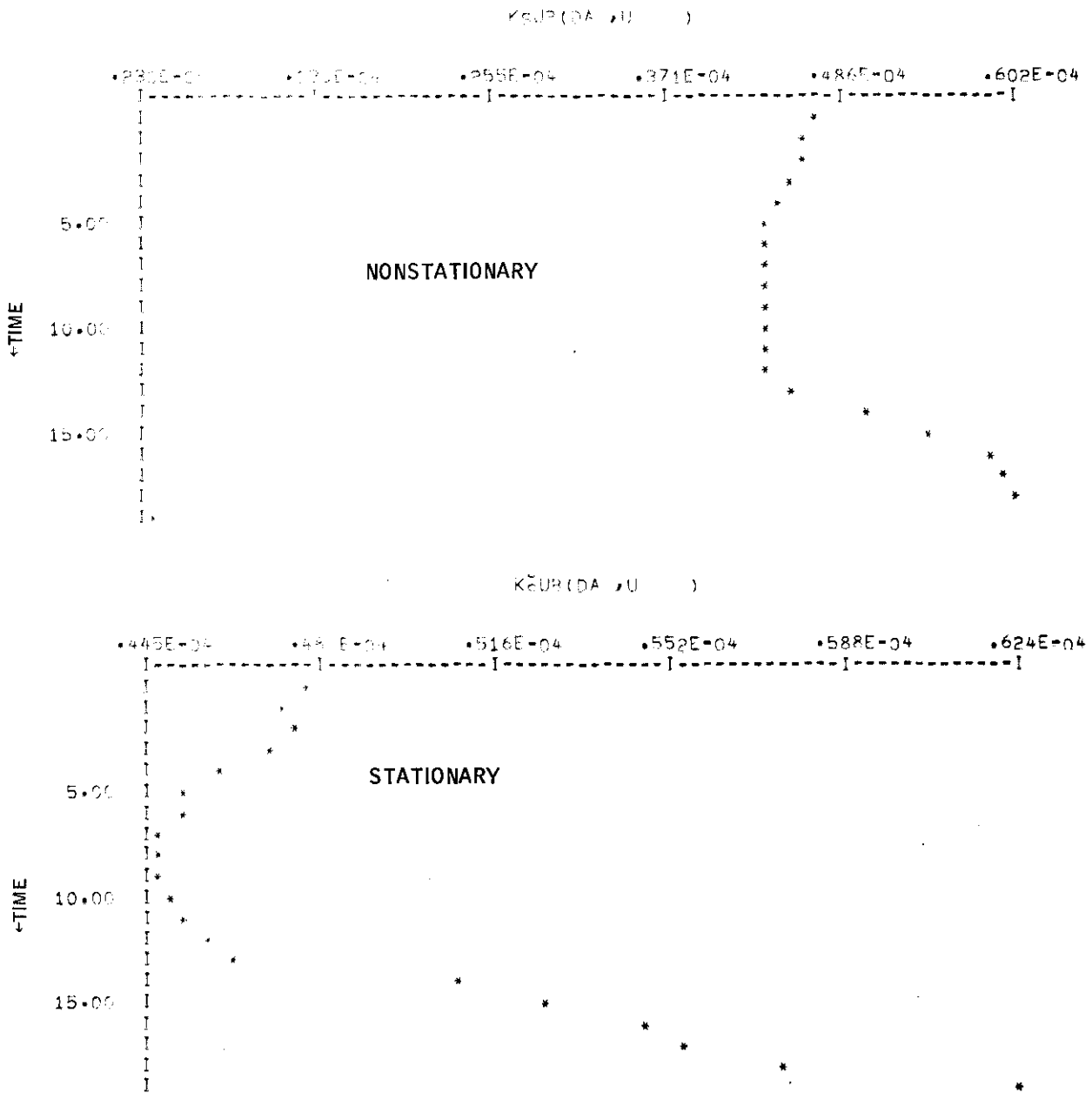


Figure 73. Optimal Controller Gain Plots (continued)

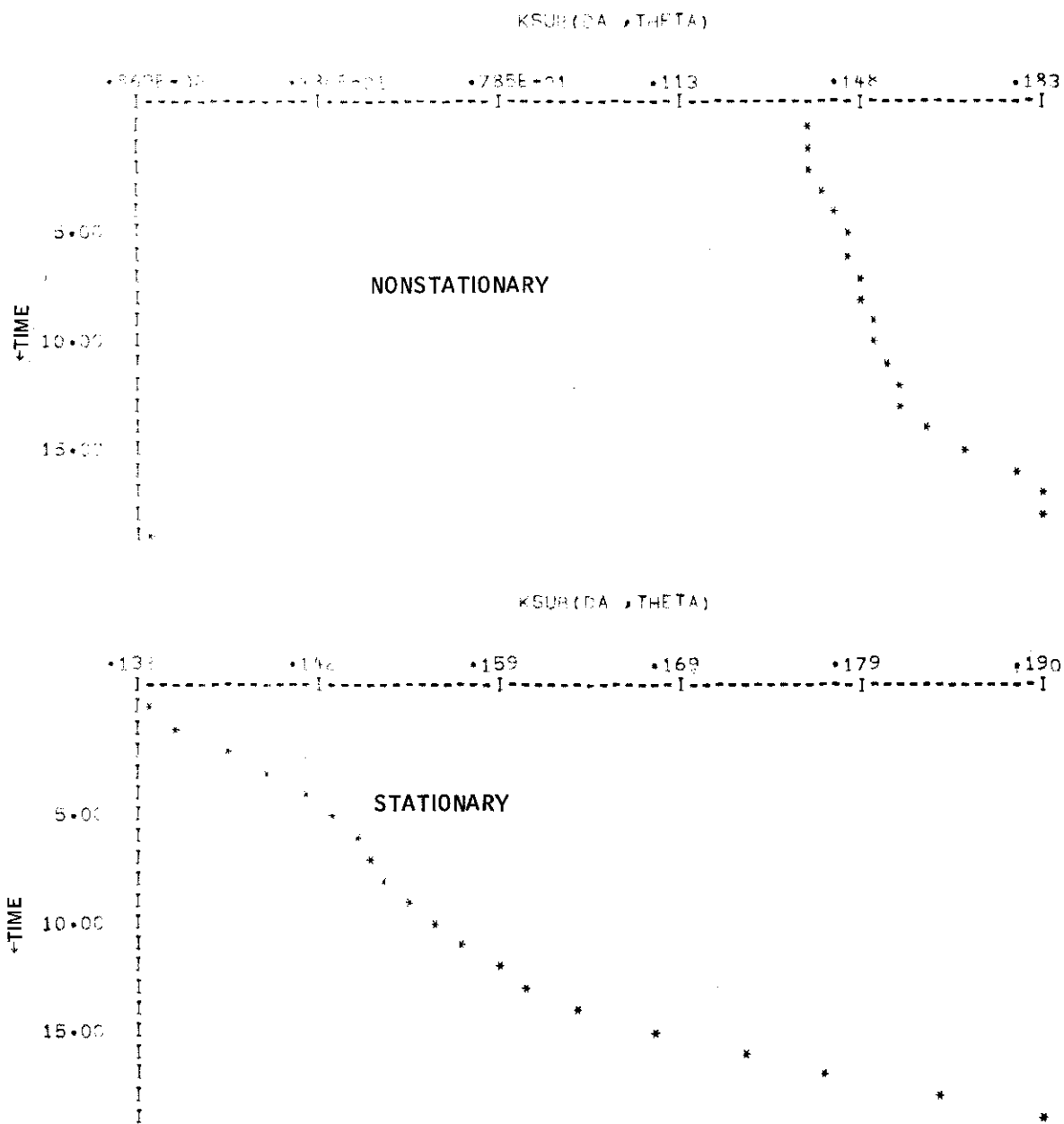


Figure 73. Optimal Controller Gain Plots (continued)

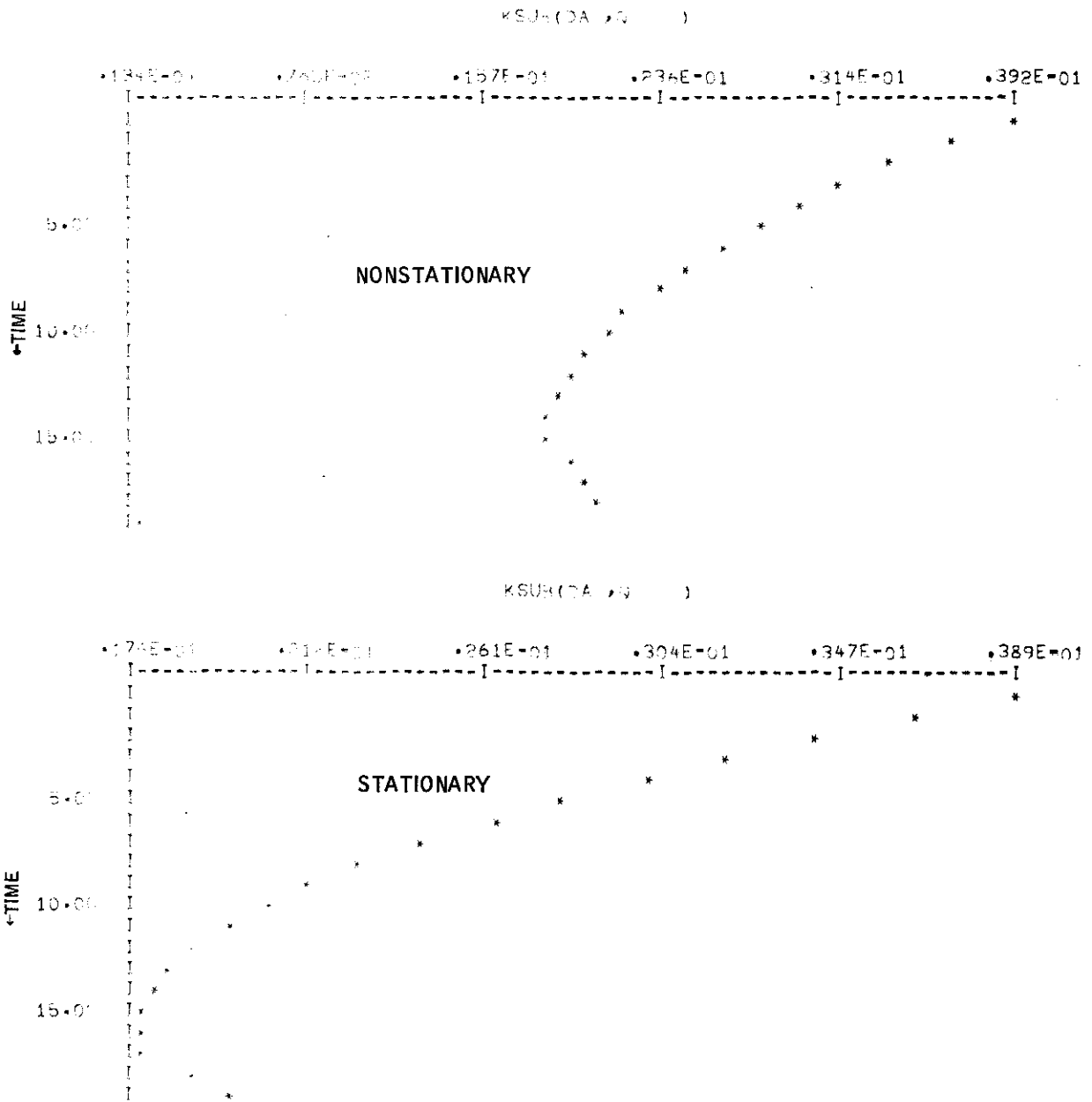


Figure 73. Optimal Controller Gain Plots (continued)

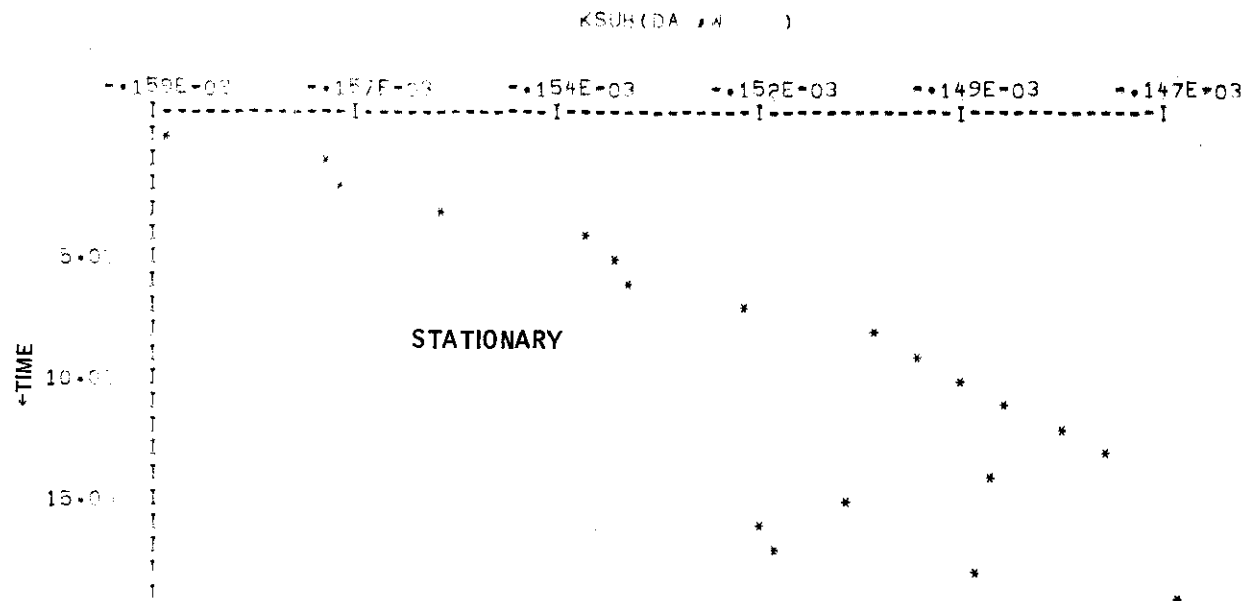
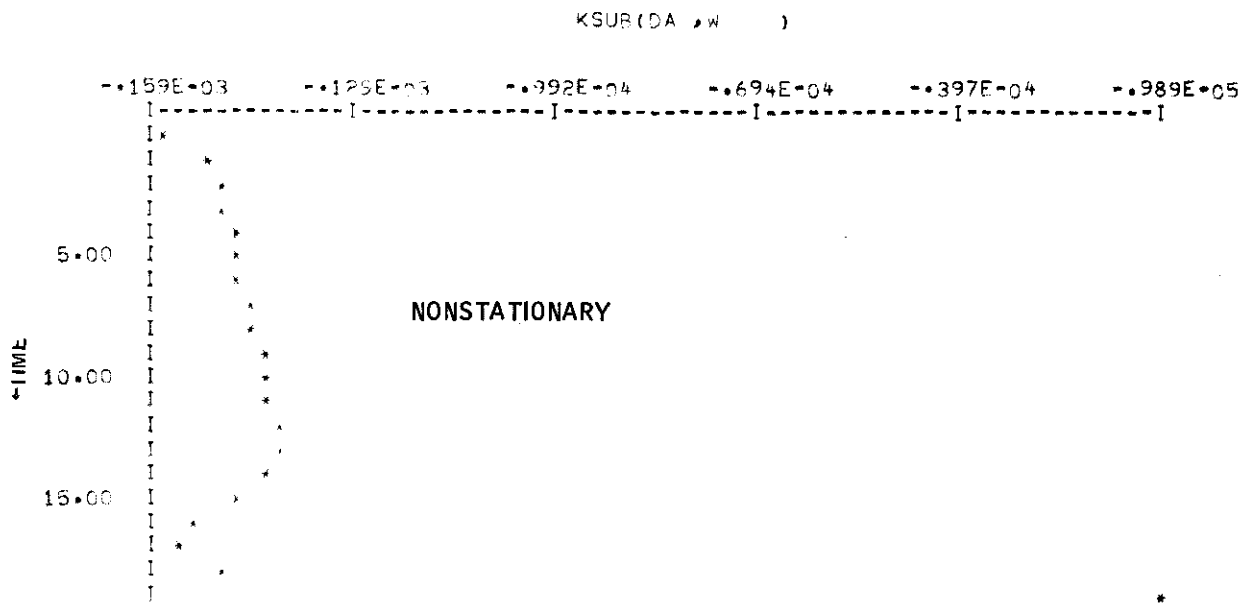


Figure 73. Optimal Controller Gain Plots (continued)

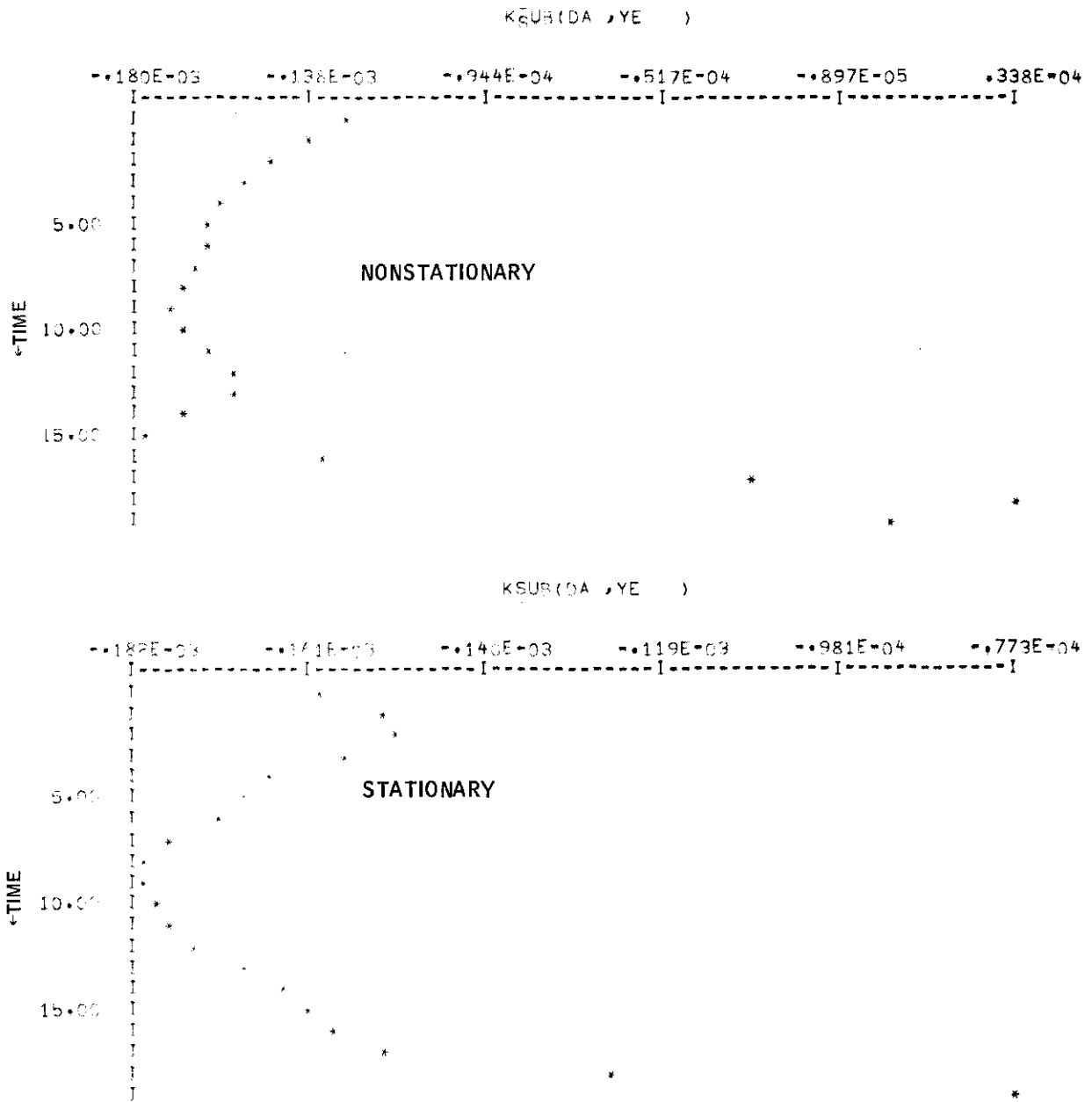


Figure 73. Optimal Controller Gain Plots (continued)

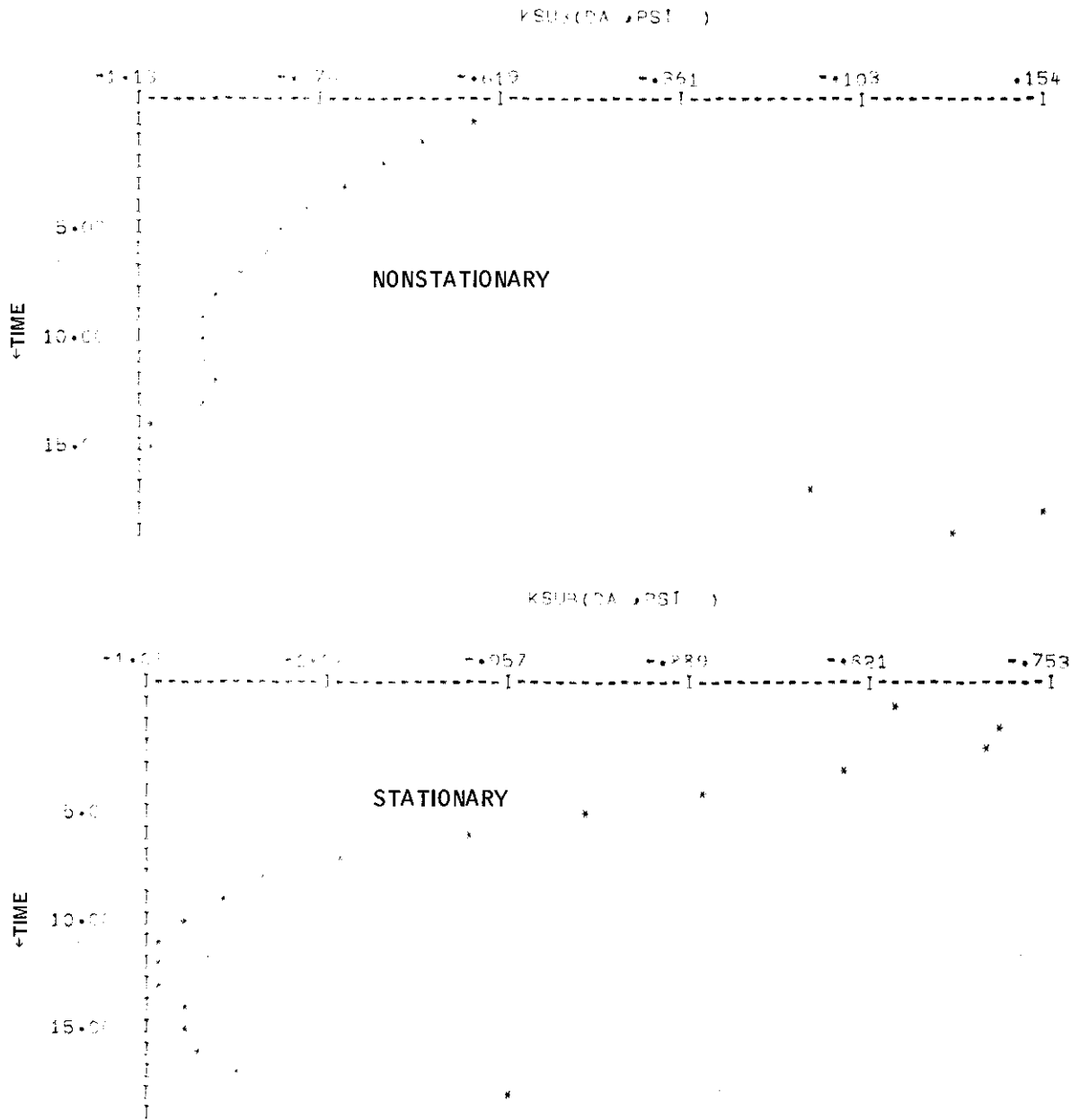


Figure 73. Optimal Controller Gain Plots (continued)

Contrails

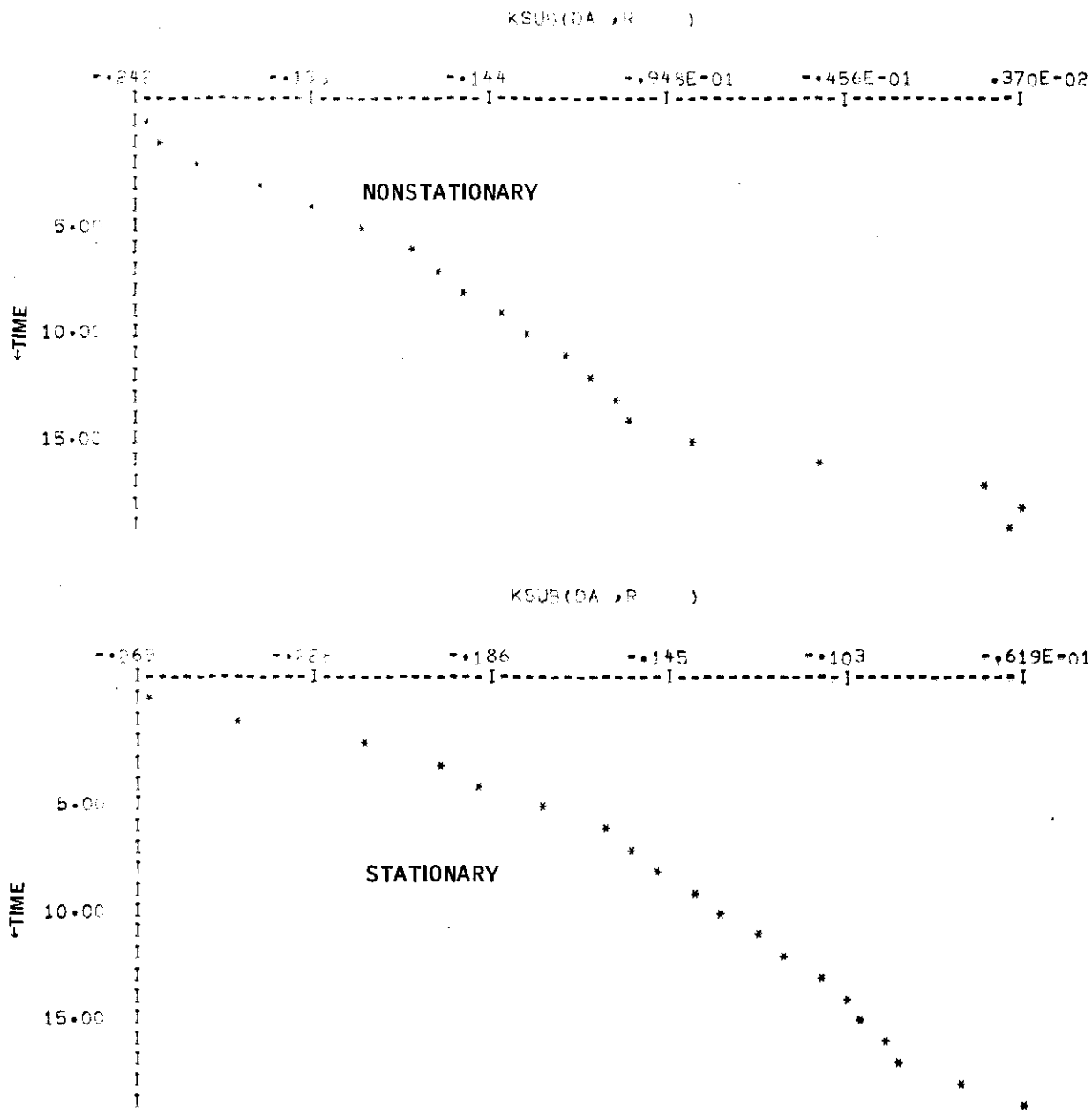


Figure 73. Optimal Controller Gain Plots (continued)

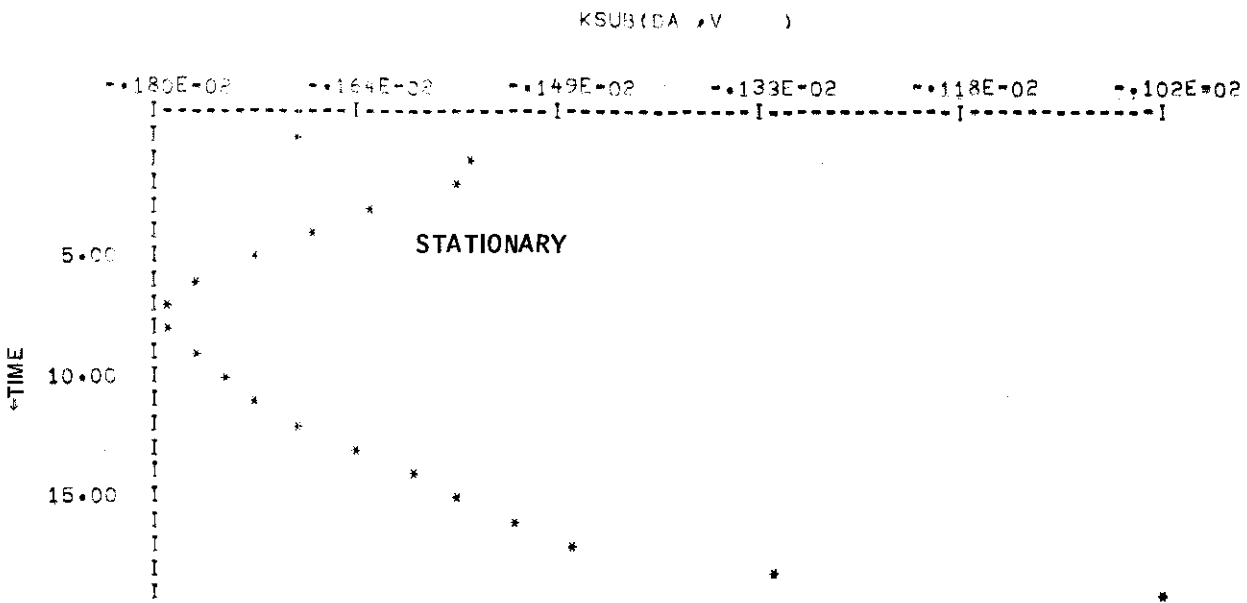
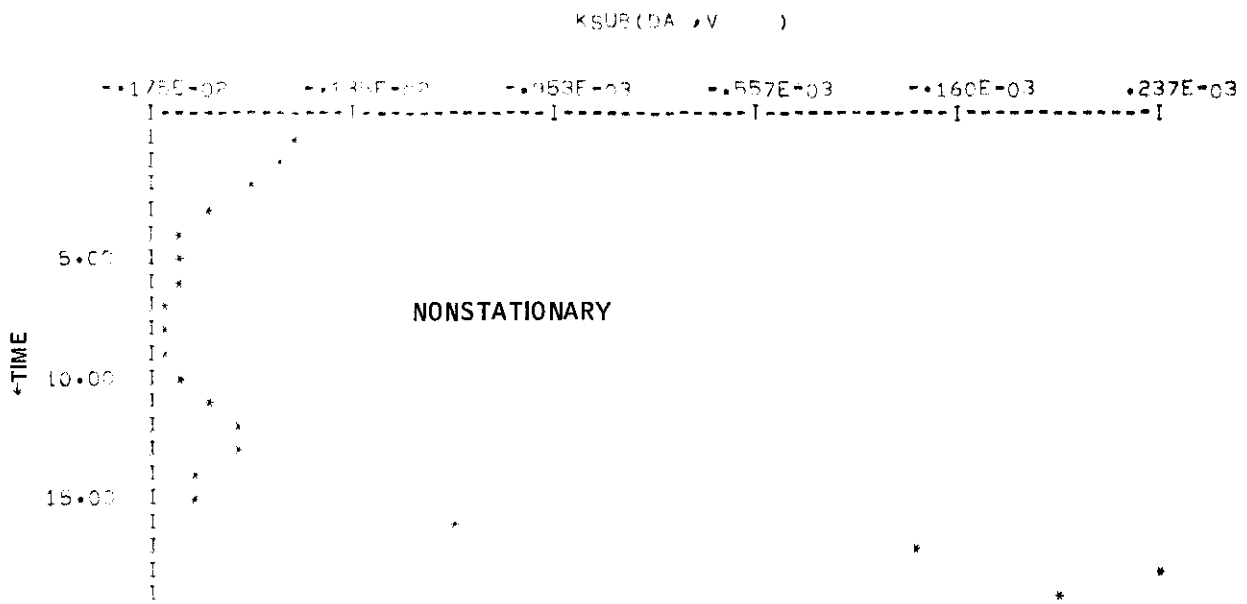


Figure 73. Optimal Controller Gain Plots (continued)

Contrails

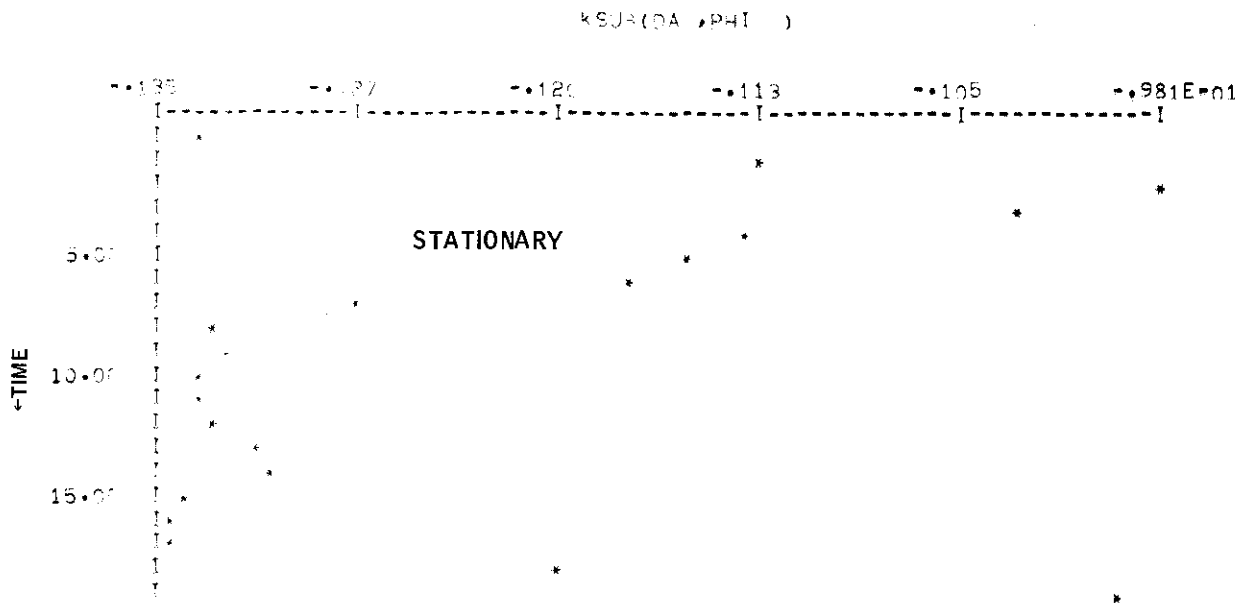
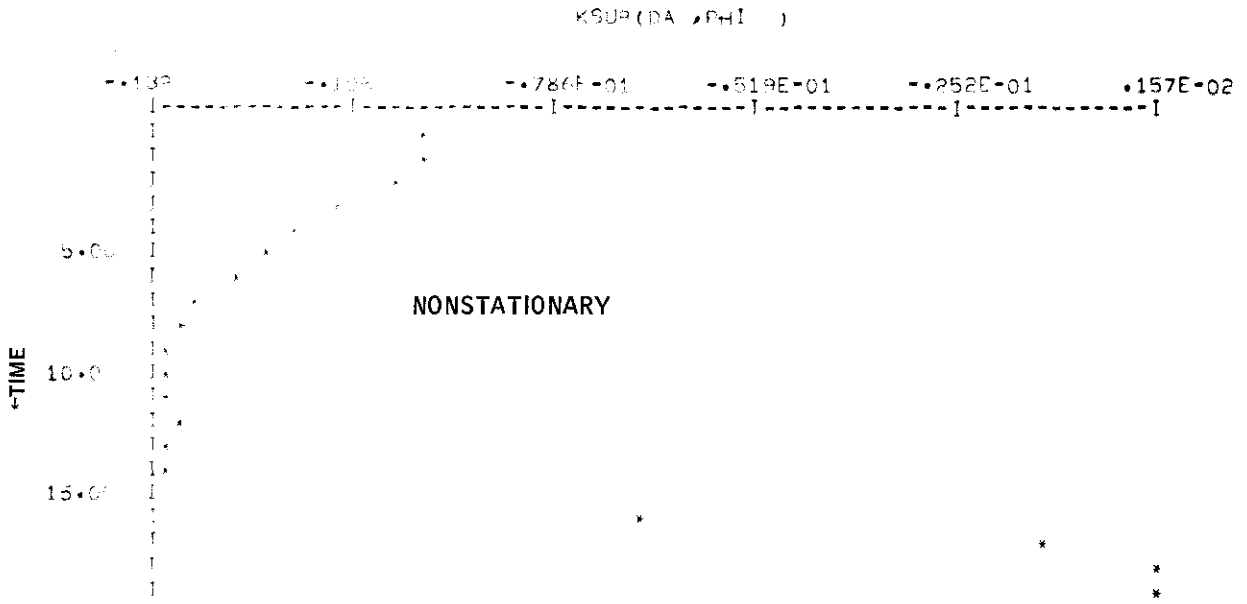


Figure 73. Optimal Controller Gain Plots (continued)

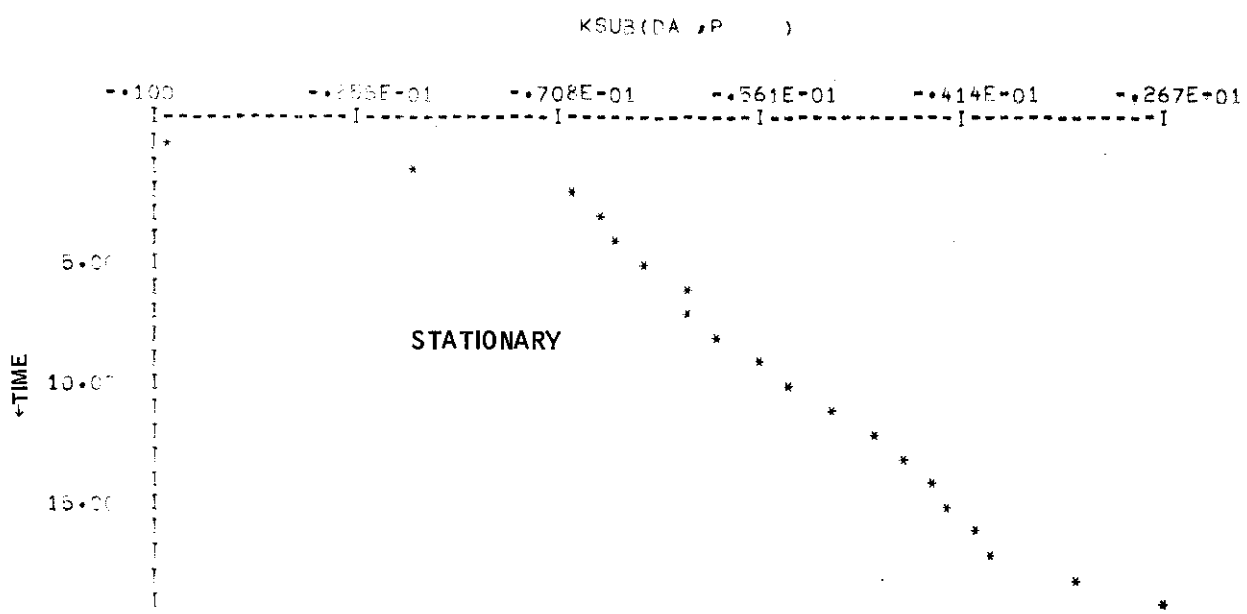
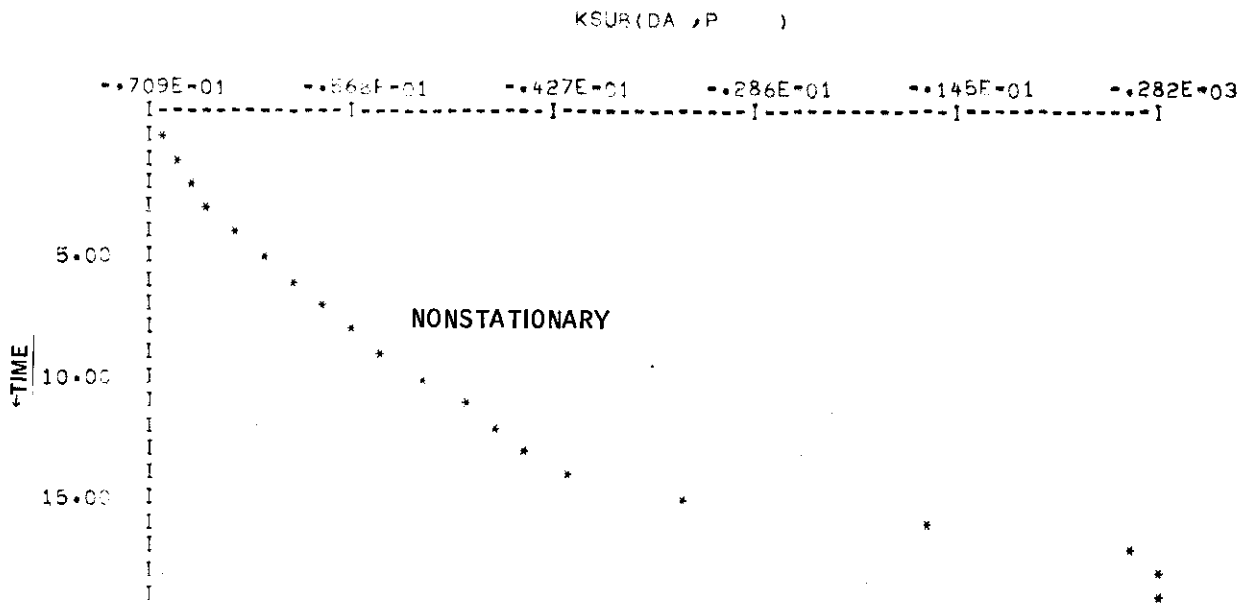


Figure 73. Optimal Controller Gain Plots (continued)

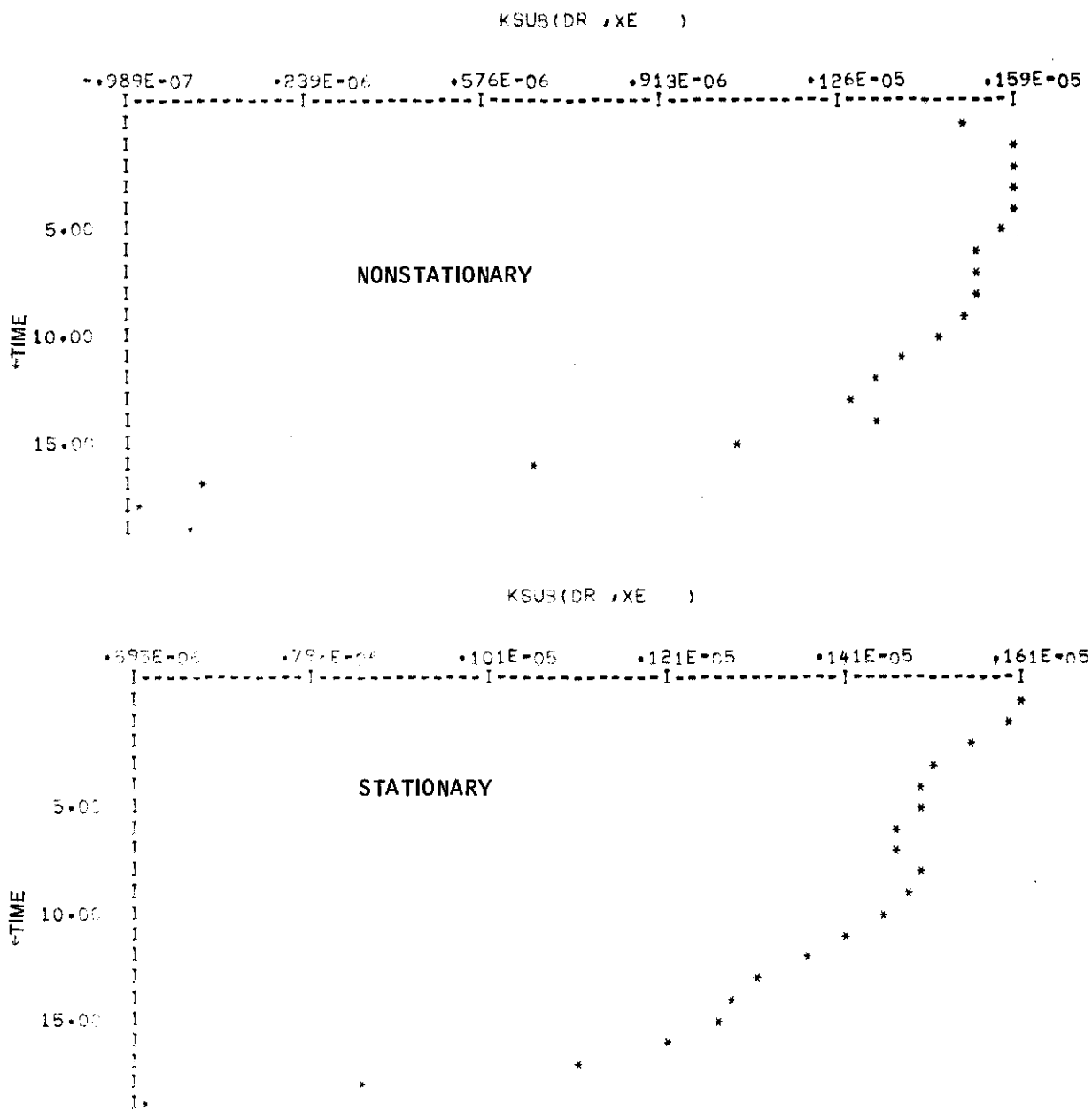


Figure 73. Optimal Controller Gain Plots (continued)

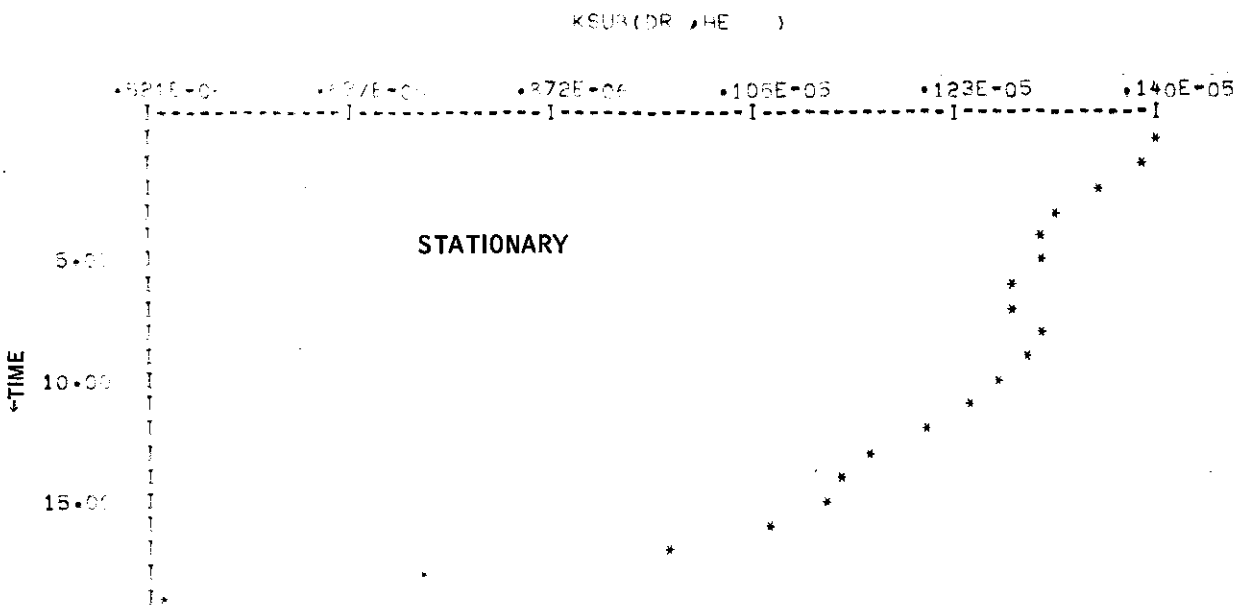
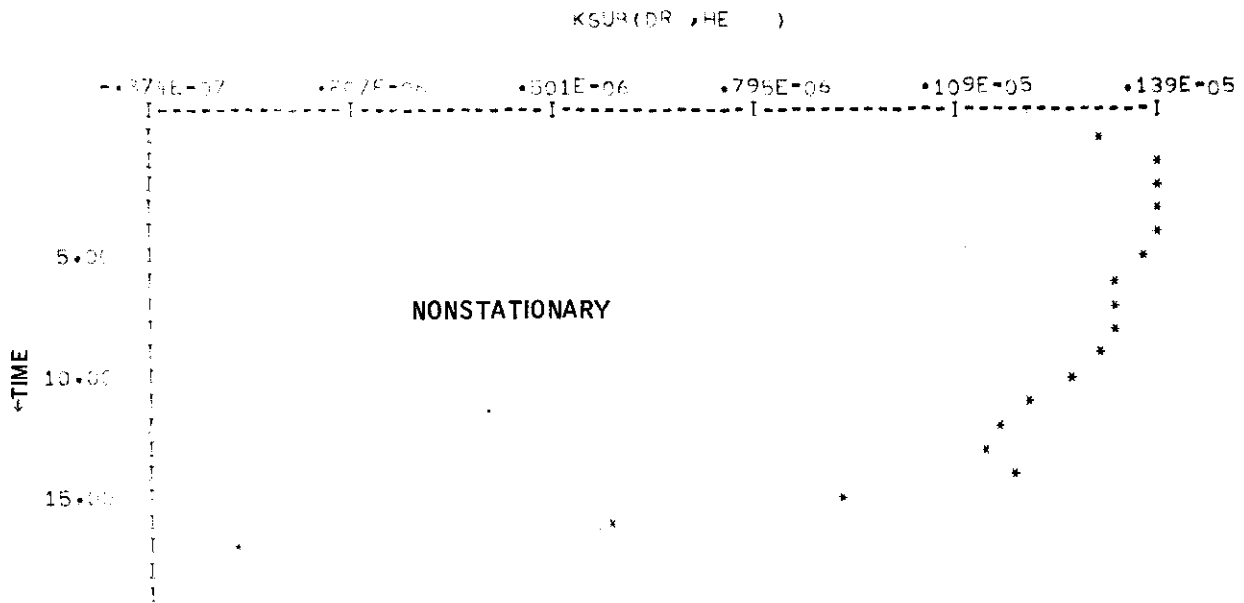


Figure 73. Optimal Controller Gain Plots (continued)

Contrails

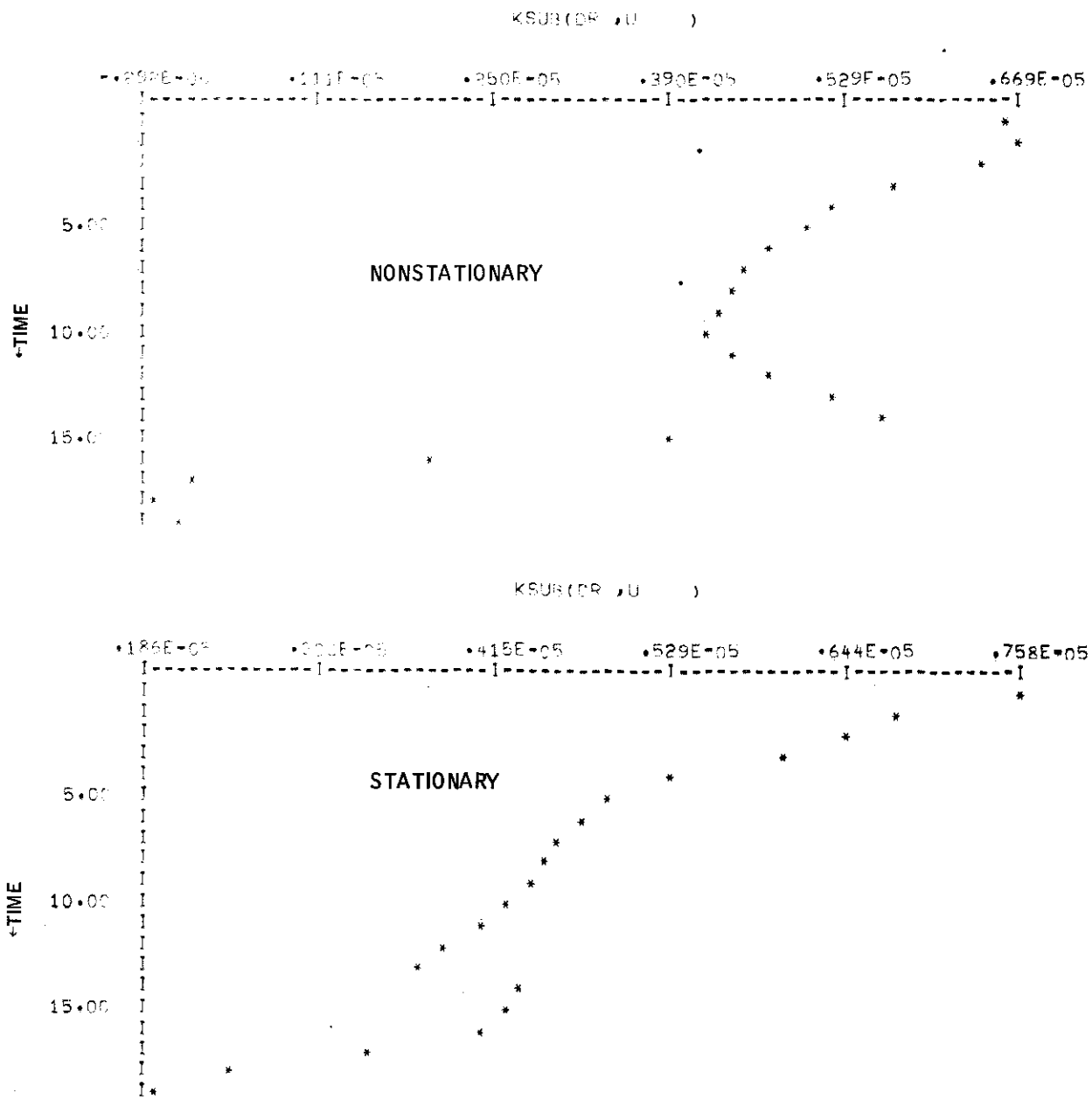


Figure 73. Optimal Controller Gain Plots (continued)

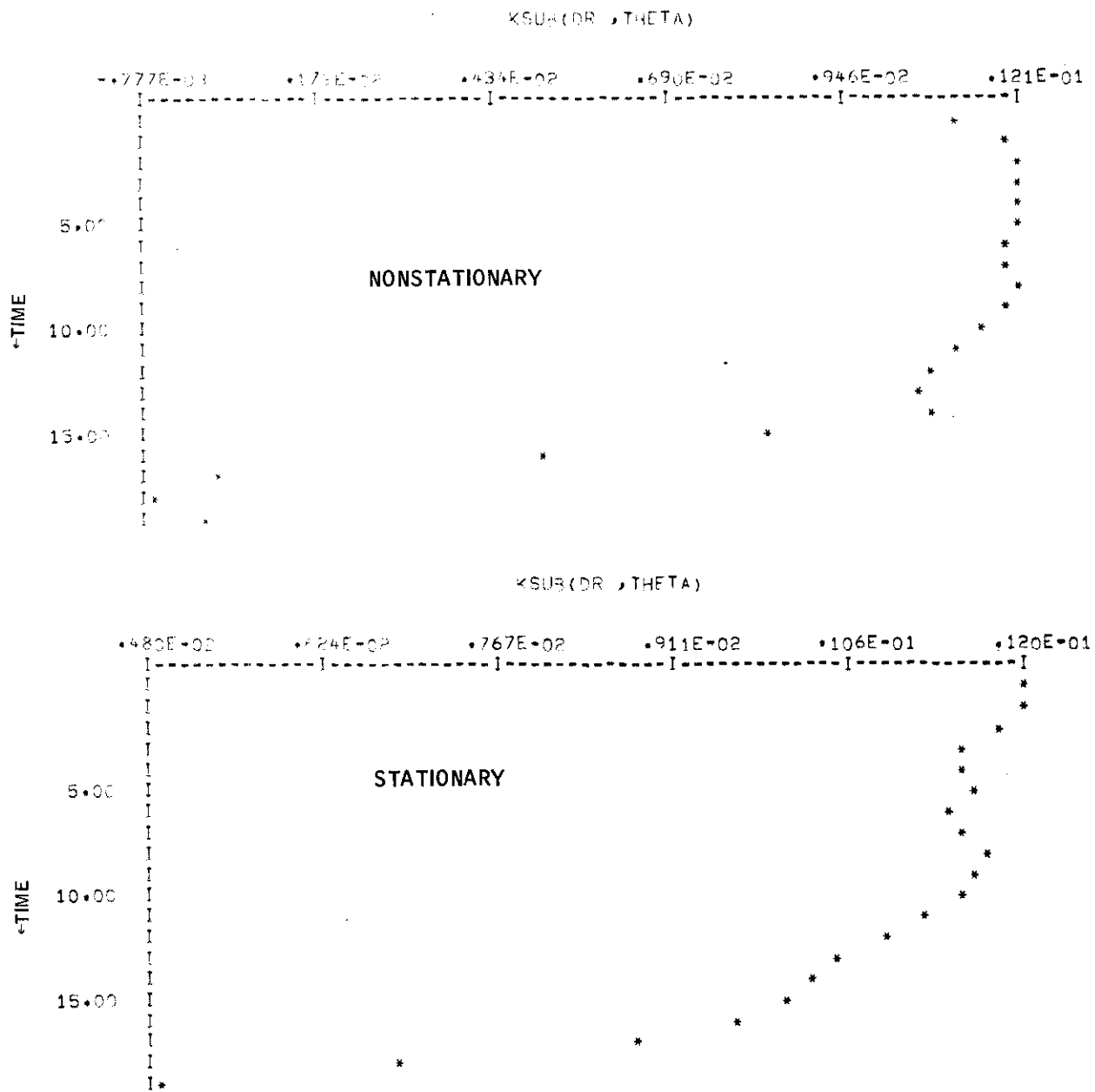


Figure 73. Optimal Controller Gain Plots (continued)

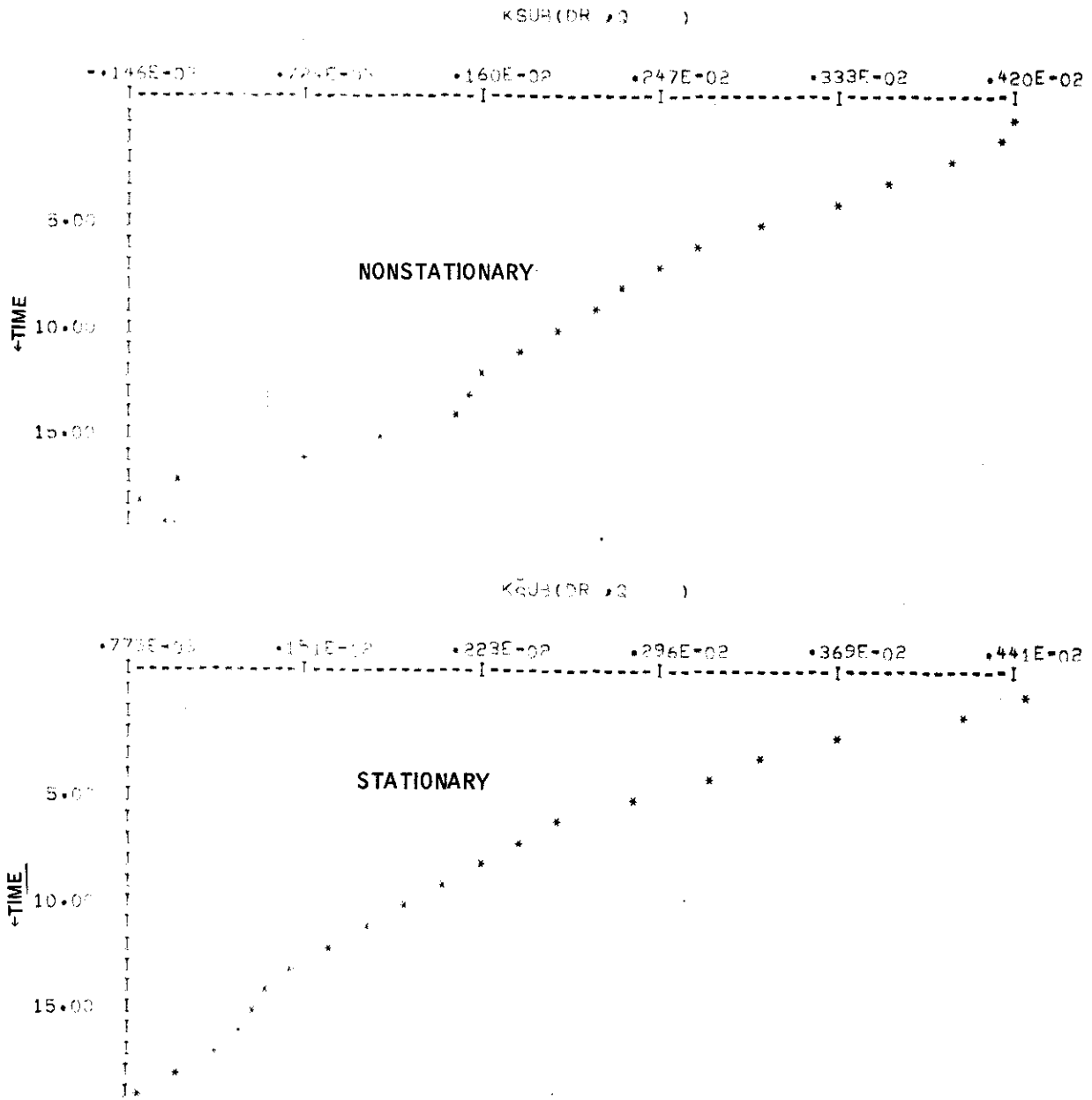


Figure 73. Optimal Controller Gain Plots (continued)

Contrails

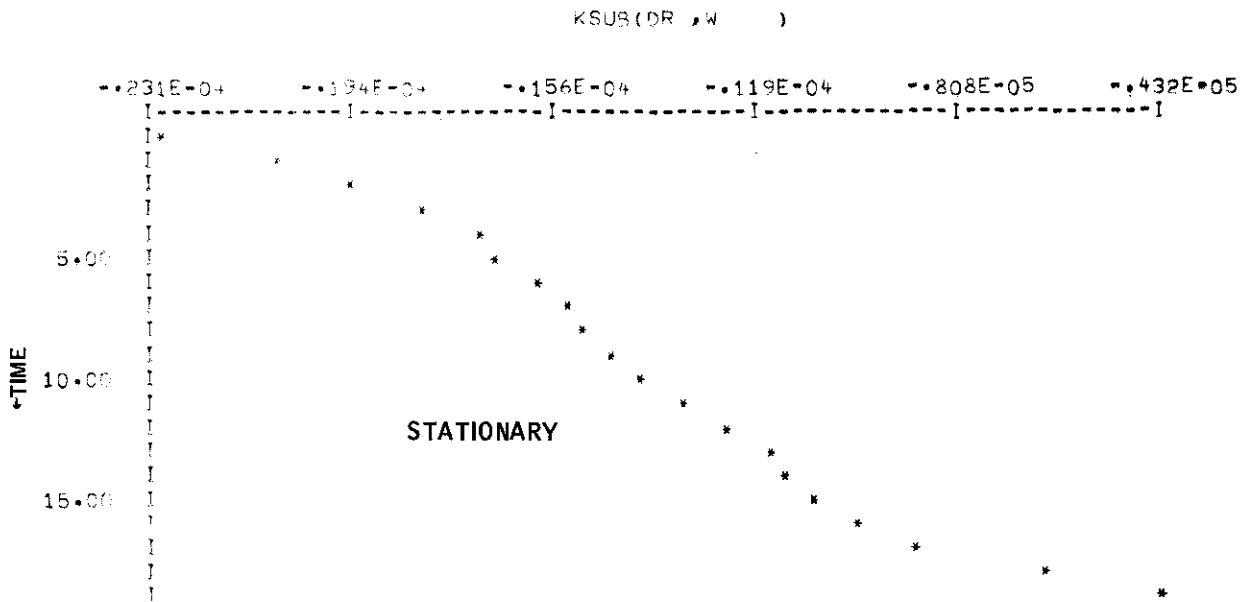
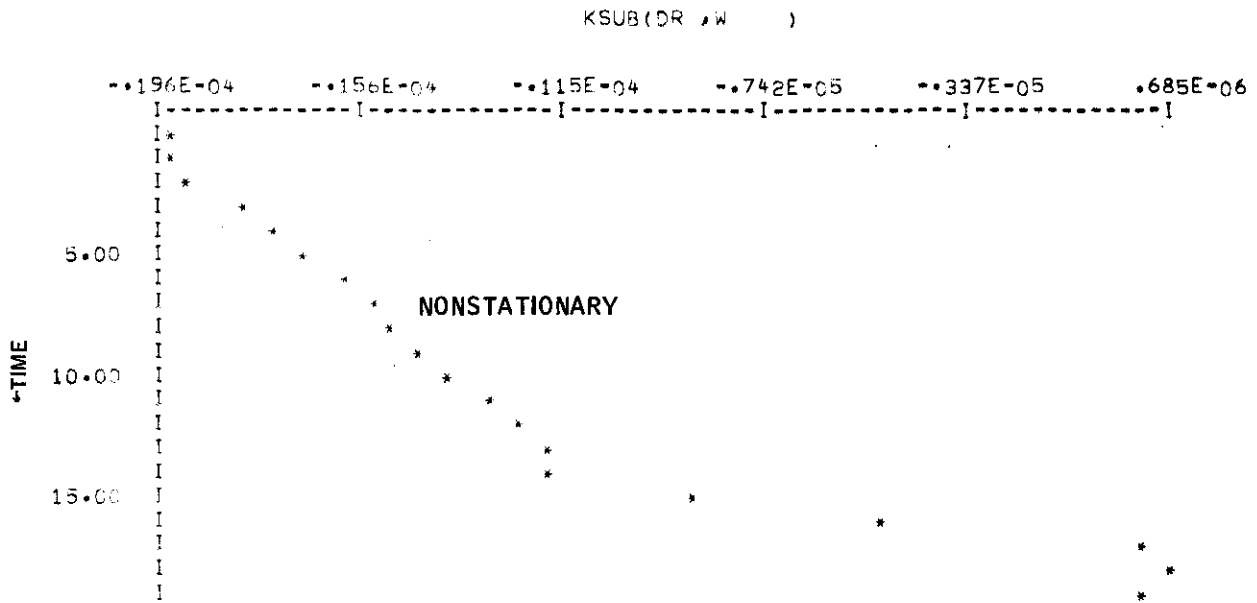


Figure 73. Optimal Controller Gain Plots (continued)

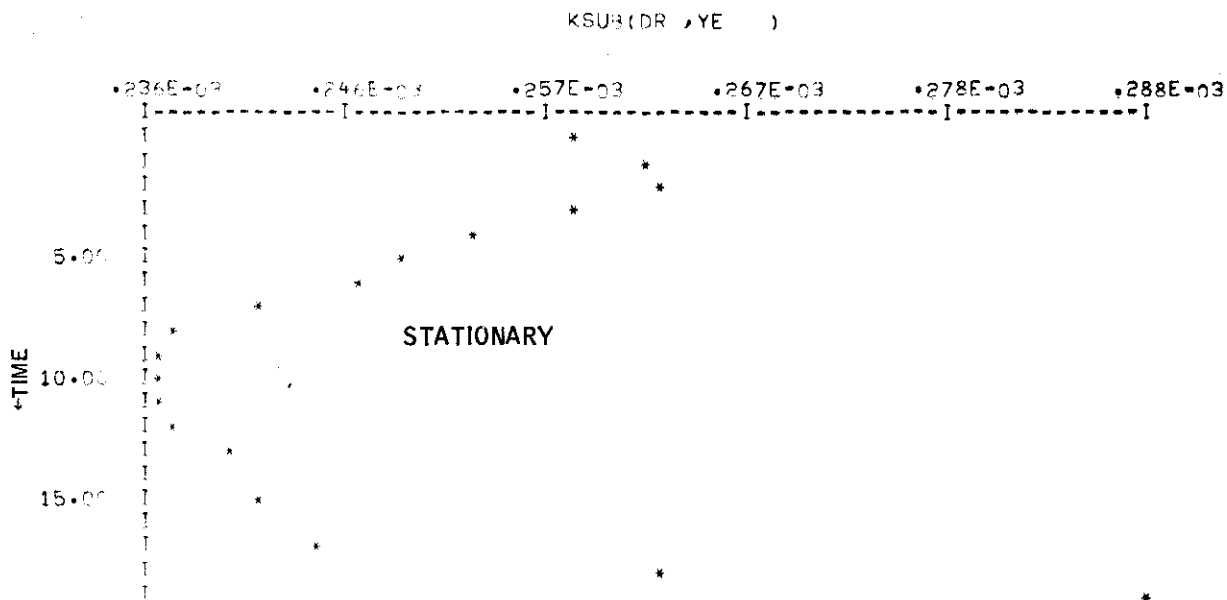
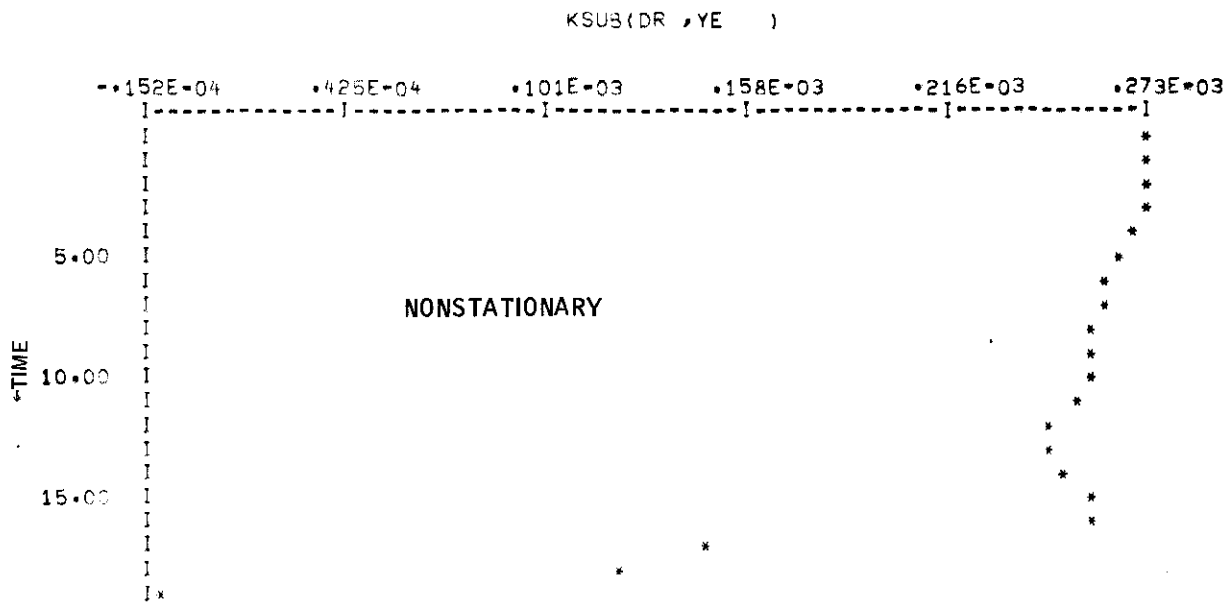


Figure 73. Optimal Controller Gain Plots (continued)

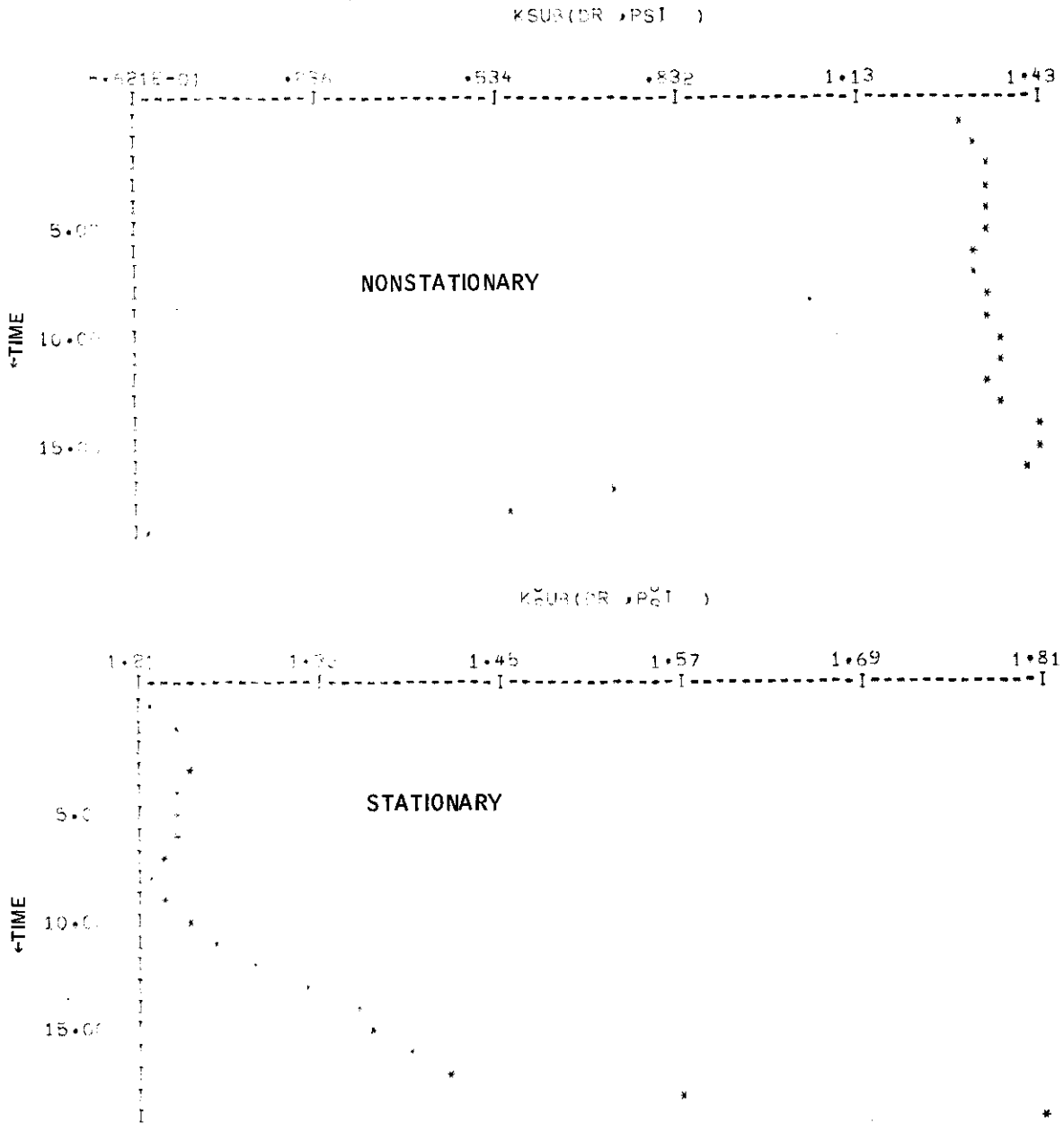


Figure 73. Optimal Controller Gain Plots (continued)

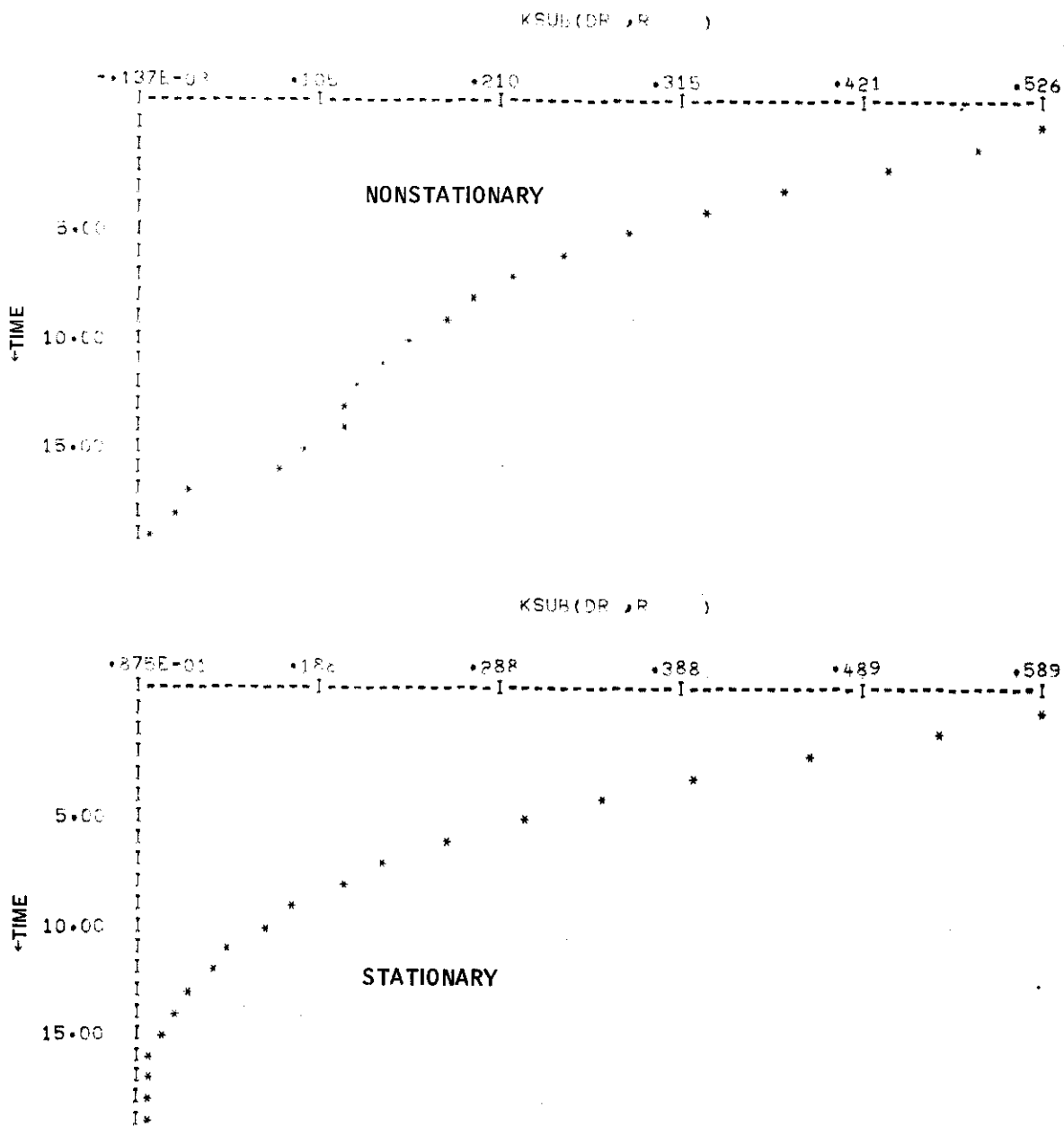


Figure 73. Optimal Controller Gain Plots (continued)

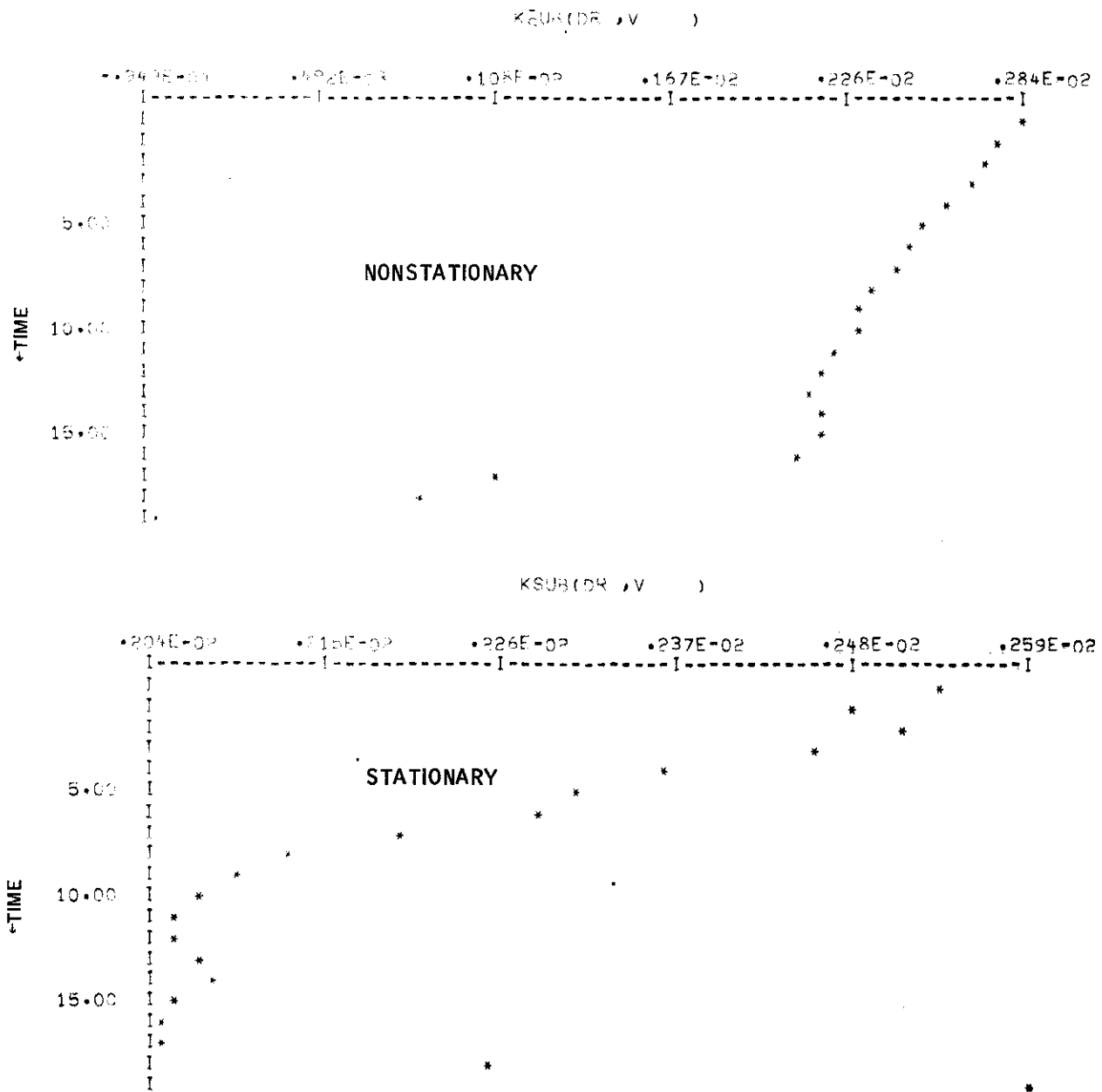


Figure 73. Optimal Controller Gain Plots (continued)

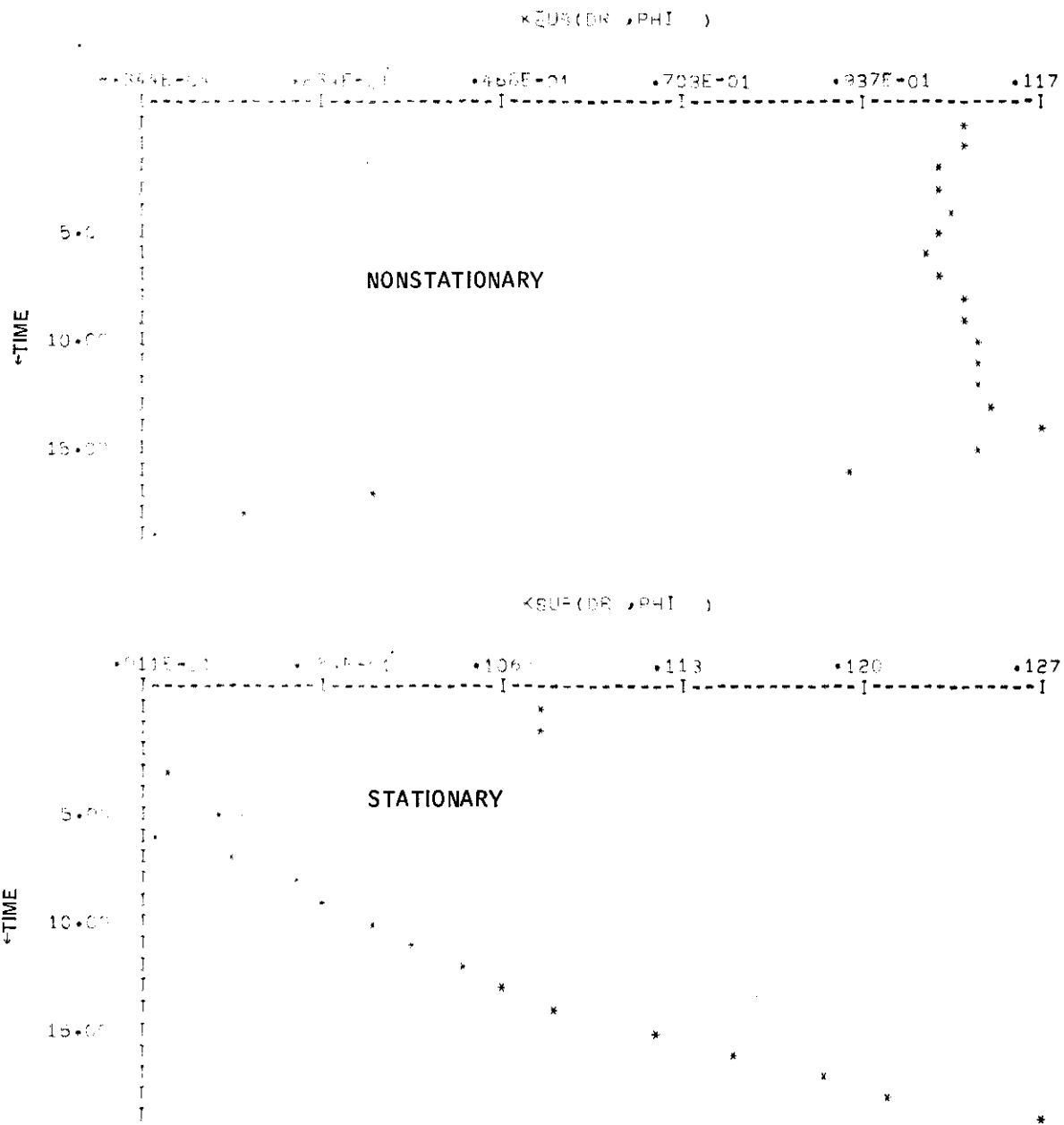


Figure 73. Optimal Controller Gain Plots (continued)

Contrails

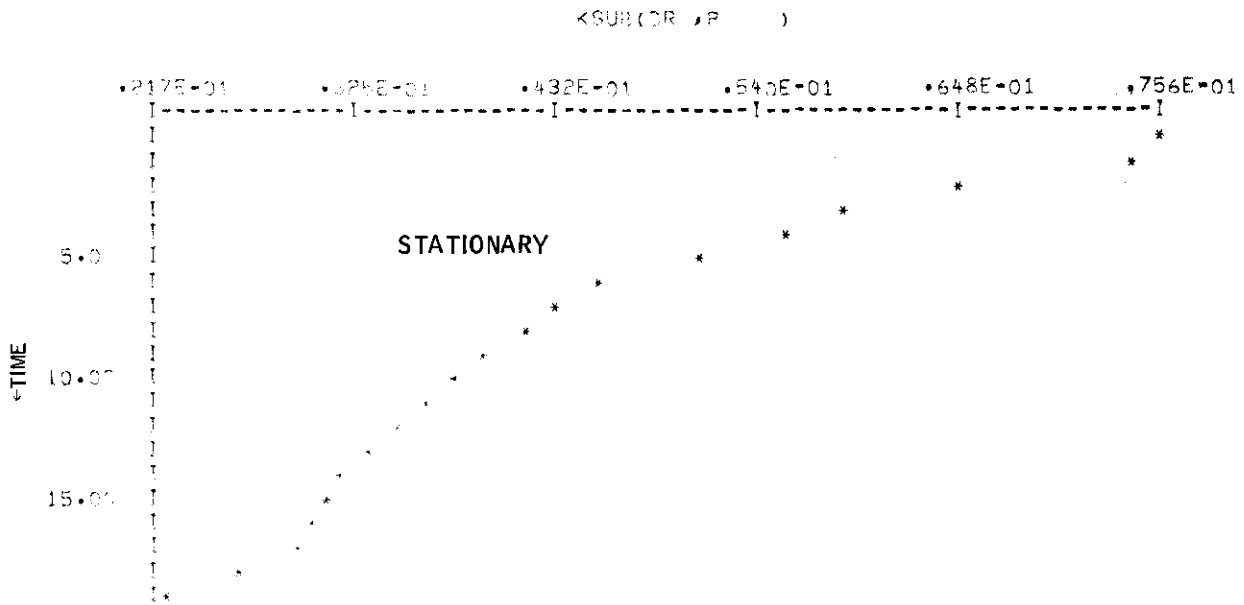
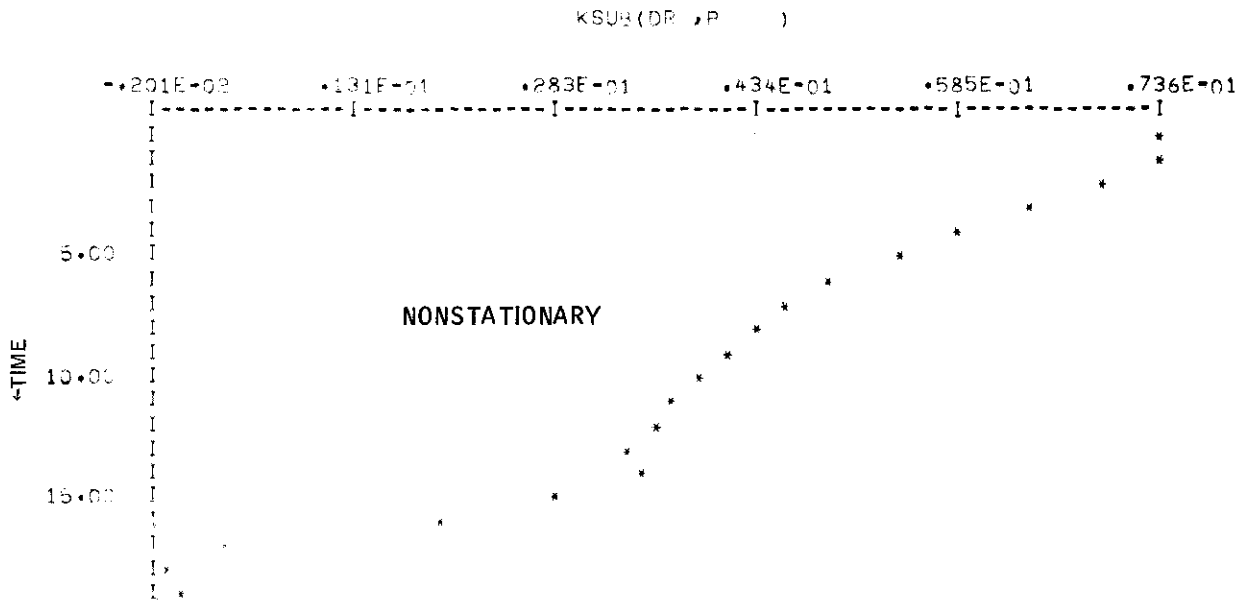


Figure 73. Optimal Controller Gain Plots (continued)

Contrails

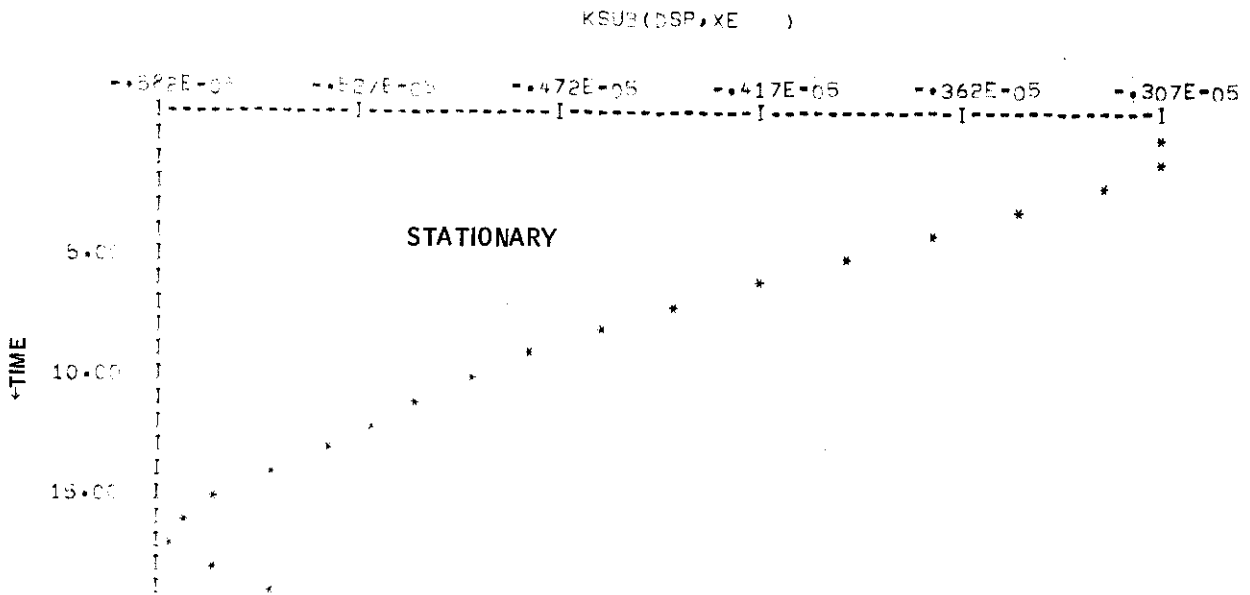
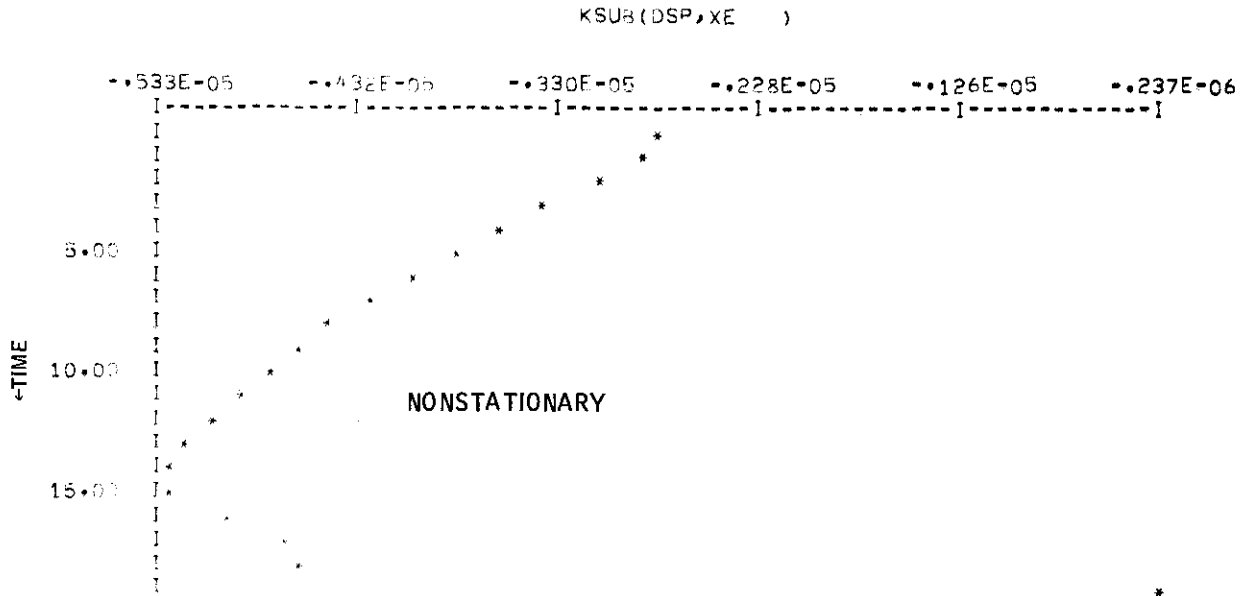


Figure 73. Optimal Controller Gain Plots (continued)

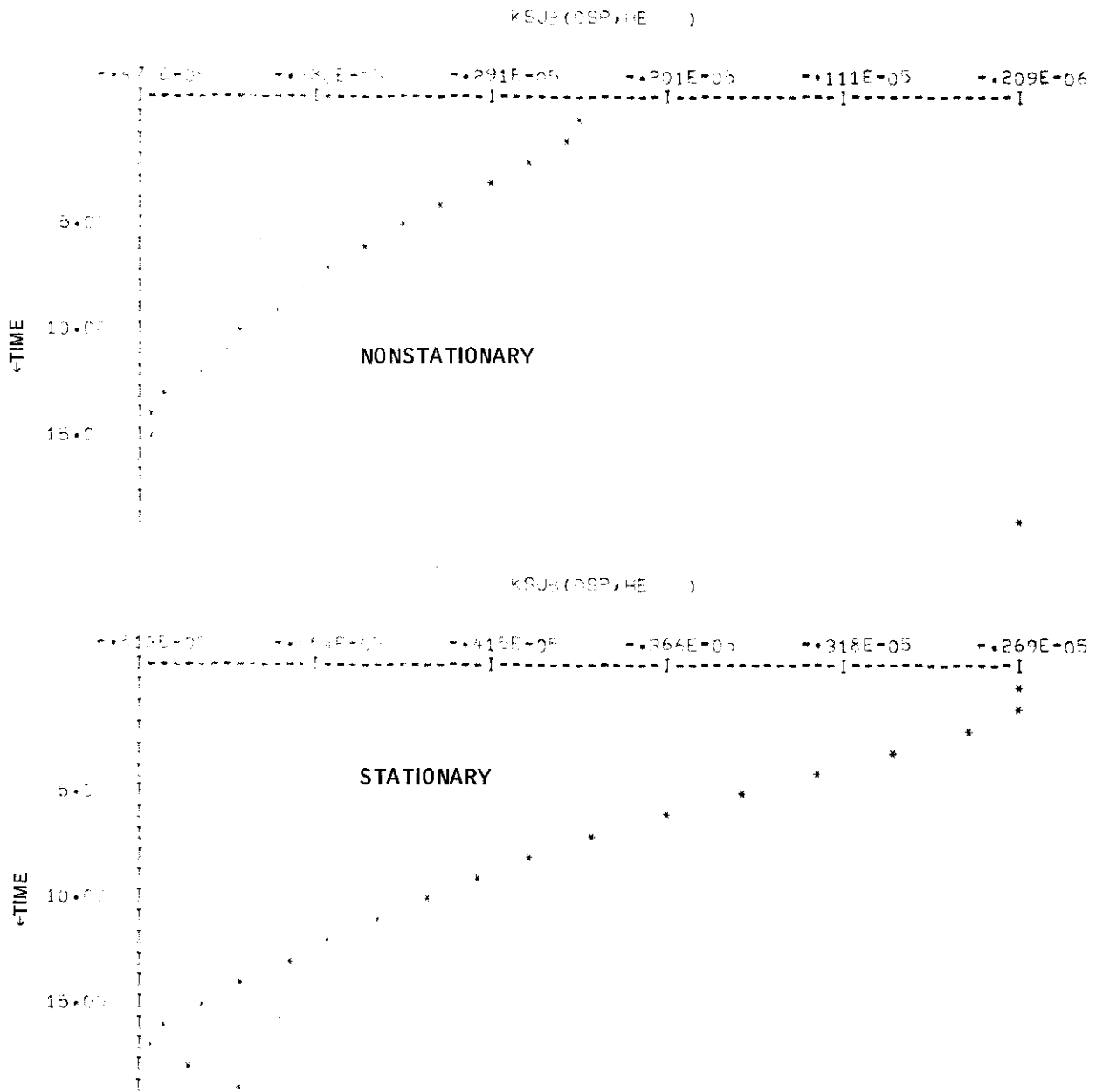


Figure 73. Optimal Controller Gain Plots (continued)

Contrails

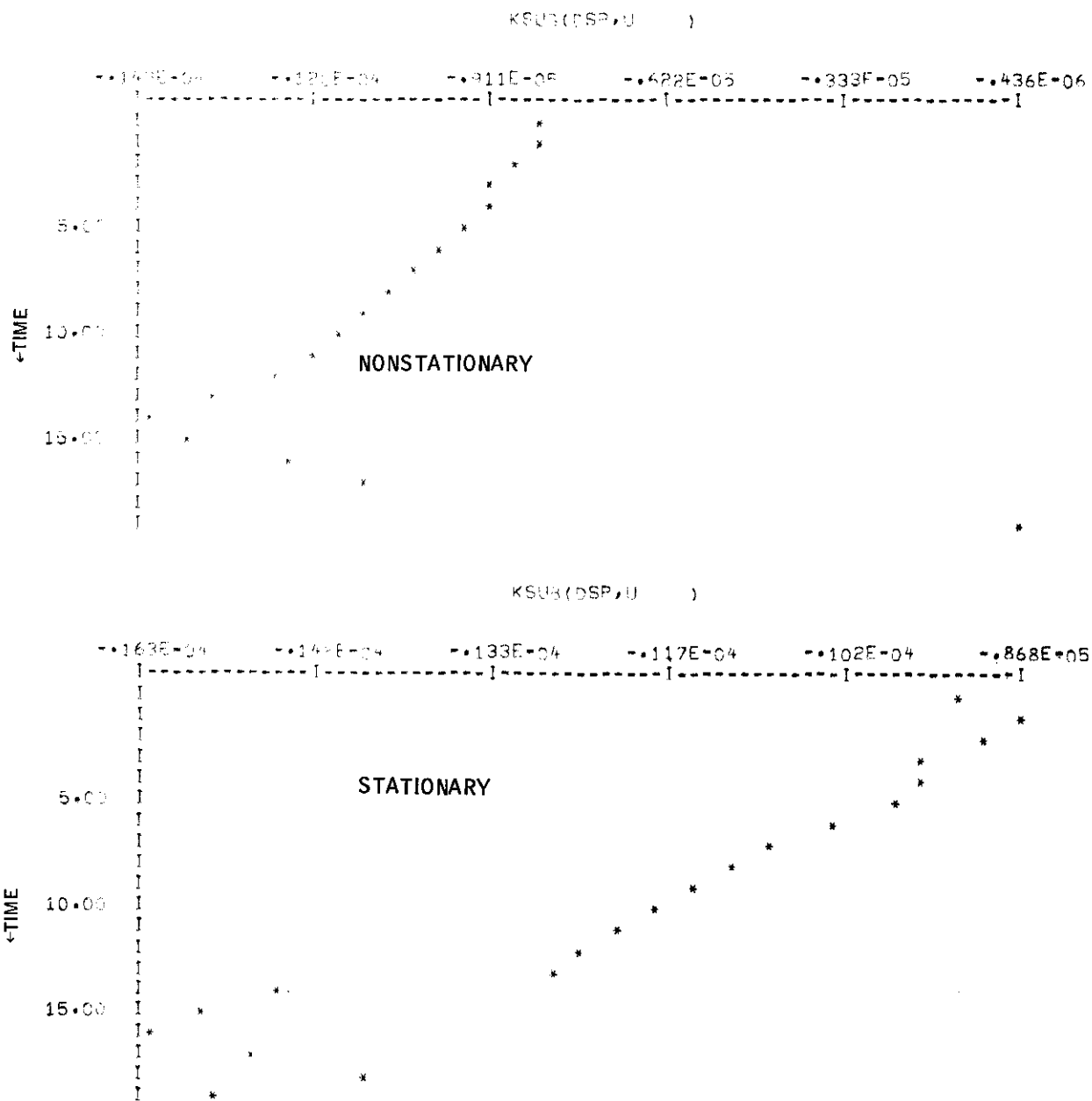


Figure 73. Optimal Controller Gain Plots (continued)

Contrails

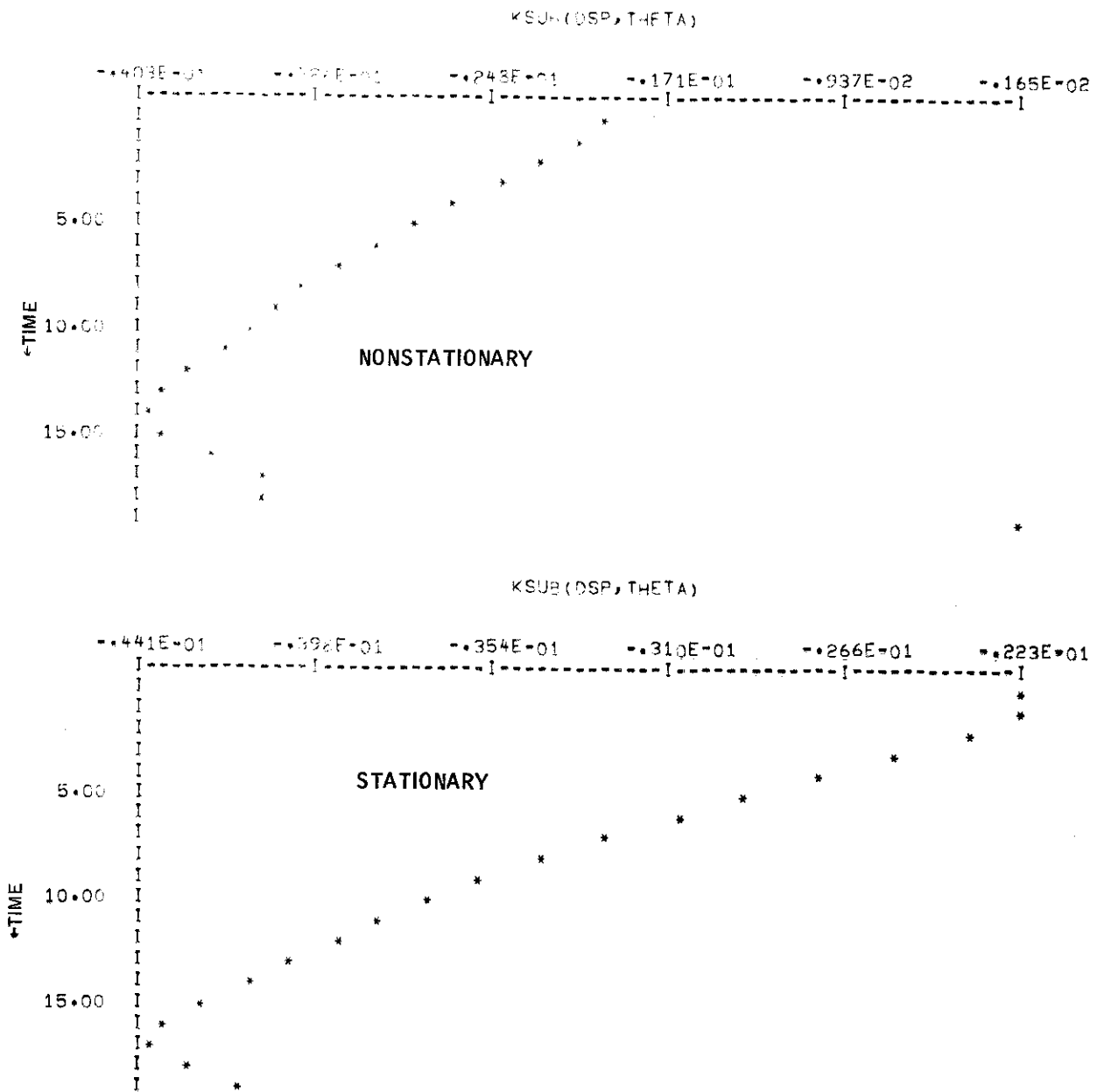


Figure 73. Optimal Controller Gain Plots (continued)

Contrails

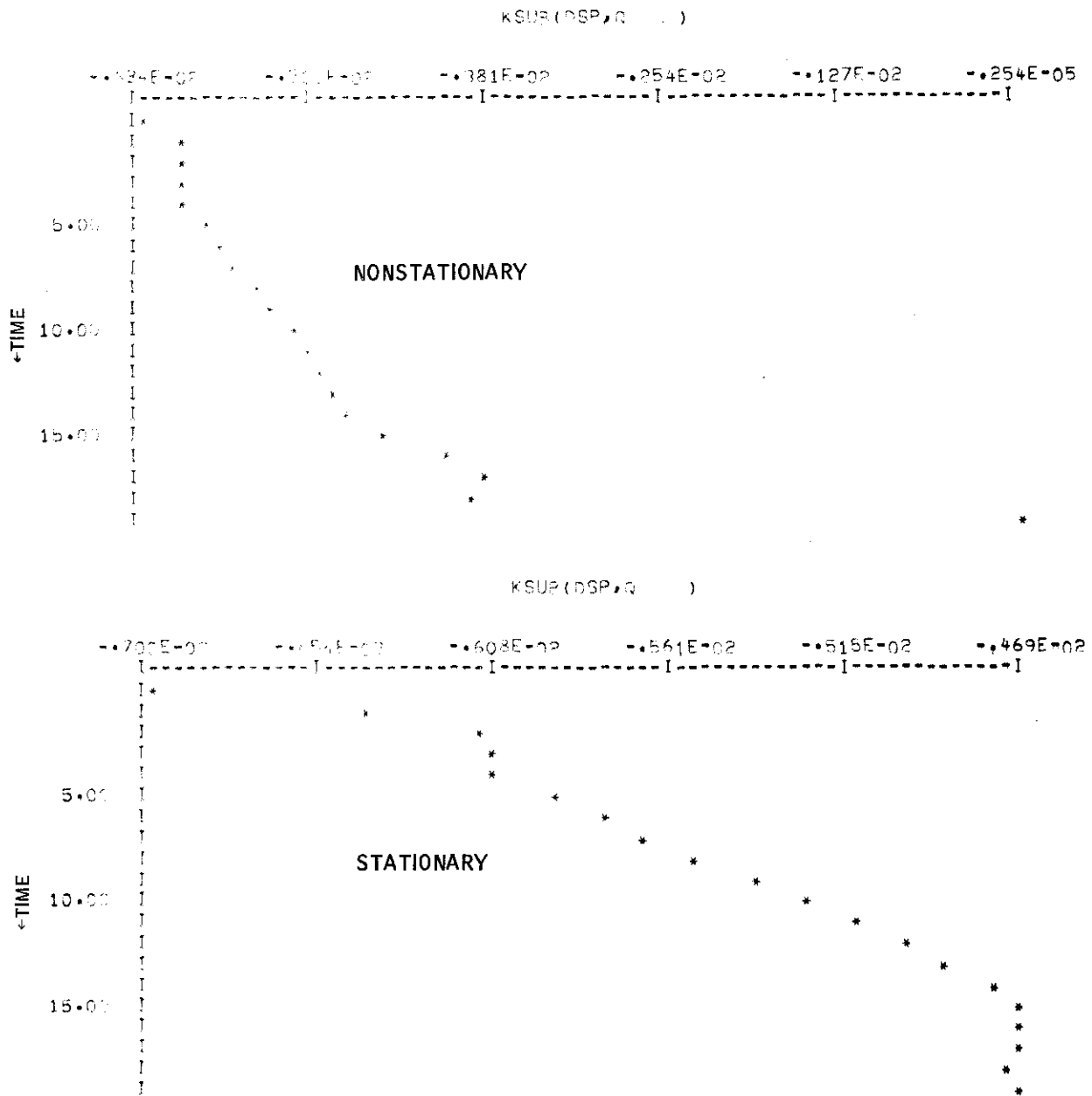


Figure 73. Optimal Controller Gain Plots (continued)

Contrails

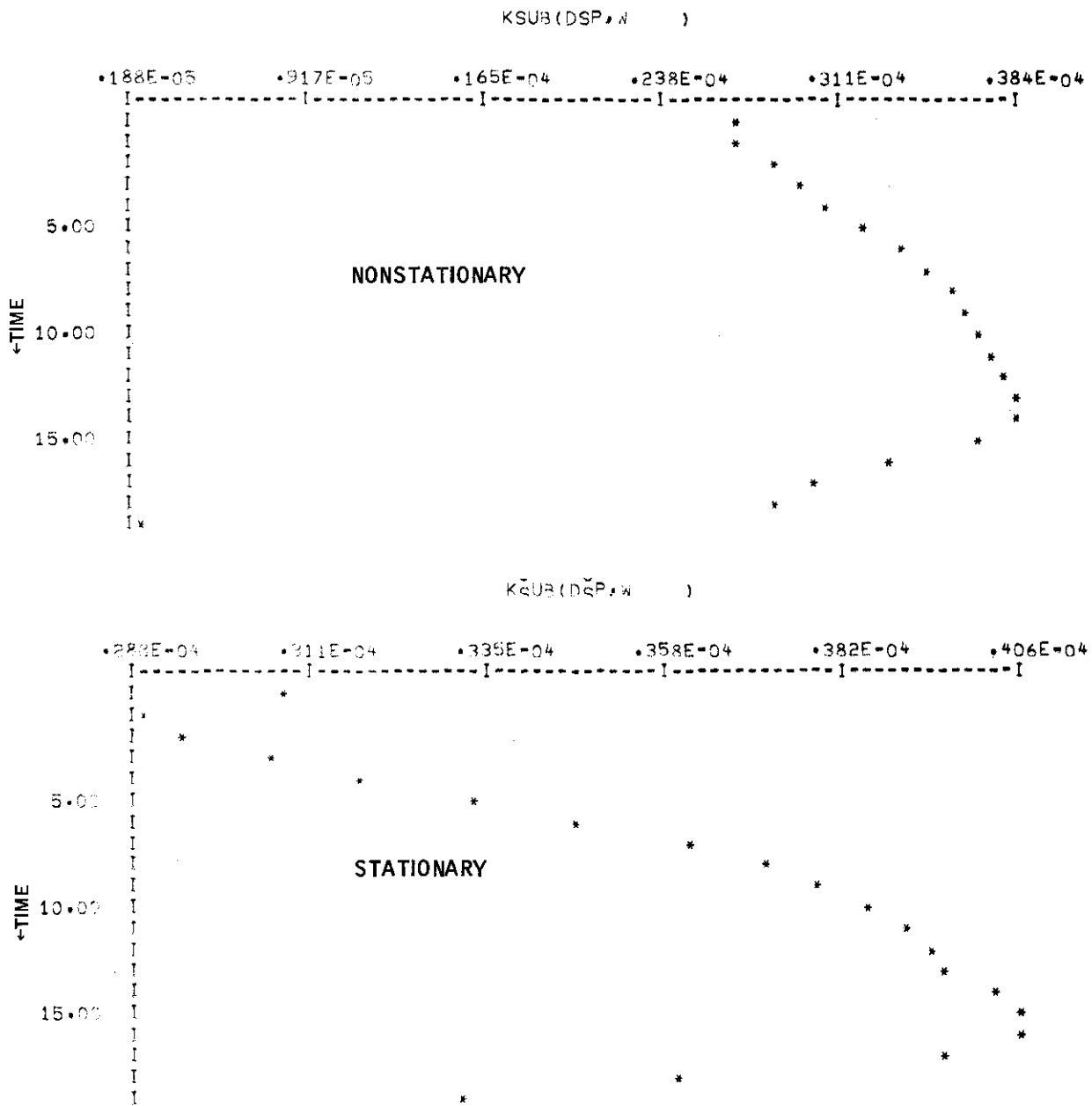


Figure 73. Optimal Controller Gain Plots (continued)

Contrails

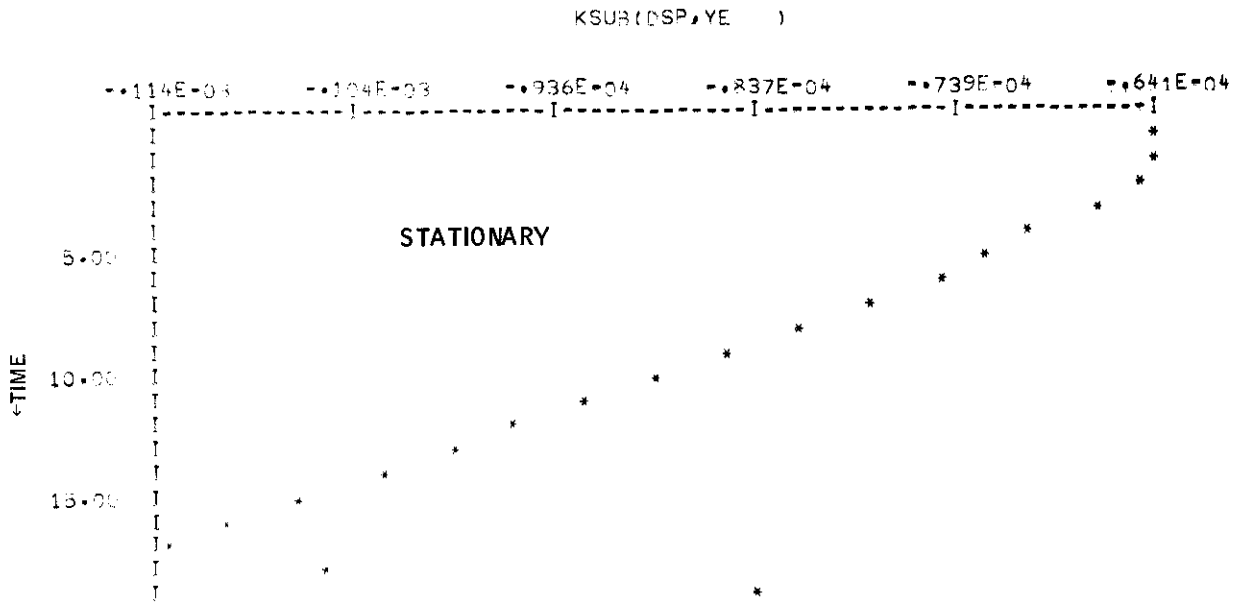
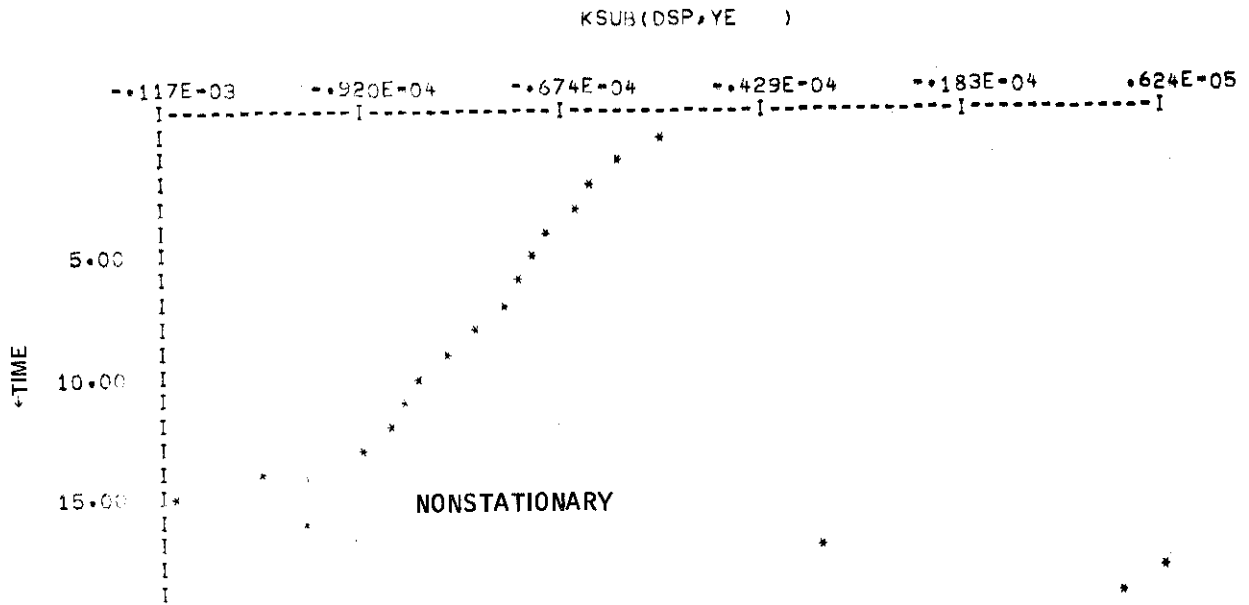


Figure 73. Optimal Controller Gain Plots (continued)

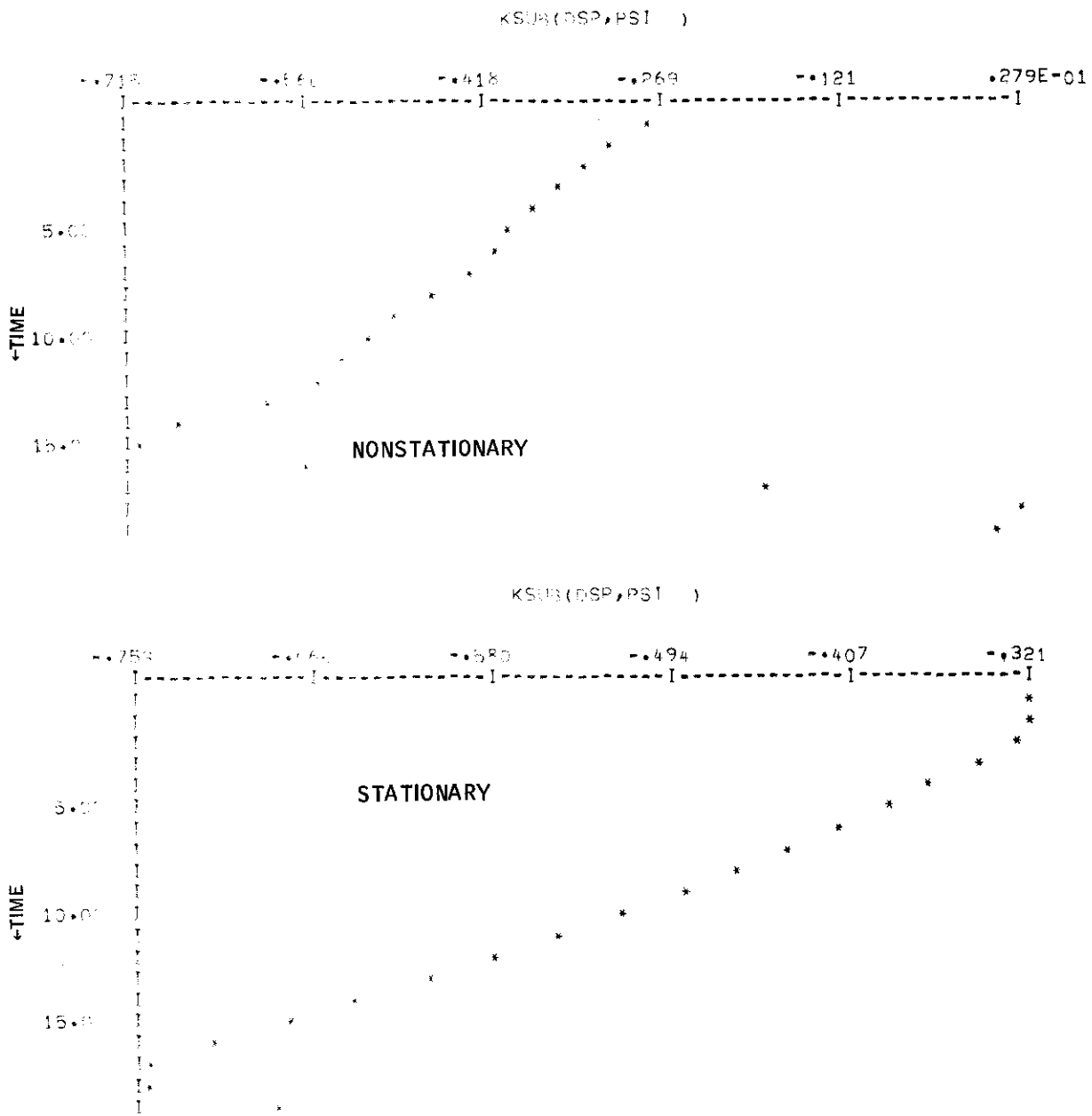


Figure 73. Optimal Controller Gain Plots (continued)

Contrails

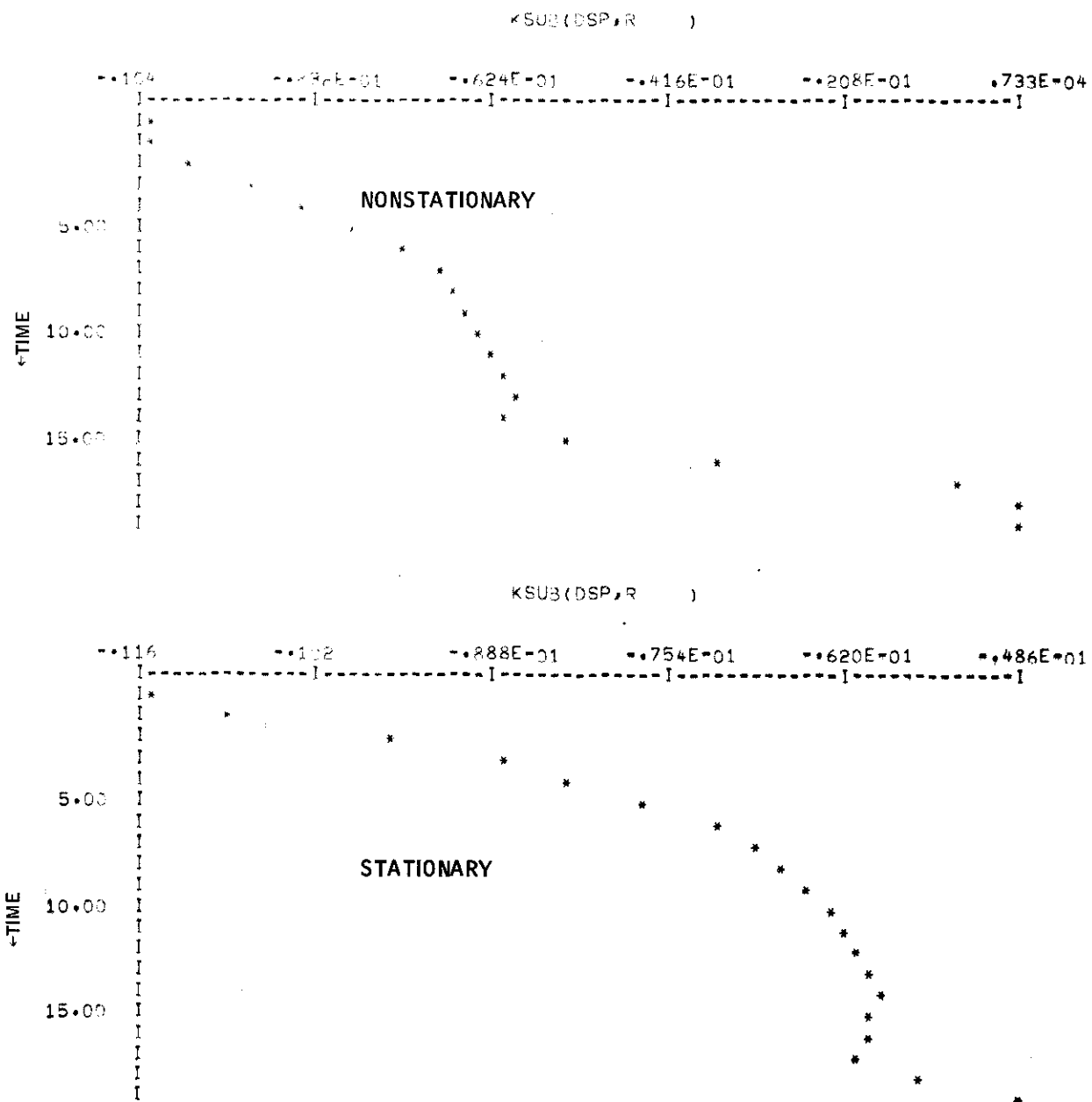


Figure 73. Optimal Controller Gain Plots (continued)

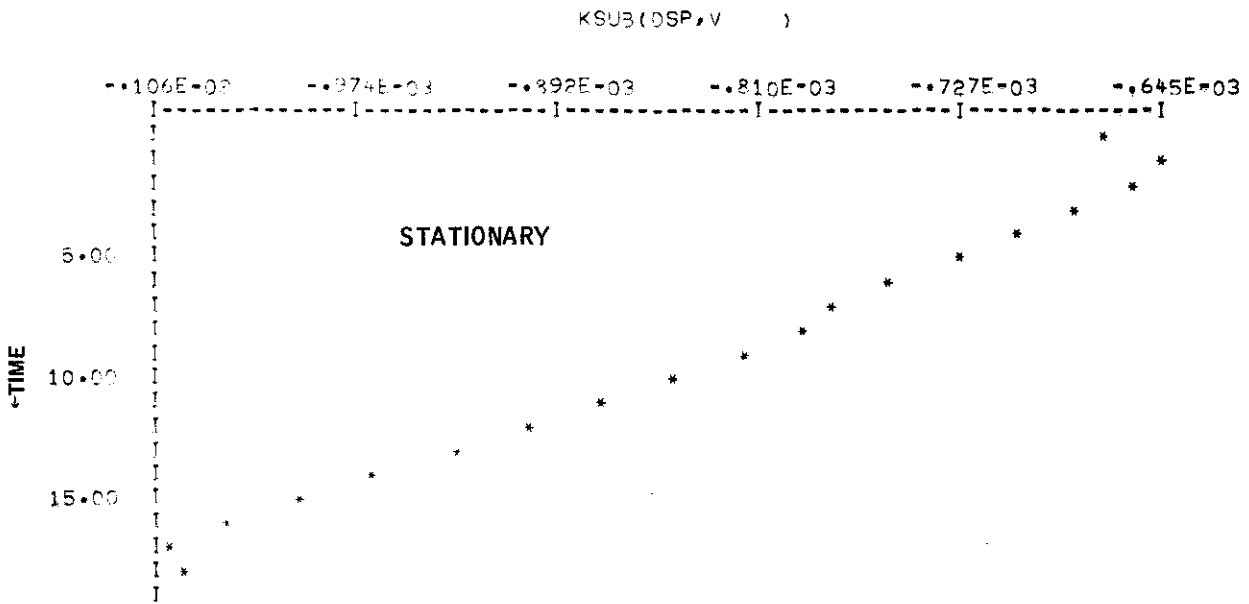
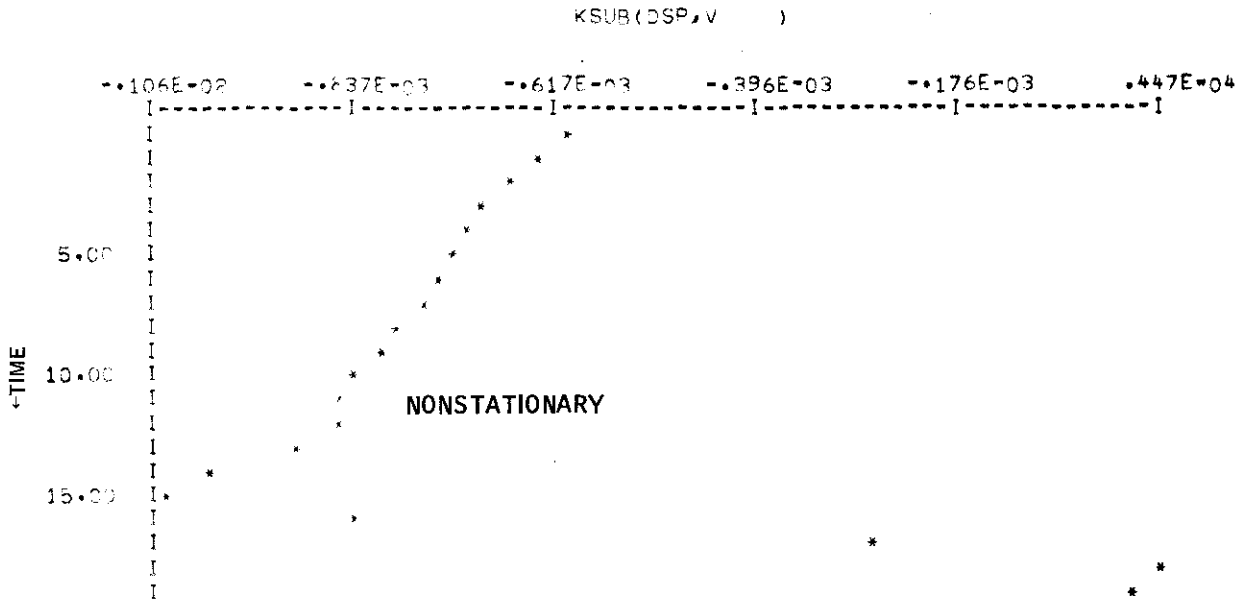


Figure 73. Optimal Controller Gain Plots (continued)

Contrails

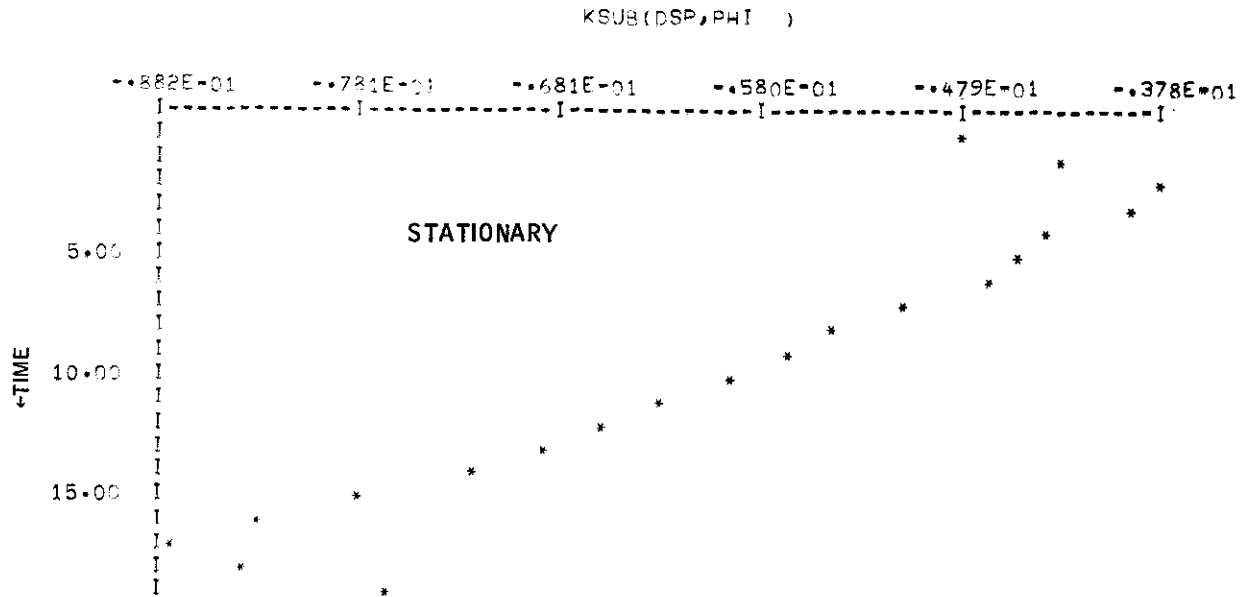
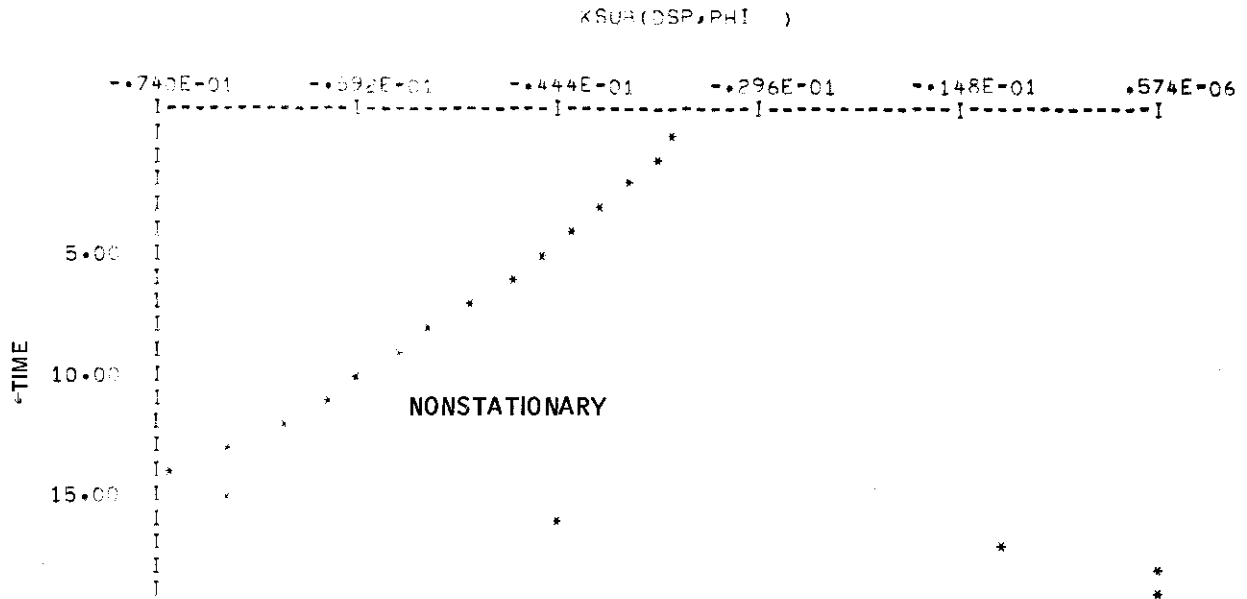


Figure 73. Optimal Controller Gain Plots (continued)

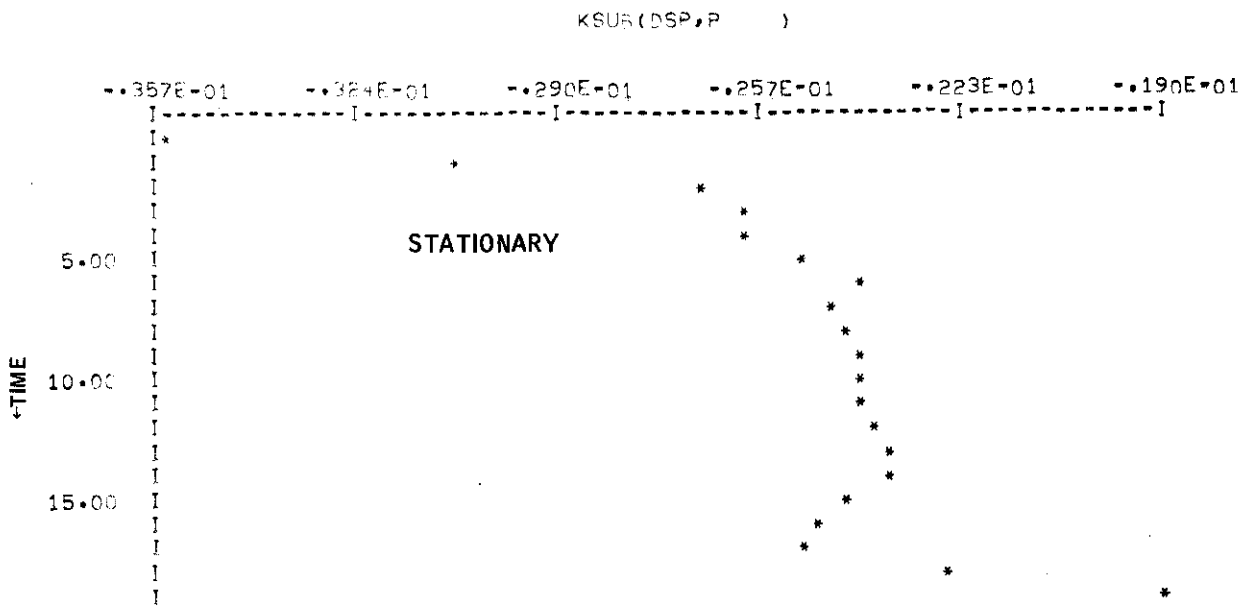
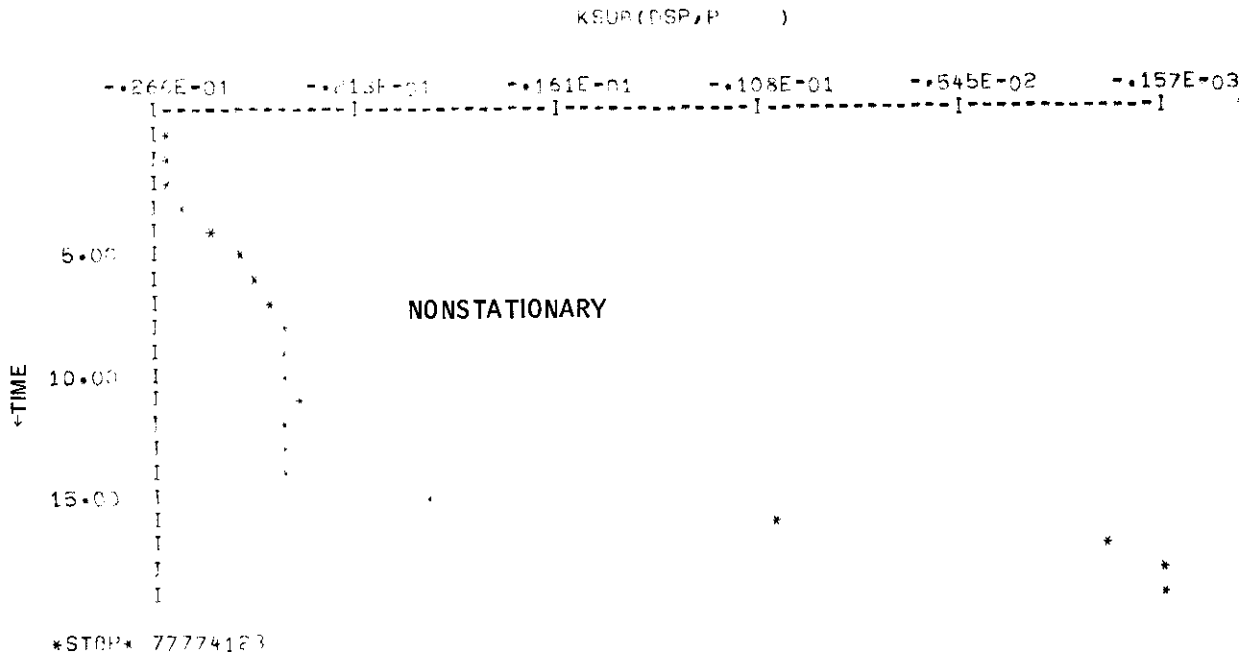


Figure 73. Optimal Controller Gain Plots (concluded)

STATIONARY, FREE AND NONSTATIONARY SPECTRUMS

The stationary and nonstationary controllers were compared with respect to the frozen-point closed-loop eigenvalues of the aircraft transition matrices.

Figure 74 shows the program for finding the eigenvalue spectrum of the aircraft at the frozen-time points. The spectrums corresponding to the aircraft with fixed-gain controller, airframe only, and with the time varying controller are shown at each data point in Figure 75. Note increased dampings and the stabilization of the position and attitude states.

Contrails

```

4FORTRAN LS,00
1:   DIMENSION F(17,17),G1(17,4),G2(17,3),H(21,17),D(21,4),Q(21,21)
2:   DIMENSION AK(4,18)
3:   DO 10 L=1,20
4:   READ(6)((F(I,J),J=1,17),I=1,17)
5:   READ(6)((G1(I,J),J=1,4),I=1,17)
6:   READ(6)((G2(I,J),J=1,3),I=1,17)
7:   READ(4)((H(I,J),J=1,17),I=1,21)
8:   READ(4)((L(I,J),J=1,4),I=1,21)
9:   READ(4)((Q(I,J),J=1,21),I=1,21)
10:  LL=21-L
11:  DO 20 M=1,LL
12:  20 READ(2)((AK(I,J),J=1,18),I=1,4)
13:  REWIND 2
14:  DO 11 I=1,17
15:  DO 11 J=1,17
16:  DO 11 K=1,4
17:  11 F(I,J)=F(I,J)+G1(I,K)*AK(K,J)
18:  TIME=L-1
19:  WRITE(9,3,1)TIME
20:  30 FORMAT(1H1/7X,59H- CLOSED LOOP ROOTS (DISCOP) FOR CONTROL WEIGHTS:
21:  110000. AT FR,3,4HSEC./)
22:  CALL ROOT(F,17)
23:  10 CONTINUE
24:  END

```

```

1:   SUBROUTINE ROOT(A,NX)
2:   DIMENSION A(NX,NX),RR(80)
3:   LWR=9
4:   CALL HESSEN(NX,A,NX)
5:   CALL GRCALL(NX,A,RR,MM,NX)
6:   WRITE(LWR,900)
7:   900 FORMAT(///74H          REAL          IMAG          DAMP
8:   IING          FREQ/)
9:   MM=MM/2
10:  DO 901 K=1,MM
11:  I=2*K-1
12:  II=2*K
13:  IF(RR(II).EQ.0.) GOTO 903
14:  FREQ=SQRT(RR(I)*RR(I)+RR(II)*RR(II))
15:  DAMP=ABS(RR(I))/FREQ
16:  WRITE(LWR,904)RR(I),RR(II),DAMP,FREQ
17:  904 FORMAT(4E20.8)
18:  GOTO 901
19:  903 WRITE(LWR,802)RR(I),RR(II)
20:  901 CONTINUE
21:  802 FORMAT(2E20.8)
22:  RETURN
23:  END

```

Figure 74. Eigenvalue Spectrum Program Listing

Contrails

CLOSED LOOP ROOTS AT .000SEC.

ROOTS OF A/C FRAME AT .000SEC.

REAL	IMAG	REAL	IMAG
-.34426327E-01	.00000000E 00	-.34426327E-01	.00000000E 00
-.34426327E-01	.00000000E 00	-.34426327E-01	.00000000E 00
-.34426327E-01	.00000000E 00	-.34426327E-01	.00000000E 00
-.34426327E-01	.00000000E 00	-.34426327E-01	.00000000E 00
-.34426327E-01	.00000000E 00	-.34426327E-01	.00000000E 00
-.14693385E-02	.62066482E-02	-.63233021E-01	.00000000E 00
-.82580375E-01	.00000000E 00	-.12746926E 01	.00000000E 00
-.13639452E 00	.00000000E 00	-.68212634E-01	.14958388E 01
-.16674493E 00	.00000000E 00	.00000000E 00	.00000000E 00
-.12167703E 00	.13006176E 00	.00000000E 00	.00000000E 00
-.12706507E 01	.00000000E 00	-.33400219E-02	.00000000E 00
-.74473323E-01	.14958737E 01	-.27407776E-01	.81259815E-01
-.53333.13E 00	.12644271E 01	-.50473045E 00	.17410152E 01
		.00000000E 00	.00000000E 00

CLOSED LOOP ROOTS (DISCP) FOR CONTROL WEIGHTS= 1000. AT

.000SEC.

REAL	IMAG	DAMPING	FREQ
-.34426327E-01	.00000000E 00		
-.34426327E-01	.00000000E 00		
-.34426327E-01	.00000000E 00		
-.34426327E-01	.00000000E 00		
-.34426327E-01	.00000000E 00		
-.15625444E-02	.64446009E-02	.23563091E 00	.66313216E-02
-.80197431E-01	.00000000E 00		
-.91842136E-01	.00000000E 00		
-.28593029E 00	.47494569E 00	.51577230E 00	.55437311E 00
-.20096872E 00	.00000000E 00		
-.12685772E 01	.00000000E 00		
-.26621273E 00	.14821498E 01	.17609304E 00	.15117735E 01
-.12307023E 01	.18213996E 01	.55986581E 00	.21982094E 01

Figure 75. Eigenvalue Spectrums

Contrails

CLOSED LOOP ROOTS AT 1.000SEC. REPTS OF A/C FRAME AT 1.000SEC.

REAL	IMAG	REAL	IMAG
-.37788856E-01	.00000000E 00	-.37788856E-01	.00000000E 00
-.37788856E-01	.00000000E 00	-.37788856E-01	.00000000E 00
-.37788856E-01	.00000000E 00	-.37788856E-01	.00000000E 00
-.37788856E-01	.00000000E 00	-.37788856E-01	.00000000E 00
-.37788856E-01	.00000000E 00	-.37788856E-01	.00000000E 00
-.40861253E-02	.67246887E-02	-.62719448E-01	.00000000E 00
-.89032665E-01	.00000000E 00	-.13719559E 01	.00000000E 00
-.12568159E 00	.00000000E 00	-.85002979E-01	.16192409E 01
-.20841872E 00	.00000000E 00	.00000000E 00	.00000000E 00
-.12530873E 00	.13516527E 00	.00000000E 00	.00000000E 00
-.13718116E 01	.00000000E 00	-.36663012E-02	.00000000E 00
-.89358141E-01	.16192289E 01	-.26928097E-01	.78043273E-01
-.55857183E 00	.13045287E 01	-.52881299E 00	.12784632E 01
		.00000000E 00	.00000000E 00

CLOSED LOOP ROOTS (DISCOP) FOR CONTRBL WEIGHTS= 10000. AT 1.000SEC.

REAL	IMAG	DAMPING	FREQ
-.37788856E-01	.00000000E 00		
-.37788856E-01	.00000000E 00		
-.37788856E-01	.00000000E 00		
-.37788856E-01	.00000000E 00		
-.37788856E-01	.00000000E 00		
-.40637551E-02	.67732923E-02	.51447525E 00	.78988350E*02
-.85314930E-01	.00000000E 00		
-.97556155E-01	.00000000E 00		
-.34166722E 00	.48195680E 00	.57833420E 00	.59077817E 00
-.97278326E 00	.00000000E 00		
-.13490308E 01	.00000000E 00		
-.26062988E 00	.16160821E 01	.15921546E 00	.16369634E 01
-.12772858E 01	.18878297E 01	.56037693E 00	.22793333E 01

Figure 75. Eigenvalue Spectrums (continued)

Contrails

CLOSED LOOP ROOTS AT 2.000SEC.

ROOTS OF A/C FRAME AT 2.000SEC.

REAL	IMAG	REAL	IMAG
-.41303573E-01	.00000000E 00	-.41303573E-01	.00000000E 00
-.41303573E-01	.00000000E 00	-.41303573E-01	.00000000E 00
-.41303573E-01	.00000000E 00	-.41303573E-01	.00000000E 00
-.41303573E-01	.00000000E 00	-.41303573E-01	.00000000E 00
-.41303573E-01	.00000000E 00	-.41303573E-01	.00000000E 00
-.50658408E-02	.70569783E-02	-.54077331E-01	.00000000E 00
-.84475366E-01	.00000000E 00	-.14529392E 01	.00000000E 00
-.12715864E 00	.00000000E 00	-.10418060E 00	.17174806E 01
-.22680412E 00	.00000000E 00	.00000000E 00	.00000000E 00
-.11591733E 00	.12284415E 00	.00000000E 00	.00000000E 00
-.14527789E 01	.00000000E 00	-.36025698E-02	.00000000E 00
-.10726565E 00	.17175086E 01	-.26014455E-01	.77513507E-01
-.61546402E 00	.14502170E 01	-.58928484E 00	.14258967E 01
		.00000000E 00	.00000000E 00

CLOSED LOOP ROOTS (DISCP) FOR CONTRL WEIGHTS= 10000. AT 2.000SEC.

REAL	IMAG	DAMPING	FREQ
-.41303573E-01	.00000000E 00		
-.41303573E-01	.00000000E 00		
-.41303573E-01	.00000000E 00		
-.41303573E-01	.00000000E 00		
-.41303573E-01	.00000000E 00		
-.50770382E-02	.71754625E-02	.57759825E 00	.87899992E-02
-.93715691E-01	.00000000E 00		
-.10185261E 00	.00000000E 00		
-.37540357E 00	.41150108E 00	.67396598E 00	.55701413E 00
-.11337419E 01	.00000000E 00		
-.13971649E 01	.00000000E 00		
-.26661383E 00	.17267477E 01	.15259409E 00	.17472094E 01
-.13122881E 01	.20292489E 01	.54301345E 00	.24165665E 01

Figure 75. Eigenvalue Spectrums (continued)

Contrails

CLOSED LOOP ROOTS AT 3.000SEC.

ROOTS OF 1/C FRAME AT 3.000SEC.

REAL	IMAG	REAL	IMAG
-.45020312E-01	.00000000E 00	-.45020312E-01	.00000000E 00
-.45020312E-01	.00000000E 00	-.45020312E-01	.00000000E 00
-.45020312E-01	.00000000E 00	-.45020312E-01	.00000000E 00
-.45020312E-01	.00000000E 00	-.45020312E-01	.00000000E 00
-.45020312E-01	.00000000E 00	-.45020312E-01	.00000000E 00
-.51945629E-02	.75658567E-02	-.48860193E-01	.00000000E 00
-.98180156E-01	.00000000E 00	-.15400055E 01	.00000000E 00
-.12641717E 00	.00000000E 00	-.11808564E 00	.18082149E 01
-.11189052E 00	.12872929E 00	.00000000E 00	.00000000E 00
-.25172744E 00	.00000000E 00	.00000000E 00	.00000000E 00
-.15399110E 01	.00000000E 00	-.35488833E-02	.00000000E 00
-.12155063E 00	.18082812E 01	-.25410536E-01	.75416394E-01
-.65623550E 00	.15409240E 01	-.63213491E 00	.15161505E 01
		.00000000E 00	.00000000E 00

CLOSED LOOP ROOTS (DISCRP) FOR CONTRL WEIGHTS= 10000. AT 3.000SEC.

REAL	IMAG	DAMPING	FREQ
-.45020312E-01	.00000000E 00		
-.45020312E-01	.00000000E 00		
-.45020312E-01	.00000000E 00		
-.45020312E-01	.00000000E 00		
-.45020312E-01	.00000000E 00		
-.51934417E-02	.76577186E-02	.56128921E 00	.92527018E-02
-.99283313E-01	.00000000E 00		
-.10566262E 00	.00000000E 00		
-.37034292E 00	.39520062E 00	.68378618E 00	.54160633E 00
-.12597039E 01	.00000000E 00		
-.14882921E 01	.00000000E 00		
-.27993624E 00	.18197058E 01	.15204737E 00	.18411121E 01
-.13476972E 01	.21328769E 01	.53416781E 00	.25229846E 01

Figure 75. Eigenvalue Spectrums (continued)

Contrails

CLOSED LOOP ROOTS AT 4.000SEC.

ROOTS OF A/C FRANK AT 7.000SEC.

REAL	IMAG	REAL	IMAG
-.48979674E-01	.00000000E 00	-.48979674E-01	.00000000E 00
-.48979674E-01	.00000000E 00	-.48979674E-01	.00000000E 00
-.48979674E-01	.00000000E 00	-.48979674E-01	.00000000E 00
-.48979674E-01	.00000000E 00	-.48979674E-01	.00000000E 00
-.48979674E-01	.00000000E 00	-.48979674E-01	.00000000E 00
-.59374256E-02	.77363343E-02	-.46753165E-01	.00000000E 00
-.10179632E 00	.00000000E 00	-.16301294E 01	.00000000E 00
-.12561655E 00	.00000000E 00	-.13051101E 00	.19032812E 01
-.11263805E 00	.13121616E 00	.00000000E 00	.00000000E 00
-.27779386E 00	.00000000E 00	.00000000E 00	.00000000E 00
-.16300932E 01	.00000000E 00	-.41578161E-02	.00000000E 00
-.13362364E 00	.19033602E 01	-.24858019E-01	.68452741E-01
-.69691777E 00	.16310865E 01	-.67430286E 00	.16059047E 01
		.00000000E 00	.00000000E 00

CLOSED LOOP ROOTS (DISCOP) FOR CONTROL WEIGHTS= 10000. AT 4.000SEC.

REAL	IMAG	DAMPING	FREQ
-.48979674E-01	.00000000E 00		
-.48979674E-01	.00000000E 00		
-.48979674E-01	.00000000E 00		
-.48979674E-01	.00000000E 00		
-.48979674E-01	.00000000E 00		
-.59425897E-02	.77912096E-02	.60645831E 00	.97988428E-02
-.10197766E 00	.00000000E 00		
-.10946464E 00	.00000000E 00		
-.35680459E 00	.41564113E 00	.65136028E 00	.54778377E 00
-.13934538E 01	.00000000E 00		
-.15983650E 01	.00000000E 00		
-.28993026E 00	.19130685E 01	.14984145E 00	.19349136E 01
-.13711490E 01	.22368401E 01	.52261262E 00	.26236432E 01

Figure 75. Eigenvalue Spectrums (continued)

Contrails

CLOSED LOOP ROOTS AT 5.000SEC.

ROOTS OF A/C FRAME AT 5.000SEC.

REAL	IMAG	REAL	IMAG
-.53215289E-01	.00000000E 00	-.53215289E-01	.00000000E 00
-.53215289E-01	.00000000E 00	-.53215289E-01	.00000000E 00
-.53215289E-01	.00000000E 00	-.53215289E-01	.00000000E 00
-.53215289E-01	.00000000E 00	-.53215289E-01	.00000000E 00
-.53215289E-01	.00000000E 00	-.53215289E-01	.00000000E 00
-.69193212E-02	.77980359E-02	-.42935093E-01	.00000000E 00
-.10489058E 00	.00000000E 00	-.17024360E 01	.00000000E 00
-.12926164E 00	.00000000E 00	-.14432117E 00	.15976264E 01
-.10993213E 00	.13064649E 00	.00000000E 00	.00000000E 00
-.28244895E 00	.00000000E 00	.00000000E 00	.00000000E 00
-.17024306E 01	.00000000E 00	-.50200480E-02	.00000000E 00
-.14705144E 00	.19977164E 01	-.24402902E-01	.62871699E-01
-.73728107E 00	.17691357E 01	-.71609220E 00	.17460709E 01
		.00000000E 00	.00000000E 00

CLOSED LOOP ROOTS (DISCOP) FOR CONTROL WEIGHTS= 10000. AT 5.000SEC.

REAL	IMAG	DAMPING	FREQ
-.53215289E-01	.00000000E 00		
-.53215289E-01	.00000000E 00		
-.53215289E-01	.00000000E 00		
-.53215289E-01	.00000000E 00		
-.53215289E-01	.00000000E 00		
-.69311097E-02	.78343210E-02	.66261726E 00	.10460291E-01
-.10708879E 00	.00000000E 00		
-.11352291E 00	.00000000E 00		
-.35304974E 00	.35987513E 00	.66184586E 00	.53342291E 00
-.15036257E 01	.00000000E 00		
-.16729755E 01	.00000000E 00		
-.29282204E 00	.20086167E 01	.14425816E 00	.20298487E 01
-.13925174E 01	.23664376E 01	.50715413E 00	.27457479E 01

Figure 75. Eigenvalue Spectrums (continued)

Contrails

CLOSED LOOP ROOTS AT 6.000SEC.

ROOTS OF A/C FRAME AT 6.000SEC.

REAL	IMAG	REAL	IMAG
-.57777648E-01	.00000000E 00	-.57777648E-01	.00000000E 00
-.57777648E-01	.00000000E 00	-.57777648E-01	.00000000E 00
-.57777648E-01	.00000000E 00	-.57777648E-01	.00000000E 00
-.57777648E-01	.00000000E 00	-.57777648E-01	.00000000E 00
-.57777648E-01	.00000000E 00	-.57777648E-01	.00000000E 00
-.81490700E-02	.76839214E-02	-.38572154E-01	.00000000E 00
-.10666535E 00	.00000000E 00	-.17713700E 01	.00000000E 00
-.13433839E 00	.00000000E 00	-.15843871E 00	.20891454E 01
-.10541366E 00	.12812794E 00	.00000000E 00	.00000000E 00
-.28441735E 00	.00000000E 00	.00000000E 00	.00000000E 00
-.17713904E 01	.00000000E 00	-.44494036E-02	.00000000E 00
-.16087315E 00	.20892493E 01	-.24849471E-01	.62088128E-01
-.77788548E 00	.19087338E 01	-.75963851E 00	.18874615E 01
		.00000000E 00	.00000000E 00

CLOSED LOOP ROOTS (DISCRP) FOR CONTROL WEIGHTS= 10000. AT 6.000SEC.

REAL	IMAG	DAMPING	FREQ
-.57777648E-01	.00000000E 00		
-.57777648E-01	.00000000E 00		
-.57777648E-01	.00000000E 00		
-.57777648E-01	.00000000E 00		
-.57777648E-01	.00000000E 00		
-.81645225E-02	.77166486E-02	.72675960E 00	.11234153E=01
-.11391941E 00	.00000000E 00		
-.11753436E 00	.00000000E 00		
-.34832325E 00	.36696992E 00	.68843963E 00	.50596048E 00
-.14029352E 01	.00000000E 00		
-.17392323E 01	.00000000E 00		
-.29420185E 00	.21009492E 01	.13867973E 00	.21214481E 01
-.14131454E 01	.24991454E 01	.49221166E 00	.28710116E 01

Figure 75. Eigenvalue Spectrums (continued)

Contrails

CLOSED LOOP ROOTS AT 7.000SEC.

ROOTS OF A/C FRAME AT 7.000SEC.

REAL	IMAG	REAL	IMAG
-.62729204E-01	.00000000E 00	-.62729204E-01	.00000000E 00
-.62729204E-01	.00000000E 00	-.62729204E-01	.00000000E 00
-.62729204E-01	.00000000E 00	-.62729204E-01	.00000000E 00
-.62729204E-01	.00000000E 00	-.62729204E-01	.00000000E 00
-.62729204E-01	.00000000E 00	-.62729204E-01	.00000000E 00
-.92767990E-02	.96775134E-02	-.37762579E-01	.00000000E 00
-.10923990E 00	.00000000E 00	-.18467901E 01	.00000000E 00
-.13930526E 00	.00000000E 00	-.17165702E 00	.21862941E 01
-.10714446E 00	.13069426E 00	.00000000E 00	.00000000E 00
-.28736076E 00	.00000000E 00	.00000000E 00	.00000000E 00
-.18468328E 01	.00000000E 00	-.53338050E-02	.00000000E 00
-.17375634E 00	.21863935E 01	-.24663779E-01	.62297038E-01
-.82084606E 00	.20496591E 01	-.80438667E 00	.20298076E 01
		.00000000E 00	.00000000E 00

CLOSED LOOP ROOTS (DISCOP) FOR CONTRL WEIGHTS= 10000. AT 7.000SEC.

REAL	IMAG	DAMPING	FREQ
-.62729204E-01	.00000000E 00		
-.62729204E-01	.00000000E 00		
-.62729204E-01	.00000000E 00		
-.62729204E-01	.00000000E 00		
-.62729204E-01	.00000000E 00		
-.92926717E-02	.97125908E-02	.69131461E 00	.13442030E-01
-.11570699E 00	.00000000E 00		
-.12139570E 00	.00000000E 00		
-.34374175E 00	.38472662E 00	.66627009E 00	.51591953E 00
-.17143349E 01	.00000000E 00		
-.18260075E 01	.00000000E 00		
-.29747635E 00	.21946484E 01	.13431797E 00	.22147175E 01
-.14373302E 01	.26353883E 01	.47881251E 00	.30018643E 01

Figure 75. Eigenvalue Spectrums (continued)

Contrails

CLOSED LOOP ROOTS AT 8.000SEC.

ROOTS OF A/C FRAME AT 8.000SEC.

REAL	IMAG	REAL	IMAG
-.68129436E-01	.00000000E 00	-.68129436E-01	.00000000E 00
-.68129436E-01	.00000000E 00	-.68129436E-01	.00000000E 00
-.68129436E-01	.00000000E 00	-.68129436E-01	.00000000E 00
-.68129436E-01	.00000000E 00	-.68129436E-01	.00000000E 00
-.68129436E-01	.00000000E 00	-.68129436E-01	.00000000E 00
-.10338955E-01	.95497069E-02	-.37626550E-01	.00000000E 00
-.11250872E 00	.00000000E 00	-.19241016E 01	.00000000E 00
-.14371573E 00	.00000000E 00	-.18527422E 00	.22872106E 01
-.10952907E 00	.13394400E 00	.00000000E 00	.00000000E 00
-.29188573E 00	.00000000E 00	.00000000E 00	.00000000E 00
-.19241515E 01	.00000000E 00	-.49052220E-02	.00000000E 00
-.18696494E 00	.22872930E 01	-.25234531E-01	.60527342E-01
-.86453506E 00	.21900195E 01	-.84963510E 00	.21713360E 01
		.00000000E 00	.00000000E 00

CLOSED LOOP ROOTS (DISCR) FOR CONTROL WEIGHTS= 10000. AT 8.000SEC.

REAL	IMAG	DAMPING	FREQ
-.68129436E-01	.00000000E 00		
-.68129436E-01	.00000000E 00		
-.68129436E-01	.00000000E 00		
-.68129436E-01	.00000000E 00		
-.68129436E-01	.00000000E 00		
-.11741138E 00	.00000000E 00		
-.10359163E-01	.95760273E-02	.73431859E 00	.14107185E*01
-.12527470E 00	.00000000E 00		
-.35137140E 00	.40211710E 00	.65799424E 00	.53400377E 00
-.12171553E 01	.00000000E 00		
-.19087186E 01	.00000000E 00		
-.29549131E 00	.22930715E 01	.12780589E 00	.23120320E 01
-.14623980E 01	.27721894E 01	.46658345E 00	.31342690E 01

Figure 75. Eigenvalue Spectrums (continued)

Contrails

CLOSED LOOP ROOTS AT 9.000SEC.

ROOTS OF A/C FRAME AT 9.000SEC.

REAL	IMAG	REAL	IMAG
-.74052534E-01	.00000000E 00	-.74052534E-01	.00000000E 00
-.74052534E-01	.00000000E 00	-.74052534E-01	.00000000E 00
-.74052534E-01	.00000000E 00	-.74052534E-01	.00000000E 00
-.74052534E-01	.00000000E 00	-.74052534E-01	.00000000E 00
-.74052534E-01	.00000000E 00	-.74052534E-01	.00000000E 00
-.11345441E-01	.93522413E-02	-.35859670E-01	.00000000E 00
-.11458667E 00	.00000000E 00	-.19986311E 01	.00000000E 00
-.14823075E 00	.00000000E 00	-.19987026E 00	.23857857E 01
-.10811350E 00	.13375242E 00	.00000000E 00	.00000000E 00
-.29647097E 00	.00000000E 00	.00000000E 00	.00000000E 00
-.19986799E 01	.00000000E 00	-.41436901E-02	.00000000E 00
-.20121833E 00	.23858560E 01	-.26011962E-01	.59652955E-01
-.90806470E 00	.23288213E 01	-.89446803E 00	.23110756E 01
		.00000000E 00	.00000000E 00

CLOSED LOOP ROOTS (DISCOP) FOR CONTROL WEIGHTS= 10000. AT 9.000SEC.

REAL	IMAG	DAMPING	FREQ
-.74052534E-01	.00000000E 00		
-.74052534E-01	.00000000E 00		
-.74052534E-01	.00000000E 00		
-.74052534E-01	.00000000E 00		
-.74052534E-01	.00000000E 00		
-.12132282E 00	.00000000E 00		
-.11369601E-01	.93719015E-02	.77164039E 00	.14734326E 01
-.12909728E 00	.00000000E 00		
-.35436129E 00	.39228285E 00	.67032927E 00	.52863765E 00
-.19157517E 01	.00000000E 00		
-.19826305E 01	.00000000E 00		
-.29357601E 00	.23914240E 01	.12184729E 00	.24093766E 01
-.14894886E 01	.29089873E 01	.45575940E 00	.32681468E 01

Figure 75. Eigenvalue Spectrums (continued)

Contrails

CLOSED LOOP ROOTS AT 10.000SEC.

ROOTS OF A/C FRAME AT 10.000SEC.

REAL	IMAG	REAL	IMAG
-.80599608E-01	.00000000E 00	-.80599608E-01	.00000000E 00
-.80599608E-01	.00000000E 00	-.80599608E-01	.00000000E 00
-.80599608E-01	.00000000E 00	-.80599608E-01	.00000000E 00
-.80599608E-01	.00000000E 00	-.80599608E-01	.00000000E 00
-.80599608E-01	.00000000E 00	-.80599608E-01	.00000000E 00
-.12326535E-01	.90602543E-02	-.34549007E-01	.00000000E 00
-.11637335E 00	.00000000E 00	-.20725472E 01	.00000000E 00
-.15245017E 00	.00000000E 00	-.21437125E 00	.24828768E 01
-.10709579E 00	.13372003E 00	.00000000E 00	.00000000E 00
-.30162815E 00	.00000000E 00	.00000000E 00	.00000000E 00
-.20725934E 01	.00000000E 00	-.31135475E-02	.00000000E 00
-.21542376E 00	.24829351E 01	-.26977336E-01	.58693416E-01
-.95154632E 00	.24654478E 01	-.93903298E 00	.24484503E 01
		.00000000E 00	.00000000E 00

CLOSED LOOP ROOTS (DISCOP) FOR CONTRL WEIGHTS= 10000. AT 10.000SEC.

REAL	IMAG	DAMPING	FREQ
-.80599608E-01	.00000000E 00		
-.80599608E-01	.00000000E 00		
-.80599608E-01	.00000000E 00		
-.80599608E-01	.00000000E 00		
-.80599608E-01	.00000000E 00		
-.12416346E 00	.00000000E 00		
-.12353161E-01	.90737312E-02	.80594594E 00	.15327530E-01
-.13277337E 00	.00000000E 00		
-.35090011E 00	.38807613E 00	.67068587E 00	.52319592E 00
-.20096831E 01	.00000000E 00		
-.20585844E 01	.00000000E 00		
-.29368672E 00	.24872614E 01	.11726174E 00	.25045401E 01
-.15193398E 01	.30450529E 01	.44646430E 00	.34030487E 01

Figure 75. Eigenvalue Spectrums (continued)

Contrails

CLOSED LOOP ROOTS AT 11.000SEC.

ROOTS OF A/C FRAME AT 11.000SEC.

REAL	IMAG	REAL	IMAG
-.87899924E-01	.00000000E 00	-.87899924E-01	.00000000E 00
-.87899924E-01	.00000000E 00	-.87899924E-01	.00000000E 00
-.87899924E-01	.00000000E 00	-.87899924E-01	.00000000E 00
-.87899924E-01	.00000000E 00	-.87899924E-01	.00000000E 00
-.87899924E-01	.00000000E 00	-.87899924E-01	.00000000E 00
-.13319379E-01	.86369998E-02	-.33222586E-01	.00000000E 00
-.11776668E 00	.00000000E 00	-.21455689E 01	.00000000E 00
-.15642227E 00	.00000000E 00	-.22903651E 00	.25786333E 01
-.10574194E 00	.13325862E 00	.00000000E 00	.00000000E 00
-.30730079E 00	.00000000E 00	.00000000E 00	.00000000E 00
-.21456099E 01	.00000000E 00	-.19351583E-02	.00000000E 00
-.22934320E 00	.25786803E 01	-.28064726E-01	.57740295E-01
-.99514316E 00	.25993729E 01	-.98352330E 00	.25829597E 01
		.00000000E 00	.00000000E 00

CLOSED LOOP ROOTS (DISCOP) FOR CONTRL WEIGHTS= 10000. AT 11.000SEC.

REAL	IMAG	DAMPING	FREQ
-.87899924E-01	.00000000E 00		
-.87899924E-01	.00000000E 00		
-.87899924E-01	.00000000E 00		
-.87899924E-01	.00000000E 00		
-.87899924E-01	.00000000E 00		
-.12705767E 00	.00000000E 00		
-.13348190E-01	.86441027E-02	.83936822E 00	.15902663E-01
-.13632334E 00	.00000000E 00		
-.34553267E 00	.37843630E 00	.67427348E 00	.51245181E 00
-.20994414E 01	.00000000E 00		
-.21328338E 01	.00000000E 00		
-.29462114E 00	.25827121E 01	.11333927E 00	.25994622E 01
-.15521788E 01	.31797965E 01	.43866527E 00	.35384128E 01

Figure 75. Eigenvalue Spectrums (continued)

Contrails

CLOSED LOOP ROOTS AT 12.000SEC.

ROOTS OF A/C FRAME AT 12.000SEC.

REAL	IMAG	REAL	IMAG
-.96120967E-01	.00000000E 00	-.96120967E-01	.00000000E 00
-.96120967E-01	.00000000E 00	-.96120967E-01	.00000000E 00
-.96120967E-01	.00000000E 00	-.96120967E-01	.00000000E 00
-.96120967E-01	.00000000E 00	-.96120967E-01	.00000000E 00
-.96120967E-01	.00000000E 00	-.96120967E-01	.00000000E 00
-.14323167E-01	.80518103E-02	-.31784913E-01	.00000000E 00
-.11860929E 00	.00000000E 00	-.22174589E 01	.00000000E 00
-.16012730E 00	.00000000E 00	-.24389434E 00	.26726084E 01
-.10389675E 00	.13218568E 00	.00000000E 00	.00000000E 00
-.31351359E 00	.00000000E 00	.00000000E 00	.00000000E 00
-.22174925E 01	.00000000E 00	-.53637959E-03	.00000000E 00
-.24450225E 00	.26726459E 01	-.29306102E-01	.56854793E-01
-.10387788E 01	.27300764E 01	-.10278800E 01	.27141031E 01
		.00000000E 00	.00000000E 00

CLOSED LOOP ROOTS (DISCOP) FOR CONTRL WEIGHTS= 10000. AT 12.000SEC.

REAL	IMAG	DAMPING	FREQ
-.96120967E-01	.00000000E 00		
-.96120967E-01	.00000000E 00		
-.96120967E-01	.00000000E 00		
-.96120967E-01	.00000000E 00		
-.96120967E-01	.00000000E 00		
-.13020481E 00	.00000000E 00		
-.14358707E-01	.80481804E-02	.87231677E 00	.16460427E-01
-.13969288E 00	.00000000E 00		
-.34138011E 00	.36053547E 00	.68755377E 00	.49651405E 00
-.21854184E 01	.00000000E 00		
-.22050853E 01	.00000000E 00		
-.29756071E 00	.26759446E 01	.11051721E 00	.26924379E 01
-.15881716E 01	.33126865E 01	.43230672E 00	.36737149E 01

Figure 75. Eigenvalue Spectrums (continued)

Contrails

CLOSED LOOP ROOTS AT 13.000SEC.

ROOTS OF A/C FRAME AT 13.000SEC.

REAL	IMAG	REAL	IMAG
-.10548581E 00	.00000000E 00	-.10548581E 00	.00000000E 00
-.10548581E 00	.00000000E 00	-.10548581E 00	.00000000E 00
-.10548581E 00	.00000000E 00	-.10548581E 00	.00000000E 00
-.10548581E 00	.00000000E 00	-.10548581E 00	.00000000E 00
-.10548581E 00	.00000000E 00	-.10548581E 00	.00000000E 00
-.11891895E 00	.00000000E 00	-.30314556E-01	.00000000E 00
-.15325779E-01	.72746311E-02	-.22883036E 01	.00000000E 00
-.16380918E 00	.00000000E 00	-.25890225E 00	.27647600E 01
-.10172583E 00	.13063358E 00	.00000000E 00	.00000000E 00
-.31983665E 00	.00000000E 00	.00000000E 00	.00000000E 00
-.22883285E 01	.00000000E 00	.12578740E-02	.00000000E 00
-.25935417E 00	.27647899E 01	-.30784191E-01	.56950289E-01
-.10824044E 01	.28570984E 01	-.10720722E 01	.28414365E 01
		.00000000E 00	.00000000E 00

CLOSED LOOP ROOTS (DISCOP) FOR CNTRL WEIGHTS= 10000. AT 13.000SEC.

REAL	IMAG	DAMPING	FREQ
-.10548581E 00	.00000000E 00		
-.10548581E 00	.00000000E 00		
-.10548581E 00	.00000000E 00		
-.10548581E 00	.00000000E 00		
-.10548581E 00	.00000000E 00		
-.13407781E 00	.00000000E 00		
-.15410025E-01	.72127007E-02	.90570157E 00	.17014463E-01
-.14258882E 00	.00000000E 00		
-.34120253E 00	.34554812E 00	.70261832E 00	.48561577E 00
-.22732145E 01	.34993913E-02	.99999882E 00	.22732172E 01
-.30147380E 00	.27677271E 01	.10828421E 00	.27840976E 01
-.16223632E 01	.34445518E 01	.42609754E 00	.38074926E 01

Figure 75. Eigenvalue Spectrums (continued)

Contrails

CLOSED LOOP ROOTS AT 14.000SEC.

ROOTS OF A/C FRAME AT 14.000SEC.

REAL	IMAG	REAL	IMAG
-11629597E 00	00000000E 00	-11629597E 00	00000000E 00
-11629597E 00	00000000E 00	-11629597E 00	00000000E 00
-11629597E 00	00000000E 00	-11629597E 00	00000000E 00
-11629597E 00	00000000E 00	-11629597E 00	00000000E 00
-11629597E 00	00000000E 00	-11629597E 00	00000000E 00
-11913862E 00	00000000E 00	-29290763E-01	00000000E 00
-16066598E-01	68593704E-02	-23584939E 01	00000000E 00
-17466957E 00	00000000E 00	-27388365E 00	28550999E 01
-10016289E 00	12748108E 00	00000000E 00	00000000E 00
-30936584E 00	00000000E 00	00000000E 00	00000000E 00
-23585095E 01	00000000E 00	65796416E-02	00000000E 00
-27421557E 00	28551234E 01	-34014924E-01	73562121E-01
-11177303E 01	29896244E 01	-11079004E 01	29746403E 01
		00000000E 00	00000000E 00

CLOSED LOOP ROOTS (DISSEP) FOR CNTRL WEIGHTS= 10000. AT 14.000SEC.

REAL	IMAG	DAMPING	FREQ
-11629597E 00	00000000E 00		
-11629597E 00	00000000E 00		
-11629597E 00	00000000E 00		
-11629597E 00	00000000E 00		
-11629597E 00	00000000E 00		
-13667733E 00	00000000E 00		
-16156204E-01	68322141E-02	92103072E 00	17541439E-01
-14621078E 00	00000000E 00		
-34120982E 00	34896352E 00	69911872E 00	48805704E 00
-23293597E 01	00000000E 00		
-23430494E 01	00000000E 00		
-31168997E 00	28576852E 01	10842774E 00	28746331E 01
-16576280E 01	35716658E 01	42097645E 00	39375789E 01

Figure 75. Eigenvalue Spectrums (continued)

Contrails

CLOSED LOOP ROOTS AT 15.000SEC.

ROOTS OF A/C FRAME AT 15.000SEC.

REAL	IMAG	REAL	IMAG
-.12895388E 00	.00000000E 00	-.12895388E 00	.00000000E 00
-.12895388E 00	.00000000E 00	-.12895388E 00	.00000000E 00
-.12895388E 00	.00000000E 00	-.12895388E 00	.00000000E 00
-.12895388E 00	.00000000E 00	-.12895388E 00	.00000000E 00
-.12895388E 00	.00000000E 00	-.12895388E 00	.00000000E 00
-.12052835E 00	.00000000E 00	-.29529046E-01	.00000000E 00
-.17138985E-01	.53846842E-02	-.24289739E 01	.00000000E 00
-.17760603E 00	.00000000E 00	-.28839595E 00	.29444425E 01
-.10094971E 00	.13058097E 00	.00000000E 00	.00000000E 00
-.31870704E 00	.00000000E 00	.00000000E 00	.00000000E 00
-.24289820E 01	.00000000E 00	.80866172E-02	.00000000E 00
-.28862808E 00	.29444595E 01	-.35387972E-01	.74918278E-01
-.11299112E 01	.30305789E 01	-.11199753E 01	.30151240E 01
		.00000000E 00	.00000000E 00

CLOSED LOOP ROOTS (DISCOP) FOR CONTRL WEIGHTS= 10000 AT 15.000SEC.

REAL	IMAG	DAMPING	FREQ
-.12895388E 00	.00000000E 00		
-.12895388E 00	.00000000E 00		
-.12895388E 00	.00000000E 00		
-.12895388E 00	.00000000E 00		
-.12895388E 00	.00000000E 00		
-.17231417E-01	.53310516E-02	.95532475E 00	.18037235E*01
-.13440488E 00	.00000000E 00		
-.14930670E 00	.00000000E 00		
-.28788486E 00	.41577788E 00	.56926163E 00	.50571626E 00
-.24174946E 01	.00000000E 00		
-.23797384E 01	.00000000E 00		
-.31266040E 00	.29474693E 01	.10548575E 00	.29640061E 01
-.16836432E 01	.36237387E 01	.42135693E 00	.39957648E 01

Figure 75. Eigenvalue Spectrums (continued)

Contrails

CLOSED LOOP ROOTS AT 16.000SEC.

ROOTS OF A/C FRAME AT 16.000SEC.

REAL	IMAG	REAL	IMAG
-.14401335E 00	.00000000E 00	-.14401335E 00	.00000000E 00
-.14401335E 00	.00000000E 00	-.14401335E 00	.00000000E 00
-.14401335E 00	.00000000E 00	-.14401335E 00	.00000000E 00
-.14401335E 00	.00000000E 00	-.14401335E 00	.00000000E 00
-.14401335E 00	.00000000E 00	-.14401335E 00	.00000000E 00
-.12129803E 00	.00000000E 00	-.29300704E-01	.00000000E 00
-.18258970E-01	.26080859E-02	-.24979133E 01	.00000000E 00
-.17795458E 00	.00000000E 00	-.30315117E 00	.30313998E 01
-.10074550E 00	.13067272E 00	.00000000E 00	.00000000E 00
-.33986916E 00	.00000000E 00	.00000000E 00	.00000000E 00
-.24979127E 01	.00000000E 00	-.97435384E-02	.00000000E 00
-.30331021E 00	.30314124E 01	-.36795601E-01	.76088451E-01
-.11438073E 01	.30339960E 01	-.11334830E 01	.30171835E 01
		.00000000E 00	.00000000E 00

CLOSED LOOP ROOTS (DISCOP) FOR CONTRL WEIGHTS= 10000. AT 16.000SEC.

REAL	IMAG	DAMPING	FREQ
-.14401335E 00	.00000000E 00		
-.14401335E 00	.00000000E 00		
-.14401335E 00	.00000000E 00		
-.14401335E 00	.00000000E 00		
-.14401335E 00	.00000000E 00		
-.18336182E-01	.25156367E-02	.99071954E 00	.18507944E+01
-.13157695E 00	.00000000E 00		
-.15233181E 00	.00000000E 00		
-.16876802E 00	.43033582E 00	.36510417E 00	.46224622E 00
-.24425515E 01	.00000000E 00		
-.24909169E 01	.00000000E 00		
-.33655290E 00	.30305913E 01	.11037339E 00	.30492214E 01
-.17237086E 01	.36537001E 01	.42669057E 00	.40399265E 01

Figure 75. Eigenvalue Spectrums (continued)

Contrails

CLOSED LOOP ROOTS AT 17.000SEC.

ROOTS OF A/C FRAME AT 17.000SEC.

REAL	IMAG	REAL	IMAG
-.16227730E 00	.00000000E 00	-.16227730E 00	.00000000E 00
-.16227730E 00	.00000000E 00	-.16227730E 00	.00000000E 00
-.16227730E 00	.00000000E 00	-.16227730E 00	.00000000E 00
-.16227730E 00	.00000000E 00	-.16227730E 00	.00000000E 00
-.16227730E 00	.00000000E 00	-.16227730E 00	.00000000E 00
-.15224533E-01	.00000000E 00	-.28816086E-01	.00000000E 00
-.12159080E 00	.00000000E 00	-.25653432E 01	.00000000E 00
-.23605352E-01	.00000000E 00	-.31803484E 00	.31157362E 01
-.17274199E 00	.00000000E 00	.00000000E 00	.00000000E 00
-.99987014E-01	.13014100E 00	.00000000E 00	.00000000E 00
-.38852799E 00	.00000000E 00	.99572047E-02	.00000000E 00
-.25653333E 01	.00000000E 00	-.37404211E-01	.66807448E-01
-.31814451E 00	.31157462E 01	-.11492450E 01	.29472003E 01
-.11604762E 01	.29674307E 01	.00000000E 00	.00000000E 00

CLOSED LOOP ROOTS (DISCOP) FOR CONTRL WEIGHTS= 10000. AT 17.000SEC.

REAL	IMAG	DAMPING	FREQ
-.16227730E 00	.00000000E 00		
-.16227730E 00	.00000000E 00		
-.16227730E 00	.00000000E 00		
-.16227730E 00	.00000000E 00		
-.16227730E 00	.00000000E 00		
-.15225979E-01	.00000000E 00		
-.23687355E-01	.00000000E 00		
-.12102234E 00	.00000000E 00		
-.15516423E 00	.00000000E 00		
-.17789783E-01	.29126781E 00	.60963461E-01	.29181058E 00
-.25581793E 01	.73054720E-03	.99999996E 00	.25581794E 01
-.32482608E 00	.31171785E 01	.10364396E 00	.31340571E 01
-.17870673E 01	.36459363E 01	.44012620E 00	.40603524E 01

Figure 75. Eigenvalue Spectrums (continued)

Contrails

CLOSED LOOP ROOTS AT 18.000SEC.

ROOTS OF A/C FRAME AT 18.000SEC.

REAL	IMAG	REAL	IMAG
-.18495925E 00	.00000000E 00	-.18495925E 00	.00000000E 00
-.18495925E 00	.00000000E 00	-.18495925E 00	.00000000E 00
-.18495925E 00	.00000000E 00	-.18495925E 00	.00000000E 00
-.18495925E 00	.00000000E 00	-.18495925E 00	.00000000E 00
-.18495925E 00	.00000000E 00	-.18495925E 00	.00000000E 00
-.13157572E-01	.00000000E 00	-.18495925E 00	.00000000E 00
-.11643363E 00	.00000000E 00	-.24992565E-01	.00000000E 00
-.28735118E-01	.00000000E 00	-.26302855E 01	.00000000E 00
-.16706014E 00	.00000000E 00	-.33284319E 00	.31941872E 01
-.92525592E-01	.12219950E 00	.00000000E 00	.00000000E 00
-.49701780E 00	.00000000E 00	.00000000E 00	.00000000E 00
-.26302584E 01	.00000000E 00	-.14010949E-01	.00000000E 00
-.33293445E 00	.31941979E 01	-.39961415E-01	.61095963E-01
-.11712372E 01	.27090477E 01	-.11579601E 01	.26773337E 01
		.00000000E 00	.00000000E 00

CLOSED LOOP ROOTS (DISCOP) FOR CONTROL WEIGHTS= 10000. AT 18.000SEC.

REAL	IMAG	DAMPING	FREQ
-.18495925E 00	.00000000E 00		
-.18495925E 00	.00000000E 00		
-.18495925E 00	.00000000E 00		
-.18495925E 00	.00000000E 00		
-.18495925E 00	.00000000E 00		
-.13118301E-01	.00000000E 00		
-.70741767E-01	.00000000E 00		
-.28967359E-01	.00000000E 00		
-.13233640E-01	.11931860E 00	.11023419E 00	.12005023E 00
-.15576273E 00	.00000000E 00		
-.26265942E 01	.00000000E 00		
-.28504241E 01	.00000000E 00		
-.35456275E 00	.31924006E 01	.11038588E 00	.32120299E 01
-.17864391E 01	.34614207E 01	.45862252E 00	.38952276E 01

Figure 75. Eigenvalue Spectrums (continued)

Contrails

CLOSED LOOP ROOTS AT 19.000SEC.

ROOTS OF A/C FRAME AT 19.000SEC.

REAL	IMAG	REAL	IMAG
-.21274249E 00	.00000000E 00	-.21274249E 00	.00000000E 00
-.21274249E 00	.00000000E 00	-.21274249E 00	.00000000E 00
-.21274249E 00	.00000000E 00	-.21274249E 00	.00000000E 00
-.21274249E 00	.00000000E 00	-.21274249E 00	.00000000E 00
-.21274249E 00	.00000000E 00	-.21274249E 00	.00000000E 00
-.12489183E-01	.00000000E 00	-.20869598E-01	.00000000E 00
-.10757573E 00	.00000000E 00	-.26920899E 01	.00000000E 00
-.31413622E-01	.00000000E 00	-.34599882E 00	.32641168E 01
-.83672578E-01	.11134600E 00	.00000000E 00	.00000000E 00
-.16834691E 00	.00000000E 00	.00000000E 00	.00000000E 00
-.60881226E 00	.00000000E 00	.62213290E-02	.00000000E 00
-.26920363E 01	.00000000E 00	-.35483514E-01	.91807263E-01
-.34608825E 00	.32641284E 01	-.11737563E 01	.24259966E 01
-.11876837E 01	.24749644E 01	.00000000E 00	.00000000E 00

STOP 77774123

CLOSED LOOP ROOTS (DISCOP, FOR CONTROL WEIGHTS= 1000. AT 19.000SEC.

REAL	IMAG	DAMPING	FREQ
-.21274249E 00	.00000000E 00		
-.21274249E 00	.00000000E 00		
-.21274249E 00	.00000000E 00		
-.21274249E 00	.00000000E 00		
-.21274249E 00	.00000000E 00		
-.11829071E-01	.00000000E 00		
-.35941624E-01	.00000000E 00		
-.53089722E-01	.50283319E-01	.72603603E 00	.73122710E-01
-.87698404E-01	.00000000E 00		
-.13296335E 00	.00000000E 00		
-.85429444E 00	.00000000E 00		
-.26936350E 01	.00000000E 00		
-.34970008E 00	.32618574E 01	.10659803E 00	.32805493E 01
-.15539923E 01	.26583809E 01	.50466316E 00	.30792663E 01

Figure 75. Eigenvalue Spectrums (concluded)

SECTION VIII VARIANCE CONTRIBUTION AND CRITICAL PARAMETER IDENTIFICATION

The variance contribution matrix as developed in Section VIII of Volume I, is used to show how to identify the important contributors to the weapon delivery performance.

This identification is facilitated if the starting value of the covariance matrix is diagonal. In this case, the impact covariance matrix can be written in terms of the components.

$$X = \sigma_1^2 (\phi_1 \phi_1') + \sigma_2^2 (\phi_2 \phi_2') + \dots + \sigma_n^2 (\phi_n \phi_n')$$

where ϕ_i , $i = 1, \dots, n$ are the column vectors of the transition (sensitivity) matrix ϕ as shown in Table XI. For the release error variances shown in Table XII, the components of the nominal impact variances are given in Table XIII, together with the impact variances. By inspection of Table XIII the following identifications are made:

The important contributors to the down-range error variance σ_{xe}^2 are:

- The longitudinal velocity states, u , v and the pitch attitude θ .

The important contributors to the cross-range error variance σ_{ye}^2 are:

- The side velocity component v and the yaw angle ψ .

Therefore, for the weapon delivery, the most critical states requiring tight control are u , v , w , θ , and ψ for weapons stationed near the cg of the aircraft.

These conclusions are based on the weapon dynamics only. For the aircraft-plus-weapon combination, one starts out with a diagonal aircraft initial covariance matrix and develops the total transition matrix from dive to impact given by

$$\phi = \phi_b H + \phi_a$$

where

Contrails

ϕ_a = aircraft transition matrix at release

H_+ = discrete transition matrix at release

ϕ_b = weapon transition matrix at impact

The columns of this matrix together with the initial error variances determine the main contributors.

It is interesting to note that, by properly correlating the errors, a reduction in impact variances is possible. It is conjectured that the optimal weapon delivery controller which controls the evolution of the error covariance matrix essentially does that. Inspection of Figure 70 shows that the contribution of the release cross-covariance term $E\{u\theta\}$ to the down-range impact variance is negative.

A program listing for computing the contributions of diagonal variances is given in Figure 76. Figure 77 shows the outputs of this program. For each state impact variance, the first row shows the initial release variances, the second row shows the multipliers (sensitivity coefficients), the third row shows the variance components, and the fourth row shows the sum of the components.

Table XI. Sensitivity Matrix ϕ of a Weapon

	x_e	h_e	u	θ	q	w	y_e	ψ	r	v
x_e	1.0	$.32 \times 10^{-5}$	$.29 \times 10^2$	$.98 \times 10^7$	$.41 \times 10^1$	$.21 \times 10^2$	0	0	0	0
h_e	0	.996	$.21 \times 10^2$	$.14 \times 10^8$	$.68 \times 10^2$	$.31 \times 10^2$	0	0	0	0
u	0	$.5 \times 10^{-6}$.82	$.19 \times 10^5$.503	$.45 \times 10^{-1}$	0	0	0	0
θ	0	0	$.6 \times 10^{-7}$.60	$.11 \times 10^{-5}$	$.13 \times 10^{-5}$	0	0	0	0
q	0	0	$.37 \times 10^{-9}$.79	$.19 \times 10^{-6}$	$.20 \times 10^{-8}$	0	0	0	0
w	0	0	$.14 \times 10^{-9}$.13	$.31 \times 10^{-3}$	$.93 \times 10^{-8}$	0	0	0	0
y_e	0	0	0	0	0	0	2.0	$.14 \times 10^8$	$.35 \times 10^2$	$.50 \times 10^2$
ψ	0	0	0	0	0	0		1.0	$.24 \times 10^{-5}$	$.36 \times 10^{-5}$
r	0	0	0	0	0	0	0	0	$.19 \times 10^{-6}$	$.80 \times 10^{-11}$
v	0	0	0	0	0	0	0	0	$.25 \times 10^{-3}$	$.15 \times 10^{-6}$

Table XII. Release Error Variances

$\sigma_{x_e}^2$	$\sigma_{h_e}^2$	σ_u^2	σ_θ^2	σ_q^2	σ_w^2	$\sigma_{y_e}^2$	σ_ψ^2	σ_r^2	σ_v^2
100	100	100	10^{-6}	10^{-6}	25	100	10^{-4}	10^{-4}	25

Table XIII. Components of Nominal Impact Variances

	x_e	h_e	u	θ	q	w	y_e	ψ	r	v
$\sigma_{x_e}^2 = .36189 \times 10^4$	100	$+ .32 \times 10^{-3}$	$+ .29 \times 10^4$	$+ .98 \times 10^1$	$+ .41 \times 10^{-5}$	$+ .52 \times 10^3$	$+ 0$	$+ 0$	$+ 0$	$+ 0$
$\sigma_{h_e}^2 = .2970 \times 10^4$	0	$+ .996 \times 10^2$	$+ .207 \times 10^4$	$+ .14 \times 10^2$	$+ .68 \times 10^{-4}$	$+ .77 \times 10^3$	$+ 0$	$+ 0$	$+ 0$	$+ 0$
$\sigma_u^2 = .833 \times 10^2$	0	$+ .5$	$+ .82 \times 10^2$	$+ .18 \times 10^{-1}$	$+ .51 \times 10^6$	$+ .11 \times 10^1$	$+ 0$	$+ 0$	$+ 0$	$+ 0$
$\sigma_\theta^2 = .39 \times 10^{-4}$	0	$+ 0$	$+ .6 \times 10^{-5}$	$+ .6 \times 10^{-6}$	$+ 0$	$+ .32 \times 10^{-4}$	$+ 0$	$+ 0$	$+ 0$	$+ 0$
$\sigma_q^2 = .88 \times 10^{-7}$	0	$+ 0$	$+ .37 \times 10^{-7}$	$+ .79 \times 10^{-9}$	$+ 0$	$+ .51 \times 10^{-7}$	$+ 0$	$+ 0$	$+ 0$	$+ 0$
$\sigma_w^2 = .38 \times 10^{-6}$	0	$+ 0$	$+ .14 \times 10^{-7}$	$+ .13 \times 10^{-6}$	$+ 0$	$+ .23 \times 10^{-6}$	$+ 0$	$+ 0$	$+ 0$	$+ 0$
$\sigma_{y_e}^2 = .27 \times 10^4$	0	$+ 0$	$+ 0$	$+ 0$	$+ 0$	$+ 0$	$+ 100$	$+ .14 \times 10^4$	$+ 0$	$+ .12 \times 10^4$
$\sigma_\psi^2 = .19 \times 10^{-3}$	0	$+ 0$	$+ 0$	$+ 0$	$+ 0$	$+ 0$	$+ 0$	$+ .1 \times 10^{-3}$	$+ 0$	$+ .9 \times 10^{-4}$
$\sigma_r^2 = .22 \times 10^{-9}$	0	$+ 0$	$+ 0$	$+ 0$	$+ 0$	$+ 0$	$+ 0$	$+ 0$	$+ .19 \times 10^{-10}$	$+ .2 \times 10^{-9}$
$\sigma_v^2 = .39 \times 10^{-5}$	0	$+ 0$	$+ 0$	$+ 0$	$+ 0$	$+ 0$	$+ 0$	$+ 0$	$+ .25 \times 10^{-7}$	$+ .38 \times 10^{-5}$

Contrails

```

A=00
*FORTRAN LS,GB
1: DIMENSION PHI(20,20),PSI(10,10),XR(10),PSIXR(10,11),IH(10),SIG(3),
2: CEP(2)
3: 1 FORMAT(8E10.4)
4: READ(2)PHI
5: READ(5,1)XR
6: DO 10 I=1,10
7: DO 10 J=1,10
8: 10 PSI(I,J)=PHI(I,J)*PHI(I,J)
9: DO 11 I=1,10
10: DO 11 J=1,10
11: 11 PSIXR(I,J)=PSI(I,J)*XR(J)
12: DO 12 I=1,10
13: PSIXR(I,11)=0.
14: DO 12 J=1,10
15: 12 PSIXR(I,11)=PSIXR(I,11)+PSIXR(I,J)
16: READ(5,2)IH
17: 2 FORMAT(10A4)
18: DO 20 I=1,10
19: WRITE(9,30)IH(I)
20: 30 FORMAT(1H1/7X,A4)
21: WRITE(9,31)
22: 31 FORMAT(/115H      XE      HE      PSI      U      R      THETA
23: 10      W      YE      V//)
24: WRITE(9,32)(PSI(I,J),J=1,10)
25: 32 FORMAT(10E12.5)
26: WRITE(9,33)
27: 33 FORMAT(//)
28: WRITE(9,32)(XR(J),J=1,10)
29: WRITE(9,33)
30: WRITE(9,32)(PSIXR(I,J),J=1,10)
31: WRITE(9,33)
32: WRITE(9,34)PSIXR(I,11)
33: 34 FORMAT(6H SUM =E12.5)
34: 20 CONTINUE
35: SIG(1)=SQRT(PSIXR(1,11))
36: SIG(2)=SQRT(PSIXR(7,11))
37: SIG(3)=SQRT(PSIXR(2,11))
38: CALL CEPC(SIG,CEP)
39: 2030 FORMAT(///7X,16H CEP HORIZONTAL=E15.8,14H CEP VERTICAL=E15.8/)
40: WRITE(9,2030)CEP(1),CEP(2)
41: END

```

Figure 76. Variance Contribution Program Listing

```

XE
  HE      U      THETA      Q      W      YE      PSI      R      V
•10000E 01 •32865E-05 •29863E 02 •9885E 07 •41849E 01 •20908E 02 •00000E 00 •52039E-11 •15509E-16 •18952E-14
•10000E 03 •10000E 03 •10000E 03 •10000E-05 •25000E 02 •10000E 03 •10000E-03 •10000E-03 •10000E 03 •25000E 02
•10000E 03 •32865E-03 •29863E 04 •9885E 01 •41849E-05 •52270E 03 •00000E 00 •52039E-15 •15509E-20 •47381E-15
SUM = .36185E 04

```

```

HE
  HE      U      THETA      Q      W      YE      PSI      R      V
•00000E 00 •99629E 00 •20780E 02 •14032E 08 •68179E 02 •31139E 02 •00000E 00 •00000E 00 •00000E 00 •00000E 00
•10000E 03 •10000E 03 •10000E 03 •10000E-05 •25000E 02 •10000E 03 •10000E-03 •10000E-03 •10000E 03 •25000E 02
•00000E 00 •99629E 00 •20780E 04 •14032E 02 •68179E-04 •77849E 03 •00000E 00 •00000E 00 •00000E 00 •00000E 00
SUM = .29702E 04

```

```

U
  HE      U      THETA      Q      W      YE      PSI      R      V
•00000E 00 •54897E-06 •82203E 00 •18895E 05 •50336E 00 •45637E-01 •00000E 00 •00000E 00 •00000E 00 •00000E 00
•10000E 03 •10000E 03 •10000E 03 •10000E-05 •25000E 02 •10000E 03 •10000E-03 •10000E-03 •10000E 03 •25000E 02
•00000E 00 •54897E-04 •82203E 02 •18895E-01 •50336E-06 •11409E 01 •00000E 00 •00000E 00 •00000E 00 •00000E 00
SUM = .83363E 02

```

Figure 77. Variance Contribution Program Outputs

THETA										
XE	HE	U	THETA	Q	W	YE	PSI	R	V	
.00000E 00	.51653E+14	.62963E+07	.60319E 00	.11235E+05	.13050E+05	.00000E 00	.00000E 00	.00000E 00	.00000E 00	.00000E 00
.10000E 03	.10000E 03	.10000E 03	.10000E+05	.10000E+05	.25000E 02	.10000E 03	.10000E+03	.10000E+03	.25000E 02	
.00000E 00	.51653E+12	.62963E+05	.60319E+06	.11235E+11	.32625E+04	.00000E 00	.00000E 00	.00000E 00	.00000E 00	.00000E 00
SUM * .39524E+04										
Q										
XE	HE	U	THETA	Q	W	YE	PSI	R	V	
.00000E 00	.40369E+15	.37068E+09	.79635E+03	.19038E+06	.20427E+08	.00000E 00	.00000E 00	.00000E 00	.00000E 00	.00000E 00
.10000E 03	.10000E 03	.10000E 03	.10000E+05	.10000E+05	.25000E 02	.10000E 03	.10000E+03	.10000E+03	.25000E 02	
.00000E 00	.40369E+13	.37068E+07	.79635E+09	.19038E+12	.51067E+07	.00000E 00	.00000E 00	.00000E 00	.00000E 00	.00000E 00
SUM * .88931E+07										
W										
XE	HE	U	THETA	Q	W	YE	PSI	R	V	
.00000E 00	.21308E+12	.14845E+09	.13162E 00	.30946E+03	.93874E+08	.00000E 00	.00000E 00	.00000E 00	.00000E 00	.00000E 00
.10000E 03	.10000E 03	.10000E 03	.10000E+05	.10000E+05	.25000E 02	.10000E 03	.10000E+03	.10000E+03	.25000E 02	
.00000E 00	.21308E+10	.14845E+07	.13162E+06	.30946E+09	.23469E+06	.00000E 00	.00000E 00	.00000E 00	.00000E 00	.00000E 00
SUM * .38148E+06										

Figure 77. Variance Contribution Program Outputs (continued)

```

YE
  XE      HE      U      THETA      Q      W      YE      PSI      R      V
.00000E 00 .00000E 00 .00000E 00 .00000E 00 .00000E 00 .00000E 00 .10000E 01 .14081E 08 .35392E 02 .50931E 02
.10000E 03 .10000E 03 .10000E 03 .10000E+05 .10000E+08 .25000E 02 .10000E 03 .10000E+03 .10000E+03 .25000E 02
.00000E 00 .00000E 00 .00000E 00 .00000E 00 .00000E 00 .00000E 00 .10000E 03 .14081E 04 .35392E+02 .12733E 04
SUM = .27814E 04

```

```

PSI
  XE      HE      U      THETA      Q      W      YE      PSI      R      V
.00000E 00 .00000E 00 .00000E 00 .00000E 00 .00000E 00 .00000E 00 .00000E 00 .10000E 01 .24198E+05 .36152E+05
.10000E 03 .10000E 03 .10000E 03 .10000E+05 .10000E+05 .25000E 02 .10000E 03 .10000E+03 .10000E+03 .25000E 02
.00000E 00 .00000E 00 .00000E 00 .00000E 00 .00000E 00 .00000E 00 .00000E 00 .10000E+03 .24198E+09 .90380E+04
SUM = .19038E+03

```

```

R
  XE      HE      U      THETA      Q      W      YE      PSI      R      V
.00000E 00 .00000E 00 .00000E 00 .00000E 00 .00000E 00 .00000E 00 .00000E 00 .00000E 00 .19283E+04 .83969E+11
.10000E 03 .10000E 03 .10000E 03 .10000E+05 .10000E+05 .25000E 02 .10000E 03 .10000E+03 .10000E+03 .25000E 02
.00000E 00 .00000E 00 .00000E 00 .00000E 00 .00000E 00 .00000E 00 .00000E 00 .00000E 00 .19283E+10 .20992E+09
SUM = .22921E+09

```

Figure 77. Variance Contribution Program Outputs (continued)

VE	HE	U	THETA	Q	W	YE	PSI	R	V
.0000E 00	.0000E 00	.0000E 00	.0000E 00	.0000E 00	.0000E 00	.0000E 00	.0000E 00	.25036E-03	.15500E-04
.1000E 03	.1000E 03	.1000E 03	.1000E-05	.1000E-05	.2500E 02	.1000E 03	.1000E-03	.1000E-03	.2500E 02
.0000E 00	.0000E 00	.0000E 00	.0000E 00	.0000E 00	.0000E 00	.0000E 00	.0000E 00	.25036E-07	.38750E-05

SUM = .39001E-05

CEP HORIZONTAL = .67145803E 02 CEP VERTICAL = .63558791E 02

STEP 77774123

Figure 77. Variance Contribution Program Outputs (concluded)

SECTION IX

CONCLUSIONS AND RECOMMENDATIONS

The following conclusions were drawn from the demonstration example:

- The results of the stationary-nonstationary comparison analysis indicated that no appreciable difference existed between the delivery performances obtained from the fixed and the time-varying controllers. This led us to believe that the use of fixed optimal gains in the weapon delivery controller would be sufficient.
- It has been observed that the steady-state values of the performance measure for a frozen-time point linear data is considerably higher than that of the finite-time model. For this reason, the weapon delivery performance evaluation (i. e. , computation of the total covariance and the CEP) should be based on the finite-time (i. e. , nonstationary) model.
- An aircraft using the optimal controller with a perfect measurement system reduced the CEP 10 to 1 with respect to a free airframe.
- The contribution matrix of an iron bomb indicated that: (a) the longitudinal states, u , w , and θ were the prime contributors to the down-range impact variances, and (b) the lateral states ψ and v were the major contributors to the cross-range impact covariance.

Limitations inherent in the example included:

- Only order-of-magnitude checks were made on the time-varying data generated in the demonstration example. More elaborate checking via data transformation as explained on page 105 of Volume I is needed to validate the data prior to extensive parametric study of a given system.
- The aerodynamic data tables for the airframe used in the demonstration example are limited to a maximum Mach number of 0.8.

The primary emphasis in this study has been on the model and software development and the demonstration of their use. These have been achieved. For future work, a detailed parametric error analysis study using ADAPS is recommended.

Unclassified

Security Classification

DOCUMENT CONTROL DATA - R & D		
(Security classification of title, body of abstract and indexing annotation must be entered when the overall report is classified)		
1. ORIGINATING ACTIVITY (Corporate author) Honeywell Inc. Systems and Research Division, Research Dept. Minneapolis, Minnesota 55413	2a. REPORT SECURITY CLASSIFICATION Unclassified	
	2b. GROUP NA	
3. REPORT TITLE DEVELOPMENT OF WEAPON DELIVERY MODELS AND ANALYSIS PROGRAMS Volume III. Testing and Demonstration of the Armament Delivery Analysis Programming System (ADAPS)		
4. DESCRIPTIVE NOTES (Type of report and inclusive dates) Final Technical Report 5 October 1970-5 October 1971		
5. AUTHOR(S) (First name, middle initial, last name) A. Ferit Konar Michael D. Ward		
6. REPORT DATE April 1972	7a. TOTAL NO. OF PAGES 191	7b. NO. OF REFS 0
8a. CONTRACT OR GRANT NO. F33615-71-C-1059 b. PROJECT NO. 8219 c. Task No. 821904 d.	9a. ORIGINATOR'S REPORT NUMBER(S) 12261-FR1, Vol. III 9b. OTHER REPORT NO(S) (Any other numbers that may be assigned this report) AFFDL-TR-71-123, Vol. III	
10. DISTRIBUTION STATEMENT Approved for public release; distribution unlimited.		
11. SUPPLEMENTARY NOTES	12. SPONSORING MILITARY ACTIVITY Air Force Flight Dynamics Laboratory Air Force Systems Command Wright-Patterson Air Force Base, Ohio	
13. ABSTRACT 45433 The testing and use of ADAPS is demonstrated by performing an analysis with a specified iron bomb (M117) and a representative tactical fighter-bomber aircraft (F4). The demonstration example revealed no appreciable performance difference between the time-invariant and time-varying optimal controllers for the weapon delivery process. The contribution matrix of an iron bomb indicated that the major contributors to the CEP are the velocity and the attitude-state errors at release.		

Unclassified

Security Classification

14. KEY WORDS	LINK A		LINK B		LINK C	
	ROLE	WT	ROLE	WT	ROLE	WT
Weapon Delivery modeling Error analysis CEP Optimal control						

Unclassified